

**Metabolomics and proteomics to understand fuel use in a  
rat model of high and low exercise capacity**

by

Katherine A. Overmyer

A dissertation submitted in partial fulfillment  
of the requirements for the degree of  
Doctor of Philosophy  
(Molecular and Integrative Physiology)  
in the University of Michigan  
2014

Doctoral Committee:

Professor Charles F. Burant, Chair  
Professor Susan V. Brooks-Herzog  
Professor Gregory D. Cartee  
Assistant Professor David B. Lombard

© Katherine Overmyer 2014

## **Acknowledgements**

A number of people contributed to the work presented in this study: Charles R. Evans, Nathan R. Qi, Catherine E. Minogue, Joshua J. Carson, Christopher J. Chermide-Scabbo, Mary K. Treutelaar, Lauren G. Koch, Steven L. Britton, David J. Pagliarini, Joshua J. Coon, Charles F. Burant.

In addition to the individuals listed above, there are many more that deserve acknowledgement for their help and support during my graduate career: Thomas Hancock, Abby Burant, Mahmoud El Azzouny, Tanu Soni, Heidi IglayReger, Arun Das, Hiroyuki Mori, Ormond MacDougald, Yu-yu Ren, Jun Li, Liz Limback, Melanie Schmitt, Molly Kalahar, Lori Heckenkamp, Jeongsoon Park, David Lombard, Greg Cartee, and Sue Brooks.

## Table of Contents

Acknowledgements	ii
List of Tables	vi
List of Figures	vii
List of Appendices	viii
List of Abbreviations	ix
Abstract	x
Chapter 1 - Introduction	1
1.1 - Aim and Scope	2
1.2 - Study overview	3
Chapter 2 - Importance of fuel preference	5
2.1 - A brief history	5
2.1.1 - Studies linking fuel use and high exercise capacity	6
2.1.2 - Fuel selection and metabolic health	8
2.1.3 - Fuel selection and longevity	10
2.2 - Mechanisms for adaptive fuel selection	11
2.2.1 - Fuel availability	12
2.2.2 - Substrate entry into the cell	15
2.2.3 - Glycogenolysis and glycolysis	16
2.2.4 - Substrate entry into the mitochondria	19
2.2.5 - Mitochondrial enzyme activity	20
2.3 - Model for high and low exercise capacity	21
2.3.1 - Beginnings of the HCR-LCR model	22
2.3.2 - Fuel selection in HCR and LCR	24
2.4 - Summary	25
Chapter 3 - Metabolomics to define fuel use during exercise	26

3.1 - Introduction	26
3.2 - Methods	27
3.2.1 - Animal protocol and study design	27
3.2.2 - Indirect calorimetry	29
3.2.3 - Muscle glycogen	29
3.2.4 - Western blot for AMPK	30
3.2.5 - Confirmation data set	30
3.2.6 - Statistical analysis and graphing	30
3.2.7 - Muscle and plasma metabolites	31
3.3 - Results	32
3.3.1 - HCR have greater whole-body fat oxidation	33
3.3.2 - HCR spare muscle glycogen	34
3.3.3 - HCR maintain complete fat oxidation	35
3.3.4 - Changes in amino acids with exercise	38
3.3.5 - AMP kinase phosphorylation	38
3.3.6 - Metabolite changes coincident with exhaustion	39
3.4 - Discussion	42
3.5 - Summary	45
Chapter 4 - Post-translational modifications that occur with exercise	47
4.1 - Introduction	47
4.2 - Methods	49
4.2.1 - Animal protocol and study design	49
4.2.2 - Mitochondrial isolations	49
4.2.3 - Generation of peptides	50
4.2.4 - Phospho and Acetyl-site enrichment	52
4.2.5 - Proteomic LC-MS/MS analysis	52
4.2.6 - Proteome data processing and normalization	53
4.2.7 - Sirt3 Western Blot	55
4.2.8 - Statistical analysis and graphing	55
4.3 - Results	56
4.3.1 - HCR and LCR mitochondrial proteome	56

4.3.2 - Protein modification	58
4.3.3 - The acetylome is most dynamic with exercise	59
4.3.4 - Sirt 3	62
4.3.5 - Integrating proteomics data	62
4.4 - Discussion	63
4.5 - Summary	66
Chapter 5 - Isotopic tracers to understand fuel use during exercise	67
5.1 - Introduction	67
5.2 - Methods	68
5.2.1 - Animal protocol and study design	68
5.2.2 - Muscle and serum metabolites	70
5.2.3 - Statistical analysis and graphing	71
5.3 - Results	71
5.3.1 - Injection of Valine leads to 70% serum enrichment	71
5.3.2 - HCR have greater valine nitrogen transfer	72
5.3.3 - Nitrogen transfer to other Amino Acids	74
5.3.4 - Valine degradation	74
5.3.5 - HCR have greater BCAA metabolism	77
5.4 - Discussion	79
5.5 - Summary	80
Chapter 6 - Study implications	82
6.1 - Model for enhanced exercise capacity	82
6.2 - Implications to health and longevity	83
6.3 - Future Directions	84
Appendices	86
References	109

## List of Tables

Table 3.1 HCR weigh less and run further than LCR	33
Table 3.2 Metabolites correlated with fuel use and exhaustion	41
Table 4.1 Number of proteins identified in mitochondria	57
Table 4.2 The Top 25 differentially expressed or modified proteins	63
Table 5.1 Valine injected animals body weight and running time	70
Table A.1 Metabolomics data set	88
Table B.1 Confirmation metabolomics data set	93
Table C.1 Proteomic data set, mitochondrial proteins	99
Table C.2 Proteomic data set, phospho-sites	100
Table C.3 Proteomic data set, acetyl-sites	105

## List of Figures

Figure 2.1 Fuel shift with fasting and feeding	14
Figure 2.2 Glycolysis and glycogenolysis	19
Figure 3.1 Study design	28
Figure 3.2 HCR have higher fat oxidation throughout exercise	34
Figure 3.3 HCR spare muscle glycogen	35
Figure 3.4 HCR have greater changes in acylcarnitines with exercise	37
Figure 3.5 Muscle AMPK is phosphorylated near exhaustion	39
Figure 3.6 Metabolites that increase with exhaustion	42
Figure 4.1 Differentially expressed proteins between HCR and LCR	58
Figure 4.2 Mitochondrial protein acetylation is dynamic with exercise	59
Figure 4.3 HCR have less mitochondrial protein acetylation than LCR	61
Figure 4.4 SIRT3 expression in the mitochondria	62
Figure 5.1 Valine injection does not effect running capacity	70
Figure 5.2 Valine enrichment in serum and muscle	73
Figure 5.3 HCR have greater isotope enrichment in downstream metabolites	76
Figure 5.4 HCR have greater valine metabolism during exercise	78
Figure 6.1 HCR have enhanced capacity to oxidize fatty acids and BCAA	83



## List of Appendices

A. Metabolomics data set	87
B. Confirmation metabolomics data set	93
C. Proteomic data sets	98

## List of Abbreviations

ATGL: Adipose triglycerol lipase

BCAA: Branched-chain amino acids

CPT1: Carnitine palmitoyl transferase I

FA: Fatty acids

GC-MS: Gas chromatography mass spectroscopy

GP: Glycogen phosphorylase

HCR: High capacity running rat

HIB: beta-hydroxyisobutyrate, the main end product of Valine metabolism

HK: Hexokinase

HSL: Hormone sensitive lipase

KIV: Keto-isovaleric acid, the first product of Valine metabolism

KIC: Keto-isocaproic acid, the first product of Leucine metabolism

KMV: Keto-methylvaleric acid, the first product of Isoleucine metabolism

LC-MS: Liquid chromatography mass spectroscopy

LCR: Low capacity running rat

PDH: Pyruvate dehydrogenase

PFK: Phosphofructokinase

RQ: Respiratory Quotient

VO<sub>2</sub>: Volume of oxygen consumption

VCO<sub>2</sub>: Volume of carbon dioxide production

## Abstract

In humans, exercise capacity strongly associates with morbidity, mortality, and disease-risk. Maximal exercise capacity is a heritable trait, and rats selectively bred for high and low exercise capacity mimic phenotypes observed in humans: high capacity running rats (HCR) have lower metabolic-disease risk and increased longevity compared to low capacity running rats (LCR). In prior *in vitro* studies HCR skeletal muscle was shown to have higher fatty acid (FA) oxidizing capacity than LCR. We hypothesized that HCR would have enhanced FA utilization during *in vivo* exercise. In this study we use metabolomics and proteomics approaches to test this hypothesis and to explore metabolic differences between HCR and LCR during an increasing-intensity treadmill protocol (speed increasing 1 m/min every 2 min). Using indirect calorimetry, we found that during exercise HCR maintain high FA utilization, while LCR primarily utilize carbohydrates. Skeletal muscle and plasma were collected at rest, at 10 min of exercise (near exhaustion for LCR), and at 45 min of exercise (near exhaustion for HCR). Metabolite profiles showed HCR have increased muscle long-chain acyl-carnitines from rest to 10 min of exercise, indicating increased FA entry into the mitochondria of HCR. In contrast, LCR showed accumulation of short- and medium-chain muscle acylcarnitines from rest to 10 min of exercise, indicating inefficient substrate metabolism. We quantified muscle mitochondrial proteins and protein post-translational modifications (phosphorylation and acetylation) at rest and at 10 min of exercise. At rest, HCR have greater expression of enzymes within FA and branched-chain amino acid (BCAA) metabolic pathways than LCR. Compared to LCR, HCR have lower mitochondrial protein acetylation at rest and show protein deacetylation with 10 min of exercise, specifically in oxidative phosphorylation, citric acid cycle, FA and BCAA metabolic pathways. Consistent with a functional role of increased protein expression and lower protein acetylation within the BCAA pathway, HCR have greater BCAA metabolism during 10 min of exercise as measured by flux of intraperitoneally injected U-13C15N valine into catabolic intermediates. This study suggests

enhanced FA and BCAA metabolism supports high running capacity and provides evidence for FA and BCAA pathway protein expression and acetylation in mediating enhanced fuel utilization.

## **Chapter 1**

### **Introduction**

How well an individual performs on a maximal exercise test can predict longevity and risk for disease. This might seem intuitive; an endurance trained athlete is likely healthier than someone who starts breathing hard after jogging only a few meters. But training to run long-distances takes months, and the training effect on metabolic processes can be lost within a matter of weeks. So although training can improve one's immediate health outlook, much of what determines performance during a maximal exercise test — and long-term health prospects — is genetically predetermined.

The genetics and underlying molecular mechanisms of exercise capacity are unknown. Certain medical conditions, like asthma and anemia, can impair delivery of oxygen to working muscle and thus limit exercise capacity. Similarly, mutations within genes involved in energy metabolism, for example glycogen phosphorylase, can limit energy production for contracting muscle. However, what yields Olympic-level exercise capacity, and associated longevity, or even more subtle differences in exercise capacity, are less well understood.

This is an important problem to address. We can imagine that someday, having this knowledge of exercise capacity and how it associates with health and longevity will lead to targeted and/or therapeutic approaches to maximize the number of healthy years we can enjoy.

## 1.1 Aim and Scope

My thesis focuses on understanding this intrinsic (non-trained) component of exercise capacity. In this study, I aim to better understand the underlying physiology of animals divergent for intrinsic exercise capacity. The implication is that the physiological mechanisms that differ with running capacity likely impact overall health. Although there are many potential mechanisms for increased exercise capacity, I will focus on the concept of fuel preference: selectively utilizing fatty acids or carbohydrates for energy production.

Preference towards fat utilization during exercise is linked to better exercise capacity. Trained long-distance athletes use fat more efficiently. This is due to a coordinated, physiological response to the stress of exercise and involves up-regulation of specific genes related to fat metabolism. In contrast, an individual with poor metabolic health uses fats inefficiently during exercise and even at rest, has impaired switching between fats and carbohydrates for energy production. Thus, fuel preference appears to relate to both exercise capacity and overall health.

The original research presented in this thesis is focused specifically on fuel use during a maximal exercise test on a treadmill. During this test, the speed increases at regular intervals until individuals exhaust. As you might imagine, fuel preference is dynamic and changes depending on the intensity of activity. At rest, roughly 85% of energy comes from fatty acids. As intensity increases, an individual a) needs more fuel to meet increasing energy demands and b) changes fuel preference, shifting towards greater carbohydrate use as speed increases. We take advantage of this shift in fuel preference as intensity increases to examine possible underlying factors for fuel preference.

My study uses rats bred for high and low intrinsic running capacity. The rats have a heterogeneous genetic background and are the product of selective breeding for intrinsic exercise capacity. This rat model mimics the associated health aspects of exercise capacity that we see in humans: the high capacity rats are lean, less susceptible to diet induced obesity and insulin resistance, and longer lived. By using a rat model, we can control for environmental factors, such as diet and physical activity, that can be more difficult to control for in human studies.

## 1.2 Study overview

This thesis focuses on how mechanisms for fuel preference might support increased exercise capacity and overall health. To achieve this aim, the following chapters are organized around three points: the background and current knowledge about fuel selection (Chapter 2), my original research which tests hypotheses about fuel utilization in rats bred for high and low running capacity (Chapters 3, 4, 5), and implications of the current study and future directions (Chapter 6).

In the second chapter, I will go through some of the key evidence linking fuel preference to exercise capacity and metabolic health. I will discuss some potential mechanisms for adaptive fuel preference, and when and why these mechanisms fail to adequately explain fuel preference. Then I will end this chapter by talking about the rat model for high and low exercise capacity and why it is a good model for uncovering mechanisms of fuel preference and exercise capacity. This chapter will set up the rationale and motivation for the original research that follows.

Chapters 3, 4, and 5 describe a series of experiments to understand fuel utilization in rats bred for high and low exercise capacity. In Chapter 3, I use metabolomic profiling to define fuel use in high and low capacity running rats. These data led to the hypothesis that exhaustive exercise induces changes in enzyme acetylation, a post-translation modification that affects enzyme activity. In Chapter 4, I use proteomic analysis to investigate post-translational modifications that occur with exercise in high and low capacity running rats, and I compare changes in protein acetylation vs. changes in protein phosphorylation with exercise. Data in Chapters 3 and 4 give evidence for the importance of two key metabolic pathways: fatty acid oxidation and branched-chain amino acid oxidation. In Chapter 5, I will describe my study using a stable isotope tracer to investigate *in vivo* flux of the branched-chain amino acid valine.

The final chapter, Chapter 6, I will highlight conclusions, implications, and future directions of the study. In particular, I will discuss the importance of fatty acid and branched-chain amino acid metabolism to exercise capacity and metabolic health

and the need for continued research to better understand the role of post-translation modifications like acetylation in supporting fuel preference.



## **Chapter 2**

### **Importance of fuel preference**

The previous chapter gave a brief introduction and overview of the study. This next chapter will highlight the current knowledge about fuel preference, first focusing on why fuel preference is linked to exercise capacity and health, second focusing on how fuel preference might be regulated, and third explaining the advantage of using a genetically complex animal model to better understand high running capacity.

#### **2.1 A brief history**

The earliest studies to understand fuel use start with Antoine-Laurent de Lavoisier. His work in the late 1700s provided the first strides towards understanding respiration and metabolism. Lavoisier was a French chemist interested in animal respiration and the phenomenon of heat production. He designed an ice-calorimeter to demonstrate that heat produced per unit of CO<sub>2</sub> was the same for both a candle flame and a live guinea pig, and with these results he famously claimed 'respiration is combustion'. Lavoisier was the first to recognize that the inspired air, 'oxygine' as he named it, was consumed in both combustion and respiration. Further, when Lavoisier measured respiration and pulse in a human volunteer, he showed that oxygen consumption varied based on activity, with exercise requiring more oxygen than resting, and eating more than fasting (Karamanou and Androustos, 2013; West, 2013).

An important concept derived from the measurement of oxygen consumption and CO<sub>2</sub> production is the respiratory quotient (RQ; CO<sub>2</sub>/O<sub>2</sub>). In the mid-1800s French chemists Regnault and Reiset recognized that the ratio of CO<sub>2</sub> produced and O<sub>2</sub> consumed was dynamic with different diets (Wilder, 1959). This fluctuation in the RQ stems from the differences in O<sub>2</sub> required for combustion of different chemical fuels (glucose, fatty acids, proteins). A glucose molecule (C<sub>6</sub>H<sub>12</sub>O<sub>6</sub>) will require 6 O<sub>2</sub> to produce 6 CO<sub>2</sub> and 6 H<sub>2</sub>O resulting in a ratio of 1:1 of CO<sub>2</sub>:O<sub>2</sub> (RQ = 1). While a molecule of fat, for example palmitic acid (C<sub>16</sub>H<sub>32</sub>O<sub>2</sub>), will require 23 O<sub>2</sub> to produce 16 CO<sub>2</sub> and 16 H<sub>2</sub>O resulting in a ratio of 16:23 of CO<sub>2</sub>:O<sub>2</sub> (RQ = 0.7) (Wilmore and Costill, 2004). For whole-body respiration, the RQ provides an estimate of relative carbohydrate vs. fat oxidation: lower RQ values indicate higher fat use, while higher RQ values indicate greater carbohydrate use.

Since Lavoisier's work and the development of calorimetry techniques to study fuel use, scientists have continued to use this knowledge to understand oxidation of fat, carbohydrates and protein for energy. Another founder of metabolic research, Carl von Voit, combined measurements of nitrogen with RQ to begin expressing metabolism in terms of the amount of protein, carbohydrate and fat stored and oxidized (Mitchell, 1937). Voit's students Rubner, Atwater, and Lusk each continued work on fuel use and metabolism. Rubner and Atwater used a bomb calorimeter to measure combustion of fat, protein and carbohydrate (Buchholz and Schoeller, 2004), and they established how much metabolic energy was produced from fat (8.9 kcal/g), carbohydrates (4 kcal/g), and protein (4 kcal/g) (Widdowson, 1955). And Lusk advanced the knowledge of diabetic, exercise, and intermediary metabolism using indirect calorimetry (Du Bois, 1933). These scientists stemming from the lineage of Lavoisier laid down the foundation for the study of fuel use in exercise, health, and longevity.

### *2.1.1 Studies linking fuel use and high exercise capacity*

Respiration during exercise has been of interest ever since Lavoisier first demonstrated respiration increases with work. In 1923, Hill and Lupton showed that O<sub>2</sub> respiration increases proportionally with increasing speed of running until a

maximum limit is reached, that is, when increasing work does not produce an increase in oxygen consumption (Hill and Lupton, 1923). Hill believed this maximal oxygen consumption could be used to assess exercise capacity of individuals with metabolic, cardiac, or other conditions that limited long-duration exercise. Within the last 20 years, several large-scale studies have found that maximal oxygen consumption strongly associates with morbidity and mortality in humans (Blair et al., 1996; Church et al., 2004; Lee et al., 2010). In addition, it also associates with risk for metabolic syndrome (Whaley et al., 1999), insulin resistance and diabetes (Larsen et al., 2012; Leite et al., 2009; Wei et al., 1999), cancer (Peel et al., 2009), and heart disease (Kodama et al., 2009).

Beyond assessing maximal oxygen consumption, Hill and his contemporaries focused on fuel use during exercise. Moderate intensity exercise leads in increased fat oxidation (decreasing RQ) and high intensity exercise leads to greater carbohydrate oxidation (increasing RQ) (Hill and Lupton, 1923; Romijn et al., 1993). By the 1920s, researchers understood that high-intensity exercise, which would elicit maximum oxygen consumption, was associated with high carbohydrate use, breakdown of glycogen and accumulation of blood lactate. Hill (1923) writes, "the very great rise of the R.Q., during and after violent effort, is a sign that the acid production is considerable." For nearly a century, researchers have been developing techniques to better understand the decreased fat use and increased carbohydrate use during high intensity exercise, and it remains an unsolved problem in exercise physiology (Jeppesen and Kiens, 2012).

The problem of fuel selection is important because fuel preference directly relates to exercise capacity and maximal oxygen consumption. Maximum oxygen consumption occurs when carbohydrate use is high, but it is significantly correlated with maximal fat oxidation during an increasing-intensity bout of exercise (Nordby et al., 2006; Venables et al., 2005). By using fat for fuel, instead of carbohydrate, the limited glycogen stores are spared, and thus exhaustion is delayed. Animal models with lower fat oxidation have faster glycogen breakdown during exercise and lower exercise capacity (Fernandez et al., 2008; Huijsman et al., 2009). In contrast, animal models with high exercise capacity have increased daily fat oxidation (Narkar et al.,

2011; Perez-Schindler et al., 2012; Quinn et al., 2013; Rogowski et al., 2013; Yamamoto et al., 2011), or greater fat oxidation during an increasing-intensity bout of exercise compared to control animals (Hakimi et al., 2007). Exercise training, which often yields increases in exercise capacity, also leads to increased fat oxidation during exercise (Coggan et al., 2000; Helge et al., 2007; Schrauwen et al., 2002; Tunstall et al., 2002). Given this evidence, we can conclude that fat oxidation during increasing-intensity exercise is critical for high oxygen consumption and exercise capacity.

We have focused primarily on fat and carbohydrate use because these fuels account for 85-95% of the total fuel used during exercise (Wagenmakers et al., 1991). However, amino acids can contribute a small percentage to energy production. In particular, branched-chain amino acids (BCAA) — valine, leucine, and isoleucine — contribute the most towards energy production in skeletal muscle (Wagenmakers et al., 1991). BCAA metabolism increases with onset of exercise (van Hall et al., 1996; Wagenmakers et al., 1989), and training leads to increases in muscle BCAA enzyme activity (Fujii et al., 1995; Shimomura et al., 1995). Gene expression of BCAA enzymes appear to be co-regulated with genes for fat oxidation: both pathways are increased in active vs. inactive twins (Leskinen et al., 2010; Pietilainen et al., 2008) and in high-capacity running rats vs. low-capacity running rats (Kivela et al., 2010). Dietary BCAA supplementation does not substantially alter exercise capacity (Blomstrand et al., 1991; MacLean and Graham, 1993), but knocking out muscle-specific branched-chain aminotransferase in mice significantly reduces exercise capacity (She et al., 2010). This evidence gives importance to the role of BCAA metabolism in exercise, even though BCAA contribute only a minor amount to overall energy production.

### *2.1.2 Fuel selection and metabolic health*

In addition to fuel selection being important for exercise capacity, fuel selection is a critical component of metabolic health. Pathophysiological states such as diabetes and insulin resistance are characterized by metabolic inflexibility - the failure to appropriately switch between glucose and fat oxidation (Kelley and Mandarino, 2000;

Thyfault et al., 2006). In normal individuals, fat oxidation is high in the fasted state and declines with insulin stimulation. However, in individuals with insulin resistance, the transition from high fat to high carbohydrate oxidation is blunted (Galgani et al., 2008). This disruption in metabolic flexibility is also associated with accumulation of lipid species within liver and muscle tissues (Kelley and Mandarino, 2000). In insulin resistance there is greater flux of fatty acids into the tissue (Bonen et al., 2004) but also greater incomplete fat oxidation, which might support insulin resistance (Koves et al., 2008; Muoio and Koves, 2007).

Studies have shown that manipulation of fat and glucose metabolism can lead to increased insulin sensitivity. Carnitine palmitoyl transferase I (CPTI) is essential for long-chain fatty acid entry into the mitochondria. Inhibiting fat oxidation with CPTI inhibitors (Oxfenicine, etomoxir, or excess malonyl-CoA) can improve insulin sensitivity (Bouzakri et al., 2008; Keung et al., 2013; Koves et al., 2008; Timmers et al., 2012). This improvement in insulin sensitivity occurs despite increased accumulation of lipid species within skeletal muscle and decreased fat oxidation. This data might seem counterintuitive, but it highlights the importance of matching fuel income with fuel oxidation. In cases when fuel requirements are low (at rest) increasing fat uptake relative to oxidation has negative consequences, and limiting fat oxidation can improve balance between fat and carbohydrate oxidation. In the case of exercise, when fuel requirements are high, increased fat uptake and oxidation is beneficial. Restoring the balance between fuel uptake and fuel use might underlie part of insulin-sensitizing benefits of exercise (Goodpaster and Brown, 2005). As mentioned in the previous section, fat use during exercise is critical to exercise capacity and positively correlates with insulin sensitivity (Hall et al., 2010).

In addition to disruption in fat and glucose metabolism, insulin resistance is associated with changes in BCAA utilization. BCAA pathway enzyme expression decreases with diabetes (Mullen and Ohlendieck, 2010), and BCAA enzyme gene expression positively correlates with insulin sensitivity (Pietilainen et al., 2008; Sears et al., 2009). In insulin resistance, circulating BCAA are elevated (Batch et al., 2013; Huffman et al., 2009; Wang et al., 2011). These elevated levels of BCAA correlate with insulin resistance (Fiehn et al., 2010; Menni et al., 2013; Xu et al., 2013) and

are predictive of development of diabetes (Wang et al., 2011). Weight loss improvement of insulin resistance associates with decreased circulating BCAA levels (Magkos et al., 2013; Shah et al., 2012).

The dynamics of BCAA metabolism with insulin resistance is not well understood. It could be that BCAA metabolism is increased with insulin resistance, as both BCAA and downstream metabolites are elevated in diabetes/insulin resistance (Batch et al., 2013; Fiehn et al., 2010; Menni et al., 2013; Newgard et al., 2009; Xu et al., 2013). However, it is more likely that BCAA metabolism is decreased in insulin resistance. Elevated BCAA coincides with decreased BCAA-related enzyme activity in animal models of insulin resistance (Doisaki et al., 2010). The mRNA expression of BCAA metabolic enzymes decreases with insulin resistance and is restored with insulin sensitizing thiazolidinedione (TZD) treatment (Sears et al., 2009). The elevation of BCAA and intermediary metabolites in insulin resistance might also indicate an imbalance of input and oxidation.

### *2.1.3 Fuel selection and longevity*

Exercise capacity is strongly associated with morbidity and mortality and is one of the best predictors of healthspan in humans (Blair et al., 1996; Church et al., 2004; Kodama et al., 2009; Lee et al., 2010). As expected from this relationship,  $VO_2$ max, a measurement of exercise capacity, decreases with age (Hollenberg et al., 1998; Hollenberg et al., 2006). Notably, aging is also associated with changes in lipid metabolism (Houtkooper et al., 2011; Tomas-Loba et al., 2013) and down-regulation of genes involved in mitochondrial metabolism and electron-transport chain (de Magalhaes et al., 2009; Zahn and Kim, 2007).

In recent years, modulations in diet and gene expression have been shown to increase lifespan in model organisms; importantly several of these manipulations target nutrient signaling and metabolism: IGF-1, mTOR, sirtuins, growth hormone, and calorie restriction (Giblin et al., 2014; Lopez-Otin et al., 2013). The metabolic response to these manipulations is thought to be an integral to the extension of lifespan (Anderson and Weindruch, 2010).

In a number of these long-lived organisms, there is elevated fat oxidation. The long-lived Ames dwarf mice and growth hormone receptor knockout mice have substantially lower 24-hr RQ measurements than control mice, indicating greater fatty acid oxidation (Westbrook et al., 2009). Long-lived mitochondrial mutations (in *C. elegans*) have elevated FA utilization and display upregulation of energy producing pathways (Munkacsy and Rea, 2014). Caloric restriction, which extends life and prevents much of the age-related decline in metabolic gene expression (Park and Prolla, 2005) also leads to increased fat oxidation in *Drosophila* (Katewa et al., 2012), mice (Bruss et al., 2010) and humans (Huffman et al., 2012). Consistent with a role of lipid metabolism in longevity, long-lived mice (calorie restriction, *Irs1*  $-/-$ , and Ames dwarf) show elevations in plasma lipids (Wijeyesekera et al., 2012).

In addition to alterations in fat oxidation in long-lived models, there also appear to be modifications in BCAA metabolism; however this relationship is more complex. Long-lived Ames dwarf mice have lower circulating BCAA, which might indicate greater utilization (Eto, 2013; Wijeyesekera et al., 2012). Calorie restriction also leads to lower levels of plasma BCAA in dogs (Richards et al., 2013). However, long-lived *daf-2* mutants (*C. elegans*) with disrupted insulin/insulin-like signaling pathway have elevated BCAA and lower expression of BCAA metabolic enzymes (Fuchs et al., 2010; Martin et al., 2011). The inconsistency of BCAA metabolism among long-lived mutants might depend on whether insulin signaling is disrupted. As we discussed in the previous section BCAA are elevated with increasing insulin resistance (Fiehn et al., 2010; Menni et al., 2013; Xu et al., 2013). We conclude that while BCAA metabolism is modulated in some of the long-lived models, up- or down-regulation of BCAA metabolism does not consistently track with increased or decreased lifespan.

## **2.2 Mechanisms for adaptive fuel selection**

In the previous section, we reviewed the historical interest in fuel selection, and the strong association between fuel selection and exercise capacity, metabolic health, and longevity. Together, this knowledge motivates the continued study of fuel selection and mechanisms for adaptive fuel selection in response to environmental

changes. Regulation of fuel selection is an integrated process that allows for energy supply to meet energy demand despite, and in response to, environmental instability. In fact, metabolic health depends on appropriate changes in fat, glucose, and protein use in response to fasting, feeding, and exercise. These dynamic changes in fuel use aid in our understanding of the various levels of control that drive fuel selection.

Given the complexity of the regulation, I will focus our attention to some of the best explanations for fuel selection, starting with regulation of fuel availability, fuel entry into the cell, glycogenolysis and glycolysis, substrate entry into the mitochondria, and mitochondrial enzyme activity.

### *2.2.1 Fuel availability*

Fuel availability is probably one of the largest contributors to fuel selection. Intermittent food uptake maintains fuel availability. Incoming fuel (food) can be used immediately for energy production or stored and used later during fasting or starving conditions. The system is regulated in a way that minimizes large sustained changes in glucose availability, which serves the purpose of maintaining glucose for the brain. Circulating hormones like insulin and glucagon augment glucose control. Insulin signaling after feeding leads to increased glucose uptake in peripheral tissues (muscle, adipose, and liver) and increased fatty acid storage in adipose tissue, while glucagon signaling during fasting leads to increased glucose production from the liver and stimulates fatty acid release from adipose tissue.

What results from this system is a see-saw between fat and glucose availability and utilization during periods of fasting and feeding (**Figure 2.1**). The key modulators of circulating fuel availability are 1) fuel uptake, which will be discussed in the next section, and 2) fuel release from stored sources, which will be the main focus of this section.

In the fasted condition, glucose supply is primarily regulated by the liver (Ramnanan et al., 2011). The liver will synthesize glucose in times of fasting and under exercise. This process utilizes stored forms of carbohydrate (glycogen) to form glucose, which is then released into circulation. The process of glycogen breakdown in the liver is mediated by glucagon (Ramnanan et al., 2011).



Fat is primarily stored as triglyceride (3 fatty acid chains + a glycerol backbone) in the adipose tissue and within skeletal muscle. Triglyceride storage accounts for the most dense and largest fuel reserve in the body (Horowitz, 2003). In times of energy need, triglycerides are broken down to yield free fatty acids and glycerol. These free fatty acids can then be oxidized for energy production. Triglyceride breakdown is catalyzed by lipases: hormone sensitive lipase (HSL) and adipose triglyceride lipase (ATGL) in tissue (Lass et al., 2011), and lipoprotein lipase in blood vessels (Horowitz, 2003).

HSL hydrolyzes many lipid types (triglycerol, diacylglycerol, cholesterylester) (Lass et al., 2011). As the name implies, HSL is acutely regulated by hormones. Insulin can suppress HSL activity (Campbell et al., 1992), and  $\beta$ -adrenergic stimulation by catecholamines can activate HSL (Clifford et al., 2000). During exercise, HSL can be activated both by increased catecholamine levels and by decreased circulating insulin (Horowitz, 2003). Mice with HSL-null mutation have decreased plasma fatty acids under fasting and moderate intensity exercise, and because fatty acids are an important source of fuel during exercise, these animals have lower running capacity (Fernandez et al., 2008). HSL is also present in skeletal muscle and likely mediates the breakdown of intramuscular triglycerides (IMTG) (Horowitz, 2003). Although catecholamines can increase muscle HSL activity, calcium can also play a role in HSL stimulation (Horowitz, 2003).

ATGL, identified in 2004, specifically catalyzes reaction of triacylglycerol into diacylglycerol and a fatty acid (Lass et al., 2011). Like HSL, ATGL is also stimulated by  $\beta$ -adrenergic activity (Haemmerle et al., 2006). Increased lipid oxidation under fasting and exercise conditions does not occur in ATGL-null mice and these null-animals have proportionally greater carbohydrate oxidation (Huijsman et al., 2009; Schoiswohl et al., 2010). Together, ATGL and HSL activity accounts for greater than 95% of the lipolysis in adipose (Schweiger et al., 2006) and skeletal muscle (Alsted et al., 2013).

How much does fuel availability control fuel utilization? If a substrate supply is limited, as is the case in for glucose under fasting conditions or fatty acids in ATGL- or HSL-null mice, then energy demand will be met with the alternative substrate.

Increasing fuel availability by direct infusion of lipid, glucose, or amino acids will lead to increased oxidation of those substrates (Coyle et al., 1997; Horowitz et al., 1997; Odland et al., 1998a; White and Brooks, 1981). But even at high availability there is substrate competition leading to shifts in fuel preference (Coyle et al., 1997; Horowitz et al., 1997) suggesting some further cellular or mitochondrial regulation of fuel selection.

Further evidence for cellular regulation of fuel selection is the fact that exercise training leads to greater fat oxidation during exercise, but does not lead to substantial increases in lipolysis (Klein et al., 1994). Horowitz (2003) explains that trained individuals have a better balance between fat availability and utilization than untrained, and in both, fat supply is not limiting. Fat supply is also not limiting at high exercise intensity, when carbohydrate oxidation increases and fat oxidation declines (Jeppesen and Kiens, 2012). Infusion of fatty acids was unable to prevent the decline in fat oxidation at higher exercise intensities (Romijn et al., 1995), again giving importance to a cellular/mitochondrial regulation of fuel selection.

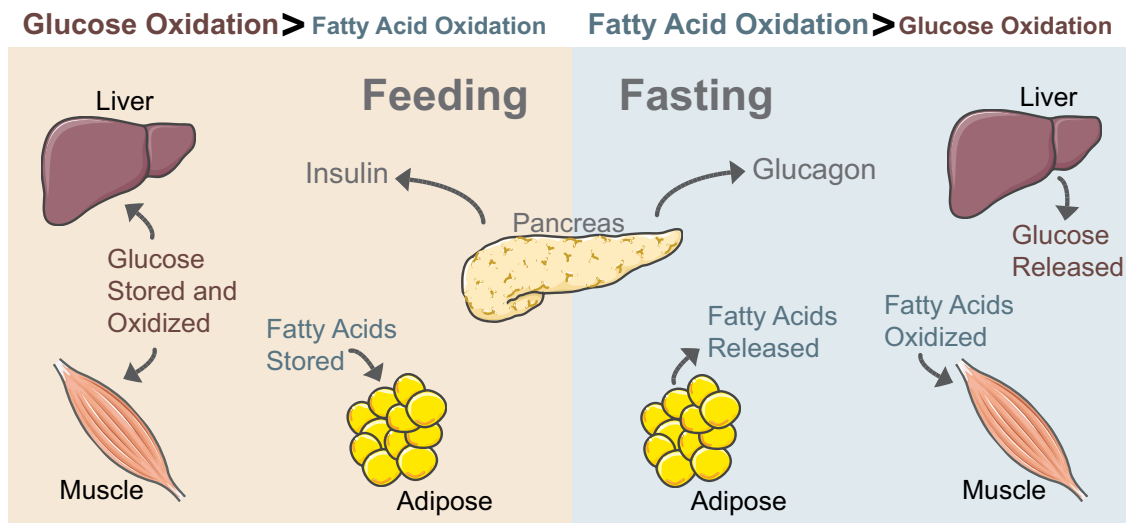


**Figure 2.1 Fuel shift with fasting and feeding.** With food, glucose and fat become plentiful, both are stored (although glucose is stored to a smaller degree) and primarily glucose is oxidized for energy production. During fasting, blood glucose is maintained by glucose production from the liver. Glucose is primarily reserved for oxidation in the brain, and lipids are released from the adipose tissue to supply fat as a fuel source for energy production in the peripheral tissues (muscle, liver, etc.). Hormones insulin and glucagon secreted from the pancreas augment changes in fuel availability.

### *2.2.2 Substrate entry into the cell*

Increasing fuel availability can increase fuel uptake, but this is through regulated transporters that facilitate fuel uptake. Because skeletal muscle is a primary consumer of these fuels (Turner et al., 2014), we will focus on regulation of glucose and fatty acid entry into the skeletal muscle.

Glucose enters skeletal muscle through glucose transporters GLUT1 and GLUT4. GLUT1 is found at low levels in skeletal muscle, whereas GLUT4 is acutely regulated by insulin and contractions (Richter and Hargreaves, 2013). GLUT4 is maintained in intracellular vesicles; upon insulin- or contraction-stimulation, GLUT4 translocates to the sarcolemma and t-tubules (Lauritzen et al., 2008; Lauritzen et al., 2010). Deletion of GLUT4 from skeletal muscle results in decreased stimulated glucose uptake (Zisman et al., 2000). Under non-stimulated conditions, glucose transport into cells is limiting and thus shifts fuel selection away from glucose oxidation; however, under fed or exercise conditions glucose transport is sufficient and glucose phosphorylation inside the cell is more rate-limiting for glucose utilization (Wasserman and Ayala, 2005).

Fatty acid entry into skeletal muscle is regulated by fatty acid transporter (FAT/CD36), fatty acid binding proteins (FABPpm and FABP4), and fatty acid transport protein 1 (FATP1) (Kiens, 2006; Nickerson et al., 2009). FAT/CD36, FABPpm and FABP4, but not FATP1, are more directly associated with increases in lipid oxidation (Jeppesen et al., 2012; Yoshida et al., 2013). Like GLUT4, FAT/CD36 is translocated to the sarcolemma under insulin and contraction stimulated conditions (Bonen et al., 2004). Overexpression of FAT/CD36 in skeletal muscle increases fat-oxidation during exercise (Ibrahimi et al., 1999; Yoshida et al., 2013). However, insulin-stimulated translocation (Luiken et al., 2002) and overexpression of FAT/CD36 in myocytes increased triglyceride synthesis and not fat oxidation (Garcia-Martinez et al., 2005). Though overexpression of fatty acid transports tends to lead to increased lipid uptake and oxidation (Nickerson et al., 2009), the possibility of increased triglyceride synthesis suggests other intracellular mechanisms help direct fatty acids towards oxidation or triglyceride synthesis.

These fatty acid transporters might also facilitate lipid entry into the mitochondria. FAT/CD36, FABPpm, and FATP1 have been found in mitochondria fractions (Guitart et al., 2014; Smith et al., 2011; Stump et al., 1993). FAT/CD36 appears to facilitate palmitate, but not palmitoyl-CoA transport into mitochondria (Smith et al., 2011). This distinction might suggest a role for this protein in supporting IMTG generated fatty acid entry into the mitochondria. FATP1 overexpression also leads to increased palmitate oxidation, but mitochondrial specificity of FATP1 action is less well understood (Guitart et al., 2014). Unlike FAT/CD36, FABPpm mitochondrial function is not related to fat oxidation. FABPpm has sequence homology with mitochondrial aspartate aminotransferase (gene name: GOT2) (Stump et al., 1993). This protein has two distinct functions depending on subcellular localization; the mitochondrial localized protein is specific to amino acid metabolism (Holloway et al., 2007).

Like increases in fuel availability, increases in substrate transport into the cell can support higher oxidation rates. However, other downstream enzymes, like hexokinase or mitochondrial fat oxidizing genes, might also regulate fuel selection and utilization, and these will be discussed next.

### 2.2.3 *Glycogenolysis and glycolysis*

As mentioned in the previous section, hexokinase (HK) activity can be rate-limiting for glucose utilization, especially during high intensity exercise (Wasserman and Ayala, 2005). HK is the first enzyme in glycolysis (**Figure 2.2**), a process that produces energy equivalents and pyruvate, which can enter the mitochondria and support oxidative phosphorylation. Inhibition or activation of key enzymes in glycolysis and glycogenolysis (glycogen breakdown) are important for modulating fuel selection. This concept of glycolysis inhibition underlies a well-cited explanation for fuel selection, the glucose fatty-acid cycle presented by Randle (1963). The glucose-fatty acid cycle explains fuel selection through fatty acid availability and subsequent biochemical inhibition of glucose oxidation: increased availability of fatty acids will yield increased fat oxidation, which in turn leads to metabolite changes that allosterically down-regulate glucose oxidation.

HK catalyzes the phosphorylation of glucose. Both HK isoforms I and II are present in skeletal muscle, but HK II is more prevalent and accounts for 80% of the activity (John et al., 2011). Overexpression of HK II leads to greater glucose uptake under insulin- and contraction- stimulated conditions (Wasserman and Ayala, 2005). HK II activity is negatively regulated by glucose 6-phosphate (Richter and Hargreaves, 2013), and additionally, HK activity is modulated by transient association with the outer mitochondrial membrane (John et al., 2011). Disassociation of HK II from the mitochondria increases glucose uptake in a manner that is less tightly coupled to mitochondrial ATP production (Mailloux et al., 2011; Neary and Pastorino, 2013). HK II dissociation from the mitochondria occurs under high glucose 6-phosphate, particularly glucose 6-phosphate generated from glycogen breakdown (John et al., 2011). This transient association of HK II with the mitochondria is speculated to facilitate channeling of substrate down specific metabolic pathways (John et al., 2011).

6-Phosphofructokinase (PFK) catalyzes the reaction of fructose 6-phosphate to fructose 1,6 bisphosphate and is inhibited by citrate (Randle, 1998). In the glucose-fatty acid cycle, increasing fatty acid oxidation was linked to elevations in NADH/NAD and Acetyl-CoA/CoA. The accumulation of acetyl-CoA would lead to increased production of citrate, which would inhibit PFK. Inhibition of PFK would lead to accumulation of upstream glucose 6-phosphate and inhibition of HK (Randle, 1998). The citrate-mediated inhibition of PFK in skeletal muscle is not well supported by *in vivo* results (Jeukendrup, 2002; Randle, 1998). However, PFK is also activated by AMP and inhibited by AMP-kinase (AMPK) activation and these mechanisms might also be important regulators of PFK (Hue and Taegtmeyer, 2009).

Though not incorporated in the glucose-fatty acid cycle, glycogen breakdown (glycogenolysis) is relevant to glucose uptake and fuel selection under fasting and exercise. Glucagon signaling (in liver), beta adrenergic signaling and muscle contraction can stimulate glycogenolysis (Jensen et al., 2011). Rapid glycogenolysis that occurs with increasing intensity exercise (Gollnick et al., 1974) will lead to elevations of glucose 6-phosphate and inhibition of hexokinase (Richter and Hargreaves, 2013). Additionally, rapid glycogen breakdown is associated with

decreased fat oxidation (Jeppesen and Kiens, 2012); while low glycogen content or the inability to break down glycogen is associated with increased fat utilization (Orngreen et al., 2009; Roepstorff et al., 2005). Glycogen phosphorylase (GP) regulates glycogenolysis, and GP activity is modulated by allosteric inhibitors and activators, phosphorylation, and acetylation (Jensen et al., 2011; Zhang et al., 2012). Allosteric activators of GP include AMP and IMP, and allosteric inhibitors are ATP, glucose 6-phosphate, and  $FAD^+$ . This allosteric regulation makes glycogen phosphorylase responsive to the energy state of the cell (Chebotareva et al., 2005; Jensen et al., 2011).

In summary, regulation of glycolysis and glycogenolysis are important for fuel selection and maintained energy supply during exercise. Inhibition of HK, PFK, or GP lead to impaired exercise capacity and greater fat oxidation (Fueger et al., 2003; Haller and Vissing, 2004; Wasserman and Ayala, 2005). In the next sections we will cover regulation of metabolite entry into the mitochondria and mitochondrial enzyme activity.

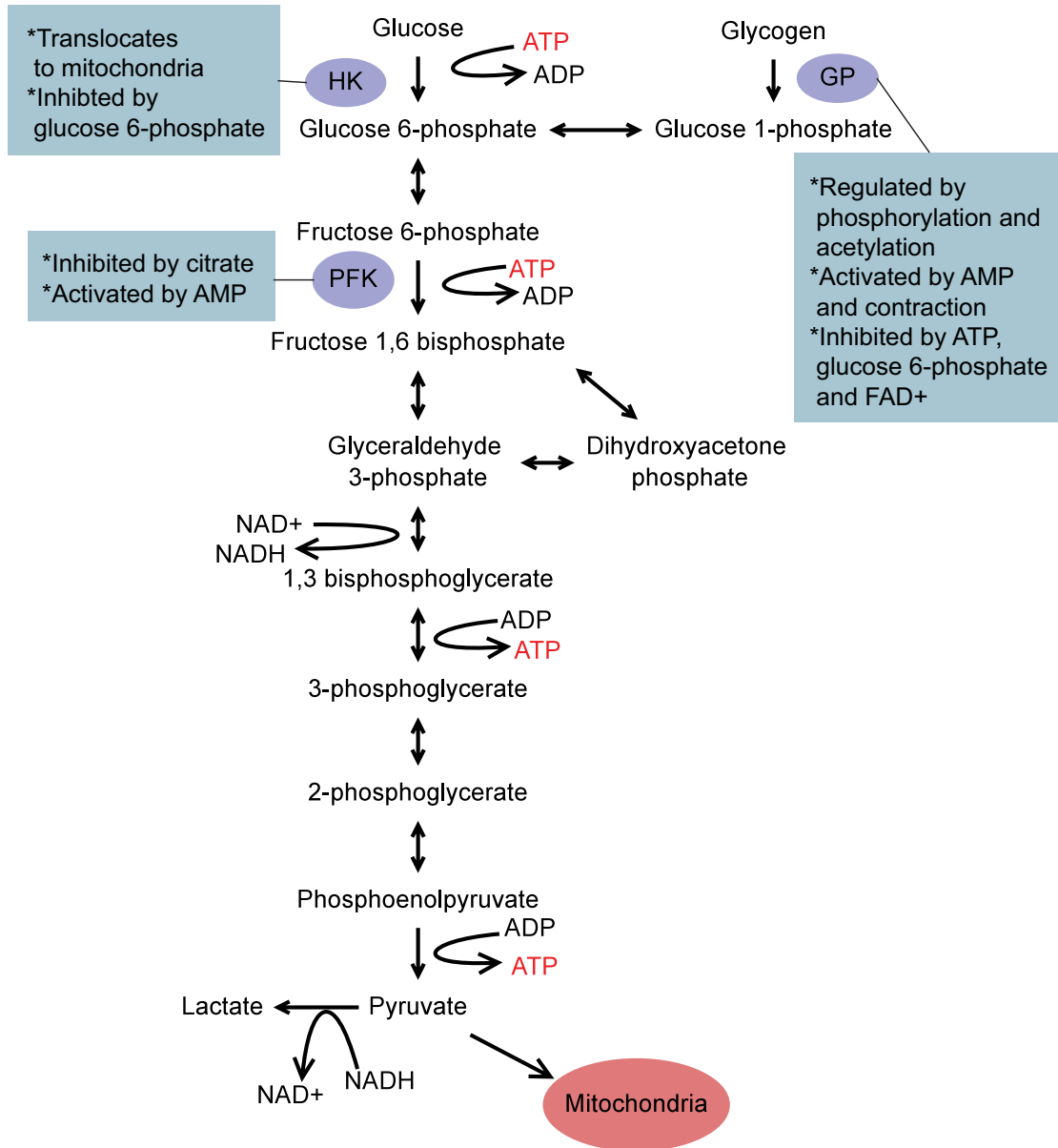


**Figure 2.2 Glycolysis and glycogenolysis.** Glucose and glycogen are broken down to pyruvate through several enzyme-catalyzed reactions, and produces a net 2 ATP and 2 NADH and 2 pyruvate molecules. Important regulated enzymes are highlighted in blue: hexokinase (HK), phosphofructokinase (PFK), and glycogen phosphorylase (GP).

#### 2.2.4 Substrate entry into the mitochondria

Entry of fatty acids into mitochondria is yet another site of fuel regulation. Long-chain fatty acids or fatty-acyl CoAs enter the mitochondria via specific transporters. We have already discussed the potential role of CD36 in mediating fatty acid (palmitate) entry into the mitochondria and now will focus on long-chain fatty acyl-

transporters carnitine palmitoyltransferase I and II (CPTI/CPTII). CPTI is located on the outer mitochondrial membrane, while CPTII is located on the inner mitochondrial membrane. CPTI reacts with long-chain acyl-CoA in the cytosol and replaces the CoA moiety with carnitine, forming an acyl-carnitine and allowing the acyl group to pass through the mitochondrial membrane (Ramsay and Zammit, 2004). CPTII converts the fatty-acyl carnitine back to fatty-acyl CoA, which can then undergo beta-oxidation in the mitochondria.

CPTI activity is inhibited by malonyl-CoA (Ramsay and Zammit, 2004), and CPTI activity can be further reduced under conditions of lower pH (Starritt et al., 2000). The inhibition of CPTI by malonyl-CoA provides a mechanism by which cells can modulate between fatty acid oxidation and fatty acid synthesis. Malonyl-CoA is generated from acetyl-CoA by the enzyme Acetyl-CoA carboxylase (ACC), and malonyl-CoA can serve as a precursor for fatty acid elongation (Kerner et al., 2014). Consistently, inhibition of CPTI, with chemical inhibitor etomoxir, leads to decreased fat oxidation and increased glucose oxidation and fatty acid synthesis (Schrauwen et al., 2013). However, muscle malonyl-CoA concentrations *in vivo* are fairly constant in humans under different exercise intensities despite changes in fuel selection (Odland et al., 1998b), suggesting that malonyl-CoA availability is not modulating exercise-induced changes in fuel selection.

CPTI catalyzes the addition of a carnitine moiety onto fatty acyl-groups. Reduced carnitine levels with increasing intensity exercise is associated with lower fatty acid oxidation (van Loon et al., 2001), and is suggestive that carnitine availability is limiting for fatty acid oxidation (Jeppesen and Kiens, 2012). Supplementation with L-carnitine can improve metabolic flexibility (Noland et al., 2009; Power et al., 2007), but there is only indirect evidence that L-carnitine supplementation improves fat oxidation during exercise (Wall et al., 2011). Furthermore, even at reduced levels, carnitine concentrations are well above the  $K_m$  for CPTI (0.2 - 0.5 mM) and thus changes in free-carnitine with exercise should have minimal effect on CPTI activity (Sahlin et al., 2008).

### 2.2.5 Mitochondrial enzyme activity



Mitochondrial enzyme activity is the final regulatory step in fuel selection. Glucose-derived carbons, fatty acids, and amino acids all enter the mitochondria and broken down to produce NADH and FADH<sub>2</sub>. Which are then passed to the electron transport chain for oxidative phosphorylation.

Glucose oxidation can be tightly controlled through mitochondrial pyruvate dehydrogenase complex (PDHc) and this control is one of the main mechanisms of the glucose-fatty acid cycle (Randle, 1998). Pyruvate generated from glycolysis is converted to acetyl-CoA by PDHc. PDHc is inactive when phosphorylated and allosterically inhibited by acetyl-CoA and NADH (Hue and Taegtmeyer, 2009). Increased fatty acid derived acetyl-CoA and NADH will inhibit PDHc and thus limit glucose derived carbons from entering the citric acid cycle through acetyl-CoA. PDHc activity increases with increasing intensity exercise (Constantin-Teodosiu et al., 1991; Howlett et al., 1998), and is modulated primarily by changes in phosphorylation status.

Fatty oxidation in the mitochondria occurs first through beta-oxidation to produce acetyl-CoA, which can enter the citric acid cycle. Beta-oxidation is catalyzed by acyl-CoA dehydrogenase and the trifunctional protein. The acyl-CoA dehydrogenase reaction produces one FADH<sub>2</sub>, and the trifunctional protein produces one NADH and acetyl-CoA. Together, these molecules shorten the fatty acid chain by 2 carbons with each cycle. The activity of beta-hydroxyacyl-CoA dehydrogenase, a component of the trifunctional protein, is positively correlated with fat oxidation during exercise (Kiens, 2006). Additionally training increases in fatty acid oxidation are associated with the upregulation of mitochondrial components of fatty acid oxidation (Holloszy and Coyle, 1984).

### **2.3 Model for high and low exercise capacity**

In the last section we discussed the importance of fuel preference and mechanisms that might regulate fuel preference at rest and during exercise. In this section we will discuss the advantages of a genetically complex animal model that has been artificially selected for high and low running capacity (HCR and LCR). This

animal model provides the advantage of controlled diet and environment while capturing some of the important phenotypes observed in humans.

### *2.3.1 Beginnings of the HCR-LCR model*

In the late-1990's, Steve Britton and Lauren Koch began developing an animal model that could be used to model complex disease. They began with the understanding that no single genetic mutation could mimic the effect of diseases like type II diabetes, heart disease, or high blood pressure, which are known to be multi-factorial in origin. Instead, they began with the premise that a model that had genetic complexity, as well as healthy and non-healthy spectrums, would be more appropriate for the study of complex disease. Using a similar principle as used in the Dahl-salt model for high- and low- salt tolerance (Rapp, 1982), Britton and Koch latched on to the idea of selective breeding for healthy and unhealthy rats.

Although there are a variety of phenotypes considered to be healthy and unhealthy, a large-scale study concluded that cardiovascular fitness ( $VO_2\text{max}$ ) was more strongly predictive of morbidity and mortality than measurements like abnormal electrocardiogram, chronic illness, high cholesterol or high blood pressure (Blair et al., 1996). Because  $VO_2\text{max}$  is closely associated with maximum work performed during an increasing intensity protocol, cardiovascular fitness can be approximated by maximal running distance during an increasing intensity exercise test. Thus, Britton and Koch began to test the hypothesis that rats bred for high and low running capacity would diverge in traits for health and longevity (Koch and Britton, 2001).

The initial test for inheritance of exercise capacity was performed using an outbred strain of Sprague-Dawley rats, consisting of 18 male and 24 females as breeding pairs (Koch et al., 1998). Rats were introduced to the treadmill once a day for 5 days. The first two days on introduction, rats were placed on a moving treadmill (less than 10 m/min on at 15° incline) and assisted by hand if they did not keep on the treadmill. On the third through fifth days of introduction, the rats were allowed to fall onto a shock grid (1.2 mA of current at 3 Hz) if they did not keep up with the treadmill speed. The speed and time on the treadmill was minimal to reduce any

exercise training effect, but only animals that met the minimum 5 min at 10 m/min were subsequently tested for exercise capacity.

After being introduced to the treadmill, rats were tested for exercise capacity once a day for 5 days. Rats were run at a constant 15° incline at 10 m/min with speed increasing 1 m/min every 2 min. Rats were run until they exhausted. Exhaustion was defined as the third time a rat could no longer sustain treadmill running and would rather sustain 2s of shock than continue on the treadmill. At exhaustion, animals were removed from the treadmill. The best performance (in distance) over the 5-day testing period was used as the measure of maximal running capacity.

For the selective breeding, the best runners were bred together and the worst runners were bred together. In the initial test of inheritance with the Sprague-Dawley outbred strain, running capacity of the high-selected line was 70% greater than the low-selected line after 3 generations of selection (Koch et al., 1998). The segregation of running capacity with selective breeding suggested that running capacity is a heritable trait. Thus, Lauren Koch and Steven Britton decided to initiate a larger-scale selective breeding program for high and low running capacity (Koch and Britton, 2005).

For the larger-scale selection, Koch and Britton chose to begin with a heterogeneous founder population, N:NIH rats (Koch and Britton, 2001). The N:NIH outbred population began from intercrossing 8 inbred rat strains: Maudsely reactor, Wistar, Wistar Kyoto, Marshall 520, Fischer, A x C 9935 Irish, Brown Norway, and Buffalo (Hansen and Spuhler, 1984), and this population was maintained with 60 outcross families. Koch and Britton began with 96 male and 96 female non-sibling N:NIH rats for the initial selection based on high and low exercise capacity (Koch and Britton, 2001). Rats were introduced to the treadmill and tested in a similar manner as described above. Based on maximal running capacity, the top-performing 13 males and females were bred together to initiate the high capacity running (HCR) line, and the bottom-performing 13 males and females were bred together to initiate the low capacity running (LCR) line. These initial breeding pairs were the first of a rotational within-family selective breeding scheme. In this breeding scheme each of

the 13 families contributes one male and one female to the next generation and are rotationally bred with another pre-arranged family. By using a rotational breeding scheme, the rate of inbreeding per generation is estimated to be less than 1% (Koch and Britton, 2005). By 10 generations of selective breeding for high and low running capacity, the HCR and LCR diverged in running capacity by 3.1-fold (females) and 3.2-fold (males) (Koch and Britton, 2005).

### 2.3.2 Fuel selection in HCR and LCR

The rat model for high and low running capacity (HCR-LCR) has been selectively bred now for over 35 generations. Running capacity was found to be a heritable trait that has continued to diverge in this rat model since the initial heterogeneous found population (N:NIH stock) (Ren et al., 2013). Numerous studies have explored the physiological differences that occur with divergence of running capacity (Koch and Britton, 2005, 2008). Importantly, the divergence in exercise capacity was associated with the divergence in lean mass, body weight, metabolic disease risk, and lifespan (Koch et al., 2011; Naples et al., 2010; Noland et al., 2007; Novak et al., 2010; Wisloff et al., 2005).

Accumulated evidence from this rat model suggests high capacity running rats (HCR) have higher fat oxidation than the low capacity running rats (LCR). Gene expression pathway analysis shows that HCR have increased gene expression within lipid metabolism, oxidative phosphorylation, citric acid cycle, and BCAA metabolism pathways (Kivela et al., 2010). Consistent with changes in mRNA, Lessard, et al (2011) showed increased protein expression of CD36 in skeletal muscle.

*In vitro* studies using isolated skeletal muscle demonstrate that HCR muscle has greater fat oxidation capacity than LCR (Lessard et al., 2011). Increased fat oxidation in HCR vs. LCR was also demonstrated in perfused skeletal muscle (Rivas et al., 2011) and isolated mitochondria (Thyfault et al., 2009), but not in perfused hearts (Schwarzer et al., 2010). The relationship between higher oxidative capacity and fuel selection in the isolated tissue models is promising. However, better

characterization of *in vivo* fuel selection, and specifically exercise-induced changes in fuel selection are needed.

## **2.4 Summary**

- Fuel selection, or the primary fuel used for energy, changes with food intake and exercise.
- Increased fat oxidation is associated with greater exercise capacity, better metabolic health, and longevity.
- A number of enzymes and transports help regulate fuel selection by controlling fuel availability, uptake into the cells, and metabolism.
- The HCR/LCR animal model was developed to better understand the genetic link between metabolic health and high exercise capacity, and this model is valuable for understanding the underlying physiology of exercise capacity and fuel use.

## **Chapter 3**

### **Metabolomics to define fuel use during exercise**

In the previous chapter, we discussed the potential mechanisms of fuel selection. For the study discussed in this chapter, we used a metabolomics platform to understand exercise fuel use in the HCR-LCR model. This study demonstrates that HCR have higher fat oxidation during exercise and the data allow for speculation on why and how fat might be preferentially utilized. This chapter sets the groundwork for the experiments described in Chapters 4 and 5.

#### **3.1 Introduction**

Exercise capacity and cardiovascular fitness predict health and mortality (Blair et al., 1996; Church et al., 2004; Kodama et al., 2009), and yet the mechanisms supporting these associations are not fully understood. Fuel selection is a critical component to both exercise capacity and overall metabolic health. Higher exercise capacity associates with increased fat oxidation during exercise (Hall et al., 2010; Morris et al., 2013; Nordby et al., 2006; Venables et al., 2005), and poor metabolic health associates with impaired fuel switching (Kelley and Mandarino, 2000). The glucose-fatty acid cycle described by Randle et al. (1963) states that fat availability will drive fat oxidation and reciprocally lead to decreased glucose oxidation; however this theory cannot explain instances when fat availability is high, but carbohydrate is preferentially used, as is the case during high-intensity exercise and diabetes (Kelley and Mandarino, 2000; Mittendorfer and Klein, 2001; Sidossis et al., 1997). We

employ a metabolomics approach to examine the physiology underlying fuel preference during exercise.

Metabolomics is a growing field of study that employs liquid chromatography or gas chromatography coupled to mass spectrometry (LC-MS or GC-MS) or nuclear magnetic resonance spectroscopy (NMR) to quantitate tens to thousands of metabolites in a single sample. This approach allows for a system wide snapshot of a metabolic state. Previous metabolomics approaches have used to study exercise have focused on changes in serum (Pohjanen et al., 2007), plasma (Lehmann et al., 2010; Lewis et al., 2010), and urine (Enea et al., 2010). Additionally, all but one of these earlier studies (Enea et al., 2010) have focused on trained individuals or individuals with high VO<sub>2</sub>max. Metabolomics approaches comparing both high and low exercise capacity mice (Wone et al., 2011) and humans (Lustgarten et al., 2013; Morris et al., 2013) have focused on the phenotype at rest rather than the response to exercise.

The current study uses a metabolomics approach to understand exercise-induced changes in fuel use in rats with high and low intrinsic running capacity (HCR and LCR). We focus not only on changes in plasma, but also changes in muscle, as muscle is the main site of fuel utilization during exercise (Egan and Zierath, 2013). By understanding the metabolic effects that differ between HCR and LCR during exercise, we gain insight into possible mechanisms of exercise capacity and fuel selection. Additionally by studying both lines at exhaustion, we can find metabolic profiles that associate with fatigue regardless of running capacity. We find that HCR preferentially use fatty acids for fuel, and exhaustion is associated with accumulation of metabolic intermediates, short- and medium-chain acyl-carnitines.

## **3.2 Methods**

### *3.2.1 Animal protocol and study design*

HCR and LCR male rats (generation 26, age 4.5 months) were housed at the University of Michigan, and the University Committee on Use and Care of Animals,

Ann Arbor Michigan approved the study. All procedures were in compliance with University guidelines and state and federal regulations.

Exercise capacity was determined on a motorized treadmill (Columbus Instruments, Columbus, OH) with an increasing-intensity protocol, starting at 10 m/min and increasing 1 m/min every 2 min, with a constant 15° incline.

The study design is presented in **Figure 3.1**. We first conducted whole-body indirect calorimetry during the increasing-intensity exercise protocol. These same rats were then divided into groups (n=5-6) and were run for 0, 10 min, 45 min (HCR only), or to exhaustion followed by a 30 min recovery (Rec). At these time points, we immediately euthanized by decapitation and collected trunk blood and tissue. Trunk blood was used for preparing plasma and for immediate quantitation of blood glucose and lactate (Accu-Check Aviva meter and Nova Biomedical Lactate Plus meter). Tissues were immediately frozen in liquid nitrogen and stored at -80°C. For subsequent assays, frozen tissues were pulverized in liquid-nitrogen with a pre-chilled bio-pulverizer or mortar and pestle.

### Metabolomics study design

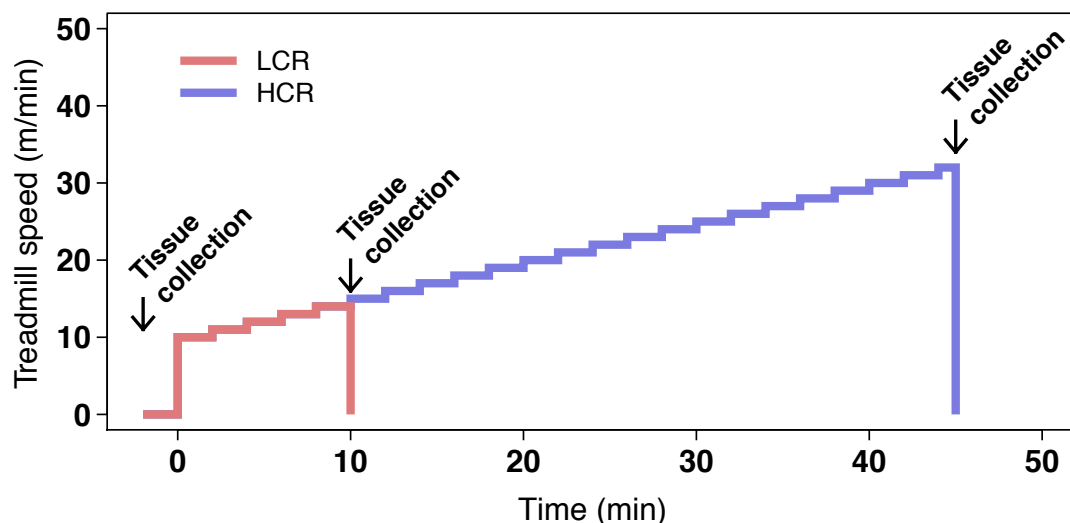


**Figure 3.1 Study design.** HCR and LCR were run on the treadmill for 0 min, 10 min, or 45 min (HCR only). At these time points, animals were euthanized and plasma and tissues were collected. During the protocol, the treadmill speed begins at 10 m/min and increases 1 m/min every 2 min.



### 3.2.2 Indirect calorimetry

Animals were run to exhaustion in sealed treadmill chambers.  $VO_2$  and  $VCO_2$  were sampled every 2 min for 5 s and were recorded using a Comprehensive Laboratory Animal Monitoring System (CLAMS, Columbus Instruments). Measurements were scaled to body mass and lean body mass, which was determined using an NMR-based analyzer (Minispec LF90II, Bruker Optics, Billerica, MA).

Non-protein RQ was used to estimate whole body carbohydrate and fat oxidation (Peronnet and Massicotte, 1991), and we adjusted estimates of carbohydrate oxidation to account for increased glycogen utilization as intensity increases (Jeukendrup and Wallis, 2005), see Equations 1-4.

Equation 1. Estimates for whole body fat oxidation.

$$\text{Fat oxidation (g/kg/min)} = 1.695 \times VO_2 - 1.701 \times VCO_2$$

Equation 2. Estimates for whole body carbohydrate oxidation at 0-40%  $VO_{2\text{max}}$ .

$$\text{Carbohydrate oxidation (g/kg/min)} = 4.585 \times VCO_2 - 3.226 \times VO_2$$

Equation 3. Estimates for whole body carbohydrate oxidation at 40-50%  $VO_{2\text{max}}$ .

$$\text{Carbohydrate oxidation (g/kg/min)} = 4.585 \times VCO_2 - 3.061 \times VO_2$$

Equation 4. Estimates for whole body carbohydrate oxidation at 50-100%  $VO_{2\text{max}}$ .

$$\text{Carbohydrate oxidation (g/kg/min)} = 4.585 \times VCO_2 - 2.962 \times VO_2$$

### 3.2.3 Muscle glycogen

Frozen gastrocnemius muscle (~50 mg) was digested in 30% KOH for 15 min at 37°C. Ethanol and  $NaSO_4$  (64% and 0.32%, final) were added to samples and allowed to incubate overnight at -20°C to precipitate glycogen. Glycogen pellets were washed twice with 10% KOH and 66% ethanol. Glycogen was dissolved with 4 N  $H_2SO_4$  at 100°C for 2 hr. Samples were neutralized with 4 N NaOH and the

resulting glucose concentration was determined with glucose (HK) assay kit from Sigma (St. Louis, MO). Glucose concentrations were normalized to starting tissue mass.

#### *3.2.4 Western blot for AMPK*

Pulverized frozen gastrocnemius muscle was extracted in buffer containing 1% Triton X-100, 20 mM HEPES, 20 mM beta-glycerophosphate, 150 mM NaCl, 10 mM NaF, 10 mM Na-Pyrophosphate, 1 mM EDTA, 1 mM Na-Orthovanadate, Roche protease inhibitor cocktail (Indianapolis, IN). After 20s sonication, samples were centrifuged at 8,000g for 10 min. Protein concentration was determined with Pierce BCA kit (Rockford, IL) and was used to normalize sample concentrations prior to loading. Sample extracts were separated by SDS-PAGE (Criterion, BioRad) and transferred to nitrocellulose membranes. After blocking with 5% non-fat dry milk in TBST, membranes were incubated overnight at 4°C with the following primary antibodies (1:1000): phospho-AMPK (Cell Signaling, #2531) and AMPK (Cell Signaling, #2532). Membranes were washed and incubated for 1 hr at 20°C with appropriate secondary antibodies conjugated to horseradish peroxidase (1:2000). After final washes, target proteins were detected with Pierce ECL solution (Rockford, IL). Band intensities were quantified using NIH ImageJ software (Schneider et al., 2012).

#### *3.2.5 Confirmation data set*

For confirming metabolite values that are coincident with exhaustion, we exercised male HCR and LCR (Generation 31 at 4.5 months of age) to quarter exhaustion (HCR only, ~15 min), half exhaustion (~6 min for LCR, ~30 min for HCR), and full exhaustion. At specified time points, animals were anesthetized with continuous inhalation of isoflurane. Tissues were collected under anesthesia and frozen immediately in liquid nitrogen; removal of heart ensured euthanasia. Tissues were stored at -80°C.

#### *3.2.6 Statistical analysis and graphing*

The R statistical and graphing environment was used for statistical analysis and generating figures (R Core Team, 2013). Data in tables and figures are presented as mean  $\pm$  standard error of the mean (SEM). Comparisons were made between HCR and LCR at 0 min, 10 min and Rec and within HCR and LCR between 0 min and other time points. Permutation t-tests, implemented in R using the *perm* package, were used for determining p-values (Fay, 2010). Permutation t-tests minimize Type I statistical errors (false positives) and are an alternative to False Discovery Rate (FDR) correction (Camargo et al., 2008). We use a significance cut-off of  $p=0.05$ .

Heatmaps were plotted using the *gplots* package "heatmap.2" function (Gregory R. Warnes, 2013).

### 3.2.7 Muscle and plasma metabolites

Total plasma non-esterified fatty acid (NEFA) was measured using Wako kit for NEFA (Richmond, VA). For specific carbon species analysis lipids were extracted from plasma using method described by Bligh and Dyer (Bligh and Dyer, 1959). Methyl esters were purified by thin layer chromatography and analyzed by gas chromatography.

For measuring glycolytic and citric acid cycle intermediates, weighed, pulverized gastrocnemius muscle samples were extracted with a solvent mixture of 8:1:1 of HPLC grade methanol:chloroform:water, with a ratio 1 mL solvent per ~30 mg of wet tissue mass. Samples were sonicated using a probe sonicator (Branson 450, 40% duty cycle, output power 4) for 20 sec and then centrifuged (16,000 x g) to pellet proteins and cell debris. Supernatant were analyzed by hydrophilic interaction chromatography - electrospray - time-of-flight mass spectroscopy (HILIC-ESI-TOF-MS) on Agilent 6220 (Santa Clara, CA) as described previously (Lorenz et al., 2011).

For acylcarnitine analysis, weighed, pulverized gastrocnemius muscle or plasma aliquots were extracted with a mixture of 8:2 of HPLC grade acetonitrile:water. Samples were probe sonicated for 20 sec (muscle only) and centrifuged (16,000 x g). Supernatant were dried by vacuum centrifugation at 45°C before being reconstituted in 9:1 mixture of mobile phases A/B used for the acylcarnitine analysis. The samples were analyzed using reversed phase liquid chromatography (RPLC)

coupled to an Agilent 6410 tandem quadrupole mass spectrometer. The column used was a Water Xbridge C18 2.5  $\mu$ , 2.1 x 50 mm (Milford, MA); mobile phase A was 5 mM ammonium acetate in water adjusted to pH 9.9 with ammonium hydroxide and mobile phase B was acetonitrile. Elution was performed at a flow rate of 0.25 mL/min, and the gradient consisted of a 7 min linear ramp from 0 to 80% B, a 3 min was at 100% B and a 6-min re-equilibration period at 0% B. Detection was performed using multiple reaction monitoring (MRM) in positive ion mode, using precursor/product ion transitions specified elsewhere (Ghoshal et al., 2005). Mass spectrometer parameters were set to 4000 V capillary voltage, 325°C gas temperature, 10 L/min gas flow, and 40 psi nebulizer pressure.

For amino acid analysis, weighed, pulverized gastrocnemius or plasma aliquots were extracted in 8:1:1 of HPLC grade methanol:chloroform:water. Muscle extracts were probe sonicated for 20 sec. Samples were centrifuged (16,000 x *g*) and supernatant were dried by vacuum centrifugation at 45°C. The dried samples were then derivatized and analyzed using Phenomenex's EZ-faast kit (Torrance, CA) and analyzed using Agilent 6890 GC with a 5973 mass selective detector (Badawy et al., 2007).

For branched-chain keto-acid analysis, plasma aliquots were extracted with 8:1:1 of HPLC grade methanol:chloroform:water and centrifuged (16,000 x *g*). Supernatant were dried by vacuum centrifugation at 45°C and reconstituted with water. Resulting samples were analyzed by reversed phase liquid chromatography coupled to ESI-TOF-MS in negative ion mode using a Waters Acquity HSS T3 1.8  $\mu$  column, with chromatographic conditions as described previously (Evans et al., 2013).

Peak areas were determined using Agilent Masshunter Quantitative Analysis software. Authentic standards were used to determine accurate mass and retention times. The data is reported as relative peak area, or in some cases, is reported as concentration as determined using stable isotope internal standards. For muscle metabolites, peak areas or exact concentrations were normalized to starting tissue mass.

### **3.3 Results**

### 3.3.1 HCR have greater whole-body fat oxidation

As in previous studies with HCR and LCR (Koch and Britton, 2001), HCR have lower body weight and higher exercise capacity (**Table 3.1**). On average, LCR ran for  $10.51 \pm 0.79$  min while HCR ran  $45.11 \pm 1.13$  min,  $p < 0.0001$ .

Oxygen consumption ( $V_{O_2}$ ) and carbon dioxide production ( $V_{CO_2}$ ) during exercise were used to estimate whole-body carbohydrate and fat oxidation (**Figure 3.2**). Amino acids can also contribute a small percentage of total fuel used during exercise (Wagenmakers et al., 1991); however, they are poorly accounted for using indirect calorimetry without accurate measurements of excreted nitrogen (urine and sweat). We will leave the discussion on amino acids for the later section 3.3.4 - Changes in amino acids with exercise.

Both HCR and LCR increase carbohydrate oxidation with onset of exercise, but at 4 min of exercise HCR and LCR begin to diverge in fuel use (**Figure 3.2A**). Carbohydrate oxidation continues to rise in LCR, but in HCR, carbohydrate use plateaus before gradually increasing again as HCR approach exhaustion. In reciprocal fashion, fat oxidation rapidly declines in LCR with onset of exercise but is maintained in HCR throughout the exercise protocol (**Figure 3.2B**). Fat oxidation begins to decrease as HCR approach exhaustion but does not drop below zero.

**Table 3.1 HCR weigh less and run further than LCR.** Data are mean  $\pm$  SEM. Asterisks indicate  $*p < 0.0001$ .

	<b>LCR (n=16)</b>	<b>HCR (n=23)</b>
Body weight (g)	$439.0 \pm 12.5$	$294.2 \pm 7.4^*$
Percent fat mass (%)	$15.6 \pm 0.6$	$3.9 \pm 0.4^*$
Percent lean mass (%)	$72.1 \pm 0.6$	$78.9 \pm 0.3^*$
Time to exhaustion (min)	$10.51 \pm 0.79$	$45.11 \pm 1.13^*$
Speedmax (m/min)	$14.63 \pm 0.40$	$31.83 \pm 0.55^*$
$VO_{2max}$ (mL/kg/min)	$26.5 \pm 0.8$	$39.4 \pm 0.5^*$
$VO_{2max}$ (mL/kg <sub>lean</sub> /min)	$36.8 \pm 1.0$	$50.0 \pm 0.6^*$

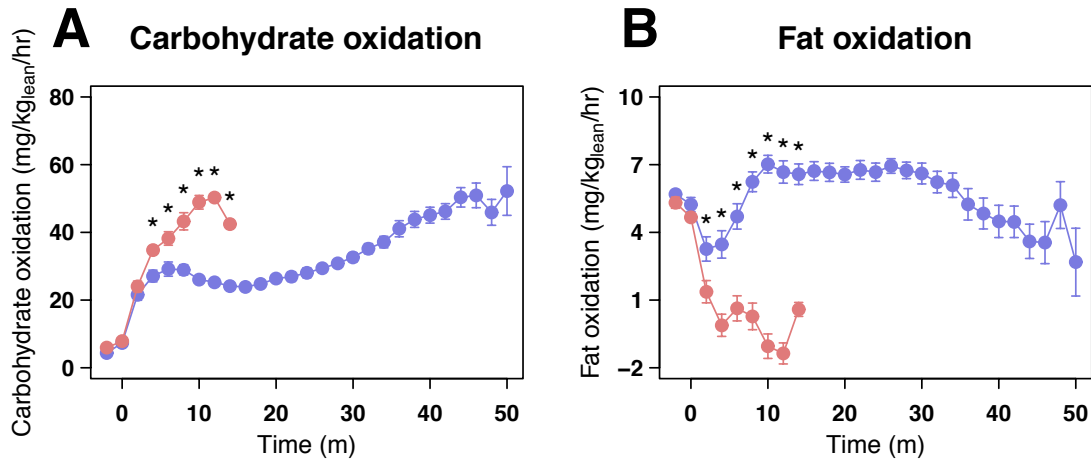


**Figure 3.2 HCR have higher fat oxidation throughout exercise.** With an increasing intensity exercise protocol, HCR run greater distance than LCR. (A) Carbohydrate oxidation and (B) fat oxidation are calculated from  $VO_2$  and  $VCO_2$  for HCR (blue) and LCR (red). Data are presented as mean  $\pm$  SEM for HCR (n=23) and LCR (n=16). Asterisks indicate \* $p < 0.05$  between HCR and LCR.

### 3.3.2 HCR spare muscle glycogen

During exercise the major inputs to glycolysis are blood glucose and muscle glycogen. As described in the study design, blood and tissues were collected at 0 min, 10 min and 45 min (**Figure 3.1**). At rest (0 min), LCR and HCR show no difference in blood glucose (**Figure 3.3A**) or muscle glycogen levels (**Figure 3.3B**). Blood glucose increases in both LCR and HCR at 10 min, while HCR have a reduction in blood glucose near exhaustion (45 min). Muscle glycogen is significantly depleted near exhaustion in both LCR (10 min) and HCR (45 min), but glycogen levels are not significantly changed in HCR from 0 to 10 min of exercise (**Figure 3.3B**). These findings are consistent with previous studies that have shown depletion of glycogen with exhaustion (Gollnick et al., 1974). These data suggest that muscle glycogen utilization, rather than glucose utilization, underlies the higher apparent carbohydrate oxidation in LCR during the first 10 min of exercise (**Figure 3.2A**).

Although HCR have significantly greater fat oxidation than LCR and maintain high fat oxidation throughout exercise, total circulating NEFA levels do not differ between HCR and LCR at any time point. Both HCR and LCR have decreased circulating NEFA at 10 min of exercise Figure 3.4.

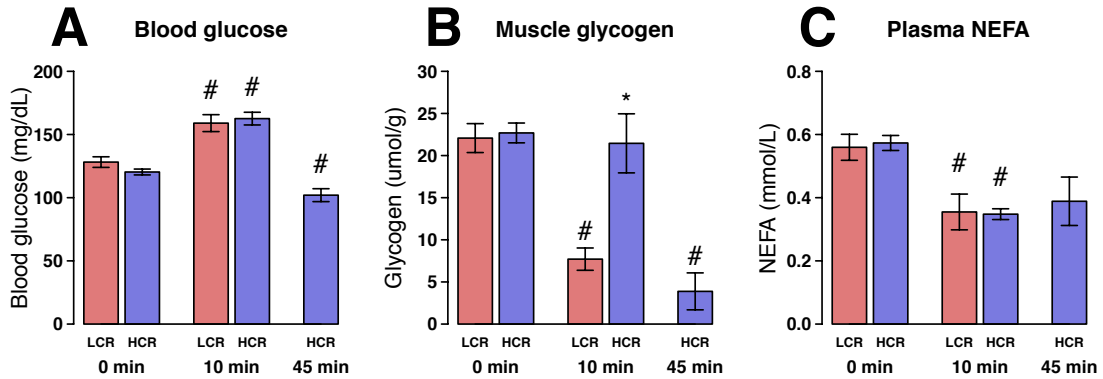


**Figure 3.3 HCR spare muscle glycogen.** Blood glucose (A), muscle glycogen (B), and plasma non-esterified fatty acids (NEFA) (C) were measured at 0 min, 10 min, and 45 min (HCR only). Values are mean  $\pm$  SEM for each group (n = 4-6). Asterisks indicate \* p<0.05 between HCR and LCR at a specific time point. Hashes indicate # p<0.05 difference from 0 min.

### 3.3.3 HCR maintain complete fat oxidation

To investigate metabolic changes related to fat oxidation, we measured total plasma fatty acids (predominately triglycerides), and muscle and plasma acyl-carnitines (**Figure 3.4A-C**). Circulating fatty acid species are similar between HCR and LCR at rest (**Figure 3.4A**). However, several muscle acylcarnitine species are lower in HCR than LCR at 0 min (**Figure 3.4B**), and several plasma acylcarnitine species are higher in HCR than LCR at 0 min, except for C5 acylcarnitine which is lower in HCR at 0 min (**Figure 3.4C**).

LCR, on the whole, show fewer changes in fatty acids and muscle acylcarnitines with exercise. Plasma 14:0 and 16:0 acylcarnitines are increased in LCR from rest to 10 min of exercise (**Figure 3.4B-C**). The increase in plasma acylcarnitines is indicative of incomplete fatty acid oxidation and parallels the decrease in fat oxidation observed with increasing intensity exercise. HCR have more dynamic changes in fatty acid species and acylcarnitines. HCR show decreases in individual circulating fatty acid species from rest to 10 min and 45 min of exercise (**Figure 3.4A**), but it should be noted that total sum of all fatty acid species do not differ between HCR and LCR at 10 min, consistent with total NEFA levels. In parallel to decreases in plasma fatty acid species, we observe that HCR have increased long-chain muscle acylcarnitines from rest to 10 min and 45 min (**Figure 3.4B**). But importantly, medium-chain acyl-carnitines are not increasing at 10 min in HCR,

which is an indication that fatty acid flux is uninhibited and efficient. The decreases in fatty acid species and increases in muscle acylcarnitines are consistent with greater flux of fatty-acyl groups into HCR mitochondria during exercise, but like LCR, plasma long-chain acylcarnitines increase in HCR near exhaustion (45 min), coincident with decline in fatty acid oxidation.



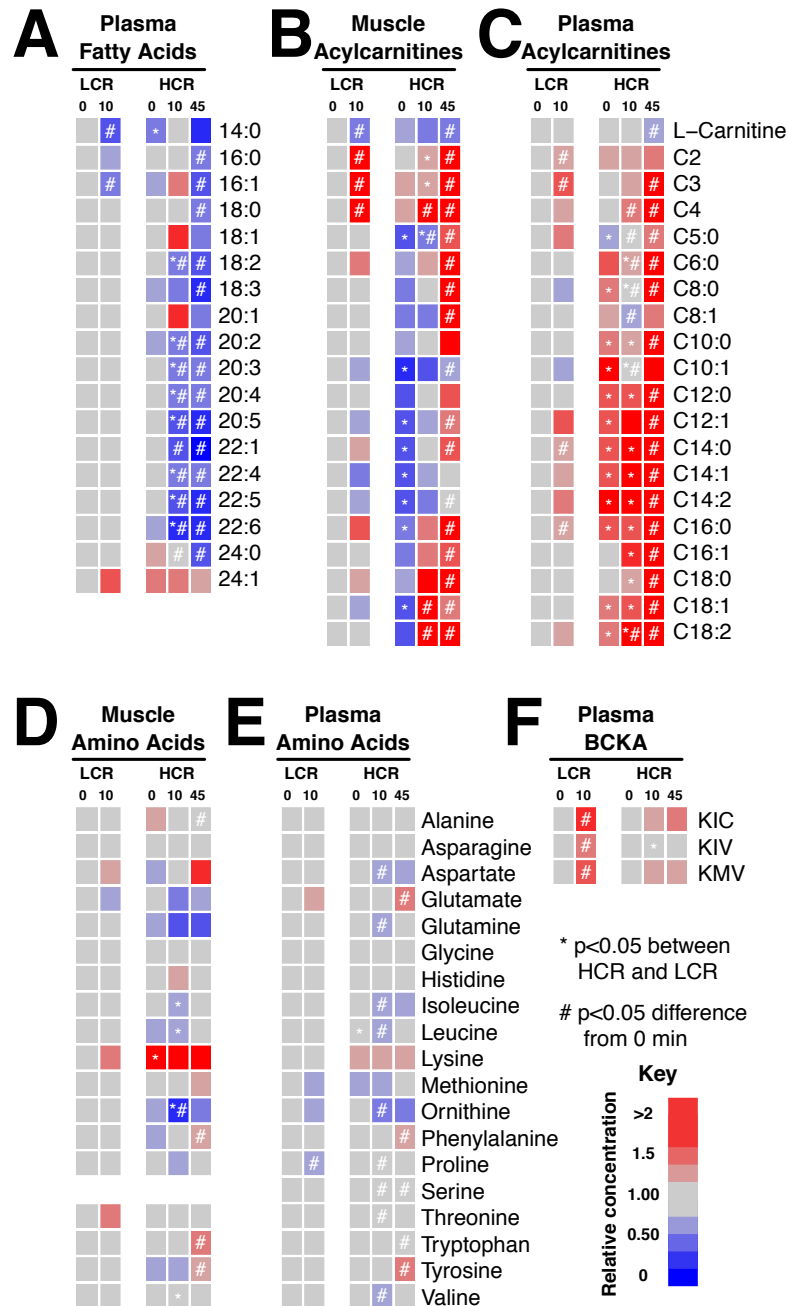


**Figure 3.4 HCR have greater changes in acylcarnitines with exercise.** The figure depicts concentrations of specific plasma fatty-acyl species (A), muscle acylcarnitine species (B), plasma acylcarnitine species (C), muscle amino acids (D), plasma amino acids (E) and plasma branched-chain keto acids,  $\alpha$ -ketoisocaproic acid (KIC),  $\alpha$ -ketoisovaleric acid (KIV), and  $\alpha$ -ketomethylvaleric acid (KMV) for each group (n=5-6). Values are presented in heat-color with red indicative of high and blue indicative low relative to LCR 0 min. Asterisks indicate \* p<0.05 between HCR and LCR at a specific time point. Hashes indicate # p<0.05 difference from baseline.

### 3.3.4 *Changes in amino acids with exercise*

Amino acids represent the third fuel source for energy production. At rest, HCR have higher muscle lysine and lower plasma leucine levels than LCR, but all other amino acids were similar between HCR and LCR (**Figure 3.4D-E**). With exercise, several amino acids decrease in HCR: muscle and plasma ornithine, plasma aspartic acid, glutamine, isoleucine, leucine, proline, threonine, and valine. Additionally, muscle branched-chain amino acids (BCAA) — leucine, isoleucine, and valine — are lower in HCR than LCR at 10 min (**Figure 3.4D**). By 45 min, several amino acids are elevated above resting levels in HCR: plasma glutamic acid, muscle and plasma phenylalanine, tyrosine, and tryptophan.

BCAA are the predominate amino acids used for fuel during exercise (Wagenmakers et al., 1991), and because these amino acids are lower in HCR than LCR at 10 min, we measured the downstream keto-acids. Leucine, isoleucine, and valine are deaminated (loss of NH<sub>3</sub>) to yield keto-isocaproic acid (KIC), keto-methylvaleric acid (KMV), and keto-isovaleric acid (KIV), respectively. These keto-acids increase in LCR with exercise and KIV levels are greater in LCR vs. HCR at 10 min (**Figure 3.4F**).

BCAA degradation can also produce the short-chain carnitines propionyl-carnitine (C3), isobutyryl-carnitine (C4), and isovaleryl-carnitine/methylbutyryl-carnitine (C5). These carnitines increase in muscle and plasma with exercise (**Figure 3.4B-C**).

### 3.3.5 *AMP kinase phosphorylation*

AMP kinase is a potential mediator of fuel selection and is driven by changes in AMP/ATP ratio (Hardie et al., 1999). HCR and LCR both have significant elevations in muscle AMP/ATP ratio near exhaustion (**Figure 3.5A**). Phosphorylation of AMPK parallels AMP/ATP and was increased in LCR at 10 min but not in HCR was not significantly different between HCR and LCR at 0 min, and LCR have increased AMPK phosphorylation at 10 min, whereas HCR have significantly increased AMPK phosphorylation at 45 min (**Figure 3.5B-C**). These data suggest that greater AMPK phosphorylation is not mediating increased fat oxidation in HCR during the first 10 min of exercise.

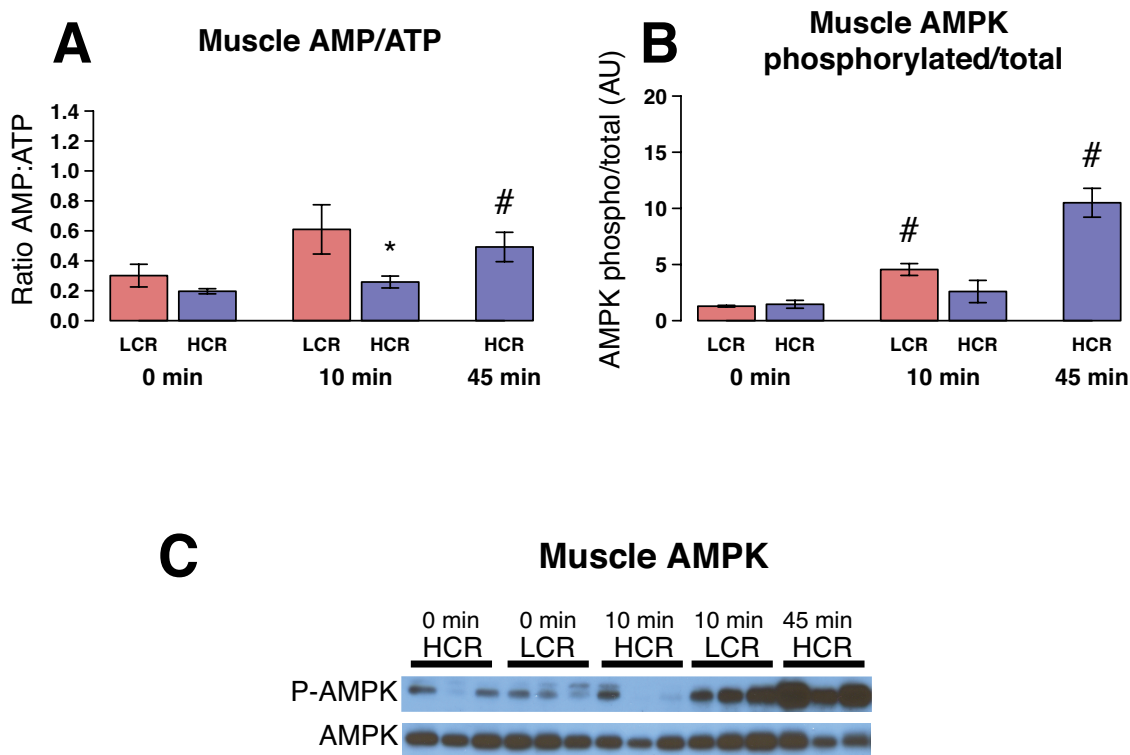


**Figure 3.5 Muscle AMPK is phosphorylated near exhaustion.** Muscle AMP:ATP (A) parallels changes in phosphorylation of AMPK (B). Representative blots for phosphorylated and total AMPK are shown in (C). Values are mean  $\pm$  SEM for each group (n = 4-6). Asterisks indicate \*  $p < 0.05$  between HCR and LCR at a specific time point. Hashes indicate #  $p < 0.05$  difference from 0 min.

### 3.3.6 Metabolite changes coincident with exhaustion

To probe for metabolite changes that are coincident with fuel selection and exhaustion, we determined correlation coefficients (Pearson  $r$ ) of metabolites with estimated fat oxidation, estimated carbohydrate oxidation and relative exhaustion (time at collection/previous time to exhaustion). We found 19 metabolites to be correlated with both fat and carbohydrate oxidation and coincident with exhaustion; most of these increased with longer exercise duration (**Table 3.2**).

To confirm changes with exhaustion, we compared these results with a second metabolomics data set in which HCR and LCR were run to quarter, half, and full exhaustion (Appendix B, **Table B.1**). Five metabolites were confirmed to change significantly with exhaustion: muscle glycogen, muscle acetylcarnitine (C2), muscle malate, muscle IMP, and plasma C5 carnitine (**Table 3.2**). Blood lactate was not

measured in the confirmation data set, but given the accumulated evidence from previous studies (Constantin-Teodosiu et al., 1991; Hill and Lupton, 1923), blood lactate is also a consistent marker of exhaustion on an increasing intensity protocol and correlated with fuel selection.

As previously highlighted, muscle glycogen levels decline with approach to exhaustion (**Figure 3.3B**) and this decline is coincident with increased carbohydrate use in both HCR and LCR. Muscle malate, a citric acid cycle intermediate, increases near exhaustion (**Figure 3.6A**). The other TCA cycle intermediates also tended to increase with exhaustion (**Table 3.2**), but only malate was found to be coincident with exhaustion in both data sets and strongly associated with fuel use. Muscle IMP (**Figure 3.6B**) is significantly lower in HCR at rest (0 min), but IMP values increase more than 5-fold in both HCR and LCR near exhaustion. The increase in IMP concentration with exhaustive exercise (Rush et al., 1995) occurs through deamination of AMP by myoadenylate deaminase (Tarnopolsky et al., 2001). Plasma C5 carnitine was also lower in HCR at 0 min (**Figure 3.6C**). Relative to the other metabolites that increased near exhaustion, changes in plasma C5-carnitine were smaller. C5-carnitine is an intermediate metabolite produced in the break down of isoleucine and/or leucine.

Muscle acetylcarnitine levels (**Figure 3.4B**) were positively correlated with carbohydrate oxidation and inversely correlated with fat oxidation (**Figure 3.6D-E**). A correlation between acetylcarnitine levels and fuel selection (RQ) has been reported previously (Kiens, 2006), but unlike previous reports (van Loon et al., 2001), we found no association between depletion of muscle L-carnitine and the decline in fat oxidation (**Figure 3.6F**), suggesting that in this model, carnitine availability is not limiting fat oxidation. Instead, acetylcarnitine accumulation is indicative of overproduction of acetyl units relative to downstream utilization through the citric acid cycle at exhaustion in both HCR and LCR. The buildup of citric acid cycle intermediate, malate, is consistent with this explanation. Finally, the similar pattern of change in metabolite levels relative to exhaustion in HCR and LCR suggests that the mechanism of exhaustion is similar in both strains, but is simply delayed in HCR.

**Table 3.2 Metabolites correlated with fuel use and exhaustion.** Table contains correlation coefficients (Pearson *r*) of metabolite values with fat oxidation, carbohydrate oxidation and percent exhaustion. An independent data set was used to confirm metabolites associated with exhaustion. In the independent data set, HCR and LCR were run to quarter (HCR only), half, and full exhaustion.

Metabolite	Correlation with Fatty Acid oxidation		Correlation with Carbohydrate oxidation		Correlation with Exhaustion		Independent Data Set: Correlation with Exhaustion	
	Pearson <i>r</i>	p-value	Pearson <i>r</i>	p-value	Pearson <i>r</i>	p-value	Pearson <i>r</i>	p-value
Muscle Glycogen *	0.49	<b>0.008</b>	-0.72	<b>&lt;0.001</b>	-0.82	<b>&lt;0.001</b>	-0.69	<b>&lt;0.001</b>
Muscle C2 Carnitine *	-0.51	<b>0.006</b>	0.80	<b>&lt;0.001</b>	0.81	<b>&lt;0.001</b>	0.65	<b>&lt;0.001</b>
Muscle Malate *	-0.61	<b>0.001</b>	0.82	<b>&lt;0.001</b>	0.87	<b>&lt;0.001</b>	0.58	<b>0.001</b>
Plasma C5:0 Carnitine *	-0.41	<b>0.030</b>	0.65	<b>&lt;0.001</b>	0.54	<b>0.002</b>	0.57	<b>0.001</b>
Muscle IMP *	-0.47	<b>0.011</b>	0.59	<b>0.001</b>	0.61	<b>&lt;0.001</b>	0.43	<b>0.019</b>
Muscle UDP-D-glucose	-0.47	<b>0.011</b>	0.76	<b>&lt;0.001</b>	0.85	<b>&lt;0.001</b>	-0.51	<b>0.005</b>
Muscle Dihydroxy-acetone-phospha	0.61	<b>0.001</b>	-0.43	<b>0.023</b>	-0.44	<b>0.012</b>	0.43	<b>0.019</b>
Muscle Succinate	-0.44	<b>0.018</b>	0.65	<b>&lt;0.001</b>	0.70	<b>&lt;0.001</b>	0.16	0.413
Muscle AMP	-0.62	<b>&lt;0.001</b>	0.63	<b>&lt;0.001</b>	0.55	<b>0.001</b>	0.14	0.475
Muscle GDP	-0.49	<b>0.008</b>	0.48	<b>0.010</b>	0.37	<b>0.039</b>	0.07	0.737
Muscle GMP	-0.60	<b>0.001</b>	0.57	<b>0.002</b>	0.43	<b>0.017</b>	0.02	0.912
Muscle Creatine	-0.39	<b>0.041</b>	0.50	<b>0.007</b>	0.60	<b>&lt;0.001</b>	0.01	0.969
Muscle Malonyl-CoA	0.44	<b>0.019</b>	-0.47	<b>0.012</b>	-0.52	<b>0.003</b>	0.00	0.980
Muscle ADP	-0.60	<b>0.001</b>	0.61	<b>0.001</b>	0.53	<b>0.002</b>	-0.15	0.442
Muscle IDP	-0.59	<b>0.001</b>	0.57	<b>0.001</b>	0.42	<b>0.018</b>	-0.20	0.294
Muscle Creatine-phosphate	0.62	<b>&lt;0.001</b>	-0.59	<b>0.001</b>	-0.63	<b>&lt;0.001</b>	-0.30	0.108
Blood Lactate	-0.51	<b>0.007</b>	0.70	<b>&lt;0.001</b>	0.78	<b>&lt;0.001</b>	n.d.	
Plasma 14:0 Fatty Acid	0.46	<b>0.016</b>	-0.39	<b>0.042</b>	-0.39	<b>0.035</b>	n.d.	

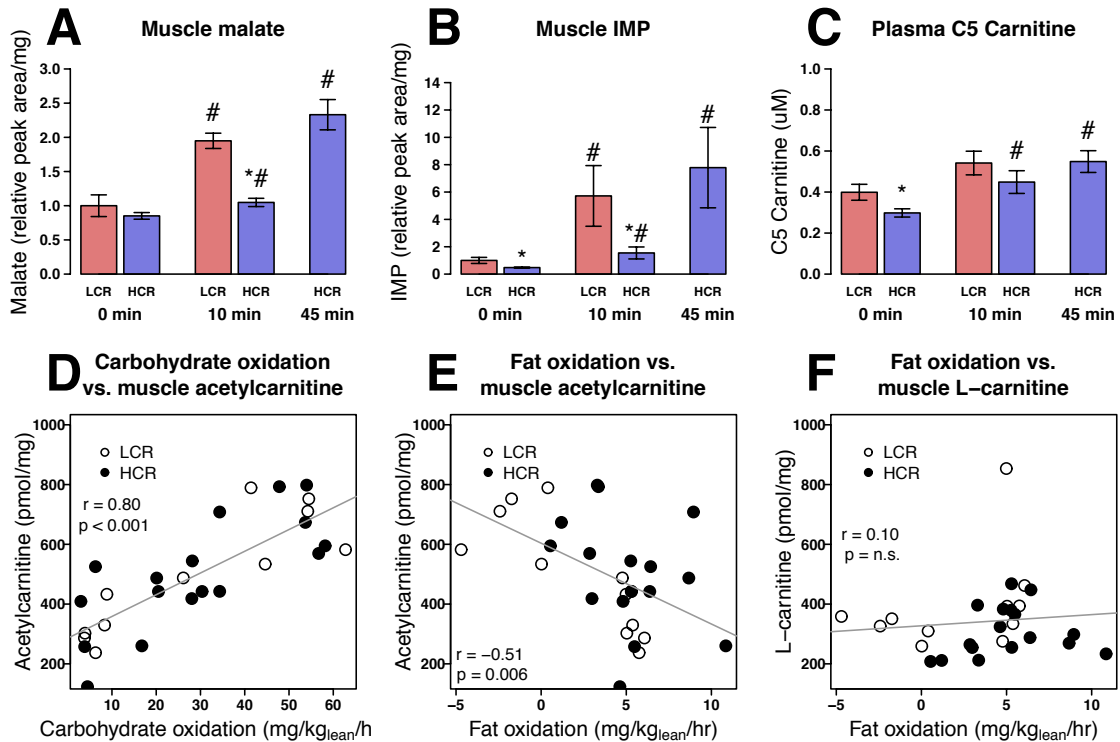


**Figure 3.6 Metabolites that increase with exhaustion.** Muscle malate (A), blood lactate (B) and muscle acetylcarntine (C) values are shown at 0, 10 and 45 min of exercise as mean  $\pm$  SEM for each group (n = 4-6). Muscle acetylcarntine (C2) is also strongly correlated with previous estimates of carbohydrate oxidation (D) and fat oxidation (E) at 0, 10, and 45 min of exercise. Muscle L-carnitine (F) was not correlated with fat oxidation. \*  $p < 0.05$  between HCR and LCR at a specific time point; #  $p < 0.05$  difference from baseline.

### 3.4 Discussion

In this study we use indirect calorimetry and metabolomics to define fuel use during an increasing-intensity exercise protocol. These data reveal that HCR have enhanced fat oxidation throughout exercise and delayed glycogen depletion vs. LCR. We found that metabolic intermediates, malate, acetylcarntine, and C5-carnitine, were associated with exhaustion and correlated with fuel selection.

Given these data and evidence from the literature, we propose that fat oxidation and delayed glycogen depletion support higher exercise capacity. Our data are consistent with other reports showing fat oxidation is higher in individuals with higher exercise capacity (Hall et al., 2010; Morris et al., 2013; Nordby et al., 2006; Venables et al., 2005), and that disruption of fatty acid oxidizing genes results in poor running

capacity (Fernandez et al., 2008; Huijsman et al., 2009). We can speculate what mechanisms might underlie the difference in fuel preference between HCR and LCR.

There is little to no evidence that circulating fuel availability is driving fuel use differences between HCR and LCR. Increased lipid availability during exercise can lead to increased fat oxidation (Romijn et al., 1995). However, in our study HCR and LCR have comparable levels of NEFA and glucose at rest and 10 min of exercise despite differences in fuel use. Even when comparing circulating lipid species, we do not find a difference between HCR and LCR at rest, with the exception of C14:0, which is lower in HCR. Decreases in lipids with exercise in HCR might be indicative of greater lipolysis of serum triglycerides, but the total sum of lipids was not different between HCR and LCR at 0 or 10 min of exercise. Although we did not measure intramuscular triglycerides, we measure specific fatty acids in muscle (stearic, oleic, and palmitic), only stearic acid was significantly different between HCR and LCR, and was lower in HCR at 10 min of exercise (**Table A.1**).

Although fat availability is likely not driving differences in fuel use, it could be that HCR and LCR have differences in fuel uptake with exercise. Previous reports found that HCR have greater protein expression of fatty acid transporter CD36 (Lessard et al., 2009). The rise in muscle acyl-carnitine in HCR suggest greater fatty acid entry into the mitochondria with exercise, and this could be due to differences in fatty acid transport. Free carnitine availability is a proposed limiting factor for fatty acid entry into mitochondria (Jeppesen and Kiens, 2012; Jeukendrup, 2002). In this study, free L-carnitine decreases with exercise but does not correlate with fat oxidation, suggesting that L-carnitine is not limiting. It could be the case that CPTI activity is different between HCR and LCR, but total CPTI protein is not different between the strains (DeMarco et al., 2012; Rivas et al., 2011). LCR have notable increases in medium-chain plasma acyl-carnitines with exercise indicating production and export of acyl-carnitines from the tissue and likely greater incomplete fatty acid oxidation. Fatty acid transporters could be mediating increased fat oxidation, but we suspect that other mechanisms are also contributing to the difference in fuel use.

Our data support the reciprocal relationship between fat and carbohydrate oxidation. Glycogen depletes as animals approach exhaustion and coincident with

lower fat oxidation. The metabolic products of immediately downstream of glycolysis — lactate and acetylcarnitine — were elevated with exhaustion and inversely correlated to fat oxidation. This reciprocal relationship between fat and carbohydrate oxidation has been well established (Randle, 1998). Glycogen breakdown and acetylcarnitine production increase with increasing-intensity exercise (Constantin-Teodosiu et al., 1991; Gollnick et al., 1974; Hiatt et al., 1989; Sahlin, 1990; van Loon et al., 2001). Glycogen phosphorylase activity, which mediates glycogen breakdown, increases with exercise (Jensen et al., 2011). HCR maintain muscle glycogen for longer; this might suggest HCR and LCR have differences in allosteric inhibitors/activators or differences in muscle recruitment and contraction mediated activation of glycogen phosphorylase.

Pyruvate dehydrogenase (PDH) activity increases with increasing intensity exercise (Howlett et al., 1998). Increased PDH activity might support increasing acetylcarnitine with increasing intensity. Acetylcarnitine accumulation with exhaustion signifies that acetyl-CoA is being made in excess of what can be used in the tissue. This excess can occur through the rapid production of acetyl-coA from glycolysis, but it also means that there is some limit on down-stream utilization - either in the citrate cycle or oxidative phosphorylation. Excess acetyl-CoA is converted to acetylcarnitine by the enzyme carnitine acetyl-transferase (CrAT). CrAT is highly expressed and active in skeletal muscle (Marquis and Fritz, 1965; Noland et al., 2009). Over-expression of CrAT in myotubes increased acetylcarnitine production, but also increased PDH activity and decreased fat oxidation. These data suggest a role of acetylcarnitine production in supporting changes in fuel preference.

Beyond fat and carbohydrate use, our data give evidence for changes in BCAA metabolism with exercise and exhaustion. At 10 min of exercise, BCAA decrease in plasma of HCR and muscle BCAA is lower in HCR than LCR. Downstream BCAA metabolites (KIV, C3-carnitine, and C5-carnitine) are increased at exhaustion. Decreased muscle and plasma BCAA in HCR suggest greater BCAA degradation in HCR vs. LCR, and increased KIV and downstream metabolites in LCR with 10 min of exercise might indicate incomplete BCAA degradation in LCR. BCAA degradation is likely a important component of exercise capacity. Plasma BCAA levels inversely



correlate with exercise capacity (Morris et al., 2013), and knocking out a key enzyme in BCAA metabolism leads to decreased exercise capacity (She et al., 2010).

As with all studies, there are some limitations. The indirect calorimetry was performed using an increasing-intensity exercise protocol - this is necessary to accurately measure  $\text{VO}_2\text{max}$ , but determining fuel use on this type of protocol is less accurate due to non-steady state conditions. Therefore, we present the data as a best estimate of fuel use during this protocol. Our second assessment of fuel use employed targeted metabolomics. A targeted metabolomics approach inherently biases our results towards previously detected metabolites and known metabolic pathways, but at the same time allows for greater confidence in the metabolites we report. And finally, in exploring which metabolites associate with exhaustion, we assume that there are common factors related to exhaustion in both HCR and LCR. It is possible that HCR and LCR exhaust for different reasons. Our data might suggest that HCR have more extreme case of metabolic stress near exhaustion - severely depleted glycogen, lower blood glucose, extreme elevations in muscle and plasma acyl-carnitines and robust phosphorylation of AMPK at 45 min. Although, HCR and LCR might experience different metabolic extremes near exhaustion, the metabolites that are altered with exhaustion in both animals (muscle glycogen, blood lactate, muscle acetylcarnitine, and muscle IMP) are well described in the literature as associating with exhaustion (Constantin-Teodosiu et al., 1991; Hiatt et al., 1989; Rush et al., 1995; Sahlin, 1990; van Loon et al., 2001).

Ultimately these data lead us to conclude that HCR's maintained fat oxidation and delayed glycogen utilization support increased running capacity. Mechanisms driving fuel preference are still unknown, although we find that accumulation of metabolic intermediates malate, acetylcarnitine, C5 carnitine, and lactate are correlate with use and coincident with exhaustion, suggesting that fuel use is dependent on mitochondrial oxidative capacity.

### **3.5 Summary**

- HCR have greater fat oxidation during an increasing intensity exercise protocol.

- Fuel availability does not differ between HCR and LCR before exercise.
- HCR have evidence for increased BCAA metabolism with exercise
- 5 metabolites: plasma C5 carnitine, muscle malate, muscle IMP, muscle acetylcarnitine, and muscle glycogen are correlated with fuel selection and coincident with exhaustion.

## **Chapter 4**

### **Post-translational modifications that occur with exercise**

In the previous chapter, we assessed metabolite changes that occur with exercise. We found HCR have higher fat oxidation throughout exercise compared to LCR. Because fuel preference is driven by both fuel availability and enzyme activity. In this chapter we will look at proteomic differences between HCR and LCR at rest and examine changes in enzyme modification (phosphorylation and acetylation) that occur with 10 min of exercise.

#### **4.1 Introduction**

Fuel availability and enzyme activity modulate fuel preference. With a metabolomics approach we identified difference in fuel use between HCR and LCR. We used metabolite values to infer mechanisms that might lead to these differences and the overall phenotype. We expand on our understanding of molecular mechanisms of fuel selection by looking directly at the proteome. *In vivo*, enzyme activity is affected by amount of enzyme available and modifications to the enzyme. Amount of available enzyme is controlled by transcriptional activity and protein ubiquitination, which act in opposition to control enzyme synthesis and breakdown. These processes regulate enzyme availability on the time scale of minutes to hours, while acute regulation of enzyme activity is achieved through enzyme modifications and allosteric regulation. Thus to understand difference in fuel use with exercise, we

must look for both enzyme availability and protein modifications that occur with exercise.

There is some evidence that increased availability of enzymes within the fat oxidation pathway can support increased fat-use during exercise and increased exercise capacity. Particularly, adaptation in response to exercise training is associated with increased transcription of HADH, FABP, FAT/CD36, and CPT1 (Holloszy and Coyle, 1984). Active vs. inactive twins have greater expression of genes within the fat oxidization pathway, as do rats bred for high vs. low running capacity (Kivela et al., 2010; Pietilainen et al., 2008). However, there is contradictory evidence that increased availability of fat oxidizing enzymes — occurring with high-fat food intake — is not sufficient to increase fat-use during exercise or running capacity (Hall et al., 2010). While enzyme availability is important, other factors, like enzyme modification, might be equally important in directing fuel use.

Certain modifications to enzymes, like phosphorylation and acetylation, can support changes in fuel use. Phosphorylation of enzymes has been increasingly studied since glycogen phosphorylase was demonstrated to have altered activity when phosphorylated (Fischer and Krebs, 1955). A number of other metabolic enzymes are modified by phosphorylation: pyruvate dehydrogenase (PDH), branched-chain keto acid dehydrogenase (BCKDH), acetyl-CoA carboxylase, and changes in phosphorylation of these enzymes occur with exercise and modify enzyme activity (Howlett et al., 1998; Jeppesen and Kiens, 2012; Lynch et al., 2002). In contrast to phosphorylation, enzyme modification by acetylation is a more recent discovery, with publications in 2010 demonstrating that most metabolic enzymes are acetylated on one or more lysine residues (Wang et al., 2010; Zhao et al., 2010). Relatively few acetylation sites have been assessed for functional consequence (Xiong and Guan, 2012), however enzyme acetylation changes with fasting and re-feeding and with calorie restriction are associated with changes in fuel preference suggesting that acetylation can modify fuel use.

We used proteomic analysis to better understand fuel use in HCR and LCR with exercise. Indirect calorimetry and metabolomic analysis presented in Chapter 3 - Metabolomics to define fuel use during exercise show that HCR have delayed

glycogen utilization and greater fat-use during exercise than LCR, despite LCR having similar fat-availability. We hypothesize that HCR and LCR have differences in enzyme availability, which is suggested from gene-expression data (Kivela et al., 2010), and we expect HCR and LCR might have differential enzyme modification that could help explain differences in fuel preference.

## **4.2 Methods**

### *4.2.1 Animal protocol and study design*

HCR and LCR male rats (generation 31) were housed at the University of Michigan, and the University Committee on Use and Care of Animals, Ann Arbor Michigan approved the study. All procedures were in compliance with University guidelines and state and federal regulations.

At 11 weeks of age, exercise capacity was determined as described previously 3.2.1 - Animal protocol and study design. The following week, the HCR and LCR rats were divided into rest and 10 min run groups (n=5), and were given ad libitum access to food prior to the experiments. Rats in the rest group were allowed to rest on stationary treadmills for 10 min, and animals in the Run group were run on the treadmill for 10 min (treadmill starting at 10 m/min and increasing 1/min every 2 min). After these time points, rats were immediately anesthetized by inhaled isoflurane (~30s) and then euthanized by decapitation. Trunk blood was used for preparing serum, and tissues were harvested and immediately frozen in liquid nitrogen. Tissues were stored at  $-80^{\circ}\text{C}$ . Both right and left extensor digitorum longus muscles (EDL) were used for subsequent proteomic analysis.

### *4.2.2 Mitochondrial isolations*

Crude mitochondria were enriched using previously described methods (Pagliarini et al., 2008), with some modifications for the current study. Rat EDL tissue was initially homogenized by crushing with a mortar and pestle (Coors) under liquid nitrogen, and all subsequent steps were carried out at  $4^{\circ}\text{C}$ . The homogenate was then transferred into a Potter-Elvehjem glass/teflon homogenizer along with 8

mL of MSHE buffer (220mM mannitol, 70mM sucrose, 5mM HEPES pH 7.4, 1mM EGTA), supplemented with protease inhibitors, deacetylase inhibitors and 0.5% BSA, for further homogenization. After homogenization with 5 strokes at 1000 rpm, the resulting homogenate was decanted into a new 15 mL tube. The homogenizer was rinsed with an additional 2 mL of MSHE, which was then added to the homogenate. The sample was centrifuged at 800 x g for 10 min in bench-top conical centrifuge. Any lipid that formed at the top of the supernatant was carefully aspirated. The supernatant, containing the mitochondria, was gently drawn off with a pipet-aid and transferred to an ultra-clear 12 mL centrifuge tube. The samples were centrifuged at 8000 x g for 10 min, and the resulting supernatant and any loose material was aspirated and discarded, leaving a dark brown pellet with a light brown halo around the center. An additional 10 mL of MSHE buffer was added to the pellet, which was resuspended by washing from the side of the tube until homogenous using as few pipetting strokes as possible. The sample was centrifuged an additional time at 8000 x g for 10 min and the crude mitochondria were resuspended in 1 mL of MSHE using the same method as before. Crude mitochondria were transferred to a 1.5 mL microfuge tube and centrifuged at 8,000 x g for 10 min in bench-top microfuge. The supernatant was aspirated and discarded. The pellet was re-suspended in MSHE (without BSA) and centrifuged at 8,000 x g for 10 min in bench-top centrifuge. The supernatant was aspirated and discarded, and the crude mitochondrial pellet was flash frozen in liquid N<sub>2</sub> and stored at -80°C until ready for use.

#### *4.2.3 Generation of peptides*

Mitochondrial cell pellets were re-suspended in approximately 500µL of lysis buffer (50mM Tris (pH 8), 8M urea, 40mM NaCl, 2mM MgCl<sub>2</sub>, 50mM NaF, 50mM β-glycerophosphate, 1mM sodium orthovanadate, 10mM sodium pyrophosphate, mini EDTA-free protease inhibitor (Roche Diagnostics, Indianapolis, IN), phosSTOP phosphatase inhibitor (Roche Diagnostics, Indianapolis, IN), and deacetylase inhibitors) and lysed on ice with a probe sonicator. Protein content was evaluated using a BCA assay (Thermo Fisher Scientific, San Jose, CA).

Proteins were reduced with 5mM dithiothreitol (incubation at 58°C for 30 minutes) and alkylated with 15mM iodoacetamide (incubation in the dark, at ambient temperature, for 30 minutes). Alkylation was quenched by adding an additional 5mM dithiothreitol (incubation at ambient temperature for 15 minutes). Proteins were enzymatically digested in a two-step process. First, proteinase LysC (Wako Chemicals, Richmond, VA) was added to each sample at a ratio of 1:100 (enzyme:protein) and the resulting mixtures were incubated at 37°C for 3 hours. Next, samples were diluted to a final concentration of 1.5 M urea (pH 8) with a solution of 50mM Tris and 5mM CaCl<sub>2</sub>. Sequencing-grade trypsin (Promega, Madison, WI) was added to each sample at a ratio of 1:50 (enzyme:protein) and the resulting mixtures were incubated at ambient temperature overnight. Digests were quenched by bringing the pH to ~2 with trifluoroacetic acid and immediately desalted using C18 solid-phase extraction columns (SepPak, Waters, Milford, MA).

Desalted material was labeled with TMT 10-plex isobaric labels (Thermo-Pierce, Rockford, IL). Only eight of the ten labels were used per experiment for the comparison of two biological replicates across each the four conditions. Prior to quenching the TMT reactions, ~5µg of material from each TMT channel was combined into a test mix and analyzed by LC-MS/MS to evaluate labeling efficiency and obtain optimal ratios for sample recombination. Following quenching, tagged peptides were combined in equal amounts by mass (~500µg per channel) and desalted. All experiments had ≥ 99% labeling efficiency, calculated by the number labeled peptides divided by the total number of peptide identifications.

Labeled peptides were fractionated by strong cation exchange (SCX) using a polysulfoethylaspartamide column (9.4×200mm; PolyLC) on a Surveyor LC quaternary pump (Thermo Scientific). Each dried and mixed TMT sample was resuspended in buffer A, injected onto the column, and subjected to the following gradient for separation: 100% buffer A from 0-2 min, 0-15% buffer from 2-5 min, and 15-100% buffer B from 5-35 min. Buffer B was held at 100% for 10 minutes and then the column was washed extensively with buffer C and water prior to recalibration. Flow rate was held at 3.0 mL/min throughout the separation. Buffer compositions were as follows: buffer A [5mM KH<sub>2</sub>PO<sub>4</sub>, 30% acetonitrile (pH 2.65)], buffer B [5mM

KH<sub>2</sub>PO<sub>4</sub>, 350mM KCl, 30% acetonitrile (pH 2.65)], buffer C [50mM KH<sub>2</sub>PO<sub>4</sub>, 500mM KCl (pH 7.5)]. Twelve fractions were collected over the first 50-minute elution period and were immediately frozen, lyophilized, and desalted. A small portion of each, 5%, was extracted and used for protein analysis. The remaining material was retained for phospho and acetyl lysine enrichment.

#### *4.2.4 Phospho and Acetyl-site enrichment*

Phosphopeptides were enriched using immobilized metal affinity chromatography (IMAC) with magnetic beads (Qiagen, Valencia, CA). Following equilibration with water, the magnetic beads were incubated with 40mM EDTA (pH 8.0) for 1 hour, with shaking. Next, the beads were washed four times with water and incubated with 30mM FeCl<sub>3</sub> for 1 hour, with shaking. Beads were then washed four times with 80% acetonitrile/0.15% TFA. Each of the 12 fractions were re-suspended in 80% acetonitrile/0.15% TFA and incubated with the magnetic beads for 45 minutes, with shaking. Following this incubation, all unbound peptides were collected for subsequent acetyl lysine enrichment. Bound peptides were washed three times with 80% acetonitrile/0.15% TFA and eluted with 50% acetonitrile, 0.7% NH<sub>4</sub>OH. Eluted peptides were immediately acidified with 4% FA, frozen, and lyophilized. Each phospho peptide fraction was re-suspended in 20 $\mu$ L 0.2% FA for LC-MS/MS analysis.

Peptides unbound by IMAC enrichment were pooled into 6 fractions. Each fraction was dissolved in 50mM HEPES (pH 7.5)/100mM KCl buffer, combined with approximately 50 $\mu$ L pan-acetyl lysine antibody-agarose conjugate (Immunechem), and rotated overnight at 4°C. Samples were rinsed eight times with 50mM HEPES (pH 7.5)/100mM KCl buffer prior to elution with 0.1% TFA. Eluted peptides were then desalted, frozen, and lyophilized. Each acetyl lysine fraction was re-suspended in 20 $\mu$ L 0.2% FA for LC-MS/MS analysis.

#### *4.2.5 Proteomic LC-MS/MS analysis*

Proteomic LC-MS/MS analysis. All experiments were performed using a NanoAcquity UPLC system (Waters, Milford, MA) coupled to an Orbitrap Fusion (Q-



OT-qIT) mass spectrometer (Thermo Fisher Scientific, San Jose, CA). Reverse-phase columns were made in-house by packing a fused silica capillary (75 $\mu$ m i.d., 360  $\mu$ m o.d, with a laser-pulled electrospray tip) with 1.7 $\mu$ m diameter, 130 Å pore size Bridged Ethylene Hybrid C18 particles (Waters) to a final length of 30cm. The column was heated to 60°C for all experiments. Samples were loaded onto the column for 12 minutes in 95:5 buffer A [water, 0.2% formic acid, and 5% DMSO]:buffer B [acetonitrile, 0.2% formic acid, and 5% DMSO] at a flow-rate of 0.30 $\mu$ L/min. Peptides were eluted using the following gradient: an increase to 7% B over 1 min, followed by a 42 min linear gradient from 7% to 18% B, followed by a 28 min linear gradient from 18% to 27% B, followed by a final 1 min ramp to 75% B which was held for 3 minutes. The column was equilibrated with 5% buffer B for an additional 25 min. Precursor peptide cations were generated from the eluent through the utilization of a nanoESI source. Phospho and acetyl enriched fractions were each analyzed in duplicate.

Mass spectrometry instrument methods consisted of MS1 survey scans (8e5 target value; 60,000 resolution; 350Th – 1400Th) that were used to guide ten subsequent data-dependent MS/MS scans (0.7Th isolation window, HCD fragmentation; normalized collision energy of 37; 5e4 target value, 60,000 resolution). Dynamic exclusion duration was set to 60s, with a maximum exclusion list of 500 and an exclusion width of 0.55Th below and 2.55Th above the selected average mass. Maximum injection times were set to 100ms for all MS1 scans, 120ms for MS/MS scans in whole protein analyses, and 200ms for MS/MS scans in phospho and acetyl enrichment analyses.

#### *4.2.6 Proteome data processing and normalization*

Data was processed using the in-house software suite COMPASS (Wenger et al., 2011b). OMSSA (Geer et al., 2004) (version 2.1.8) searches were performed against a target-decoy database (Uniprot (rat), [www.uniprot.org](http://www.uniprot.org), August 19, 2013). Searches were conducted using a 3Da precursor mass tolerance and a 0.01Da product mass tolerance. A maximum of 3 missed tryptic cleavages were allowed. The fixed modifications specified were carbamidomethylation of cysteine residues, TMT 10-

plex on peptide N-termini, and TMT 10-plex on lysine residues. The variable modifications specified were oxidation of methionine and TMT 10-plex on tyrosine residues. Additional variable modifications were specified for phospho-peptide analyses (phosphorylation of threonine, serine, and tyrosine residues) and acetyl-peptide analyses (acetylation of lysine residues). Note that the acetylation modification mass shift was set to -187.1523 Da to account for the difference between an acetyl group and a TMT 10-plex tag, which enables the use of TMT 10-plex as a fixed modification on lysine residues, even for acetylated peptides. TMT quantification of identified peptides was performed within COMPASS as described previously (Phanstiel et al., 2011). Peptides identified within each of 12 fractions were grouped into proteins according to previously reported rules (Nesvizhskii and Aebersold, 2005) using COMPASS. Protein quantification was performed by summing all of the reporter ion intensities within each channel for all peptides uniquely mapping back to a given protein. Protein, phospho-peptide, and acetyl-peptide experiment sets were processed separately.

Phosphopeptide localization was performed using Phosphinator software within COMPASS, as described previously (Phanstiel et al., 2011). This program both localized phosphorylation sites and combined quantitative data for phospho-isoforms across all 12 fractions. All phosphosites had to be localized for a given phospho-peptide to be included in subsequent quantitative analysis.

Acetylpeptide localization was performed using LoToR software within COMPASS. Briefly, for each peptide spectral match (PSM) that contained an acetyl modification, theoretical fragmentation spectra were generated by performing *in silico* fragmentation of every possible peptide isoform. Each theoretical spectrum was then compared to the experimental spectrum using mass tolerances of 0.025Th. A peptide was declared localized if one isoform matched at least one peak more than any other isoform matched. Localized acetylated peptides were grouped together on acetylated positions and reporter ion intensities were summed.

To generate a list of rat mitochondrial proteins, Entrez GeneIDs from the mouse MitoCarta compendium of mitochondrial proteins (Pagliarini et al., 2008) were mapped to NCBI HomoloGene group ID according to build 67. All rat genes

corresponding to these groups were then mapped to UniProt identifiers using the UniProtKB ID mapping table (July 2013).

To account for variation in mitochondrial preparation, all quantitative data was normalized at the mitochondrial protein level. Only mitochondrial proteins were included in our analysis. All quantitative values were log<sub>2</sub> transformed and mean normalized. To normalize phosphorylation and acetylation data for protein differences, the value for each phospho and acetyl isoform reporter ion channel had subtracted from it the quantitative value of that channel from the corresponding protein.

#### *4.2.7 Sirt3 Western Blot*

Western blot for SIRT3. Frozen gastrocnemius tissues collected from female HCR and LCR rats (generation 33, 6 month of age) at 0, 10, and 45 min of treadmill exercise were used for mitochondrial isolations. Isolated mitochondria were extracted in buffer containing 1% Triton X-100, 20mM HEPES, 20mM beta-glycerophosphate, 150mM NaCl, 10mM NaF, 10mM Na-Pyrophosphate, 1mM EDTA, protease inhibitor cocktail (Roche) and phosphatase inhibitor cocktail (Thermo Scientific). After 20s sonication, samples were centrifuged at 8,000 x g for 10 min. Protein concentration was determined with Pierce BCA kit (Rockford, IL) and was used to normalize sample concentrations prior to loading. Sample extracts were separated by SDS-PAGE (Criterion, BioRad) and transferred to a nitrocellulose membrane. After blocking with 5% non-fat dry milk in TBS-T, the membrane was incubated overnight at 4°C with anti-SirtT3 primary antibody (1:1000, Cell Signaling #D22A3, generously provided by David Lombard). The membrane was washed and incubated for 1 hr at 20°C with appropriate secondary antibodies conjugated to horseradish peroxidase (1:2000). After final washes, target proteins were detected with Pierce ECL solution (Rockford, IL).

#### *4.2.8 Statistical analysis and graphing*

Statistical analysis and graphing was performed in the R environment (R Core Team, 2013). Protein and modification site fold-changes were calculated by

averaging protein-normalized values for each condition and calculating the difference of averages. Comparisons were made between HCR and LCR at rest and 10 min exercise and within strain between rest and 10 min exercise. Pathway enrichment analysis was performed through Enrichr (Chen et al., 2013). For statistics on pathway changes, each acetyl-site within a pathway for each individual samples were compared between groups. Thus, a pathway with 40 acetyl-sites and n=4 per group would be compared 4x40 with 4x40. This analysis gives equal weight to individual acetylation sites within a pathway, but maintains variance between individual, biological samples. For all comparisons, p-values were determined by permutation t-test using R perm package (Fay, 2010).

Rank products (Hong et al., 2006) approach was used to rank differentially expressed and modified proteins. The combined rank score was used to generate a list of top 25 proteins differentiating between HCR and LCR at 10 min of exercise.

## 4.3 Results

### 4.3.1 HCR and LCR mitochondrial proteome

We performed isobaric-tagged proteomic analysis on mitochondria isolated from EDL collected from HCR and LCR males before and after 10 min of exercise. In total, 428 proteins were identified, and of those 174 were significantly different between HCR and LCR when normalized for mitochondrial mass (**Table 4.1**). Although HCR tend to have greater mitochondrial content within skeletal muscle than LCR (Rivas et al., 2011; Seifert et al., 2012), our data show that mitochondrial composition differs by 40% between HCR and LCR. Many mitochondrial proteins identified had lower expression in HCR vs. LCR.

Full tables with the relative expression of all identified proteins can be found in Appendix C. The most down-regulated proteins in HCR include mitochondrial encoded Mt-atp8, Mt-co2; and the most up-regulated is Acadsb, an enzyme involved in breakdown of isoleucine (**Figure 4.1**). KEGG Pathway enrichment analysis revealed differential protein expression in oxidative phosphorylation, fatty acid metabolism, BCAA degradation, aminoacyl tRNA biosynthesis, fatty acid elongation,

butanoate metabolism. Of the identified proteins within the enriched pathways, we see that 12 of the 18 proteins in oxidative phosphorylation are down in HCR vs. LCR, while 7 of the 9 fatty acid metabolism proteins are up in HCR vs. LCR. BCAA Degradation and fatty acid elongation proteins are up in HCR, while 7 of the 7 proteins within the Aminoacyl tRNA biosynthesis pathway are down in HCR. Given the lower expression of mitochondrially encoded proteins Mt-atp8, Mt-co2 and tRNA biosynthetic proteins, it seems likely that mitochondrial biogenesis is different between HCR and LCR. Also, HCR have specific enrichment for fatty acid and BCAA metabolic enzymes.

Comparing this data with a recent proteomic study with HCR and LCR heart tissue, we extend the HCR-LCR proteome by 15-fold. The previous proteomic study employed 2D-gel electrophoresis (Burniston et al., 2011) on whole tissue lysates, where as the current study focuses specifically on the mitochondrial proteome. Proteins *Acca2*, *Cox4i1*, and *Cox5* were consistently overexpressed in HCR in both studies.

**Table 4.1 Number of proteins identified in mitochondria.** This table includes number of phosphorylation sites and acetylation sites.

	Proteome	Phosphoproteome	Acetylome
Number of MitoCarta proteins identified	428	73	85
HCR vs LCR p<0.05 (Up in HCR)	174 (22)		
Number of identified modification sites		131	241
HCR Rest vs LCR Rest p<0.05 (Up in HCR Rest)		8 (7)	13 (0)
HCR Run vs LCR Run p<0.05 (Up in HCR Run)		3 (3)	10 (0)
HCR Run vs HCR Rest p<0.05 (Up in HCR Run)		0 (0)	4 (2)
LCR Run vs LCR Rest p<0.05 (Up in LCR Run)		3 (2)	2 (0)

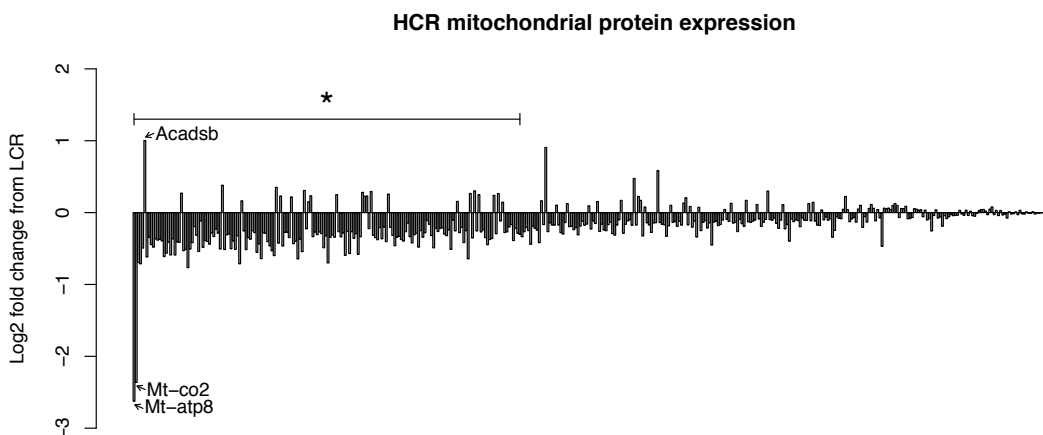


**Figure 4.1 Differentially expressed proteins between HCR and LCR.** Expression (log<sub>2</sub> fold change) of each identified protein show that most proteins have lower expression in HCR relative to LCR. Asterisk \* over the left side of the graph indicates protein expression is significantly different between HCR and LCR.

#### 4.3.2 Protein modification

The phosphoproteome and acetylome were determined after enrichment for peptides containing phospho- and acetyl-sites. We identified 131 phosphorylation sites on 73 proteins and 241 acetylation sites on 85 proteins. We normalized the expression each phospho- and acetyl-site to the expression of the total protein. For example, expression of modified K171 on Sdha was normalized to overall expression of Sdha. **Table 4.1** shows the number of protein phosphorylation and acetylation sites that were found to be significantly different between HCR and LCR at rest and after 10 min running.

At rest, there are 7 phospho-sites on 6 proteins that are significantly more phosphorylated in HCR than LCR: Abcb8, Cox6b1, Cpox, Ldha (2 sites), Mitch2, Vdac2, and there were 13 acetyl-sites on 11 proteins that were significantly less acetylated in HCR at rest: Sdha, Etf1, Hspd1 (2 sites), Crat, Aco2, Dld, Ndufs1, Ivd (2 sites), Got2, and Hadha. When we look at pathway enrichment analysis for phosphorylation and acetylated sites we see that there is more acetylation enrichment in oxidative phosphorylation, BCAA degradation, propionate metabolism, and fatty acid metabolism pathways. There is relatively equal phosphorylation and

acetylation enrichment in the citrate cycle and more phosphorylation enrichment within the reductive carboxylate cycle.

We compared fold-change Run/Rest for the proteome, phosphoproteome, and acetylome, to assess what proteome changes occur with 10 min of exercise (**Figure 4.2**). There are only minor changes in the proteome and phosphoproteome with exercise, but the acetylome changes more dynamically with exercise. Both HCR and LCR have decreases in acetylation state with 10 min of exercise; however, HCR have greater decreases in acetylation state. These data suggest that enzyme modification by acetylation might be more prevalent in pathways related to fuel preference.

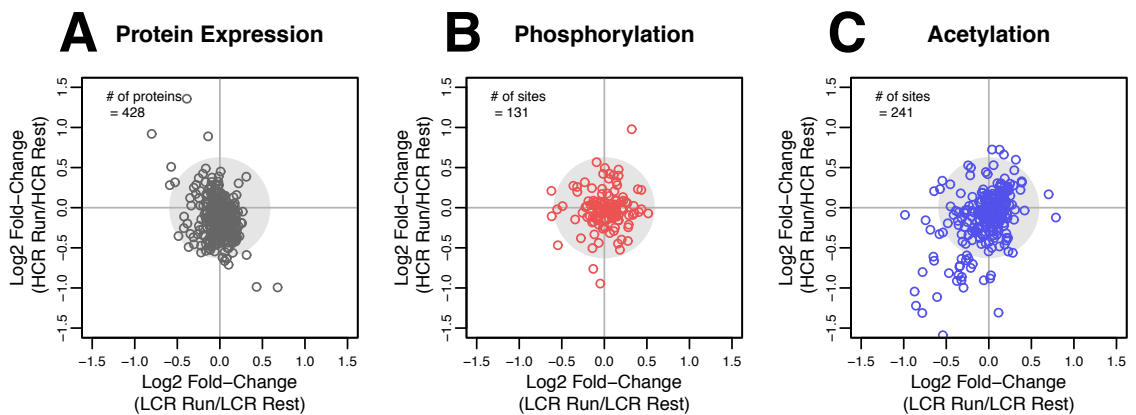


**Figure 4.2 Mitochondrial protein acetylation is dynamic with exercise.** Log<sub>2</sub> fold-change (Run/Rest) values for HCR and LCR were used to plot changes with exercise in the proteome (A), phosphoproteome (B), and acetylome (C).

#### 4.3.3 The acetylome is most dynamic with exercise

Overall, mitochondrial acetylation was lower in HCR at rest (**Figure 4.3A**), and this difference was amplified following exercise (**Figure 4.3B**). KEGG pathway analysis revealed that these acetylation sites were enriched within the oxidative phosphorylation, citric acid cycle, BCAA degradation, propionate metabolism and FA metabolism pathways. By estimating the relative level of acetylation of all peptides within each of these pathways, we found that there was significantly lower mitochondrial acetylation in each pathway in HCR compared to LCR, both at rest and following exercise (**Figure 4.3C**). In addition, HCR had significant deacetylation in 4 of the 5 acetyl-rich pathways after 10 min of exercise, while LCR had no significant pathway changes in acetylation, Consistent with differential fatty acid oxidation

between HCR and LCR at 10 min of exercise, relative acetyl-site occupancy on fatty acid metabolic enzymes is lower in HCR (**Figure 4.3D**).



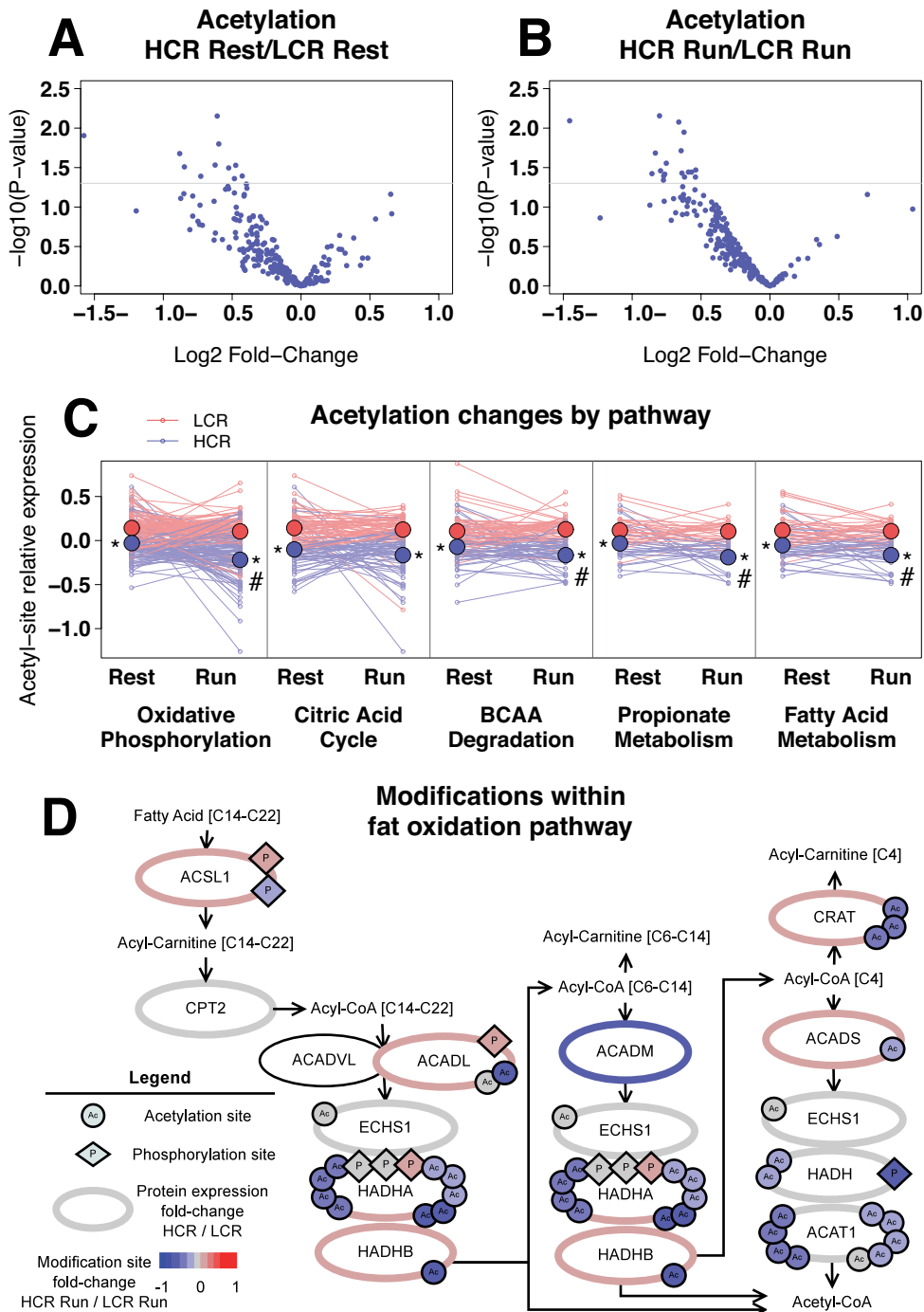


**Figure 4.3 HCR have less mitochondrial protein acetylation than LCR.**  $\text{Log}_2$  fold-change (HCR/LCR) values for the 141 acetyl-lysine sites were plotted against p-values at rest (A) and at 10 min run (B) ( $n=5$ ). For each enriched pathway (C), relative acetyl-site occupancy (small circles) and average pathway acetylation (large circles) are given for each group ( $n=5$ ). The fat oxidation pathway (D) is less acetylated in HCR with exercise. Proteins (ellipses) are labeled by gene symbol with identified acetylation (circle) and phosphorylation (diamond) sites. The color scale designates  $\text{log}_2$  fold-change (HCR/LCR comparison for protein; or HCR Run/LCR Run comparison for acetylation and phosphorylation).

#### 4.3.4 Sirt 3

The enriched pathways are targets of the lysine deacetylase SIRT3 (Rardin et al., 2013). Malate dehydrogenase, succinate dehydrogenase subunit A, and hydroxyacyl-CoA dehydrogenase subunit A, which are known targets of SIRT3 (Finley et al., 2011; Hebert et al., 2013; Rardin et al., 2013), are among the proteins most differentially acetylated in mitochondria of HCR and LCR (see Appendix C, **Table C.3**), suggesting a role of SIRT3 in mediating the differences in acetylation. However, we found no difference in the SIRT3 levels between HCR and LCR in mitochondrial extracts by proteomic analysis (Appendix C, **Table C.1**) or by Western blotting (**Figure 4.4**). If SIRT3 is mediating these differences, then it is due to differential activation of SIRT3.

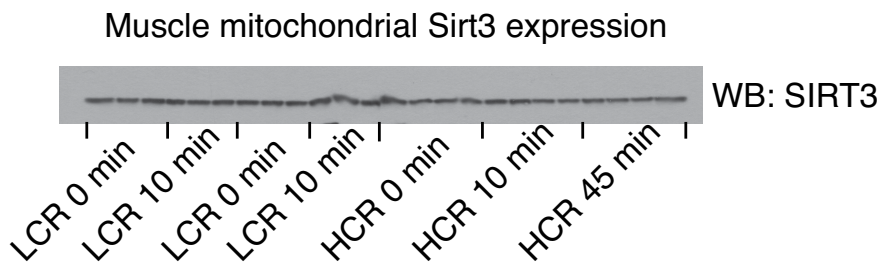


**Figure 4.4 SIRT3 expression in the mitochondria.** Mitochondrial proteins isolated from gastrocnemius tissue of HCR and LCR were separated by SDS-PAGE. Anti-Sirt3 antibody (Cell Signaling) was used to detect SIRT3 expression.

#### 4.3.5 Integrating proteomics data

We used a rank products approach to rank the most differentiating proteins in each of the data sets: proteome, phosphoproteome and acetylome. Rank products accounts for both fold-change and p-value to generate a rank score (Hong et al., 2006). The combined rank score for an individual protein across the data sets incorporates both protein abundance and post-translation modification. The top 25 proteins that differentiate HCR-run and LCR-run are presented in **Table 4.2**. Many of these top 25 proteins are involved in the electron transport chain and fatty acid metabolism, and a few are involved in citric acid cycle, BCAA metabolism, and transcriptional regulation. Differential expression/modification of these proteins are

consistent with metabolomic differences observed in HCR vs. LCR at 10 min of exercise.

**Table 4.2 The Top 25 differentially expressed or modified proteins.** Rank products approach accounts for protein fold-change and p-value. The combined rank score of protein expression, protein phosphorylation, and protein acetylation for each protein was used to identify the top 25 proteins differentially expressed between HCR and LCR at 10 min of exercise.

Gene name	Primary Pathway
Cox7c	Electron transport chain
Fh	Citric acid cycle
Cox7b	Electron transport chain
Acadsb	BCAA metabolism
Cox5a	Electron transport chain
Ndufc1	Electron transport chain
Acot13	Fatty acid metabolism
Cox6b1	Electron transport chain
Ndufa4	Electron transport chain
Uqcrq	Electron transport chain
Eci2	Fatty acid metabolism
LOC683884	Fatty acid metabolism
Dlst	Glucose metabolism
Sod2	Oxoreductase
Etfdh	Fatty acid metabolism/Electron transport chain
Hadha	Fatty acid metabolism
Suclg1	Citric acid cycle
Mt-atp8	Electron transport chain
Mt-co2	Electron transport chain
Lrpprc	Transcriptional regulation
Drg2	Cell proliferation
Mrps35	Transcriptional regulation
Ucp3	Mitochondrial Uncoupling
Hk2	Glucose metabolism
Acadm	Fatty acid metabolism

#### 4.4 Discussion

Proteomic analysis of HCR and LCR EDL mitochondria show that HCR have higher expression of proteins within fatty acid and BCAA metabolic pathways, but lower expression of proteins within tRNA synthesis. There were 7 phosphorylation sites and 13 acetylation sites that were different between HCR and LCR at rest. With

exercise, we found that protein acetylation decreases in both strains but these decreases were greater in HCR. The pathways that were differentially acetylated at rest and 10 min of exercise were oxidative phosphorylation, citrate cycle, and fatty acid and BCAA metabolic pathways.

We previously demonstrated that HCR have increased fatty acid oxidation during exercise compared to LCR (see Chapter 3 - Metabolomics to define fuel use during exercise). Akin to adaptations observed with exercise training (Holloszy et al., 1998; Kiens et al., 1993), we find that non-trained HCR have upregulation of enzymes within the FA oxidation pathway (Appendix A, Table C.1).

In the previous chapter, elevation of metabolite intermediates near exhaustion - malate, acetylcarnitine, and C5-carnitine - were suggestive of a mitochondrial regulation of fuel selection. The excess production of acetyl-units and build up of citric acid cycle intermediates are evidence of imbalance between acetyl-unit production and downstream metabolism through the citric acid cycle and electron transport chain. In this study, we show that HCR and LCR have differential expression of proteins with the electron transport chain. Normalized to mitochondrial content, many of the electron transport proteins were lower in HCR than LCR. The combined rank product of protein expression, phosphorylation, and acetylation, demonstrates that expression and modification of proteins in the electron transport chain represent a predominate difference between HCR and LCR at 10 min of exercise. Further studies will be needed to understand the functional consequence of these modifications of electron transport chain proteins and their role in fuel selection differences with running.

Accumulated evidence suggests that deacetylation of enzymes within fatty acid and BCAA pathways increases activity of these enzymes (Hallows et al., 2011; Hirschey et al., 2010; Rardin et al., 2013; Still et al., 2013). HCR's greater fatty acid oxidation during exercise is consistent with a functional consequence of lower protein acetylation in the fatty acid metabolism pathway. Our finding of rapid mitochondrial protein deacetylation with exercise provides an additional mechanism by which animals can increase substrate oxidation in response to increased energy demand.

Change in lysine acetylation of mitochondrial proteins is a balance between NAD<sup>+</sup>-dependent SIRT3 deacetylase activity (Lombard et al., 2007) and non-enzymatic addition of acetyl groups to lysine (Wagner and Payne, 2013). In contrast to the lower acetylation observed with exercise training and calorie restriction (Palacios et al., 2009), the lower level of acetylation observed in HCR is not explained by SIRT3 content (**Figure 4.4**). Rather, the dynamic deacetylation is likely due to SIRT3 activation by expected increases in mitochondrial NAD<sup>+</sup> that occurs with exercise (White and Schenk, 2012). In addition, the differences in acetyl-unit availability may also contribute to the observed differences in acetylation between HCR and LCR. Acetylcarnitine accumulation with increasing exercise intensity is a consistent phenomenon (Constantin-Teodosiu et al., 1991; Gollnick et al., 1974; Hiatt et al., 1989; Sahlin, 1990; van Loon et al., 2001), and like others (Kiens, 2006), we have shown that acetylcarnitine levels correlate positively with carbohydrate oxidation and negatively with FA oxidation. Increases in acetyl-unit availability in LCR from 0 to 10 min of exercise could potentially lead to increased or maintained acetylation of lysine residues.

There are a few caveats to this study. The first is that mitochondria were isolated from the EDL muscle rather than gastrocnemius, which was used previously in the metabolomics study. Others have shown differences in fuel use and protein expression in EDL vs. soleus or red gastrocnemius muscle (Rivas et al., 2011). In general, greater differences in protein expression were observed between HCR and LCR in the EDL (Rivas et al., 2011). Secondly, the protein modifications described here are relative small fold-changes and thus might not have large functional consequences. However, dynamic-range suppression with an isobaric tag proteomic approach leads to lower apparent fold-change (Wenger et al., 2011a), thus the actual proteome changes in HCR and LCR are greater than they appear. Finally, there is high variability in the data, which is likely a combination of variation in individual animals and variability in the mitochondrial isolations. Future studies will need to be performed to understand the true biological variability and the consistency of change that occurs with exercise. Analysis of several data sets by

western blotting with pan-acetyl-lysine antibody show consistent trends of lower protein acetylation in HCR with 10 min of exercise (data not shown).

In summary, HCR and LCR have differential expression of many mitochondrial proteins, and HCR have higher expression of proteins involved in fatty acid and BCAA metabolic pathways. Mitochondrial protein acetylation, but not protein expression or phosphorylation, is robustly modified with exercise. HCR have lower protein acetylation with fatty acid and BCAA pathways, consistent with greater metabolic flux through these pathways. Thus, regulation of mitochondrial enzymes by changes in protein expression and acute post-translational modification offer additional explanations for fuel preference at rest and during exercise.

#### **4.5 Summary**

- 40% of the mitochondrial proteome of the EDL is differentially expressed between HCR and LCR.
- Within the proteome, fatty acid and BCAA metabolic pathways are enriched in HCR, while tRNA synthesis pathway is more enriched in LCR.
- Acetylation is dynamic with exercise; both HCR and LCR have deacetylation with 10 min of exercise.
- HCR have less acetylation in oxidative phosphorylation, fatty acid metabolism, and BCAA degradation pathways.

## Chapter 5

### Isotopic tracers to understand fuel use during exercise

In the previous chapter we find that HCR compared to LCR have decreased mitochondrial protein acetylation at rest and with exercise. The most differentially acetylated pathways include oxidative phosphorylation, citrate cycle, BCAA degradation and fatty acid metabolism. We know from the data presented in Chapter 3 that HCR have greater fat oxidation during exercise and that accumulation of metabolites in glycolysis and BCAA metabolism associate with exhaustion. Depletion of BCAA in HCR at 10 min of exercise indicates greater BCAA degradation and decreased acetylation state of BCAA enzymes is also linked to greater pathway flux. In this chapter we explore the kinetics of BCAA metabolism in HCR and LCR using an *in vivo* isotopic tracer approach and confirm increased BCAA metabolism in HCR with exercise.

#### 5.1 Introduction

BCAA metabolism is associated with metabolic health and exercise capacity. Circulating BCAA levels are elevated in individuals with obesity, diabetes, and poor metabolic health (Batch et al., 2013; Connor et al., 2010; Newgard et al., 2009; Wang et al., 2011). Plasma levels of BCAA correlate with insulin resistance and predict development of diabetes (Fiehn et al., 2010; Menni et al., 2013; Wang et al., 2011; Wurtz et al., 2013; Xu et al., 2013). Additionally, Morris et al. (2013) found that

circulating BCAA at rest correlate with exercise capacity, suggesting that pathway kinetics might differ between healthy and non-healthy individuals.

In most tissues BCAA metabolism is localized within the mitochondria, the exception being in the brain. The BCAA (leucine, isoleucine and valine) share enzymes for the first two reactions of BCAA degradation. The first reaction is catalyzed by branched-chain amino-acid transferase (BCAT) and results in the transfer of nitrogen to an alpha-keto acid. This first reaction is a reversible and allows for nitrogen transfer between the BCAA and glutamate. The second reaction is catalyzed by the branched-chain keto acid dehydrogenase (BCKDH) complex. This complex is similar in structure to pyruvate dehydrogenase and alpha ketoglutarate dehydrogenase; it is comprised of 4 subunits and the E1alpha subunit has a phosphorylation site that regulates activity of this enzyme. Although muscle BCKDH complex activity is low at rest, the BCKDH is dephosphorylated (Rush et al., 1995) and activated during exercise (Wagenmakers et al., 1991; Wagenmakers et al., 1989). The other enzymes involved in BCAA metabolism are specific to each amino acid. What regulates activity of these downstream enzymes is unknown. The data presented in Chapter 4 suggest a role for protein acetylation in modifying BCAA enzyme activity.

We probe BCAA metabolism by introducing U-<sup>13</sup>C<sup>15</sup>N valine *in vivo* with and without exercise and measure enrichment of isotope labeling in downstream metabolites by metabolomics. Because HCR have decreases in circulating BCAA with exercise (Chapter 3) and lower protein acetylation within the BCAA pathway, we hypothesized that HCR would have increased valine metabolism with exercise. Additionally by exploring the BCAA metabolic pathway during exercise we hope to access how downstream metabolites (KIV and C3-carnitine) increase with exhaustion.

## **5.2 Methods**

### *5.2.1 Animal protocol and study design*



Female HCR and LCR rats (generation 31, 3 mo of age) were housed at the University of Michigan and the University Committee on Use and Care of Animals, Ann Arbor Michigan approved the study, and procedures were in compliance with the University guidelines, and state and Federal regulations. Although the previous two studies were done using male HCR and LCR, we have data that female HCR and LCR also have clear differences in running capacity and fuel preference during exercise. We chose to use female rats to be more cost-effective; female rats weigh less than male rats and thus require less isotope tracer to be injected.

Exercise capacity was determined using the increasing intensity exercise protocol described previously (3.2.1 - Animal protocol and study design), metrics are presented in **Table 5.1**. Indirect calorimetry (see 3.2.2 - Indirect calorimetry) was performed to determine the effect of intraperitoneally (IP) injected valine (100 mg/kg) vs. control injected saline on exercise capacity and fuel selection (n=6, HCR and LCR, paired comparison design). We found no significant effect of valine injection on fuel use or exercise capacity (**Figure 5.1**).

For the isotopic tracer study, animals were divided into 4 groups: LCR-Rest, LCR-Run, HCR-Rest, HCR-Run (n=4-6). All rats were IP injected with U-<sup>13</sup>C<sup>15</sup>N valine (100 mg/kg) and allowed to rest on a stationary treadmill for 10 min. Rest groups remained on the stationary treadmill for an additional 10 min, while Run groups underwent the increasing intensity treadmill running protocol (**Figure 5.2A**).

Immediately after removal from treadmill animals were briefly anesthetized with inhaled isoflurane (~30 sec) and then euthanized by decapitation. Trunk blood was used to prepare serum and tissues were harvested and immediately frozen in liquid nitrogen.

**Table 5.1 Valine injected animals body weight and running time.** Data are mean  $\pm$  SEM. Asterisks indicate \* $p < 0.05$ .

	Body weight (g)	Running time (min)
LCR-Rest (n=5)	204.8 $\pm$ 6.8	12.72 $\pm$ 1.08
LCR-Run (n=5)	204.5 $\pm$ 2.8	13.00 $\pm$ 0.77
HCR-Rest (n=4)	150.1 $\pm$ 6.7*	64.99 $\pm$ 3.44*
HCR-Run (n=6)	151.5 $\pm$ 5.8*	64.18 $\pm$ 0.91*

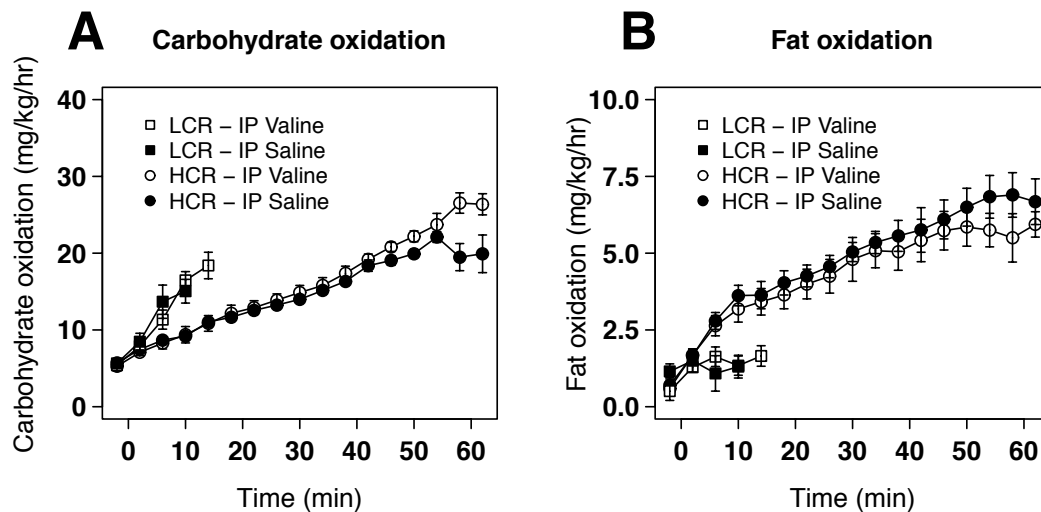


**Figure 5.1 Valine injection does not effect running capacity.** HCR and LCR were injected with valine (100 mg/kg) and run to exhaustion while sampling VO<sub>2</sub> and VCO<sub>2</sub>. Estimated carbohydrate oxidation (A) and fat oxidation (B) were not different between valine injection and control saline injection (n=6). Values are mean  $\pm$  SEM.

### 5.2.2 Muscle and serum metabolites

Frozen gastrocnemius muscle was pulverized in liquid nitrogen with a mortar and pestle. Weighed samples (~ 30 mg) were extracted with 1 mL of solvent mixture consisting of 8:1:1 HPLC grade methanol:chloroform:water. Samples were sonicated (Branson 450, 40% duty cycle, output power 4) for 20 sec and then centrifuged (16,000 x g) to pellet proteins. Serum samples were extracted in solvent mixture of 9:1 of acetonitrile and water, at an serum to solvent ratio of 1:4. Extracted serum

samples were centrifuged to pellet proteins. These extracts were used for subsequent analysis.

Glycolytic, citrate cycle intermediates were measured as described in section 3.2.7 - Muscle and plasma metabolites. For carnitine and branched-chain keto analysis, extracts were dried by vacuum centrifugation at 45°C. Dried samples were reconstituted with water and analyzed using LC-MS. For amino acid quantitation, extracts were dried by vacuum centrifugation at 45°C and resulting samples were derivatized using N-tert-butyltrimethylsilyl-N-methyltrifluoroacetamide (MTBSTFA) and analyzed by GC-MS.

Targeted metabolite quantitation was performed using Agilent Masshunter Quantitative Analysis software. Peak areas were quantitated for mass of naturally occurring isotope (M+0) and mass plus isotope shift (M+1:M+n, n being the number of potential isotope labeled carbons/nitrogens). Correction for natural isotope abundance was performed using an in-house script running in MATLAB (2012a The MathWorks, Natick, MA).

### *5.2.3 Statistical analysis and graphing*

R statistical and graphing environment was used for all subsequent processing of the data: calculating isotope enrichment, statistical analysis and graphing (R Core Team, 2013). Metabolite and enrichment data are presented as mean  $\pm$  standard error of the mean (SEM). Isotope flux comparisons were made between HCR and LCR for Rest and Run conditions and within HCR and LCR between Rest and Run and permutation p-values were used to assess significance ( $p < 0.05$ ) (Fay, 2010).

## **5.3 Results**

### *5.3.1 Injection of Valine leads to 70% serum enrichment*

Preliminary experiments confirm that IP injection of 100 mg/kg valine does not alter fuel selection or running capacity in HCR and LCR (**Figure 5.1**). Isotopic labeled U-<sup>13</sup>C<sup>15</sup>N valine was used to trace BCAA-derived carbon and nitrogen metabolism.

Animals were divided into 4 groups: LCR-Rest, HCR-Rest, LCR-Run, HCR-Run (n=4-6), and all tissue were harvested 20 min after IP-injection of U-<sup>13</sup>C<sup>15</sup>N valine (100 mg/kg) (**Figure 5.2A**). Valine isotope enrichment in serum averaged 68.6 ± 1.4% with no difference between groups (**Figure 5.2B**).

### 5.3.2 HCR have greater valine nitrogen transfer

Valine enrichment in gastrocnemius muscle was comparable to that in serum (**Figure 5.2C**). Valine isotope enrichment, as detected by mass spectrometry, was split between two main isotopes. The injected compound, U-<sup>13</sup>C<sup>15</sup>N valine, is detected 6 Daltons above the mass of unlabeled valine; thus the fully labeled valine is M+6 valine. Reversible transamination into KIV and reamination with unlabeled <sup>14</sup>N yields M+5 valine. HCR had greater M+5 and less M+6 isotope enrichment than LCR (**Figure 5.2D**). The greater M+5 enrichment suggests greater transamination and reamination in HCR. The labeled nitrogen group can be donated to any branched-chain keto-acid or to alpha-ketoglutarate to form BCAA or glutamate. Glutamate is considered main nitrogen acceptor. Muscle glutamate M+1 enrichment is greater in HCR-Run vs. LCR-Run (**Figure 5.2E**).

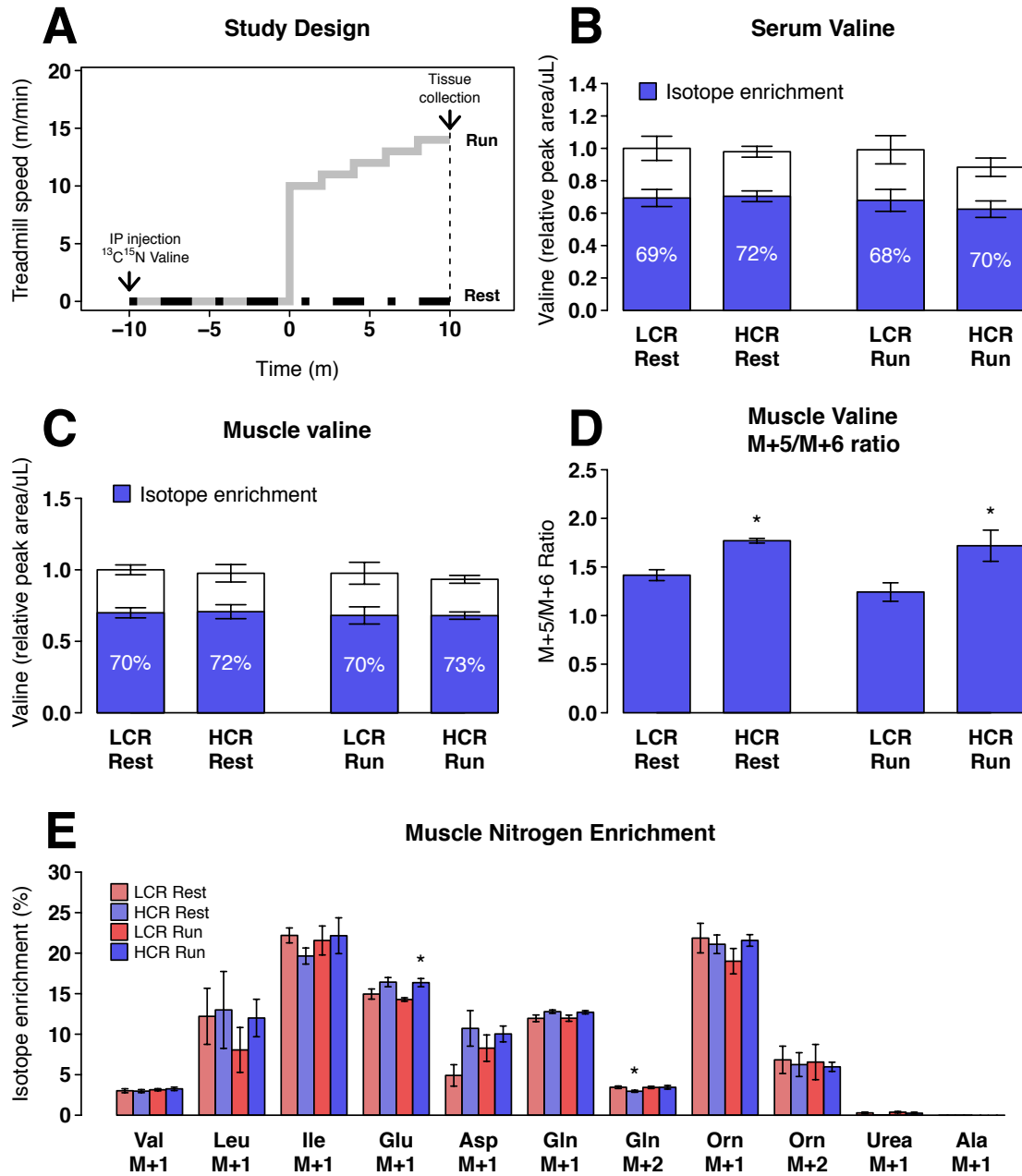


**Figure 5.2 Valine enrichment in serum and muscle.** Animals are injected with U- $^{13}\text{C}^{15}\text{N}$  valine and have 20 min exposure to isotope tracer in both Rest and Run groups (A). Valine isotope enrichment in in serum (B) and muscle (C) was similar between HCR and LCR, but valine reamination, as measured by M+5/M+6 ratio, was greater in HCR (D). Glutamate (Glu), the initial nitrogen acceptor, had greater labeled nitrogen (M+1) enrichment in HCR-Run (E). Ornithine (Orn) contained the greatest nitrogen enrichment and Urea and Alanine (Ala) were found to have little nitrogen enrichment. Values are mean  $\pm$  SEM for each group (n = 4-6). Asterisks indicate \* p<0.05 between HCR and LCR within Rest or Run groups.

### 5.3.3 Nitrogen transfer to other Amino Acids

Glutamate is universal nitrogen donor and will participate in other transamination reactions leading to the formation of aspartate (from oxaloacetate) and alanine (from pyruvate). Although formation of glutamate removes an alpha-ketoglutarate from citrate cycle, transferring this nitrogen to other amino acids can lead to the reformation of alpha-ketoglutarate, resupplying the citrate cycle with carbons. Although previous studies show elevations of BCAA to lead to increases in alanine (Houten et al., 2013), we do not observe labeled nitrogen in the gastrocnemius or serum alanine pools (**Figure 5.2E**). Instead, we observe labeled (M+1) leucine, valine, isoleucine, aspartate, glutamate, glutamine, and ornithine. Glutamine and ornithine have 2 nitrogen groups and we observe some M+2 labeling in these amino acids. With the exception of skeletal muscle glutamate (at run) and M+2 glutamine (at rest), we do not observe significant differences between HCR and LCR.

### 5.3.4 Valine degradation

The next reactions in valine degradation yield NADH and FADH<sub>2</sub> in a manner similar to beta-oxidation. The irreversible BCKDH complex generates the first NADH by converting the keto acid of valine (KIV) to isobutyryl-CoA. Percent isotope enrichment of muscle KIV was similar between HCR and LCR at rest and with running (**Figure 5.3A**). However, total and labeled (M+5) KIV are higher in LCR-Run than HCR-Run. The increase in muscle KIV with exercise in LCR is consistent with the observations of increased KIV with exhaustion (Chapter 3). The increase in KIV values suggests either greater deamination of valine or decreased degradation of KIV by BCKDH.

BCKDH activity will lead to the formation of isobutyryl-CoA, which was not directly measured in this study. Excess isobutyryl-CoA is converted to isobutyryl-carnitine. Isobutyryl-carnitine is a component of the C<sub>4</sub>-carnitine, measured by LC-MS; the other component measured as C<sub>4</sub>-carnitine is butyryl-carnitine derived from fatty acid oxidation. We observe ~35% isotope enrichment of the C<sub>4</sub>-carnitine pool, presuming enrichment of isobutyryl-carnitine is similar to enrichment of KIV, we can calculate that valine-derived carbons account 50-60% of the total C<sub>4</sub>-carnitine pool.

Both LCR and HCR have increases in total and labeled (M+4) C4-carnitine with exercise, suggesting increased flux through BCKDH with exercise (**Figure 5.3B**). However, HCR-Run had greater total and labeled C4-carnitine than LCR-Run, confirming that HCR have greater flux of valine carbons through BCKDH while LCR accumulate KIV upstream of the BCKDH complex.

Downstream reactions convert isobutyryl-CoA into  $\beta$ -hydroxyisobutyric acid ( $\beta$ -HIB) and produce another NADH and a FADH<sub>2</sub>.  $\beta$ -HIB is a primary end product of valine metabolism (Lee and Davis, 1986; Spydevold, 1979; Wagenmakers et al., 1985). With running, HCR and LCR have increased total and labeled (M+4)  $\beta$ -HIB, but there was no significant difference between HCR and LCR **Figure 5.3(C)**.

Although  $\beta$ -HIB is considered the major product of valine metabolism, propionyl-CoA and succinyl-CoA are also possible end products of valine metabolism. Generation of propionyl-CoA from  $\beta$ -HIB will yield another NADH, but consume 1 ATP. We measured propionyl-carnitine (C3-carnitine) to estimate propionyl-CoA production (**Figure 5.3D**). With running, LCR have increased total C3-carnitine similar to what was observed in Chapter 3 (**Figure 3.4B**). However, LCR have no increase in labeled (M+3) C3-carnitine. As a result, HCR-Run have greater percent enrichment and M+3 C3-carnitine than LCR-Run. Based on the low isotopic enrichment, we estimate that only 20% of the C3-carnitine pool is derived from valine metabolism. These data suggest that LCR's increase in C3-carnitine is derived from a non-valine precursor. The other intermediates in valine metabolism (methylmalonate, methylmalonylsemialdehyde, beta aminoisobutyric acid) were not detected. The remaining down-stream metabolite, succinate, increases in LCR with exercise, but there is minimal labeling (M+3) within the succinate pool (**Figure 5.3E**). These data suggest that valine-derived carbons do not contribute to citric acid cycle flux.

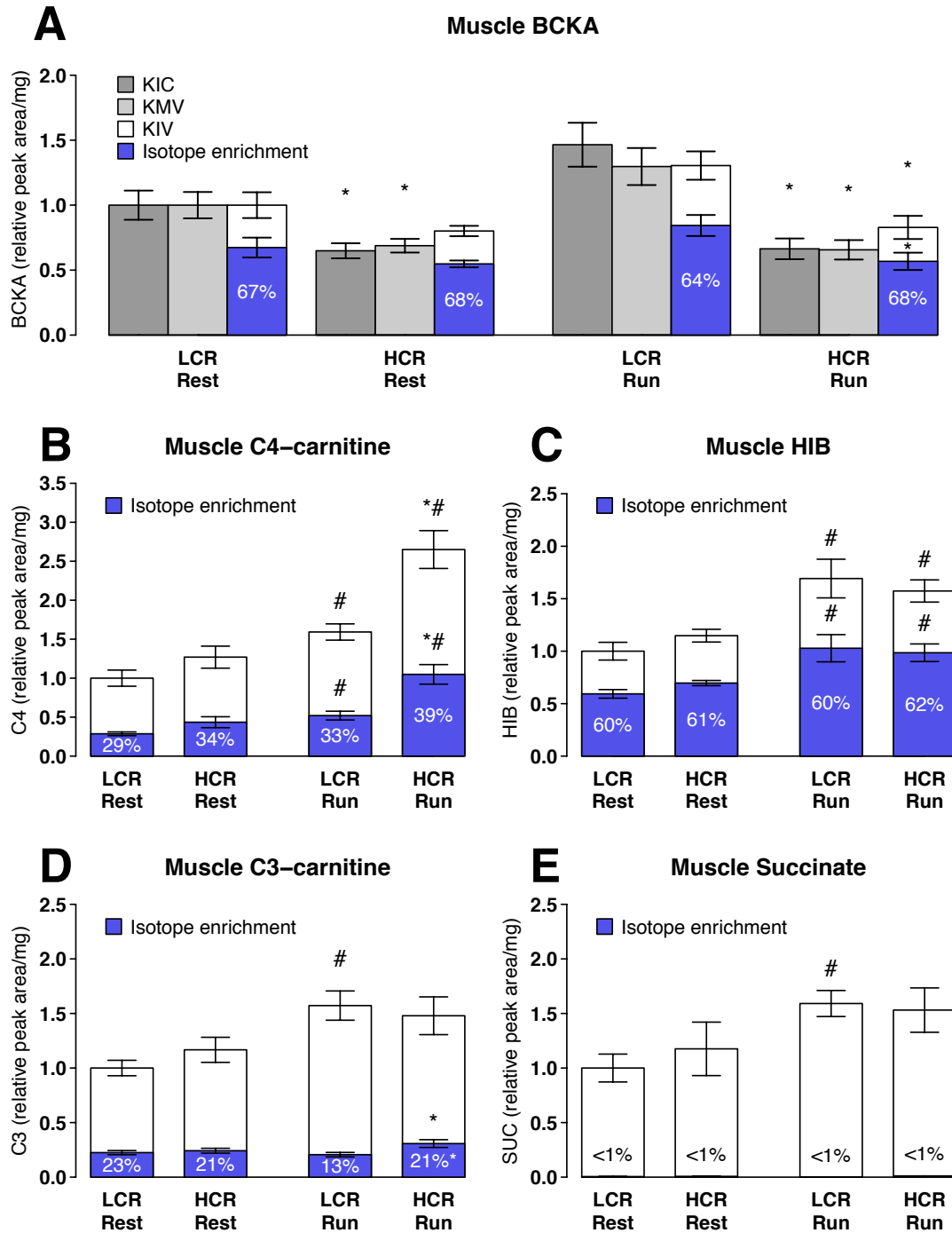


**Figure 5.3 HCR have greater isotope enrichment in downstream metabolites.** HCR and LCR show differences in relative concentration of metabolites downstream of valine: KIV (A), isobutyryl-carnitine (C4) (B),  $\beta$ -hydroxyisobutyrate ( $\beta$ -HIB) (C), and propionyl-carnitine (C3) (D). LCR-Run have greater KIV and other BCKA, while HCR have greater C4-carnitine. Values are mean  $\pm$  SEM for each group (n = 4-6). Asterisks indicate \* p<0.05 between HCR and LCR at a specific time point. Hashes indicates # p<0.05 difference from Rest.



### 5.3.5 HCR have greater BCAA metabolism

Metabolite flux through a pathway is the rate at which the precursor metabolite is broken down to product metabolite. We estimate flux through various parts of the BCAA pathway by looking at ratios of product to precursor isotope-labeled metabolites (**Figure 5.4**). We find subtle differences between HCR and LCR flux at rest, but greater differences between HCR and LCR flux with exercise. From the product:precursor ratio of KIV:valine, it appears that LCR have greater flux through BCAT enzyme (**Figure 5.4A**). However, if we consider that HCR also have greater reaminated valine (M+5) to the fully labeled valine (M+6), it is likely that flux through BCAT is similar between HCR and LCR. Flux through the BCKDH complex as estimated by C4-carnitine:KIV ratio is significantly greater in HCR-Run than LCR-Run, although both HCR and LCR increased flux through BCKDH with exercise (**Figure 5.4B**). Flux through the enzymes from Isobutyryl-CoA to HIB is estimated from the HIB:C4-carnitine ratio (**Figure 5.4C**). Because the elevated C4-carnitine in HCR-Run, there is a lower estimated flux out of isobutyryl-CoA. However flux from KIV to HIB remains overall higher in HCR-Run than LCR-Run (data not shown). The product:precursor ratio for C3-carnitine:HIB is lower in LCR with exercise and lower in LCR-Run vs. HCR-Run (**Figure 5.4D**). This trend holds true for the limited flux from C3-carnitine to Succinate (**Figure 5.4E**).

In **Figure 5.4** we also highlight the relative expression of acetylation and phosphorylation sites within the valine degradation pathway, as identified in Post-translational modifications that occur with exercise. Of the eight enzymes identified to have acetylation sites, 6 are less acetylated in HCR-Run than LCR-Run. Of the 6 phosphorylation sites identified, 5 are associated with the BCKDH complex. Dephosphorylation of BCKDHA is the most well known site of BCAA regulation. It is likely both acetylation state and phosphorylation state play a role in regulating BCAA metabolism.

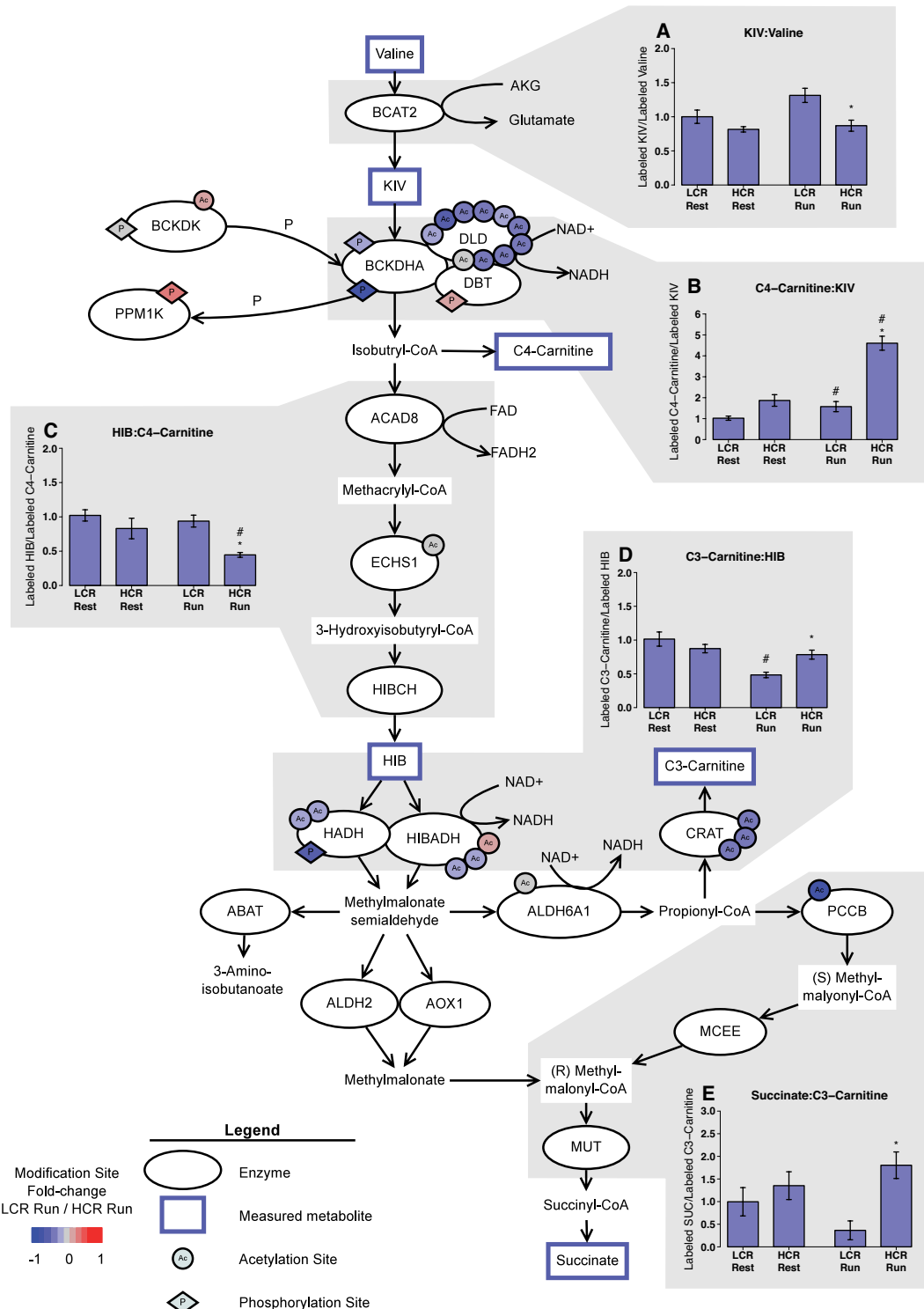


**Figure 5.4 HCR have greater valine metabolism during exercise.** Isotope enrichment of product vs. precursor metabolite estimates flux through the shaded portions of the pathway (A-E). Product:precursor relationships are relative to LCR-Rest (n=4-6). Many of these enzymes were identified as having acetylation sites (see Chapter 3 - Metabolomics to define fuel use during exercise). For each acetylation site, we show relative acetylation state as  $\log_2$  fold change (LCR Run/HCR Run).

## 5.4 Discussion

The flux analysis of U-<sup>13</sup>C<sup>15</sup>N valine during exercise in HCR and LCR suggest that BCAA metabolism increases in both HCR and LCR increase BCAA metabolism with exercise, but HCR have greater nitrogen transamination and greater flux through the BCKDH complex than LCR. Our data suggest that the increase in KIV in LCR at exhaustion is indicative of less flux through the BCKDH complex, and the increase in C3-carnitine with exhaustion is derived from a non-valine precursor. Although valine contributes far less to energy production than glycogen or fatty acids, certain aspects of valine metabolism might support increased running capacity.

Nitrogen flux is important for maintaining the malate-aspartate shuttle, which allows cytosolic NADH to be taken into the mitochondria. Knocking out the BCAA transaminase enzyme (BCAT) in skeletal muscle of mice leads to significant reduction in running capacity and disruption of the malate-aspartate shuttle (She et al., 2010). The conclusion from this knockout study was that BCAA derived transamination was critical for the formation of glutamate, aspartate, glutamine and alanine. Although we do not find labeled nitrogen in the alanine pool, we observe labeled nitrogen in glutamate, aspartate and glutamine. Our data confirm that BCAA participate in nitrogen transamination at rest and during exercise, and in this capacity could support the malate-aspartate shuttle.

The second step in BCAA degradation is irreversible and catalyzed by BCKDH complex. Although muscle BCKDH complex activity is low at rest, BCKDH is dephosphorylated (Rush et al., 1995) and activated during exercise (Wagenmakers et al., 1991). Activation of skeletal muscle BCKDH complex with exercise indicates a role for BCAA metabolism in supporting exercise capacity, and increased activation of BCKDH under low glycogen conditions (van Hall et al., 1996; Wagenmakers et al., 1991) suggests BCKDH is modulated acutely to respond nutrient deficient and is associated with fuel changes in fuel selection.

Beyond changes in phosphorylation state of BCKDH E1alpha subunit, we also found evidence that enzyme acetylation could modulate activity. The Dld subunit of

BCKDH complex is heavily modified by acetylation, and we identified 10 acetyl-sites in DLD that on average had less acetyl-occupancy in HCR-Run vs. LCR-Run (**Figure 5.4**). As DLD is a subunit of the pyruvate dehydrogenase and  $\alpha$ -ketoglutarate dehydrogenase complex, future studies are warranted to dissect the potential modulation of these complexes secondary to changes in DLD acetylation.

One major caveat of this study is that by introducing a bolus of valine for the isotope tracer study, we likely create greater flux through the valine pathway than would be observed under non-elevated valine conditions. Acute ingestion of BCAA has been shown to increase activation of BCKDH at rest and during exercise (van Hall et al., 1996). However, despite this elevated valine condition, we observed increases in valine metabolism with exercise and differences in valine flux between HCR and LCR. Secondly, valine metabolism might not reflect the flux of the other BCAA. In our metabolomics analysis, we found plasma C5-carnitine was lower in HCR at rest, and elevation of C5-carnitine was associated with exhaustion. C5-carnitine is not a valine-derived metabolite, but is instead derived from leucine and isoleucine degradation. One of the most differentially expressed proteins between HCR and LCR was isoleucine-specific enzyme ACADSB (Appendix C, **Table C.1**). The upregulation of ACADSB might lead to the lower levels of C5-carnitine in HCR vs. LCR. Thus, we suspect using the isotopic tracer isoleucine would demonstrate even more dramatic differences in BCAA flux between HCR and LCR.

In conclusion, HCR have greater valine metabolism than LCR with exercise. This has implications to exercise capacity. Resting plasma BCAA levels were inversely correlated with exercise capacity (Morris et al., 2013), and disruption of proteins involved in BCAA metabolism lead to a significant decrease in running capacity (She et al., 2010). Both acetylation and phosphorylation of the BCKDH complex were modulated with exercise in HCR more than LCR, suggesting both phosphorylation and acetylation have a role in modulating BCAA metabolism.

## 5.5 Summary

- We observed similar uptake of U- $^{13}\text{C}^{15}\text{N}$  valine in HCR and LCR
- Metabolism of U- $^{13}\text{C}^{15}\text{N}$  valine increased with exercise in both HCR and LCR

- HCR have greater nitrogen transamination and reamination
- HCR also have greater flux through the BCKDH complex, resulting in less accumulation of KIV and increased production of C4-carnitine.

## Chapter 6

### Study implications

The previous chapters have focused on understanding the metabolic regulation of high and low exercise capacity. We found that HCR have higher fat oxidation during exercise than LCR, and that HCR have greater protein abundance and post-translation modifications of enzymes within fatty acid and BCAA metabolic pathways.

#### 6.1 Model for enhanced exercise capacity

Based on our results, we propose that animals with enhanced oxidative capacity have increased fatty acid and BCAA utilization. The higher capacity to oxidize these substrates is supported by the upregulation and deacetylation of proteins within these oxidative pathways (**Figure 6.1**). In conditions of increasing energy demand such as exercise, HCR are able to continue production of ATP through oxidative phosphorylation, at a time when LCR have reached their maximal oxidative capacity. When the ability to oxidize substrate becomes limiting, glycogen is mobilized and lactate is generated through anaerobic glycolysis. The buildup of acetylcarnitine, malate, and other substrates in muscle at exhaustion in both HCR and LCR points to the imbalance between the influx of substrates and ability to oxidize these substrates.

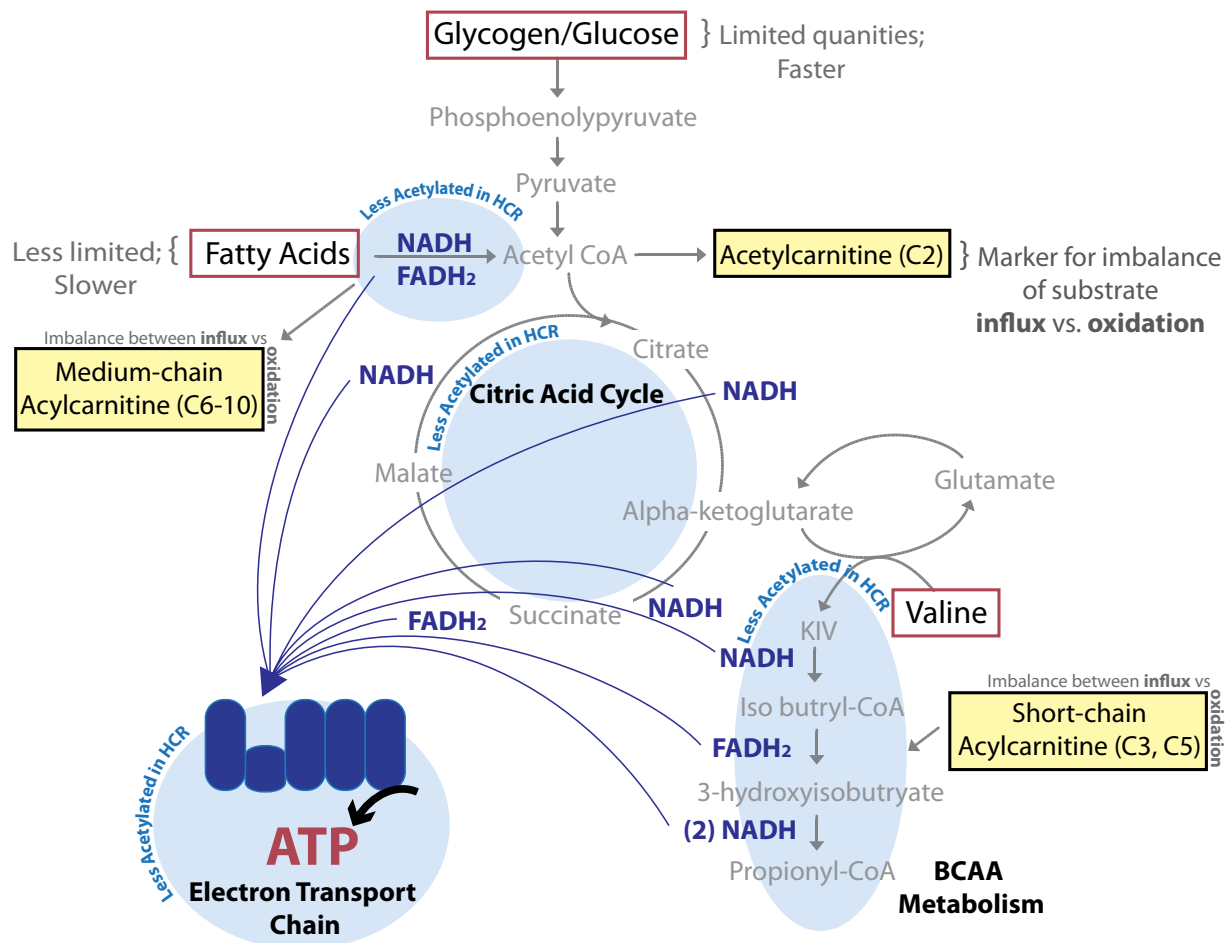


**Figure 6.1 HCR have enhanced capacity to oxidize fatty acids and BCAA.** This enhanced capacity is supported by greater protein expression and lower protein acetylation within FA and BCAA metabolic pathways, as well as the citric acid cycle and the electron transport chain. Enhanced oxidative efficiency leads to slower accumulation of metabolic intermediates such as short- and medium- chain acylcarnitines, which indicate imbalances between substrate supply and downstream oxidation.

## 6.2 Implications to health and longevity

Importantly, metabolic differences between HCR and LCR during exercise inform us about altered metabolic pathways that underlie risk for metabolic disease.

Decreased fat oxidation during exercise (Hall et al., 2010) and impaired switching between glucose and fatty acid oxidation are both linked to insulin resistance and diabetes (Kelley and Mandarino, 2000). Many studies also link altered BCAA metabolism to the development of insulin resistance and diabetes (Wang et al., 2011; Wurtz et al., 2013). Circulating BCAA levels are elevated with obesity, diabetes, and poor metabolic health (Batch et al., 2013; Connor et al., 2010;

Newgard et al., 2009; Wang et al., 2011) and correlate with measures of insulin resistance (Fiehn et al., 2010; Menni et al., 2013; Xu et al., 2013). Notably, resting plasma BCAA levels are also inversely correlated with exercise capacity (Morris et al., 2013). Based on our data, changes in the capacity of fatty acid and BCAA oxidation could be due to differential expression and post-translational modification of enzymes in fatty acid and BCAA metabolism, as well as citric acid cycle and electron transport chain. Intrinsic genetic differences could be amplified by mitochondrial protein acetylation in the setting of inactivity and over nutrition (Hirschey et al., 2011). Thus, phenotypes associated with metabolic disease, such as increased circulating BCAA and metabolic inflexibility, may reflect differences in the capacity to utilize BCAA and fatty acids.

Beyond implications to metabolic health, these data suggest a possible mechanistic link between exercise capacity and longevity. Like HCR, a number of longevity models have elevated fatty acid and BCAA oxidation, including Ames dwarf and growth hormone receptor knock-out mice (Westbrook et al., 2009) and caloric restriction in drosophila (Katewa et al., 2012), mice (Bruss et al., 2010) and humans (Huffman et al., 2012). Coincidentally, long-lived organisms with mitochondrial mutations have elevated fatty acid utilization and display upregulation of energy producing pathways (Martin et al., 2011; Munkacsy and Rea, 2014). Like these models of longevity, HCR and LCR show pathway specific differences in mitochondrial protein abundance, with 40.6% of mitochondrial proteins differentially expressed between the strains and specific upregulation of fatty acid and BCAA metabolic enzymes.

### **6.3 Future Directions**

This study leads to several new ideas that should be explored further. First, lysine acetylation is an increasingly recognized post-translational modification, and yet the functional characterization of specific lysine residues is sparse (Xiong and Guan, 2012). Consequently, our interpretation of global changes in lysine acetylation is based in changes in physiology that occur with Sirt3 disruption or calorie restriction (Hallows et al., 2011; Hebert et al., 2013; Hirschey et al., 2010; Rardin et al., 2013;



Still et al., 2013). Also, global acetylation is tissue specific (Lundby et al., 2012), and thus physiological consequences of acetylation likely differ by tissue type. Though generalizations about global acetylation are useful, characterization of specific modifications would aid our understanding about the functional consequences to metabolism and other processes.

Second, it is clear that metabolism helps regulate lysine acetylation (and other acyl-group modifications) both by regulating production of small-chain acyl groups (acetyl-CoA, propionyl-CoA, succinyl-CoA, malonyl-CoA) and by modulating NAD<sup>+</sup> availability (Choudhary et al., 2014). Thus, changes in lysine modification can be indicative of nutrient status and be responsive to a wide-range of metabolic changes. Acute changes in non-histone lysine modification are just beginning to be explored (Masri et al., 2013; Zhang et al., 2012), and further characterization of lysine modification kinetics and metabolic regulation are important next steps for understanding dynamics of protein regulation.

Third, metabolic differences between HCR and LCR likely underlie divergence in health and longevity. As discussed above, long-lived species also have changes in metabolism and mitochondrial restructuring (Munkacsy and Rea, 2014). The differences in mitochondrial content between HCR and LCR deserve further explanation. It is possible that mitochondrial dynamics (mitochondrial breakdown and mitochondrial biogenesis) is supporting metabolic and phenotypic differences in HCR and LCR. There is evidence that metabolite intermediates can act as signals to mediate changes in mitochondrial dynamics (Butler et al., 2013). By combining genetic (Ren et al., 2013) and metabolomic approaches to understand exercise capacity, we may provide important insights into the integration of signals in modulating the whole-animal response to exercise and aging.

## **Appendices**

### **A. Metabolomics data set**

Metabolomics data set (Table A.1) contains muscle and plasma metabolite values for HCR and LCR at 0, 10, and 45 min (HCR only) of exercise. Metabolite values are presented as mean  $\pm$  SEM for each group, and permutation p-values are given for each comparison.

Table A.1 Muscle and plasma metabolite values from HCR and LCR with exercise.

Metabolites by Category	Units	LCR 0 min Mean ± SEM	HCR 0 min Mean ± SEM	LCR 10 min Mean ± SEM	HCR 10 min Mean ± SEM	HCR 45 min Mean ± SEM	Permutation P-Values:				
							LCR 0 min vs LCR 10 min	HCR 0 min vs HCR 10 min	HCR 0 min vs HCR 45 min	LCR 0 min vs HCR 0 min	LCR 10 min vs HCR 10 min
<b>Metabolites by Category</b>											
<b>Muscle Metabolites:</b>											
<b>Glycolysis</b>											
Muscle Glycogen	µmol/g	22.07 ± 1.72	22.69 ± 1.18	7.71 ± 1.32	21.45 ± 3.51	3.88 ± 2.19	<b>0.0022</b>	0.77	<b>0.0022</b>	0.78	<b>0.0047</b>
Muscle Hexose	rel. peak area/mg	1 ± 0.065	0.838 ± 0.059	0.835 ± 0.068	0.985 ± 0.070	0.939 ± 0.047	0.11	0.14	0.21	0.095	0.15
Muscle Hexose-phosphoate	rel. peak area/mg	1 ± 0.202	1.53 ± 0.171	0.818 ± 0.189	1.67 ± 0.255	1.02 ± 0.236	0.51	0.67	0.11	0.08	<b>0.022</b>
Muscle Fructose-1,6-bisphosphate	rel. peak area/mg	1 ± 0.502	0.32 ± 0.175	0.92 ± 0.43	0.26 ± 0.050	0.13 ± 0.009	0.91	0.88	0.26	0.23	0.17
Muscle Dihydroxy-acetone-phosphate	rel. peak area/mg	1 ± 0.129	1.24 ± 0.111	0.677 ± 0.135	1.35 ± 0.195	0.839 ± 0.193	0.11	0.64	0.11	0.21	<b>0.02</b>
Muscle Glycerol-3-phosphate	rel. peak area/mg	1 ± 0.136	0.845 ± 0.082	1.2 ± 0.155	0.929 ± 0.081	1.07 ± 0.126	0.35	0.48	0.16	0.34	0.14
Muscle 2- and 3-Phosphoglycerate	rel. peak area/mg	1 ± 0.538	0.154 ± 0.029	0.365 ± 0.169	0.138 ± 0.028	0.070 ± 0.010	0.34	0.7	<b>0.022</b>	0.23	0.27
Muscle Phosphoenolpyruvate	rel. peak area/mg	1 ± 0.491	0.133 ± 0.019	0.442 ± 0.157	0.244 ± 0.056	0.132 ± 0.045	0.37	0.11	0.97	0.063	0.23
Muscle Lactate	rel. peak area/mg	1 ± 0.133	0.856 ± 0.119	1.24 ± 0.137	0.928 ± 0.069	1.08 ± 0.122	0.24	0.59	0.22	0.42	<b>0.044</b>
<b>Pentose Phosphate Pathway</b>											
Muscle Rib(ul)ose-5-phosphate	rel. peak area/mg	1 ± 0.112	0.79 ± 0.064	1.15 ± 0.214	0.876 ± 0.052	0.939 ± 0.084	0.58	0.3	0.19	0.16	0.24
Muscle Erythrose-4-phosphate	rel. peak area/mg	1 ± 0.19	1.46 ± 0.145	0.81 ± 0.194	1.56 ± 0.193	1.01 ± 0.202	0.48	0.71	0.11	0.087	<b>0.021</b>
<b>Citric Acid Cycle</b>											
Muscle Acetyl-CoA	rel. peak area/mg	1 ± 0.286	1.39 ± 0.179	1.73 ± 0.348	1.56 ± 0.090	2.49 ± 0.26	0.14	0.43	<b>0.0043</b>	0.27	0.62
Muscle Citrate	rel. peak area/mg	1 ± 0.025	1.03 ± 0.102	1.11 ± 0.039	1.26 ± 0.049	1.65 ± 0.094	<b>0.039</b>	0.061	<b>0.0043</b>	0.81	<b>0.042</b>
Muscle Malate	rel. peak area/mg	1 ± 0.159	0.851 ± 0.048	1.95 ± 0.112	1.05 ± 0.060	2.33 ± 0.221	<b>0.0043</b>	<b>0.031</b>	<b>0.0022</b>	0.48	<b>0.0012</b>
Muscle Succinate	rel. peak area/mg	1 ± 0.091	1.05 ± 0.111	1.55 ± 0.111	1.11 ± 0.111	1.61 ± 0.079	<b>0.0065</b>	0.71	<b>0.0065</b>	0.74	<b>0.017</b>
<b>Nucleotides and Cofactors</b>											
Muscle AMP	rel. peak area/mg	1 ± 0.246	0.626 ± 0.053	2.14 ± 0.537	0.882 ± 0.113	1.82 ± 0.29	0.08	0.55	<b>0.0022</b>	0.21	<b>0.037</b>
Muscle ADP	rel. peak area/mg	1 ± 0.167	0.791 ± 0.051	1.71 ± 0.344	0.964 ± 0.094	1.61 ± 0.222	0.089	0.15	<b>0.0043</b>	0.32	<b>0.041</b>
Muscle ATP	rel. peak area/mg	1 ± 0.054	0.959 ± 0.031	1.09 ± 0.035	1.05 ± 0.056	1.15 ± 0.043	0.19	0.21	<b>0.0087</b>	0.52	0.56
Muscle CMP	rel. peak area/mg	1 ± 0.116	1 ± 0.128	1.03 ± 0.071	1.28 ± 0.045	1.01 ± 0.082	0.82	0.056	0.97	1	<b>0.016</b>
Muscle CTP	rel. peak area/mg	1 ± 0.083	0.923 ± 0.077	1.13 ± 0.118	0.939 ± 0.129	1.32 ± 0.093	0.37	0.93	<b>0.013</b>	0.5	0.28
Muscle GMP	rel. peak area/mg	1 ± 0.138	0.919 ± 0.111	1.58 ± 0.314	0.896 ± 0.121	1.31 ± 0.063	0.11	0.91	<b>0.013</b>	0.67	<b>0.042</b>
Muscle GDP	rel. peak area/mg	1 ± 0.138	0.73 ± 0.062	1.12 ± 0.195	0.842 ± 0.045	1.19 ± 0.095	0.66	0.17	<b>0.0043</b>	0.11	0.16
Muscle GTP	rel. peak area/mg	1 ± 0.082	0.969 ± 0.081	1.23 ± 0.183	0.992 ± 0.113	1.27 ± 0.116	0.3	0.89	0.058	0.77	0.29
Muscle IMP	rel. peak area/mg	1 ± 0.223	0.476 ± 0.042	5.72 ± 2.22	1.55 ± 0.438	7.78 ± 2.94	<b>0.013</b>	<b>0.0023</b>	<b>0.0022</b>	<b>0.024</b>	<b>0.029</b>
Muscle IDP	rel. peak area/mg	1 ± 0.197	1.02 ± 0.11	2.47 ± 0.696	1.37 ± 0.222	1.91 ± 0.356	0.058	0.22	<b>0.0022</b>	0.95	0.15
Muscle ITP	rel. peak area/mg	1 ± 0.054	1.02 ± 0.077	1.21 ± 0.072	1 ± 0.133	1.2 ± 0.051	<b>0.043</b>	0.92	0.08	0.8	0.23
Muscle UMP	rel. peak area/mg	1 ± 0.201	0.872 ± 0.073	1.36 ± 0.42	0.916 ± 0.166	1.02 ± 0.091	0.53	0.82	0.23	0.56	0.38
Muscle UDP	rel. peak area/mg	1 ± 0.179	0.832 ± 0.111	1.29 ± 0.219	0.947 ± 0.112	1.12 ± 0.21	0.34	0.46	0.25	0.45	0.18
Muscle UTP	rel. peak area/mg	1 ± 0.074	0.977 ± 0.054	1.06 ± 0.084	0.988 ± 0.098	0.899 ± 0.031	0.56	0.95	0.24	0.82	0.56
Muscle XMP	rel. peak area/mg	1 ± 0.192	1.06 ± 0.181	1.22 ± 0.238	1.39 ± 0.25	1.33 ± 0.039	0.51	0.33	0.39	0.81	0.63
Muscle NAD+	rel. peak area/mg	1 ± 0.059	1.05 ± 0.054	1.04 ± 0.051	1.08 ± 0.058	1.06 ± 0.033	0.62	0.77	0.86	0.56	0.65
Muscle NADH	rel. peak area/mg	1 ± 0.107	1.1 ± 0.059	1.61 ± 0.128	1.41 ± 0.182	1.9 ± 0.208	<b>0.011</b>	0.17	<b>0.0022</b>	0.42	0.38

Table A.1

Table A.1 Cont.

Muscle NADP+	rel. peak area/mg	1 ± 0.093	1.1 ± 0.119	1.1 ± 0.108	1.01 ± 0.119	0.956 ± 0.095	0.47	0.63	0.41	0.55	0.6
Muscle NADPH	rel. peak area/mg	1 ± 0.146	1.64 ± 0.183	1.4 ± 0.234	1.68 ± 0.182	2.53 ± 0.294	0.17	0.83	<b>0.035</b>	<b>0.019</b>	0.29
Muscle FAD	rel. peak area/mg	1 ± 0.081	1.32 ± 0.06	1.21 ± 0.114	1.35 ± 0.1	1.59 ± 0.058	0.16	0.79	<b>0.0087</b>	<b>0.011</b>	0.37
Muscle FMN	rel. peak area/mg	1 ± 0.258	0.939 ± 0.104	1.45 ± 0.249	1.63 ± 0.352	1.11 ± 0.152	0.23	0.1	0.34	0.84	0.7
Muscle Coenzyme A	rel. peak area/mg	1 ± 0.187	1.1 ± 0.067	1.01 ± 0.202	0.892 ± 0.11	0.858 ± 0.095	0.95	0.15	0.065	0.63	0.59
<b>Nucleosides</b>											
Muscle Adenine	rel. peak area/mg	1 ± 0.327	1.4 ± 0.182	1.53 ± 0.6	2.27 ± 0.332	2.39 ± 0.28	0.5	<b>0.031</b>	<b>0.015</b>	0.31	0.28
Muscle Adenosine	rel. peak area/mg	1 ± 0.347	1.48 ± 0.204	1.73 ± 0.695	2.44 ± 0.379	2.6 ± 0.277	0.39	<b>0.042</b>	<b>0.013</b>	0.26	0.37
Muscle Hypoxanthine	rel. peak area/mg	1 ± 0.116	0.954 ± 0.097	0.973 ± 0.065	0.951 ± 0.052	0.997 ± 0.087	0.84	0.97	0.75	0.76	0.79
Muscle Inosine	rel. peak area/mg	1 ± 0.189	0.726 ± 0.138	1.79 ± 0.436	1.28 ± 0.193	1.56 ± 0.216	0.13	<b>0.036</b>	<b>0.011</b>	0.23	0.27
Muscle Uracil	rel. peak area/mg	1 ± 0.234	1.23 ± 0.181	1.53 ± 0.259	1.22 ± 0.197	2.24 ± 0.496	0.15	0.97	0.05	0.44	0.34
Muscle Xanthine	rel. peak area/mg	1 ± 0.217	0.798 ± 0.183	1.86 ± 0.521	1.43 ± 0.176	2.44 ± 0.429	0.18	<b>0.03</b>	<b>0.015</b>	0.51	0.44
<b>Sugar-Nucleotides</b>											
Muscle ADP-D-Glucose	rel. peak area/mg	1 ± 0.117	1.14 ± 0.189	1.44 ± 0.193	1.22 ± 0.085	1.45 ± 0.152	0.069	0.64	0.23	0.56	0.35
Muscle N-Acetyl-glucosamine-phosphate	rel. peak area/mg	1 ± 0.075	0.793 ± 0.088	0.978 ± 0.166	0.805 ± 0.080	1.06 ± 0.063	0.92	0.93	<b>0.041</b>	0.11	0.36
Muscle UDP-D-glucose	rel. peak area/mg	1 ± 0.086	1.11 ± 0.06	2.39 ± 0.179	1.36 ± 0.084	3.81 ± 0.504	<b>0.0022</b>	<b>0.049</b>	<b>0.0022</b>	0.3	<b>0.0012</b>
Muscle UDP-D-glucuronate	rel. peak area/mg	1 ± 0.316	1.9 ± 0.32	0.623 ± 0.239	2.19 ± 0.515	0.923 ± 0.373	0.34	0.66	0.078	0.082	<b>0.017</b>
Muscle UDP-N-Acetyl-D-glucosamine	rel. peak area/mg	1 ± 0.061	1.07 ± 0.058	0.914 ± 0.048	1.07 ± 0.044	1.02 ± 0.026	0.29	0.99	0.44	0.42	<b>0.036</b>
<b>Amino Acids</b>											
Muscle Alanine	µM/mg	5.63 ± 0.39	7.14 ± 0.59	5.95 ± 0.36	5.63 ± 0.41	4.88 ± 0.53	0.56	0.055	<b>0.019</b>	0.063	0.57
Muscle Glycine	µM/mg	5.02 ± 0.63	5.50 ± 0.22	4.95 ± 0.26	4.89 ± 0.39	5.62 ± 0.35	0.91	0.22	0.78	0.51	0.91
Muscle Valine	µM/mg	0.563 ± 0.044	0.532 ± 0.033	0.656 ± 0.032	0.474 ± 0.034	0.485 ± 0.026	0.2	0.25	0.3	0.57	<b>0.0065</b>
Muscle Leucine	µM/mg	0.452 ± 0.033	0.367 ± 0.031	0.485 ± 0.021	0.33 ± 0.024	0.382 ± 0.031	0.47	0.34	0.72	0.093	<b>0.0023</b>
Muscle Isoleucine	µM/mg	0.273 ± 0.020	0.234 ± 0.022	0.296 ± 0.012	0.184 ± 0.01	0.228 ± 0.020	0.36	0.058	0.84	0.22	<b>0.0012</b>
Muscle Threonine	µM/mg	1.41 ± 0.26	1.37 ± 0.03	1.94 ± 0.56	1.59 ± 0.20	1.58 ± 0.15	0.46	0.44	0.33	0.8	0.56
Muscle Proline	µM/mg	0.784 ± 0.101	0.664 ± 0.025	0.69 ± 0.073	0.637 ± 0.068	0.727 ± 0.062	0.47	0.64	0.39	0.27	0.55
Muscle Asparagine	µM/mg	0.493 ± 0.067	0.466 ± 0.061	0.466 ± 0.049	0.511 ± 0.063	0.513 ± 0.035	0.74	0.62	0.53	0.77	0.64
Muscle Aspartic Acid	µM/mg	0.418 ± 0.071	0.332 ± 0.078	0.449 ± 0.09	0.45 ± 0.09	0.71 ± 0.16	0.55	0.35	0.063	0.4	0.73
Muscle Methionine	µM/mg	0.12 ± 0.02	0.14 ± 0.02	0.138 ± 0.025	0.11 ± 0.016	0.157 ± 0.017	0.6	0.3	0.52	0.53	0.38
Muscle Glutamic Acid	µM/mg	3.74 ± 0.50	3.36 ± 0.29	2.68 ± 0.20	2.43 ± 0.32	2.84 ± 0.43	0.078	0.058	0.31	0.52	0.51
Muscle Phenylalanine	µM/mg	0.211 ± 0.02	0.165 ± 0.011	0.225 ± 0.015	0.191 ± 0.017	0.281 ± 0.024	0.62	0.28	<b>0.0022</b>	0.071	0.18
Muscle Glutamine	µM/mg	30.0 ± 9.0	20.6 ± 3.3	31.1 ± 11	14.9 ± 5.0	12 ± 2.8	0.94	0.37	0.078	0.39	0.2
Muscle Ornithine	µM/mg	0.0402 ± 0.0085	0.0281 ± 0.0074	0.0445 ± 0.0103	0.0072 ± 0.0053	0.0227 ± 0.0051	0.96	<b>0.042</b>	0.57	0.31	<b>0.0076</b>
Muscle Lysine	µM/mg	0.456 ± 0.098	1.01 ± 0.17	0.663 ± 0.067	0.9 ± 0.146	0.949 ± 0.16	0.13	0.63	0.81	<b>0.039</b>	0.12
Muscle Histidine	µM/mg	0.640 ± 0.088	0.669 ± 0.087	0.676 ± 0.101	0.762 ± 0.078	0.737 ± 0.087	0.79	0.44	0.59	0.79	0.49
Muscle Tyrosine	µM/mg	0.361 ± 0.037	0.279 ± 0.029	0.381 ± 0.031	0.294 ± 0.025	0.472 ± 0.051	0.69	0.71	<b>0.011</b>	0.12	0.055
Muscle Tryptophan	µM/mg	0.109 ± 0.010	0.092 ± 0.007	0.117 ± 0.007	0.1 ± 0.009	0.16 ± 0.015	0.52	0.52	<b>0.0022</b>	0.21	0.19
<b>Lipids</b>											
Muscle Palmitic acid	rel. peak area/mg	1 ± 0.121	0.845 ± 0.106	1.23 ± 0.174	0.812 ± 0.108	0.924 ± 0.058	0.3	0.82	0.52	0.35	0.058
Muscle Stearic acid	rel. peak area/mg	1 ± 0.122	0.717 ± 0.072	1.18 ± 0.179	0.746 ± 0.084	0.847 ± 0.056	0.41	0.79	0.18	0.076	<b>0.038</b>
Muscle Oleic acid	rel. peak area/mg	1 ± 0.29	1.12 ± 0.39	1.09 ± 0.405	0.775 ± 0.136	0.896 ± 0.205	0.77	0.49	0.66	0.9	0.45
Muscle PC 34:2	rel. peak area/mg	1 ± 0.101	1.07 ± 0.035	1.04 ± 0.022	1.22 ± 0.135	1.17 ± 0.060	0.71	0.35	0.19	0.53	0.26

Table A.1 Cont.

Muscle PC 36:4	rel. peak area/mg	1 ± 0.064	0.92 ± 0.077	1.09 ± 0.063	0.904 ± 0.042	1.01 ± 0.054	0.32	0.84	0.38	0.44	<b>0.028</b>
Muscle PC 38:6	rel. peak area/mg	1 ± 0.034	1.02 ± 0.057	1.08 ± 0.055	0.945 ± 0.075	1.18 ± 0.064	0.26	0.48	0.087	0.8	0.19
Muscle PE 38:4	rel. peak area/mg	1 ± 0.080	0.883 ± 0.057	1.02 ± 0.067	0.909 ± 0.082	1.03 ± 0.09	0.84	0.8	0.21	0.25	0.33
Muscle PE 38:6	rel. peak area/mg	1 ± 0.057	1.18 ± 0.102	1.17 ± 0.047	1.13 ± 0.097	1.35 ± 0.027	<b>0.041</b>	0.79	0.097	0.17	0.73
Muscle PG 34:1	rel. peak area/mg	1 ± 0.068	1.06 ± 0.071	1.13 ± 0.059	1.1 ± 0.088	1.25 ± 0.052	0.18	0.75	0.056	0.55	0.78
Muscle PI 38:4	rel. peak area/mg	1 ± 0.048	1 ± 0.048	1.06 ± 0.051	0.99 ± 0.036	1.14 ± 0.028	0.43	0.85	<b>0.028</b>	0.99	0.29
Muscle PS 38:4	rel. peak area/mg	1 ± 0.045	1.05 ± 0.032	1.06 ± 0.071	1.07 ± 0.036	1.18 ± 0.051	0.49	0.66	0.061	0.39	0.93
Muscle PS 40:6	rel. peak area/mg	1 ± 0.054	0.94 ± 0.051	1.1 ± 0.061	0.86 ± 0.07	1.15 ± 0.055	0.25	0.4	<b>0.019</b>	0.44	<b>0.016</b>
<b>Acylcarnitines</b>											
Muscle L-Carnitine	p mol/mg	483 ± 76.7	396 ± 19.7	313 ± 16.3	307 ± 32.3	265 ± 30.2	<b>0.0055</b>	0.051	<b>0.011</b>	0.34	0.86
Muscle C2 Carnitine	p mol/mg	339 ± 34.2	349 ± 57.3	643 ± 50.8	434 ± 33	689 ± 39.3	<b>0.0022</b>	0.21	<b>0.0022</b>	0.88	<b>0.0047</b>
Muscle C3 Carnitine	p mol/mg	3.37 ± 0.465	4.33 ± 0.839	9.75 ± 1.33	4.04 ± 0.332	20.2 ± 4.52	<b>0.0022</b>	0.75	<b>0.0022</b>	0.35	<b>0.0012</b>
Muscle C4 Carnitine	p mol/mg	4.09 ± 0.732	5.12 ± 1.45	12.3 ± 3.14	9.85 ± 1.34	15.6 ± 2.07	<b>0.0065</b>	<b>0.04</b>	<b>0.0043</b>	0.55	0.49
Muscle C5:0 Carnitine	p mol/mg	1.11 ± 0.417	0.423 ± 0.071	1.24 ± 0.202	0.712 ± 0.065	1.69 ± 0.274	0.82	<b>0.014</b>	<b>0.0043</b>	<b>0.045</b>	<b>0.017</b>
Muscle C6:0 Carnitine	rel. peak area/mg	1 ± 0.21	0.809 ± 0.177	1.43 ± 0.526	1.29 ± 0.193	2.61 ± 0.713	0.58	0.099	<b>0.013</b>	0.49	0.83
Muscle C8:0 Carnitine	rel. peak area/mg	0.274 ± 0.055	0.178 ± 0.034	0.307 ± 0.129	0.237 ± 0.038	0.507 ± 0.146	0.9	0.29	<b>0.017</b>	0.16	0.76
Muscle C8:1 Carnitine	rel. peak area/mg	1 ± 0.206	0.635 ± 0.065	0.898 ± 0.304	0.654 ± 0.074	2.13 ± 0.453	0.76	0.86	<b>0.0022</b>	0.097	0.57
Muscle C10:0 Carnitine	rel. peak area/mg	1 ± 0.192	0.697 ± 0.123	0.973 ± 0.343	1.11 ± 0.208	1.94 ± 0.685	0.96	0.13	<b>0.0022</b>	0.22	0.74
Muscle C10:1 Carnitine	rel. peak area/mg	1 ± 0.284	0.295 ± 0.032	0.805 ± 0.493	0.358 ± 0.066	0.752 ± 0.108	0.76	0.42	<b>0.0022</b>	<b>0.011</b>	0.6
Muscle C12:0-OH Carnitine	rel. peak area/mg	1 ± 0.22	0.741 ± 0.16	1.43 ± 0.512	1.1 ± 0.213	2.09 ± 0.516	0.56	0.21	<b>0.024</b>	0.35	0.62
Muscle C12:0 Carnitine	rel. peak area/mg	1 ± 0.204	0.491 ± 0.103	0.859 ± 0.249	0.951 ± 0.205	1.55 ± 0.526	0.68	0.087	0.067	0.061	0.78
Muscle C12:1 Carnitine	rel. peak area/mg	1 ± 0.218	0.473 ± 0.085	0.773 ± 0.226	0.794 ± 0.166	1.44 ± 0.468	0.48	0.13	<b>0.043</b>	<b>0.045</b>	0.95
Muscle C14:0-OH Carnitine	rel. peak area/mg	1 ± 0.227	0.906 ± 0.246	1.67 ± 0.488	1.68 ± 0.369	2.84 ± 0.64	0.25	0.13	<b>0.017</b>	0.78	0.99
Muscle C14:0 Carnitine	p mol/mg	0.986 ± 0.201	0.427 ± 0.105	1.16 ± 0.52	0.907 ± 0.225	1.54 ± 0.488	0.88	0.1	<b>0.026</b>	<b>0.043</b>	0.73
Muscle C14:1 Carnitine	rel. peak area/mg	1 ± 0.223	0.375 ± 0.071	0.649 ± 0.194	0.717 ± 0.164	0.995 ± 0.296	0.25	0.097	0.054	<b>0.024</b>	0.8
Muscle C14:2 Carnitine	rel. peak area/mg	1 ± 0.199	0.342 ± 0.069	0.702 ± 0.211	0.599 ± 0.163	0.923 ± 0.28	0.3	0.23	<b>0.041</b>	<b>0.011</b>	0.68
Muscle C16:0-OH Carnitine	rel. peak area/mg	1 ± 0.239	0.716 ± 0.214	1.79 ± 0.488	1.88 ± 0.509	3.06 ± 0.591	0.17	0.077	<b>0.0043</b>	0.38	0.88
Muscle C16:0 Carnitine	p mol/mg	1.95 ± 0.331	0.984 ± 0.209	2.99 ± 1.3	2.76 ± 0.818	4.3 ± 1.18	0.63	0.079	<b>0.0043</b>	<b>0.035</b>	0.88
Muscle C16:1 Carnitine	rel. peak area/mg	1 ± 0.216	0.532 ± 0.14	0.876 ± 0.243	1.48 ± 0.417	1.59 ± 0.437	0.66	0.064	<b>0.03</b>	0.1	0.25
Muscle C18:0 Carnitine	rel. peak area/mg	1 ± 0.183	0.783 ± 0.188	1.19 ± 0.349	2.27 ± 0.634	2.29 ± 0.652	0.65	0.069	<b>0.039</b>	0.4	0.17
Muscle C18:1 Carnitine	rel. peak area/mg	1 ± 0.189	0.457 ± 0.124	0.8 ± 0.229	1.93 ± 0.664	1.35 ± 0.38	0.51	0.043	<b>0.03</b>	<b>0.048</b>	0.17
Muscle C18:2-OH Carnitine	rel. peak area/mg	1 ± 0.192	0.748 ± 0.231	1.32 ± 0.367	2.03 ± 0.538	2.04 ± 0.451	0.48	0.054	<b>0.024</b>	0.42	0.32
Muscle C18:2 Carnitine	rel. peak area/mg	1 ± 0.176	0.488 ± 0.14	1.13 ± 0.318	2.24 ± 0.804	2.07 ± 0.516	0.73	<b>0.04</b>	<b>0.0065</b>	0.052	0.27
<b>Miscellaneous</b>											
Muscle 3-Phospho-serine	rel. peak area/mg	1 ± 0.178	0.9 ± 0.102	1.12 ± 0.254	0.821 ± 0.111	0.877 ± 0.090	0.71	0.62	0.87	0.65	0.32
Muscle Acetylphosphate	rel. peak area/mg	1 ± 0.192	1.49 ± 0.161	0.834 ± 0.202	1.61 ± 0.205	1.06 ± 0.205	0.55	0.88	0.13	0.076	<b>0.022</b>
Muscle Creatine	rel. peak area/mg	1 ± 0.087	0.888 ± 0.06	1.2 ± 0.0434	0.966 ± 0.048	1.17 ± 0.045	0.08	0.32	<b>0.0065</b>	0.34	<b>0.0058</b>
Muscle Creatine-phosphate	rel. peak area/mg	1 ± 0.161	1.19 ± 0.112	0.513 ± 0.138	1.14 ± 0.062	0.639 ± 0.115	0.05	0.68	<b>0.0087</b>	0.36	<b>0.0023</b>
Muscle Creatinine	rel. peak area/mg	1 ± 0.033	0.843 ± 0.050	1.05 ± 0.060	0.9 ± 0.061	0.966 ± 0.038	0.48	0.5	0.08	<b>0.037</b>	0.12
Muscle Deoxyuridine	rel. peak area/mg	1 ± 0.082	0.608 ± 0.023	0.936 ± 0.115	0.933 ± 0.069	0.937 ± 0.042	0.65	0.33	<b>0.0022</b>	0.095	0.98
Muscle Gluconate	rel. peak area/mg	1 ± 0.085	0.608 ± 0.118	1.15 ± 0.106	0.817 ± 0.055	1.44 ± 0.154	0.29	0.13	<b>0.0022</b>	<b>0.03</b>	<b>0.013</b>
Muscle Glucosamine-1-P and -6-P	rel. peak area/mg	1 ± 0.053	1.21 ± 0.0875	1.09 ± 0.102	1.2 ± 0.124	1.15 ± 0.085	0.49	0.91	0.59	0.069	0.53
Muscle Glutathione, oxidized	rel. peak area/mg	1 ± 0.099	0.976 ± 0.053	1.2 ± 0.137	0.676 ± 0.036	0.819 ± 0.061	0.3	<b>0.0023</b>	0.087	0.83	<b>0.0012</b>
Muscle Glutathione, reduced	rel. peak area/mg	1 ± 0.073	0.881 ± 0.057	1.07 ± 0.048	0.796 ± 0.037	0.958 ± 0.067	0.43	0.21	0.4	0.22	<b>0.0012</b>
Muscle Malonyl-CoA	rel. peak area/mg	1 ± 0.325	1.81 ± 0.269	0.568 ± 0.098	1.31 ± 0.122	0.756 ± 0.173	0.25	0.098	<b>0.0087</b>	0.091	<b>0.0012</b>

Table A.1 Cont.

Muscle N-Acetylmethionine	rel. peak area/mg	1 ± 0.118	0.882 ± 0.142	1.07 ± 0.137	0.808 ± 0.116	1.25 ± 0.164	0.72	0.69	0.13	0.53	0.18
Muscle Pantothenate	rel. peak area/mg	1 ± 0.085	0.899 ± 0.072	1.06 ± 0.057	1.02 ± 0.078	1.01 ± 0.063	0.56	0.29	0.26	0.37	0.67
Muscle Quinolinate	rel. peak area/mg	1 ± 0.157	0.82 ± 0.088	1 ± 0.243	0.62 ± 0.084	1.05 ± 0.152	1	0.13	0.25	0.35	0.15
<b>Plasma Metabolites:</b>											
<b>Glycolysis</b>											
Blood Glucose	mg/dL	128 ± 4.19	120 ± 2.32	159 ± 6.69	163 ± 5.02	102 ± 5.11	<b>0.0022</b>	<b>0.0012</b>	<b>0.0065</b>	0.14	0.68
Blood Lactate	mmol/L	1.93 ± 0.24	2.23 ± 0.325	6.28 ± 0.832	3.22 ± 0.438	8.35 ± 1.83	<b>0.0022</b>	0.1	<b>0.0022</b>	0.49	<b>0.0065</b>
<b>Amino Acids</b>											
Plasma Alanine	µM	347 ± 30.1	397 ± 34.9	375 ± 40.9	362 ± 7.85	342 ± 33.7	0.58	0.33	0.28	0.29	0.71
Plasma Glycine	µM	260 ± 8.83	288 ± 9.58	229 ± 32.3	270 ± 11	275 ± 10.3	0.35	0.23	0.39	0.058	0.21
Plasma Valine	µM	234 ± 10.4	216 ± 9.5	200 ± 22.1	186 ± 8.56	196 ± 11.9	0.18	<b>0.038</b>	0.21	0.23	0.51
Plasma Leucine	µM	176 ± 3.87	154 ± 7.59	147 ± 18.3	131 ± 4.36	148 ± 10.8	0.17	<b>0.019</b>	0.64	<b>0.035</b>	0.32
Plasma Isoleucine	µM	96.7 ± 3.69	85.8 ± 4.15	83.3 ± 7.42	70.5 ± 2.23	78.9 ± 6.05	0.14	<b>0.0023</b>	0.36	0.082	0.1
Plasma Threonine	µM	243 ± 13.8	260 ± 12.6	226 ± 22.1	211 ± 13.4	229 ± 12.2	0.49	<b>0.029</b>	0.12	0.36	0.52
Plasma Serine	µM	344 ± 23.9	385 ± 17.9	319 ± 45.6	316 ± 17.3	319 ± 17.1	0.64	<b>0.023</b>	<b>0.023</b>	0.2	0.97
Plasma Proline	µM	181 ± 10.4	182 ± 8.22	139 ± 15	156 ± 7.92	155 ± 15	<b>0.048</b>	<b>0.044</b>	0.15	0.92	0.31
Plasma Asparagine	µM	61.6 ± 4.26	67.1 ± 5.38	55.8 ± 6.96	57.5 ± 2.95	62.7 ± 4.78	0.47	0.13	0.56	0.47	0.8
Plasma Aspartic Acid	µM	14.9 ± 1.58	14 ± 0.54	13.4 ± 1.46	10.3 ± 1.35	12.2 ± 2.15	0.5	<b>0.035</b>	0.42	0.6	0.15
Plasma Methionine	µM	56.8 ± 6.04	47.1 ± 4.08	39.8 ± 5.27	43.1 ± 2.93	50.8 ± 3.44	0.065	0.46	0.49	0.2	0.55
Plasma 4-Hydroxyproline	µM	36.9 ± 4.31	35 ± 4.42	30 ± 3.92	29.4 ± 1.06	37 ± 3.72	0.31	0.24	0.72	0.74	0.91
Plasma Glutamic Acid	µM	116 ± 8.33	108 ± 4.47	143 ± 20	110 ± 9.04	165 ± 23.9	0.23	0.81	<b>0.017</b>	0.4	0.15
Plasma Phenylalanine	µM	73.3 ± 3.58	63.5 ± 3.23	73.5 ± 8.59	72.8 ± 2.71	96 ± 7.15	0.98	0.05	<b>0.0065</b>	0.082	0.91
Plasma Glutamine	µM	6359 ± 437	6093 ± 410	6412 ± 958	4423 ± 334	6197 ± 453	0.97	<b>0.0093</b>	0.88	0.66	0.053
Plasma Ornithine	µM	40.9 ± 2.72	35.6 ± 2.18	34 ± 5.03	24.8 ± 2.79	26.5 ± 3.79	0.25	<b>0.014</b>	0.074	0.16	0.13
Plasma Lysine	µM	363 ± 18.5	440 ± 31.8	333 ± 40.1	428 ± 21.8	438 ± 33.2	0.5	0.75	0.95	0.067	0.061
Plasma Histidine	µM	63.9 ± 2.21	67.5 ± 6.6	53.7 ± 12.2	67.1 ± 4.69	70.1 ± 3.67	0.45	0.95	0.74	0.65	0.32
Plasma Tyrosine	µM	100 ± 3.96	93.3 ± 6.85	105 ± 4.63	86.5 ± 7.96	150 ± 13.5	0.46	0.51	<b>0.0065</b>	0.39	0.096
Plasma Tryptophan	µM	126 ± 6.43	119 ± 5.05	109 ± 12.9	120 ± 5.51	144 ± 9.53	0.25	0.9	<b>0.043</b>	0.41	0.41
<b>Keto Acids</b>											
Plasma Keto-isovaleric acid	rel. peak area	1 ± 0.066	0.951 ± 0.030	1.43 ± 0.132	1.08 ± 0.088	1.16 ± 0.132	<b>0.015</b>	0.24	0.18	0.52	<b>0.045</b>
Plasma Keto-isocaproic acid	rel. peak area	1 ± 0.072	1.1 ± 0.099	1.79 ± 0.213	1.32 ± 0.172	1.43 ± 0.211	<b>0.0065</b>	0.3	0.18	0.44	0.13
Plasma Keto-methylvaleric acid	rel. peak area	1 ± 0.038	1.04 ± 0.056	1.56 ± 0.168	1.21 ± 0.145	1.32 ± 0.153	<b>0.013</b>	0.34	0.13	0.58	0.14
<b>Lipids</b>											
Blood Non-Esterified Fatty Acids (NEFA)	mmol/L	0.559 ± 0.041	0.573 ± 0.024	0.355 ± 0.057	0.348 ± 0.017	0.389 ± 0.077	<b>0.017</b>	<b>0.0012</b>	0.056	0.78	0.91
Plasma 14:0 Fatty Acid	nmol	1.66 ± 0.222	0.917 ± 0.178	0.64 ± 0.236	1.67 ± 0.828	0.535 ± 0.138	<b>0.017</b>	0.49	0.15	<b>0.035</b>	0.26
Plasma 16:0 Fatty Acid	nmol	113 ± 6.99	101 ± 9.33	90.1 ± 8.66	99 ± 17.2	58.9 ± 14.5	0.069	0.92	<b>0.043</b>	0.32	0.71
Plasma 16:1 Fatty Acid	nmol	7.98 ± 1.07	5.74 ± 0.574	4.8 ± 0.608	10.7 ± 4.06	3.06 ± 0.919	<b>0.039</b>	0.44	<b>0.032</b>	0.095	0.34
Plasma 18:0 Fatty Acid	nmol	75.1 ± 3.17	71.9 ± 4.2	79.6 ± 5.67	63.9 ± 14.5	42.4 ± 3.33	0.5	0.69	<b>0.0022</b>	0.54	0.35
Plasma 18:1 n7 Fatty Acid	nmol	17.6 ± 1.47	14.6 ± 1.25	15 ± 0.741	14.7 ± 2.25	7.53 ± 1.87	0.14	0.97	<b>0.013</b>	0.18	0.95
Plasma 18:1 n9 Fatty Acid	nmol	81.5 ± 6.02	84.6 ± 10.4	74.7 ± 7.49	137 ± 38.6	48.8 ± 25.7	0.48	0.25	0.24	0.81	0.11
Plasma 18:2 Fatty Acid	nmol	132 ± 7.33	113 ± 7.12	124 ± 9.25	79.2 ± 11.5	53.9 ± 2.82	0.49	<b>0.037</b>	<b>0.0022</b>	0.074	<b>0.015</b>
Plasma 18:3 n3 Fatty Acid	nmol	4.05 ± 0.362	3.3 ± 0.341	3.42 ± 0.555	2.11 ± 0.478	0.94 ± 0.066	0.35	0.078	<b>0.0022</b>	0.18	0.11

Table A.1 Cont.

Plasma 18:3 n6 Fatty Acid	nmol	0.62 ± 0.099	0.865 ± 0.074	0.69 ± 0.11	0.367 ± 0.06	0.282 ± 0.047	0.64	<b>0.0022</b>	<b>0.0022</b>	0.087	<b>0.03</b>
Plasma 20:1 Fatty Acid	nmol	1.52 ± 0.198	1.66 ± 0.257	1.4 ± 0.267	2.77 ± 0.744	0.813 ± 0.483	0.62	0.15	0.16	0.61	0.063
Plasma 20:2 Fatty Acid	nmol	2.56 ± 0.131	2.12 ± 0.167	2.45 ± 0.123	1.52 ± 0.164	1.08 ± 0.029	0.57	<b>0.032</b>	<b>0.0022</b>	0.071	<b>0.0043</b>
Plasma 20:3 Fatty Acid	nmol	3.15 ± 0.318	3.5 ± 0.326	3.54 ± 0.457	1.83 ± 0.169	1.59 ± 0.129	0.49	<b>0.0022</b>	<b>0.0022</b>	0.46	<b>0.0087</b>
Plasma 20:4 Fatty Acid	nmol	93 ± 7.68	98.9 ± 3.96	108 ± 15.9	54 ± 6.85	60.9 ± 5.83	0.47	<b>0.0022</b>	<b>0.0043</b>	0.51	<b>0.0065</b>
Plasma 20:5 Fatty Acid	nmol	6.18 ± 0.745	5.88 ± 0.673	6.03 ± 1.04	2.48 ± 0.39	1.65 ± 0.522	0.92	<b>0.0043</b>	<b>0.0043</b>	0.77	<b>0.0043</b>
Plasma 22:1 Fatty Acid	nmol	0.355 ± 0.044	0.38 ± 0.059	0.348 ± 0.047	0.163 ± 0.079	0.0467 ± 0.0154	0.94	0.05	<b>0.0022</b>	0.8	0.071
Plasma 22:4 Fatty Acid	nmol	2.21 ± 0.197	2.29 ± 0.138	2.34 ± 0.226	1.32 ± 0.128	1.27 ± 0.165	0.68	<b>0.0022</b>	<b>0.0065</b>	0.77	<b>0.0022</b>
Plasma 22:5 Fatty Acid	nmol	5.97 ± 1.42	5.92 ± 0.684	6.42 ± 1.31	2.65 ± 0.296	1.55 ± 0.235	0.82	<b>0.0022</b>	<b>0.0022</b>	0.98	<b>0.0043</b>
Plasma 22:6 Fatty Acid	nmol	13.2 ± 2.48	8.85 ± 0.964	12.2 ± 2.27	3.88 ± 0.951	2.82 ± 0.9	0.76	<b>0.0043</b>	<b>0.0043</b>	0.11	<b>0.0022</b>
Plasma 24:0 Fatty Acid	nmol	0.872 ± 0.131	1.16 ± 0.057	0.937 ± 0.182	0.878 ± 0.078	0.343 ± 0.156	0.78	<b>0.022</b>	<b>0.0022</b>	0.082	0.8
Plasma 24:1 Fatty Acid	nmol	0.803 ± 0.303	1.19 ± 0.479	1.27 ± 0.314	1.07 ± 0.151	1 ± 0.174	0.27	0.82	0.73	0.49	0.58
<b>Acylcarnitines</b>											
Plasma L-Carnitine	µM	115 ± 6.04	113 ± 8.37	106 ± 6.78	106 ± 2.8	86.3 ± 5.76	0.31	0.39	<b>0.026</b>	0.85	0.96
Plasma C2 Carnitine	µM	45.7 ± 2.66	56.8 ± 5.29	55.8 ± 1.4	58.5 ± 3.04	66.6 ± 3.17	<b>0.011</b>	0.76	0.15	0.097	0.47
Plasma C3 Carnitine	µM	2.34 ± 0.132	2.2 ± 0.191	3.82 ± 0.463	3 ± 0.408	7.85 ± 1.98	<b>0.013</b>	0.11	<b>0.0022</b>	0.56	0.21
Plasma C4 Carnitine	µM	2.11 ± 0.208	1.84 ± 0.121	2.77 ± 0.386	3.02 ± 0.438	4.51 ± 0.69	0.17	<b>0.016</b>	<b>0.0022</b>	0.28	0.67
Plasma C5:0-DC Carnitine	rel. peak area	1 ± 0.228	3.18 ± 0.473	2.01 ± 0.424	1.8 ± 0.262	4.11 ± 0.4	0.074	<b>0.027</b>	0.16	<b>0.0043</b>	0.64
Plasma C5:0 Carnitine	µM	0.399 ± 0.039	0.298 ± 0.020	0.541 ± 0.058	0.449 ± 0.055	0.549 ± 0.053	0.074	<b>0.024</b>	<b>0.0022</b>	0.024	0.27
Plasma C6:0 Carnitine	rel. peak area	1 ± 0.196	1.55 ± 0.144	0.937 ± 0.050	1.18 ± 0.077	2.3 ± 0.157	0.9	<b>0.016</b>	<b>0.011</b>	0.058	0.03
Plasma C8:0 Carnitine	µM	0.0162 ± 0.0017	0.0221 ± 0.002	0.0127 ± 0.001	0.0173 ± 0.0006	0.0317 ± 0.0030	0.14	<b>0.012</b>	<b>0.019</b>	<b>0.043</b>	<b>0.013</b>
Plasma C8:1 Carnitine	rel. peak area	1 ± 0.192	1.19 ± 0.094	0.902 ± 0.060	0.81 ± 0.0742	1.38 ± 0.089	0.83	<b>0.0093</b>	0.17	0.4	0.35
Plasma C10:0 Carnitine	rel. peak area	1 ± 0.116	1.44 ± 0.086	0.868 ± 0.040	1.31 ± 0.067	2.83 ± 0.078	0.35	<b>0.026</b>	<b>0.0022</b>	0.022	<b>0.0012</b>
Plasma C10:1 Carnitine	rel. peak area	1 ± 0.153	1.89 ± 0.173	0.801 ± 0.035	1.13 ± 0.068	2.41 ± 0.312	0.24	<b>0.0012</b>	0.18	<b>0.0065</b>	<b>0.0023</b>
Plasma C12:0 Carnitine	rel. peak area	1 ± 0.228	4.41 ± 0.829	1.59 ± 0.367	2.64 ± 0.403	8.01 ± 0.878	0.2	0.073	<b>0.017</b>	<b>0.0043</b>	0.086
Plasma C12:0 Carnitine	rel. peak area	1 ± 0.083	1.52 ± 0.113	1.04 ± 0.045	1.62 ± 0.162	5.07 ± 0.474	0.66	0.67	<b>0.0022</b>	0.011	<b>0.0012</b>
Plasma C12:1 Carnitine	rel. peak area	1 ± 0.157	1.52 ± 0.138	1.54 ± 0.222	1.87 ± 0.153	6.92 ± 0.86	0.076	0.12	<b>0.0022</b>	0.039	0.24
Plasma C14:0 Carnitine	rel. peak area	1 ± 0.139	4.35 ± 0.908	1.75 ± 0.269	3.41 ± 0.504	7.77 ± 0.781	<b>0.039</b>	0.38	<b>0.019</b>	<b>0.0022</b>	<b>0.013</b>
Plasma C14:1 Carnitine	µM	0.0355 ± 0.0018	0.055 ± 0.005	0.0434 ± 0.003	0.0677 ± 0.007	0.221 ± 0.023	0.05	0.18	<b>0.0022</b>	<b>0.0043</b>	<b>0.0012</b>
Plasma C14:2 Carnitine	rel. peak area	1 ± 0.084	1.55 ± 0.148	1.21 ± 0.061	2.07 ± 0.227	8.85 ± 1.02	0.082	0.087	<b>0.0022</b>	<b>0.019</b>	<b>0.0012</b>
Plasma C16:0 Carnitine	rel. peak area	1 ± 0.104	1.84 ± 0.169	1.37 ± 0.133	2.38 ± 0.224	8.82 ± 1.02	0.071	0.091	<b>0.0022</b>	<b>0.0087</b>	<b>0.0047</b>
Plasma C16:0 Carnitine	rel. peak area	1 ± 0.104	3.35 ± 0.79	1.18 ± 0.057	2.98 ± 0.593	4.17 ± 0.78	0.16	0.69	0.46	<b>0.0022</b>	<b>0.0012</b>
Plasma C16:1 Carnitine	µM	0.159 ± 0.009	0.245 ± 0.015	0.192 ± 0.007	0.246 ± 0.015	0.506 ± 0.045	<b>0.019</b>	0.97	<b>0.0022</b>	<b>0.0022</b>	<b>0.01</b>
Plasma C16:1 Carnitine	rel. peak area	1 ± 0.108	1.15 ± 0.133	1.09 ± 0.074	1.73 ± 0.258	7.15 ± 0.687	0.5	0.071	<b>0.0022</b>	0.41	<b>0.019</b>
Plasma C18:0 Carnitine	rel. peak area	1 ± 0.158	1.12 ± 0.123	0.978 ± 0.037	1.32 ± 0.123	3.47 ± 0.381	0.92	0.3	<b>0.0022</b>	0.55	<b>0.024</b>
Plasma C18:1 Carnitine	rel. peak area	1 ± 0.127	1.37 ± 0.113	1.01 ± 0.031	1.56 ± 0.153	4.29 ± 0.469	0.94	0.37	<b>0.0022</b>	<b>0.048</b>	<b>0.0035</b>
Plasma C18:2-OH Carnitine	rel. peak area	1 ± 0.093	1.86 ± 0.293	1.07 ± 0.084	1.78 ± 0.233	3.12 ± 0.343	0.59	0.82	<b>0.019</b>	<b>0.0035</b>	<b>0.0035</b>
Plasma C18:2 Carnitine	rel. peak area	1 ± 0.119	1.41 ± 0.085	1.22 ± 0.065	1.96 ± 0.232	5.21 ± 0.416	0.14	<b>0.027</b>	<b>0.0022</b>	<b>0.028</b>	<b>0.0023</b>
Plasma C20:0 Carnitine	rel. peak area	1 ± 0.091	1.53 ± 0.15	1.77 ± 0.348	1.28 ± 0.242	1.37 ± 0.27	0.091	0.43	0.62	<b>0.019</b>	0.31
Plasma C20:2 Carnitine	rel. peak area	1 ± 0.15	0.939 ± 0.124	1.05 ± 0.069	1.83 ± 0.291	5.65 ± 1.86	0.78	<b>0.022</b>	<b>0.0022</b>	0.73	<b>0.038</b>
Plasma C20:3 Carnitine	rel. peak area	1 ± 0.119	1.21 ± 0.123	1.04 ± 0.101	1.73 ± 0.257	4.81 ± 1.08	0.83	0.12	<b>0.0022</b>	0.25	<b>0.033</b>
Plasma C20:4 Carnitine	rel. peak area	1 ± 0.084	1.19 ± 0.1	1.23 ± 0.083	1.57 ± 0.106	4.36 ± 0.481	0.091	<b>0.026</b>	<b>0.0022</b>	0.19	<b>0.028</b>



## **B. Confirmation metabolomics data set**

A confirmation metabolomics data set (Table B.1) contains muscle and plasma metabolite values for HCR and LCR at quarter (HCR only), half, and full exhaustion. For HCR this is approximately 15 min, 30 min, and 60 min of increasing intensity exercise. For LCR this is approximately 6 min and 12 min of increasing intensity exercise. Metabolite values are presented as mean  $\pm$  SEM for each group.

Table B.1

Metabolites by Category	Units	LCR Rest (n=1)	LCR Half Exhaustion	LCR Full Exhaustion	HCR Quarter	HCR Half Exhaustion	HCR Full Exhaustion
		Mean ± SEM	Mean ± SEM (n=5)	Mean ± SEM (n=6)	Mean ± SEM (n=5)	Mean ± SEM (n=6)	Mean ± SEM (n=6)
<b>Glycolysis</b>							
Muscle Glycogen	mmol/L glucose	1.00 ± NA	0.82 ± 0.067	0.56 ± 0.12	1.12 ± 0.13	0.79 ± 0.14	0.27 ± 0.053
Muscle Hexose-phosphate	rel. peak area/mg	1.00 ± NA	2.27 ± 0.61	2.24 ± 0.44	1.39 ± 0.13	1.80 ± 0.39	1.92 ± 0.19
Muscle Fructose-1,5-bisphosphate	rel. peak area/mg	1.00 ± NA	0.62 ± 0.13	0.82 ± 0.16	0.94 ± 0.13	1.08 ± 0.086	0.76 ± 0.095
Muscle Dihydroxy-acetone-phosphate	rel. peak area/mg	1.00 ± NA	2.62 ± 0.19	3.24 ± 0.43	1.86 ± 0.38	3.04 ± 0.53	13.49 ± 3.49
Muscle Glycerol-3-phosphate	rel. peak area/mg	1.00 ± NA	1.39 ± 0.23	1.76 ± 0.24	1.08 ± 0.11	1.11 ± 0.18	3.53 ± 0.28
Muscle 2- and 3-Phosphoglycerate	rel. peak area/mg	1.00 ± NA	0.85 ± 0.095	0.91 ± 0.098	1.11 ± 0.24	1.14 ± 0.055	1.13 ± 0.093
Muscle Phosphoenolpyruvate	rel. peak area/mg	1.00 ± NA	0.71 ± 0.038	0.86 ± 0.074	0.78 ± 0.12	0.72 ± 0.066	0.95 ± 0.17
Muscle Lactate	rel. peak area/mg	1.00 ± NA	0.79 ± 0.12	0.99 ± 0.12	0.51 ± 0.041	0.65 ± 0.10	2.51 ± 0.44
<b>Pentose Phosphate Pathway</b>							
Muscle Rib(ul)ose-5-phosphate	rel. peak area/mg	1.00 ± NA	0.64 ± 0.036	0.99 ± 0.27	0.61 ± 0.068	0.78 ± 0.071	1.07 ± 0.12
Muscle Erythrose-4-phosphate	rel. peak area/mg	1.00 ± NA	2.08 ± 0.43	2.05 ± 0.53	1.55 ± 0.12	1.97 ± 0.38	1.99 ± 0.19
<b>Citric Acid Cycle</b>							
Muscle Acetyl-CoA	rel. peak area/mg	1.00 ± NA	1.26 ± 0.23	1.00 ± 0.16	0.79 ± 0.094	1.28 ± 0.12	2.02 ± 0.38
Muscle Citrate	rel. peak area/mg	1.00 ± NA	1.03 ± 0.12	1.12 ± 0.12	1.04 ± 0.14	1.63 ± 0.089	2.05 ± 0.25
Muscle Malate	rel. peak area/mg	1.00 ± NA	1.51 ± 0.28	2.31 ± 0.17	1.06 ± 0.091	1.99 ± 0.15	5.91 ± 0.92
Muscle Succinate	rel. peak area/mg	1.00 ± NA	1.92 ± 0.93	1.37 ± 0.38	0.95 ± 0.23	2.38 ± 0.60	2.62 ± 0.54
<b>Nucleotides and Cofactors</b>							
Muscle AMP	rel. peak area/mg	1.00 ± NA	0.73 ± 0.058	0.86 ± 0.11	0.85 ± 0.086	1.02 ± 0.068	1.12 ± 0.13
Muscle ADP	rel. peak area/mg	1.00 ± NA	0.86 ± 0.08	0.75 ± 0.075	0.84 ± 0.092	1.01 ± 0.075	0.94 ± 0.088
Muscle ATP	rel. peak area/mg	1.00 ± NA	0.90 ± 0.096	0.75 ± 0.084	0.88 ± 0.10	1.04 ± 0.077	0.99 ± 0.098
Muscle CMP	rel. peak area/mg	1.00 ± NA	0.52 ± 0.063	0.35 ± 0.052	0.62 ± 0.088	0.64 ± 0.084	0.64 ± 0.098
Muscle CTP	rel. peak area/mg	1.00 ± NA	0.86 ± 0.076	0.77 ± 0.07	0.90 ± 0.12	1.06 ± 0.11	1.15 ± 0.098
Muscle GMP	rel. peak area/mg	1.00 ± NA	0.54 ± 0.10	0.70 ± 0.12	0.61 ± 0.068	0.83 ± 0.044	0.74 ± 0.068
Muscle GDP	rel. peak area/mg	1.00 ± NA	0.89 ± 0.099	0.87 ± 0.056	0.92 ± 0.13	1.01 ± 0.078	1.11 ± 0.089
Muscle GTP	rel. peak area/mg	1.00 ± NA	0.93 ± 0.084	0.79 ± 0.081	0.91 ± 0.16	0.99 ± 0.12	1.17 ± 0.087
Muscle IMP	rel. peak area/mg	1.00 ± NA	0.64 ± 0.21	1.30 ± 0.32	0.31 ± 0.037	0.81 ± 0.25	2.56 ± 0.91
Muscle IDP	rel. peak area/mg	1.00 ± NA	0.58 ± 0.038	0.60 ± 0.064	0.76 ± 0.071	0.88 ± 0.12	0.80 ± 0.11
Muscle ITP	rel. peak area/mg	1.00 ± NA	0.88 ± 0.084	0.75 ± 0.071	0.89 ± 0.12	1.04 ± 0.096	1.09 ± 0.098
Muscle UMP	rel. peak area/mg	1.00 ± NA	0.51 ± 0.053	0.61 ± 0.11	0.62 ± 0.084	0.68 ± 0.058	0.65 ± 0.072
Muscle UDP	rel. peak area/mg	1.00 ± NA	0.86 ± 0.09	0.87 ± 0.085	0.97 ± 0.13	1.08 ± 0.075	1.05 ± 0.10
Muscle UTP	rel. peak area/mg	1.00 ± NA	0.86 ± 0.077	0.74 ± 0.066	0.92 ± 0.11	1.08 ± 0.10	1.11 ± 0.10
Muscle XMP	rel. peak area/mg	1.00 ± NA	0.64 ± 0.079	0.60 ± 0.11	0.85 ± 0.14	0.79 ± 0.088	0.70 ± 0.15
Muscle NAD+	rel. peak area/mg	1.00 ± NA	0.76 ± 0.073	0.65 ± 0.067	0.87 ± 0.093	0.95 ± 0.071	0.86 ± 0.097
Muscle NADH	rel. peak area/mg	1.00 ± NA	1.00 ± 0.31	0.79 ± 0.23	0.91 ± 0.14	1.04 ± 0.16	0.90 ± 0.11

Table B.1. Metabolomic analysis of HCR and LCR with exercise. HCR were run to quarter, half, and full exhaustion, and LCR were run to half and full exhaustion.

Table B.1 Cont.

Muscle NADP+	rel. peak area/mg	1.00 ± NA	0.79 ± 0.068	0.82 ± 0.092	1.02 ± 0.14	1.24 ± 0.11	1.12 ± 0.13
Muscle NADPH	rel. peak area/mg	1.00 ± NA	0.88 ± 0.068	0.77 ± 0.11	1.09 ± 0.15	1.31 ± 0.11	1.31 ± 0.17
Muscle FAD	rel. peak area/mg	1.00 ± NA	0.87 ± 0.057	0.85 ± 0.12	1.33 ± 0.14	1.59 ± 0.13	1.48 ± 0.21
Muscle FMN	rel. peak area/mg	1.00 ± NA	0.64 ± 0.06	0.70 ± 0.081	0.97 ± 0.13	1.09 ± 0.065	0.95 ± 0.13
Muscle Coenzyme A	rel. peak area/mg	1.00 ± NA	0.92 ± 0.06	0.79 ± 0.11	1.27 ± 0.13	1.44 ± 0.21	1.34 ± 0.14

**Nucleosides**

Muscle Adenine	rel. peak area/mg	1.00 ± NA	0.67 ± 0.056	1.68 ± 1.12	0.82 ± 0.024	0.97 ± 0.16	1.03 ± 0.18
Muscle Adenosine	rel. peak area/mg	1.00 ± NA	0.62 ± 0.07	2.02 ± 1.49	0.92 ± 0.068	1.06 ± 0.18	1.07 ± 0.17
Muscle Hypoxanthine	rel. peak area/mg	1.00 ± NA	0.69 ± 0.083	0.65 ± 0.059	0.65 ± 0.059	0.79 ± 0.076	0.76 ± 0.11
Muscle Inosine	rel. peak area/mg	1.00 ± NA	0.66 ± 0.16	1.88 ± 0.80	0.45 ± 0.036	0.76 ± 0.24	1.31 ± 0.20
Muscle Uracil	rel. peak area/mg	1.00 ± NA	1.95 ± 0.17	2.21 ± 0.34	1.45 ± 0.11	2.59 ± 0.39	7.51 ± 1.17
Muscle Xanthine	rel. peak area/mg	1.00 ± NA	0.91 ± 0.23	2.37 ± 1.07	0.64 ± 0.013	0.82 ± 0.20	3.28 ± 0.46

**Sugar-Nucleotides**

Muscle ADP-D-Glucose	rel. peak area/mg	1.00 ± NA	0.72 ± 0.059	0.67 ± 0.065	0.80 ± 0.11	0.94 ± 0.092	1.03 ± 0.11
Muscle N-Acetyl-glucosamine-phosphate	rel. peak area/mg	1.00 ± NA	0.74 ± 0.087	0.79 ± 0.097	0.69 ± 0.073	0.76 ± 0.067	0.85 ± 0.08
Muscle UDP-D-glucose	rel. peak area/mg	1.00 ± NA	0.76 ± 0.094	0.53 ± 0.065	1.07 ± 0.15	0.95 ± 0.089	0.83 ± 0.11
Muscle UDP-D-glucuronate	rel. peak area/mg	1.00 ± NA	0.80 ± 0.081	0.74 ± 0.068	0.87 ± 0.083	1.07 ± 0.12	0.97 ± 0.12
Muscle UDP-N-acetyl-D-glucosamine	rel. peak area/mg	1.00 ± NA	0.78 ± 0.078	0.66 ± 0.059	0.75 ± 0.07	0.81 ± 0.051	0.85 ± 0.082

**Amino Acids**

Muscle Alanine	rel. peak area/mg	1.00 ± NA	0.75 ± 0.08	0.70 ± 0.062	0.64 ± 0.053	0.72 ± 0.048	0.79 ± 0.088
Muscle Glycine	rel. peak area/mg	1.00 ± NA	1.04 ± 0.08	0.82 ± 0.072	1.04 ± 0.13	1.08 ± 0.11	1.15 ± 0.12
Muscle Valine	rel. peak area/mg	1.00 ± NA	0.73 ± 0.074	0.65 ± 0.062	0.52 ± 0.057	0.61 ± 0.05	0.78 ± 0.085
Muscle Leucine	rel. peak area/mg	1.00 ± NA	0.65 ± 0.06	0.57 ± 0.059	0.45 ± 0.058	0.53 ± 0.048	0.75 ± 0.08
Muscle Threonine	rel. peak area/mg	1.00 ± NA	0.77 ± 0.055	0.67 ± 0.072	0.80 ± 0.10	0.90 ± 0.058	0.93 ± 0.097
Muscle Proline	rel. peak area/mg	1.00 ± NA	0.73 ± 0.058	0.66 ± 0.066	0.63 ± 0.077	0.76 ± 0.059	0.91 ± 0.10
Muscle Asparagine	rel. peak area/mg	1.00 ± NA	0.48 ± 0.029	0.22 ± 0.046	0.21 ± 0.046	0.35 ± 0.076	0.23 ± 0.097
Muscle Aspartic Acid	rel. peak area/mg	1.00 ± NA	0.85 ± 0.17	0.80 ± 0.12	1.16 ± 0.14	1.37 ± 0.15	0.86 ± 0.13
Muscle Methionine	rel. peak area/mg	1.00 ± NA	0.78 ± 0.066	0.75 ± 0.10	0.70 ± 0.083	0.88 ± 0.075	1.14 ± 0.14
Muscle Glutamic Acid	rel. peak area/mg	1.00 ± NA	0.53 ± 0.075	0.41 ± 0.059	0.55 ± 0.065	0.63 ± 0.055	0.52 ± 0.067
Muscle Phenylalanine	rel. peak area/mg	1.00 ± NA	0.82 ± 0.063	0.82 ± 0.097	0.69 ± 0.065	0.84 ± 0.08	1.31 ± 0.15
Muscle Glutamine	rel. peak area/mg	1.00 ± NA	0.78 ± 0.051	0.64 ± 0.073	0.76 ± 0.095	0.83 ± 0.067	0.67 ± 0.071
Muscle Ornithine	rel. peak area/mg	1.00 ± NA	0.77 ± 0.047	0.68 ± 0.081	0.89 ± 0.14	1.05 ± 0.11	0.99 ± 0.088
Muscle Lysine	rel. peak area/mg	1.00 ± NA	1.07 ± 0.079	0.86 ± 0.12	2.03 ± 0.34	2.59 ± 0.34	2.93 ± 0.33
Muscle Histidine	rel. peak area/mg	1.00 ± NA	0.85 ± 0.088	0.73 ± 0.082	0.92 ± 0.10	1.09 ± 0.098	1.06 ± 0.11
Muscle Tyrosine	rel. peak area/mg	1.00 ± NA	0.93 ± 0.085	0.90 ± 0.13	0.72 ± 0.092	0.98 ± 0.077	1.43 ± 0.19
Muscle Tryptophan	rel. peak area/mg	1.00 ± NA	0.91 ± 0.072	0.96 ± 0.097	0.87 ± 0.13	1.15 ± 0.074	1.61 ± 0.22

**Lipids**

Muscle Palmitic acid	rel. peak area/mg	1.00 ± NA	0.91 ± 0.11	0.83 ± 0.14	1.09 ± 0.10	1.49 ± 0.12	1.23 ± 0.27
Muscle Stearic acid	rel. peak area/mg	1.00 ± NA	0.94 ± 0.12	0.81 ± 0.13	0.90 ± 0.10	1.17 ± 0.11	1.23 ± 0.31
Muscle Oleic acid	rel. peak area/mg	1.00 ± NA	0.61 ± 0.059	0.84 ± 0.18	1.91 ± 0.16	2.90 ± 0.34	1.22 ± 0.18
Muscle PC 34:2	rel. peak area/mg	1.00 ± NA	1.00 ± 0.094	1.00 ± 0.12	1.27 ± 0.15	1.42 ± 0.16	1.31 ± 0.16

Table B.1 Cont.

Muscle PC 36:4	rel. peak area/mg	1.00 ± NA	0.59 ± 0.082	0.51 ± 0.043	0.48 ± 0.052	0.53 ± 0.041	0.53 ± 0.053
Muscle PE 38:6	rel. peak area/mg	1.00 ± NA	0.73 ± 0.069	0.66 ± 0.068	0.84 ± 0.064	0.98 ± 0.096	0.92 ± 0.14
Muscle PG 34:1	rel. peak area/mg	1.00 ± NA	0.73 ± 0.067	0.64 ± 0.08	0.94 ± 0.09	1.16 ± 0.095	1.11 ± 0.19
Muscle PI 38:4	rel. peak area/mg	1.00 ± NA	0.68 ± 0.061	0.65 ± 0.063	0.66 ± 0.068	0.78 ± 0.062	0.77 ± 0.088
<b>Acylcarnitines</b>							
Muscle L-Carnitine	rel. peak area/mg	1.00 ± NA	0.68 ± 0.077	0.53 ± 0.10	0.76 ± 0.093	0.83 ± 0.04	0.50 ± 0.051
Muscle C2-Carnitine	rel. peak area/mg	1.00 ± NA	1.90 ± 0.45	3.32 ± 0.60	0.97 ± 0.28	2.46 ± 0.28	6.44 ± 1.01
Muscle C3-Carnitine	rel. peak area/mg	1.00 ± NA	1.32 ± 0.17	2.54 ± 0.49	1.03 ± 0.14	1.90 ± 0.41	10.10 ± 2.83
Muscle C4-Carnitine	rel. peak area/mg	1.00 ± NA	0.87 ± 0.073	1.06 ± 0.15	0.58 ± 0.11	1.41 ± 0.38	2.89 ± 0.58
Muscle C5:0-Carnitine	rel. peak area/mg	1.00 ± NA	0.87 ± 0.12	1.76 ± 0.16	1.24 ± 0.24	1.72 ± 0.39	3.16 ± 0.55
Muscle C6:0-Carnitine	rel. peak area/mg	1.00 ± NA	0.58 ± 0.13	1.57 ± 0.37	0.82 ± 0.17	2.80 ± 1.40	3.28 ± 0.71
Muscle C8:0-Carnitine	rel. peak area/mg	1.00 ± NA	0.72 ± 0.13	1.10 ± 0.14	0.75 ± 0.15	1.92 ± 0.82	1.41 ± 0.23
Muscle C8:1-Carnitine	rel. peak area/mg	1.00 ± NA	0.58 ± 0.098	0.74 ± 0.083	0.55 ± 0.057	0.97 ± 0.17	1.04 ± 0.18
Muscle C10:0-Carnitine	rel. peak area/mg	1.00 ± NA	0.91 ± 0.22	1.67 ± 0.30	1.17 ± 0.36	3.07 ± 1.39	2.05 ± 0.49
Muscle C10:1-Carnitine	rel. peak area/mg	1.00 ± NA	0.91 ± 0.27	1.92 ± 0.33	2.02 ± 0.81	5.28 ± 1.96	5.43 ± 1.41
Muscle C12:0-Carnitine	rel. peak area/mg	1.00 ± NA	1.22 ± 0.25	1.69 ± 0.28	1.55 ± 0.45	3.15 ± 1.04	2.29 ± 0.52
Muscle C12:1-Carnitine	rel. peak area/mg	1.00 ± NA	0.60 ± 0.12	0.96 ± 0.11	0.57 ± 0.19	1.81 ± 0.58	1.66 ± 0.42
Muscle C14:0-Carnitine	rel. peak area/mg	1.00 ± NA	1.38 ± 0.26	1.72 ± 0.29	1.77 ± 0.57	3.21 ± 0.93	2.69 ± 0.52
Muscle C14:1-Carnitine	rel. peak area/mg	1.00 ± NA	1.14 ± 0.18	1.57 ± 0.23	1.52 ± 0.53	3.00 ± 1.05	2.24 ± 0.43
Muscle C14:2-Carnitine	rel. peak area/mg	1.00 ± NA	1.14 ± 0.24	2.15 ± 0.37	1.48 ± 0.56	3.55 ± 1.79	2.66 ± 0.41
Muscle C16:0-Carnitine	rel. peak area/mg	1.00 ± NA	1.78 ± 0.16	2.44 ± 0.69	2.27 ± 0.57	3.60 ± 0.76	3.02 ± 0.47
Muscle C16:1-Carnitine	rel. peak area/mg	1.00 ± NA	1.20 ± 0.21	1.89 ± 0.37	1.95 ± 0.64	3.24 ± 0.87	2.20 ± 0.43
Muscle C18:0-Carnitine	rel. peak area/mg	1.00 ± NA	0.59 ± 0.058	1.08 ± 0.26	1.23 ± 0.50	2.20 ± 0.33	1.16 ± 0.38
Muscle C18:1-Carnitine	rel. peak area/mg	1.00 ± NA	0.43 ± 0.12	0.60 ± 0.12	0.47 ± 0.17	1.40 ± 0.19	1.12 ± 0.39
Muscle C18:2-Carnitine	rel. peak area/mg	1.00 ± NA	1.29 ± 0.23	2.32 ± 0.57	2.96 ± 1.15	5.04 ± 1.58	2.92 ± 0.60
<b>Miscellaneous</b>							
Muscle 3-Phospho-serine	rel. peak area/mg	1.00 ± NA	0.52 ± 0.066	0.41 ± 0.053	0.52 ± 0.055	0.61 ± 0.059	0.53 ± 0.067
Muscle Acetylphosphate	rel. peak area/mg	1.00 ± NA	1.14 ± 0.17	1.07 ± 0.13	0.88 ± 0.062	1.00 ± 0.13	1.07 ± 0.11
Muscle Creatine	rel. peak area/mg	1.00 ± NA	0.78 ± 0.087	0.74 ± 0.063	0.71 ± 0.061	0.80 ± 0.047	0.86 ± 0.11
Muscle Creatine-phosphate	rel. peak area/mg	1.00 ± NA	0.70 ± 0.069	0.60 ± 0.067	0.72 ± 0.082	0.84 ± 0.074	0.73 ± 0.075
Muscle Creatinine	rel. peak area/mg	1.00 ± NA	0.77 ± 0.074	0.70 ± 0.072	0.62 ± 0.067	0.72 ± 0.045	0.74 ± 0.071
Muscle Deoxyuridine	rel. peak area/mg	1.00 ± NA	0.66 ± 0.024	0.51 ± 0.079	0.91 ± 0.21	1.28 ± 0.26	0.91 ± 0.18
Muscle Glucosate	rel. peak area/mg	1.00 ± NA	0.59 ± 0.10	0.60 ± 0.047	0.42 ± 0.059	0.59 ± 0.073	0.56 ± 0.093
Muscle Glucosate-1-P and -6-P	rel. peak area/mg	1.00 ± NA	1.34 ± 0.22	1.32 ± 0.11	1.01 ± 0.11	1.16 ± 0.18	1.37 ± 0.14
Muscle Glutathione, oxidized	rel. peak area/mg	1.00 ± NA	0.68 ± 0.064	0.62 ± 0.058	0.58 ± 0.07	0.64 ± 0.053	0.64 ± 0.076
Muscle Glutathione, reduced	rel. peak area/mg	1.00 ± NA	0.68 ± 0.061	0.59 ± 0.062	0.59 ± 0.07	0.61 ± 0.041	0.59 ± 0.059
Muscle Malonyl-CoA	rel. peak area/mg	1.00 ± NA	1.92 ± 0.19	1.34 ± 0.15	2.44 ± 0.41	2.82 ± 0.40	3.20 ± 0.40
Muscle N-Acetylornithine	rel. peak area/mg	1.00 ± NA	0.67 ± 0.069	0.62 ± 0.048	0.77 ± 0.081	0.94 ± 0.082	0.82 ± 0.087
Muscle Pantothenate	rel. peak area/mg	1.00 ± NA	0.85 ± 0.061	0.76 ± 0.094	0.75 ± 0.08	0.92 ± 0.052	0.83 ± 0.12
Muscle Oumolinate	rel. peak area/mg	1.00 ± NA	0.53 ± 0.099	0.54 ± 0.096	0.52 ± 0.10	0.41 ± 0.10	0.60 ± 0.073
<b>Plasma Metabolites:</b>							
<b>Acylcarnitines</b>							
Plasma L-Carnitine	rel. peak area	1.00 ± NA	1.22 ± 0.061	1.07 ± 0.12	1.15 ± 0.082	0.98 ± 0.053	0.92 ± 0.07

Table B.1 Cont.

Plasma C2 Carnitine	rel. peak area	1.00 ± NA	1.27 ± 0.094	1.34 ± 0.085	1.28 ± 0.11	1.68 ± 0.18	1.14 ± 0.12
Plasma C3 Carnitine	rel. peak area	1.00 ± NA	1.22 ± 0.082	1.32 ± 0.062	0.95 ± 0.15	0.88 ± 0.098	1.93 ± 0.19
Plasma C4 Carnitine	rel. peak area	1.00 ± NA	1.74 ± 0.25	1.60 ± 0.11	1.11 ± 0.14	1.34 ± 0.17	1.52 ± 0.19
Plasma C5:0 Carnitine	rel. peak area	1.00 ± NA	1.45 ± 0.15	1.77 ± 0.10	0.82 ± 0.059	0.93 ± 0.17	1.21 ± 0.083
Plasma C6:0 Carnitine	rel. peak area	1.00 ± NA	1.87 ± 0.23	2.89 ± 0.51	3.14 ± 0.36	3.49 ± 0.58	3.15 ± 0.47
Plasma C8:0 Carnitine	rel. peak area	1.00 ± NA	1.66 ± 0.16	1.87 ± 0.12	2.14 ± 0.10	2.57 ± 0.12	2.31 ± 0.13
Plasma C8:1 Carnitine	rel. peak area	1.00 ± NA	1.27 ± 0.12	1.32 ± 0.091	1.09 ± 0.059	1.26 ± 0.11	1.32 ± 0.13
Plasma C10:0 Carnitine	rel. peak area	1.00 ± NA	2.28 ± 0.33	2.66 ± 0.19	3.06 ± 0.28	4.21 ± 0.28	4.31 ± 0.33
Plasma C10:1 Carnitine	rel. peak area	1.00 ± NA	1.91 ± 0.17	2.13 ± 0.23	2.38 ± 0.15	3.27 ± 0.16	3.28 ± 0.32
Plasma C12:0 Carnitine	rel. peak area	1.00 ± NA	1.73 ± 0.23	2.24 ± 0.19	2.66 ± 0.32	3.85 ± 0.36	5.64 ± 0.53
Plasma C12:1 Carnitine	rel. peak area	1.00 ± NA	1.03 ± 0.09	1.29 ± 0.12	1.09 ± 0.15	2.00 ± 0.21	2.59 ± 0.27
Plasma C14:0 Carnitine	rel. peak area	1.00 ± NA	1.74 ± 0.19	2.40 ± 0.23	2.30 ± 0.25	3.63 ± 0.24	7.18 ± 0.58
Plasma C14:1 Carnitine	rel. peak area	1.00 ± NA	1.96 ± 0.25	2.86 ± 0.33	2.58 ± 0.26	4.06 ± 0.53	7.64 ± 0.79
Plasma C14:2 Carnitine	rel. peak area	1.00 ± NA	1.87 ± 0.24	2.62 ± 0.24	2.21 ± 0.18	3.83 ± 0.37	5.66 ± 0.38
Plasma C16:0 Carnitine	rel. peak area	1.00 ± NA	1.77 ± 0.074	2.02 ± 0.24	1.90 ± 0.15	2.57 ± 0.20	5.33 ± 0.46
Plasma C16:1 Carnitine	rel. peak area	1.00 ± NA	2.04 ± 0.22	3.33 ± 0.49	2.76 ± 0.31	5.26 ± 0.45	9.23 ± 0.46
Plasma C18:0 Carnitine	rel. peak area	1.00 ± NA	2.10 ± 0.44	2.72 ± 0.47	1.98 ± 0.30	4.39 ± 0.51	7.32 ± 1.11
Plasma C18:1 Carnitine	rel. peak area	1.00 ± NA	11.56 ± 4.02	12.09 ± 3.36	8.51 ± 3.24	11.30 ± 4.80	40.49 ± 17.19
Plasma C18:2 Carnitine	rel. peak area	1.00 ± NA	2.41 ± 0.54	3.38 ± 0.55	2.57 ± 0.30	5.70 ± 1.08	9.37 ± 1.18
Plasma C20:4 Carnitine	rel. peak area	1.00 ± NA	1.53 ± 0.33	2.28 ± 0.33	1.50 ± 0.14	3.77 ± 0.42	5.09 ± 0.67

### **C. Proteomic data sets**

Appendix C contains tables with log<sub>2</sub> fold change values for quantified mitochondria proteins (Table C.1), phospho-sites (Table C.2), and acetyl-sites (Table C.3). Quantitative proteomics was performed on mitochondria isolated from skeletal muscle of HCR and LCR collected at rest and after 10 min of increasing intensity exercise.

Table C.1

Table C.1 Mitochondrial proteome fold change.

Uniprot ID	Gene Symbol	Entrez	HCR/LCR		HCR Rest / LCR Rest		HCR Run / LCR Run		LCR Run / LCR Rest		HCR Run / HCR Rest	
			log2 fold change	Permutation P-value	log2 fold change	Permutation P-value	log2 fold change	Permutation P-value	log2 fold change	Permutation P-value	log2 fold change	Permutation P-value
Q5FVL8	Abcb10	361439	-0.266	0.012	-0.301	0.143	-0.230	0.171	-0.035	0.829	0.036	0.829
Q5RKL8	Abcb8	362302	-0.175	0.058	-0.223	0.143	-0.127	0.257	0.005	0.971	0.101	0.057
D3ZXK4	Abhd11	NA	0.062	0.549	0.058	0.714	0.066	0.714	0.035	0.886	0.043	0.800
P13437	Acaa2	170465	0.308	0.010	0.311	0.114	0.305	0.086	0.220	0.029	0.213	0.200
B1WC61	Acad9	294973	-0.009	0.917	-0.032	0.714	0.014	0.914	0.059	0.714	0.105	0.400
P15650	Acadl	25287	0.154	0.098	0.252	0.114	0.056	0.714	0.173	0.143	-0.022	0.857
P08503	Acadm	24158	-0.469	0.605	-1.322	0.400	0.385	0.571	0.310	0.543	2.017	0.229
G3V796	Acadm	NA	-0.256	0.647	0.048	0.943	-0.560	0.486	-0.220	0.743	-0.828	0.314
Q6IMX3	Acads	64304	0.231	0.019	0.190	0.200	0.086	0.086	-0.020	0.829	0.062	0.686
P70584	Acadsb	25618	1.002	< 0.001	1.115	0.029	0.889	0.029	-0.138	0.686	-0.364	0.286
P17764	Acat1	25014	0.040	0.638	0.044	0.857	0.036	0.714	-0.053	0.600	-0.060	0.714
Q9ER34	Aco2	79250	0.085	0.178	0.153	0.143	0.018	0.857	0.026	0.857	-0.110	0.057
D3ZA93	Acot13	NA	0.303	0.039	0.216	0.371	0.389	0.057	-0.014	0.971	0.159	0.571
Q6IMX8	Acot2	192272	0.250	0.013	0.341	0.086	0.229	0.060	0.029	0.829	-0.153	0.257
Q499N5	Acsf2	NA	-0.461	0.024	-0.574	0.086	-0.347	0.229	-0.009	0.971	0.218	0.457
D3ZUX7	Acsf3	NA	-0.163	0.121	-0.206	0.229	-0.119	0.400	0.105	0.486	0.191	0.029
P18163	Acs1	25288	0.258	0.019	0.196	0.371	0.320	0.029	-0.096	0.543	0.029	0.886
D3ZZN3	Acs1	NA	-0.192	0.272	-0.144	0.686	-0.241	0.200	0.081	0.914	-0.016	1.000
D4A1G1	Acyp2	NA	-0.126	0.329	-0.219	0.400	-0.034	0.800	0.142	0.343	0.327	0.143
Q5BJQ0	Adck3	NA	0.047	0.640	0.064	0.686	0.031	0.857	0.158	0.057	0.125	0.571
G3V9I7	Adck5	NA	-0.265	0.076	-0.363	0.143	-0.167	0.571	-0.077	0.686	0.119	0.771
Q4QQW3	Adhfe1	362474	-0.243	0.101	-0.250	0.171	-0.236	0.457	0.060	0.800	0.074	0.686
D3ZW08	Adsl	NA	-0.288	0.044	-0.433	0.114	-0.144	0.286	-0.040	1.000	0.249	0.143
F1LN92	Afg3l2	NA	-0.058	0.419	-0.075	0.486	-0.041	0.886	0.033	0.657	0.067	0.429
D3Z9L0	Agk	NA	-0.264	0.263	-0.303	0.371	-0.226	0.571	-0.245	0.486	-0.169	0.600
G3V965	Agpat5	NA	-0.342	0.013	-0.322	0.200	-0.363	0.086	-0.006	0.943	-0.046	0.829
Q9JM53	Aifm1	83533	0.011	0.853	0.043	0.486	-0.022	0.857	0.062	0.571	-0.003	0.971
P29410	Ak2	500039	-0.084	0.670	-0.123	0.543	-0.044	0.771	-0.058	0.829	0.021	0.914
Q8CG45	Akr7a2	171445	-0.201	0.022	-0.207	0.057	-0.196	0.171	0.099	0.343	0.109	0.486
G3V9W6	Aldh3a2	NA	-0.595	0.010	-0.682	0.143	-0.508	0.171	-0.124	0.514	0.050	0.886
G3V945	Aldh5a1	NA	-0.040	0.657	-0.068	0.714	-0.013	0.886	-0.055	0.714	0.000	1.000
G3V7J0	Aldh6a1	NA	0.171	0.116	0.216	0.286	0.125	0.314	0.046	0.771	-0.046	0.771
Q64057	Aldh7a1	291450	-0.113	0.208	-0.125	0.429	-0.101	0.543	0.011	0.857	0.035	0.771
Q9JLJ3	Aldh9a1	64040	-0.425	0.006	-0.435	0.171	-0.415	0.086	-0.017	0.914	0.003	1.000
Q5U1W6	Apool	317191	-0.029	0.823	-0.069	0.829	0.011	0.943	0.000	1.000	0.080	0.714
B1WBW4	Armc10	NA	-0.253	0.004	-0.347	0.029	-0.160	0.229	0.047	0.657	0.234	0.057
Q505J9	Atad1	309532	-0.116	0.047	-0.131	0.171	-0.102	0.286	0.031	0.714	0.059	0.200
Q3KRE0	Atad3	NA	-0.094	0.225	-0.132	0.286	-0.056	0.629	-0.009	0.943	0.068	0.486
Q35567	Atic	295406	-0.422	0.011	-0.505	0.114	-0.338	0.171	-0.187	0.714	-0.020	0.886
P15999	Atp5a1	65262	-0.009	0.947	-0.058	0.714	0.039	0.857	0.057	0.743	0.154	0.514
P19511	Atp5f1	NA	0.037	0.369	0.023	0.629	0.051	0.486	-0.055	0.457	-0.027	0.600
P31399	Atp5h	641434	0.156	0.035	0.109	0.371	0.203	0.029	-0.020	1.000	0.073	0.543
P29419	Atp5i	140608	-0.011	0.931	0.108	0.771	-0.129	0.457	0.106	0.343	-0.131	0.600
P21571	Atp5j	500560	0.088	0.616	0.234	0.457	-0.058	0.886	0.008	0.943	-0.284	0.371
D3ZAF6	Atp5j2	NA	0.103	0.072	0.087	0.171	0.120	0.343	-0.062	0.743	-0.030	0.714
Q6PDU7	Atp5l	NA	-0.029	0.865	-0.067	0.800	0.009	0.971	0.129	0.657	0.204	0.457
Q66647	Atp5o	192241	0.001	0.993	0.038	0.857	-0.035	0.886	-0.166	0.571	-0.238	0.371
D3ZY50	Atpaf1	NA	-0.107	0.304	-0.112	0.457	-0.101	0.600	0.122	0.457	0.132	0.400
D3ZTW7	Atpaf2	NA	0.063	0.549	0.105	0.514	0.021	0.943	0.172	0.057	0.089	0.629
Q03344	Atpif1	NA	-0.255	0.043	-0.156	0.457	-0.355	0.029	0.230	0.086	0.030	0.857
G3V8T9	Bax	NA	-0.403	0.006	-0.420	0.086	-0.386	0.057	-0.020	0.971	0.014	0.971
B1WBN3	Bckdha	25244	-0.138	0.128	-0.154	0.229	-0.122	0.514	0.022	0.886	0.053	0.543
P35738	Bckdhh	29711	-0.101	0.336	-0.067	0.657	-0.136	0.429	0.116	0.486	0.047	0.714
Q00972	Bckdk	29603	-0.137	0.186	-0.141	0.514	-0.133	0.286	0.059	0.543	0.067	0.486
D3Z771	Bcl2l13	NA	-0.340	0.196	-0.376	0.457	-0.304	0.343	-0.045	0.943	0.026	0.971
Q5XIM0	Bcs1l	301514	-0.242	0.029	-0.301	0.029	-0.183	0.400	-0.155	0.514	-0.037	0.743
P29147	Bdh1	117099	0.225	0.471	0.165	0.743	0.285	0.400	-0.279	0.743	-0.159	0.543
Q3B8N9	Bphl	361239	-0.695	< 0.001	-0.846	0.029	-0.544	0.057	-0.061	0.743	0.241	0.200
Q35796	C1qbp	29681	-0.175	0.361	-0.521	0.143	0.171	0.371	-0.281	0.114	0.412	0.257
Q6AY04	C2orf47	NA	-0.068	0.630	-0.047	0.943	-0.090	0.714	-0.062	0.743	-0.105	0.429
Q642A4	C8orf82	NA	-0.309	0.017	-0.325	0.229	-0.294	0.086	0.055	0.771	0.086	0.486
D2GV57	Cars2	NA	-0.354	0.025	-0.469	0.257	-0.239	0.057	0.035	0.914	0.265	0.371
Q5PPN7	Ccdc51	316008	-0.250	0.026	-0.224	0.171	-0.277	0.143	0.002	1.000	-0.051	0.714
Q4V897	Ccdc90b	308820	-0.503	0.004	-0.542	0.143	-0.464	0.029	-0.043	0.857	0.035	0.914
D4AC23	Cct7	NA	-0.530	0.001	-0.638	0.029	-0.421	0.086	-0.060	0.914	0.156	0.343
D3ZQB6	Cecr5	NA	-0.389	0.003	-0.490	0.057	-0.288	0.029	-0.002	1.000	0.199	0.200
B5DER5	Chchd1	361005	-0.432	0.006	-0.468	0.057	-0.397	0.114	0.074	0.714	0.145	0.600
Q63ZY8	Chchd10	NA	0.294	0.018	0.402	0.114	0.186	0.114	-0.048	0.800	-0.263	0.143
D3ZUX5	Chchd3	NA	0.034	0.647	0.100	0.400	-0.031	0.686	0.006	0.943	-0.126	0.314
Q5BJN5	Chchd4	312559	-0.149	0.303	-0.107	0.571	-0.192	0.429	0.260	0.229	0.175	0.314
B0K020	Cisd1	NA	0.019	0.797	0.044	0.771	-0.006	0.943	-0.011	0.914	-0.060	0.743
MORAD5	Clpp	NA	-0.126	0.166	-0.176	0.057	-0.075	0.800	-0.038	0.914	0.063	0.514
Q5U2U0	Clpx	300786	-0.196	0.087	-0.192	0.314	-0.199	0.257	0.003	0.971	-0.004	0.886
Q5I0K3	Clybl	306198	0.054	0.625	0.109	0.629	0.000	1.000	0.034	0.743	-0.075	0.686
P22734	Comt	24267	-0.612	0.001	-0.601	0.057	-0.622	0.029	0.031	0.857	0.010	0.857
D3ZM21	Comtd1	NA	-0.044	0.765	-0.018	0.943	-0.069	0.914	0.101	0.714	0.050	0.829

Table C.1 Cont

D3ZK74	Coq10a	NA	0.170	0.111	0.072	0.743	0.269	0.086	-0.101	0.429	0.096	0.571
Q63159	Coq3	29309	-0.145	0.211	-0.161	0.171	-0.128	0.571	0.143	0.400	0.175	0.343
Q4G064	Coq5	NA	-0.119	0.369	-0.138	0.457	-0.100	0.771	0.105	0.686	0.143	0.257
Q68FU7	Coq6	299195	-0.160	0.099	-0.151	0.229	-0.169	0.400	0.053	0.743	0.035	0.743
Q68FT1	Coq9	NA	0.038	0.666	0.119	0.400	-0.042	0.743	0.021	0.857	-0.140	0.314
P10888	Cox411	29445	0.151	0.009	0.148	0.086	0.155	0.086	-0.076	0.286	-0.070	0.400
P11240	Cox5a	252934	0.352	0.008	0.333	0.086	0.370	0.057	-0.248	0.086	-0.211	0.286
P12075	Cox5b	94194	0.164	0.003	0.153	0.114	0.175	0.057	-0.086	0.057	-0.065	0.457
P10818	Cox6a1	25282	-0.193	0.324	-0.292	0.457	-0.093	0.571	0.104	0.743	0.303	0.286
G3V8M4	Cox6a2	NA	0.044	0.793	0.053	0.914	0.035	0.971	0.010	1.000	-0.009	0.943
D3ZD09	Cox6b1	NA	0.143	0.355	-0.137	0.514	0.423	0.057	-0.200	0.314	0.360	0.200
P11951	Cox6c2	NA	0.250	0.040	0.315	0.171	0.185	0.200	-0.032	0.800	-0.162	0.314
P35171	Cox7a2	NA	-0.002	0.976	-0.054	0.657	0.049	0.771	0.009	0.971	0.112	0.400
D3ZYX8	Cox7a2l	NA	0.043	0.225	-0.012	0.914	0.098	0.086	-0.013	0.914	0.097	0.114
P80431	Cox7b	303393	0.583	0.123	0.248	0.600	0.919	0.171	-0.800	0.143	-0.129	0.800
R80432	Cox7c	NA	0.381	0.004	0.273	0.229	0.488	0.029	-0.166	0.429	0.048	0.743
Q3B7D0	Cpx	304024	-0.337	0.019	-0.493	0.057	-0.180	0.371	-0.125	0.514	0.187	0.343
P18886	Cpt2	25413	-0.006	0.942	0.048	0.743	-0.059	0.571	0.047	0.514	-0.060	0.800
Q704S8	Crat	311849	0.125	0.085	0.103	0.429	0.147	0.029	0.064	0.257	0.108	0.429
Q5U2V5	Crsl1	366196	-0.248	0.405	-0.170	0.657	-0.326	0.486	-0.346	0.457	-0.502	0.286
P04166	Cyb5b	NA	-0.171	0.175	-0.248	0.200	-0.094	0.629	-0.012	0.886	0.143	0.514
P17178	Cyp27a1	301517	0.057	0.585	0.110	0.457	0.004	1.000	0.133	0.429	0.027	0.857
F7E2Z0	Dap3	NA	-0.372	< 0.001	-0.399	0.029	-0.345	0.086	0.010	0.971	0.064	0.543
B2GV15	Dbt	29611	0.054	0.586	0.108	0.429	0.001	1.000	0.033	0.800	-0.075	0.657
Q6AY55	Dcald	360639	-0.481	< 0.001	-0.522	0.029	-0.440	0.029	0.001	0.971	0.003	0.514
G3V734	Decr1	NA	0.113	0.285	-0.007	0.971	0.234	0.171	-0.129	0.371	0.113	0.543
D3ZDE4	Dguok	NA	-0.097	0.300	-0.021	0.943	-0.172	0.257	0.189	0.257	0.039	0.857
Q63707	Dhodh	65156	-0.175	0.177	-0.220	0.400	-0.129	0.571	-0.035	0.886	0.056	0.629
Q8VID1	Dhrs4	266686	-0.074	0.538	-0.084	0.657	-0.065	0.743	-0.025	0.829	-0.006	0.971
P08461	Dlat	81654	0.231	0.006	0.265	0.086	0.086	0.629	-0.040	0.657	-0.107	0.371
Q6P6R2	Dld	298942	0.111	0.306	0.125	0.400	0.097	0.629	-0.030	0.829	-0.058	0.714
G3V6P2	Dlst	NA	0.127	0.585	0.262	0.514	-0.009	0.971	-0.053	0.857	-0.324	0.429
B1WBV5	Dnajc11	362666	-0.366	< 0.001	-0.410	0.029	-0.322	0.057	-0.063	0.571	0.024	0.771
B2RVV0	Dnajc30	NA	-0.276	0.114	-0.407	0.257	-0.144	0.400	-0.218	0.571	0.045	0.829
D3ZDC1	Drg2	NA	-0.766	0.001	-0.544	0.114	-0.987	0.029	0.432	0.171	-0.011	0.943
P70583	Dut	NA	-0.513	< 0.001	-0.571	0.029	-0.454	0.029	-0.129	0.714	-0.012	0.857
Q62651	Ech1	64526	0.218	0.005	0.145	0.143	0.290	0.029	-0.055	0.714	0.091	0.286
P14604	Echs1	140547	0.043	0.554	0.030	0.743	0.055	0.657	-0.024	0.743	0.001	1.000
Q68G41	Eci1	NA	-0.167	0.055	-0.170	0.229	-0.164	0.143	-0.116	0.486	-0.110	0.171
Q5XIC0	Eci2	NA	0.226	0.018	0.128	0.400	0.325	0.029	-0.018	0.829	0.179	0.229
Q5XIC2	Ecsit	300447	-0.135	0.106	-0.154	0.200	-0.115	0.429	0.050	0.743	0.089	0.371
Q99372	Eln	25043	-0.640	0.001	-0.809	0.057	-0.472	0.029	-0.219	0.600	0.117	0.571
B0BNG0	Emc2	NA	-0.511	0.028	-0.567	0.171	-0.455	0.057	-0.304	0.429	-0.193	0.629
Q3V5X8	Endog	NA	-0.359	0.013	-0.487	0.086	-0.230	0.229	-0.120	0.486	0.137	0.514
P56571	ES1	NA	-0.015	0.861	0.050	0.743	-0.079	0.314	0.132	0.400	0.002	0.971
P13803	Etfa	300726	0.134	0.170	0.184	0.343	0.083	0.457	0.042	0.657	-0.060	0.829
Q68FU3	Etfb	292845	0.170	0.287	0.241	0.286	0.099	0.829	-0.080	0.771	-0.222	0.286
Q66HF3	Etfdh	295143	0.240	0.046	0.161	0.400	0.319	0.057	-0.168	0.343	-0.011	1.000
B0BNI4	Ethe1	292710	-0.176	0.094	-0.157	0.371	-0.195	0.257	0.062	0.686	0.023	0.800
D3ZTW9	Exog	NA	-0.463	0.002	-0.551	0.086	-0.376	0.057	-0.081	0.829	0.094	0.714
Q6AYQ8	Fahd1	302980	0.042	0.532	0.061	0.343	0.024	0.886	0.105	0.114	0.068	0.571
B2RVW9	Fahd2	NA	-0.121	0.215	-0.052	0.743	-0.190	0.114	0.158	0.286	0.020	0.914
Q5XIJ4	Fam210a	NA	0.012	0.914	-0.011	0.971	0.034	0.971	0.055	0.829	0.100	0.771
Q6AXX6	Fam213a	NA	-0.376	0.025	-0.409	0.171	-0.343	0.143	0.038	0.800	0.104	0.600
Q5M7V7	Fastkd2	301463	-0.127	0.460	-0.071	0.771	-0.182	0.314	0.037	0.914	-0.074	0.886
P56522	Fdxr	79122	-0.338	0.012	-0.369	0.200	-0.086	0.086	-0.030	0.943	0.033	0.857
D3ZBM3	Fech	NA	-0.043	0.731	-0.027	0.857	-0.058	0.943	0.095	0.629	0.064	0.657
Q5M964	Fh	NA	0.475	0.124	0.500	0.429	0.451	0.257	0.010	1.000	-0.039	0.743
Q3B7U9	Fkbp8	290652	-0.440	0.002	-0.519	0.086	-0.360	0.057	-0.113	0.514	0.045	0.800
Q5XJW2	Gadd45gip1	288916	-0.134	0.271	0.022	0.943	-0.290	0.171	0.196	0.400	-0.116	0.400
G3V7G8	Gars	NA	-0.404	0.019	-0.546	0.029	-0.261	0.314	0.027	0.943	0.312	0.171
D3ZY68	Gatc	NA	-0.190	0.685	-0.011	0.943	-0.369	0.457	-0.310	0.514	-0.668	0.514
Q5RK08	Gbas	498174	-0.042	0.683	-0.006	1.000	-0.079	0.571	0.190	0.143	0.116	0.571
D3ZT90	Gcdh	NA	-0.188	0.094	-0.273	0.086	-0.103	0.486	0.024	0.886	0.194	0.200
Q07803	Gfm1	114017	-0.193	0.051	-0.206	0.114	-0.180	0.200	0.032	0.714	0.059	0.457
Q5XIA8	Ghitm	290596	-0.121	0.093	-0.048	0.800	-0.195	0.086	0.078	0.429	-0.069	0.514
D3ZC10	Gk	NA	-0.163	0.105	-0.228	0.171	-0.097	0.543	-0.127	0.457	0.004	0.914
Q6AXW1	Glrx2	114022	-0.263	0.101	-0.380	0.143	-0.145	0.486	-0.052	0.857	0.184	0.257
D4ADD7	Glrx5	NA	-0.018	0.894	0.012	0.971	-0.049	0.857	0.268	0.057	0.207	0.457
P13264	Gls	24398	-0.166	0.314	0.111	0.657	-0.442	0.114	0.148	0.400	-0.405	0.143
P10860	Glud1	24399	-0.146	0.024	-0.182	0.114	-0.109	0.229	0.020	0.857	0.092	0.200
P00507	Got2	314123	0.145	0.051	0.184	0.143	0.106	0.314	0.034	0.629	-0.043	0.714
Q35077	Gpd1	60666	-0.402	0.004	-0.496	0.057	-0.308	0.114	-0.053	0.743	0.135	0.457
P35571	Gpd2	25062	-0.336	0.052	-0.333	0.229	-0.340	0.257	0.067	0.886	0.060	0.914
G3V872	Gpt2	NA	-0.570	0.017	-0.764	0.086	-0.375	0.171	-0.073	0.857	0.316	0.371
P04041	Gpx1	24404	-0.397	0.025	-0.417	0.200	-0.377	0.143	-0.041	0.800	-0.001	1.000
P97576	Grpel1	79563	-0.020	0.941	-0.023	0.943	-0.017	0.971	0.105	0.771	0.111	0.800
P24473	Gstk1	297029	-0.270	0.010	-0.326	0.057	-0.214	0.229	0.039	0.743	0.150	0.314
D3ZHF8	Guf1	NA	-0.489	< 0.001	-0.496	0.057	-0.482	0.029	-0.112	0.857	-0.097	0.343
Q9WVK7	Hadh	113965	-0.004	0.978	-0.186	0.457	0.179	0.486	-0.151	0.571	0.215	0.400
Q64428	Hadha	170670	0.234	0.006	0.264	0.143	0.204	0.029	-0.048	0.629	-0.109	0.429
Q60587	Hadhb	171155	0.271	0.001	0.339	0.029	0.203	0.143	-0.024	0.857	-0.160	0.086
F1LQ11	Hagh	NA	-0.228	0.099	-0.378	0.029	-0.079	0.800	-0.158	0.457	0.142	0.229



Table C.1 Cont.

D3ZL85	Hccs	NA	0.129	0.269	0.051	0.629	0.208	0.371	-0.228	0.229	-0.071	0.657
P29266	Hibadh	NA	-0.058	0.696	0.021	1.000	-0.137	0.629	0.108	0.629	-0.050	0.857
Q5XIE6	Hibch	301384	-0.103	0.114	-0.044	0.629	-0.162	0.114	0.143	0.171	0.025	0.800
D4A801	Hint2	NA	-0.029	0.798	0.039	0.771	-0.098	0.543	0.036	0.857	-0.101	0.543
P27881	Hk2	25059	-0.541	0.004	-0.371	0.171	-0.711	0.057	0.102	0.686	-0.238	0.200
P97519	Hmgcl	79238	-0.181	0.215	-0.134	0.486	-0.229	0.371	0.219	0.171	0.123	0.629
B0BMMW2	Hsd17b10	63864	0.045	0.438	0.086	0.257	0.004	0.943	0.117	0.200	0.035	0.714
P97852	Hsd17b4	79244	-0.543	0.004	-0.662	0.114	-0.425	0.057	-0.120	0.829	0.117	0.800
Q6MGB5	Hsd17b8	361802	-0.515	0.001	-0.613	0.029	-0.417	0.057	-0.042	0.886	0.153	0.400
Q4V8F9	Hsd12	NA	0.165	0.068	0.180	0.229	0.150	0.229	0.054	0.657	0.024	0.886
F1M953	Hspa9	NA	0.050	0.483	0.024	0.886	0.076	0.400	0.045	0.371	0.097	0.514
B5DFG4	Hspb7	50565	-0.417	0.036	-0.525	0.143	-0.309	0.171	0.071	0.800	0.287	0.343
P63039	Hspd1	289614	-0.002	0.986	0.085	0.600	-0.089	0.486	0.084	0.457	-0.090	0.543
D3ZDP2	Ict1	NA	-0.166	0.221	-0.093	0.629	-0.239	0.257	0.194	0.143	0.048	0.829
P41562	ldh1	24479	-0.279	0.083	-0.340	0.143	-0.218	0.400	-0.121	0.571	0.000	1.000
P56574	ldh2	361596	0.002	0.990	0.187	0.429	-0.184	0.257	0.101	0.543	-0.270	0.171
Q68FX0	ldh3B	94173	0.095	0.096	0.139	0.200	0.050	0.371	0.054	0.429	-0.035	0.686
Q5XIJ3	ldh3g	25179	0.101	0.537	0.145	0.686	0.057	0.714	-0.035	0.914	-0.122	0.771
Q3KR86	lmmt	312444	0.077	0.118	0.007	0.943	0.148	0.057	-0.091	0.114	0.050	0.543
D4A4L5	lscA2	NA	-0.252	0.105	-0.362	0.200	-0.142	0.429	-0.160	0.514	0.060	0.771
B2R279	lscu	NA	-0.225	0.006	-0.220	0.029	-0.230	0.171	-0.035	0.800	-0.045	0.629
P12007	lvd	24513	-0.173	0.077	-0.074	0.543	-0.273	0.171	0.138	0.343	-0.061	0.743
Q5XIM7	Kars	292028	-0.410	0.002	-0.474	0.057	-0.346	0.086	-0.042	0.829	0.087	0.400
D3ZVS2	L2hgdh	NA	-0.106	0.306	-0.039	0.743	-0.173	0.371	-0.004	1.000	-0.137	0.229
Q3ZPX9	Lace1	NA	0.030	0.840	0.166	0.371	-0.107	0.657	0.178	0.457	-0.095	0.457
D3ZFI6	Lactb	NA	-0.101	0.109	-0.141	0.171	-0.062	0.371	-0.156	0.086	-0.077	0.429
Q68FS4	Lap3	289668	-0.383	< 0.001	-0.448	0.029	-0.319	0.029	-0.073	0.714	0.057	0.457
P04642	Ldha	366355	-0.513	0.004	-0.688	0.057	-0.338	0.114	-0.041	0.886	0.309	0.171
P42123	Ldhb	24534	-0.164	0.132	-0.356	0.086	0.028	0.857	-0.229	0.057	0.155	0.314
Q77PJ4	Ldhd	307858	-0.292	0.103	-0.341	0.371	-0.242	0.171	-0.096	0.800	0.003	1.000
Q5XIN6	Letm1	305457	-0.185	0.158	-0.158	0.400	-0.212	0.371	0.056	0.657	0.002	1.000
Q5XIH4	Lias	305348	-0.364	0.007	-0.363	0.114	-0.365	0.086	0.200	0.200	0.199	0.543
F1LXAO	LOC100910710	NA	-0.105	0.280	-0.207	0.257	-0.002	0.971	-0.019	0.914	0.186	0.086
Q3MHT2	LOC100911034	NA	-0.114	0.351	0.022	0.943	-0.250	0.257	0.069	0.771	-0.203	0.200
Q6IRL2	LOC100911485	NA	-0.286	0.016	-0.308	0.171	-0.263	0.143	-0.026	0.829	0.019	0.914
D3ZCZ9	LOC100912599	NA	-0.069	0.586	-0.087	0.600	-0.052	0.914	-0.055	0.829	-0.020	0.914
D3ZFI3	LOC683884	NA	0.225	0.108	0.205	0.514	0.245	0.029	-0.055	0.886	-0.016	0.857
A9UMV7	LOC686442	NA	-0.398	0.343	-0.668	0.457	-0.128	0.686	-0.125	0.771	0.416	0.686
Q924S5	Lonp1	170916	-0.145	0.118	-0.133	0.486	-0.157	0.171	0.080	0.486	0.056	0.771
Q5SGE0	Lrpprc	313867	0.907	0.076	0.457	0.543	1.357	0.114	-0.387	0.314	0.512	0.600
G3V9Z3	Maoa	NA	-0.177	0.122	-0.214	0.286	-0.140	0.429	-0.076	0.743	-0.002	1.000
Q66HG9	Mavs	NA	-0.344	0.023	-0.314	0.143	-0.374	0.114	-0.104	0.657	-0.164	0.486
D3ZPF2	Mcat	NA	-0.390	0.053	-0.360	0.400	-0.419	0.029	0.063	0.829	0.004	0.971
Q5XIT9	Mccc2	361884	-0.061	0.388	-0.060	0.629	-0.063	0.714	0.045	0.800	0.042	0.571
D4A197	Mcee	NA	0.207	0.172	0.256	0.314	0.158	0.429	0.196	0.400	0.098	0.629
MORDI5	Mcu	NA	-0.262	0.009	-0.239	0.057	-0.285	0.086	0.039	0.943	-0.007	0.914
Q89989	Mdh1	24551	-0.040	0.759	-0.248	0.286	0.168	0.257	-0.160	0.286	0.256	0.229
P04636	Mdh2	81829	0.041	0.446	0.062	0.514	0.020	0.714	0.084	0.314	0.043	0.629
D3ZJH9	Me2	NA	-0.713	0.002	-0.934	0.086	-0.491	0.057	-0.367	0.343	0.075	0.743
Q8R4Z9	Mfn1	192647	-0.068	0.474	-0.103	0.457	-0.033	0.829	-0.004	0.971	0.066	0.657
Q920F5	Mlycd	85239	-0.267	0.061	-0.400	0.114	-0.133	0.514	-0.150	0.457	0.117	0.543
B5DFN3	Mnf1	NA	-0.151	0.094	-0.155	0.200	-0.148	0.429	0.067	0.657	0.074	0.486
P63031	Mpc1	NA	-0.021	0.912	0.179	0.571	-0.222	0.343	-0.049	0.714	-0.451	0.143
P97532	Mpst	192172	-0.101	0.376	0.003	1.000	-0.204	0.286	0.142	0.400	-0.064	0.743
Q5XIE3	Mrpl11	293666	-0.299	0.032	-0.366	0.114	-0.232	0.257	-0.057	0.829	0.077	0.657
D3ZXF9	Mrpl12	NA	-0.085	0.412	-0.111	0.600	-0.060	0.629	0.016	0.829	0.067	0.771
Q7M0E7	Mrpl14	301250	-0.286	0.003	-0.278	0.086	-0.293	0.029	0.136	0.286	0.121	0.286
D4A4A9	Mrpl19	NA	-0.345	0.012	-0.406	0.057	-0.283	0.114	0.168	0.457	0.291	0.057
Q498T4	Mrpl2	NA	-0.532	0.003	-0.662	0.086	-0.403	0.086	-0.131	0.629	0.128	0.600
B2GV62	Mrpl20	NA	-0.335	0.010	-0.279	0.171	-0.391	0.057	0.197	0.457	0.086	0.457
D3ZMR9	Mrpl21	NA	-0.120	0.281	-0.103	0.571	-0.136	0.429	0.112	0.514	0.079	0.571
POC2C0	Mrpl22	287302	-0.219	0.060	-0.184	0.343	-0.254	0.171	0.018	0.886	-0.053	0.714
Q66H47	Mrpl24	295224	-0.256	0.002	-0.266	0.057	-0.246	0.057	0.051	0.800	0.070	0.429
D3ZJY1	Mrpl28	NA	-0.287	0.005	-0.250	0.114	-0.324	0.086	0.145	0.229	0.071	0.600
POC2C1	Mrpl30	502223	-0.268	0.049	-0.303	0.286	-0.232	0.171	0.025	0.886	0.096	0.371
D4ABL7	Mrpl33	NA	-0.451	0.213	-0.518	0.371	-0.384	0.457	0.152	0.829	0.286	0.600
Q6AXT0	Mrpl37	56281	-0.316	0.001	-0.340	0.029	-0.291	0.086	-0.056	0.629	-0.006	1.000
Q5PQN9	Mrpl38	NA	-0.335	0.014	-0.343	0.143	-0.328	0.057	0.036	0.800	0.052	0.771
D4A131	Mrpl4	NA	-0.205	0.035	-0.188	0.143	-0.223	0.257	0.003	0.971	-0.032	0.857
Q4G067	Mrpl44	301552	-0.298	0.081	-0.283	0.429	-0.313	0.114	-0.094	0.771	-0.124	0.571
D4A104	Mrpl45	NA	-0.279	0.002	-0.339	0.029	-0.219	0.143	-0.009	0.971	0.112	0.371
Q5RK00	Mrpl46	293054	-0.366	0.001	-0.401	0.029	-0.332	0.086	0.021	0.857	0.090	0.457
D3ZDX7	Mrpl48	NA	-0.167	0.108	-0.114	0.429	-0.221	0.200	0.008	0.971	-0.099	0.543
Q7TF77	Mrpl49	309176	-0.343	0.009	-0.450	0.086	-0.235	0.143	-0.062	0.771	0.153	0.229
D3ZYL4	Mrpl50	NA	-0.316	0.007	-0.351	0.086	-0.281	0.086	-0.079	0.714	-0.009	0.971
B2RYW4	Mrpl53	362388	-0.206	0.501	-0.289	0.600	-0.123	0.857	-0.069	0.914	0.097	0.600
D3Z9K2	Mrpl54	NA	0.099	0.582	0.284	0.371	-0.085	0.743	0.042	0.886	-0.328	0.314
Q641X9	Mrpl9	310653	-0.371	0.004	-0.428	0.057	-0.314	0.057	0.025	0.971	0.139	0.314
D4A040	Mrps11	NA	-0.347	0.005	-0.387	0.057	-0.308	0.114	-0.047	0.829	0.031	0.800
Q5XJ37	Mrps15	298517	-0.435	0.006	-0.451	0.086	-0.420	0.057	0.144	0.486	0.175	0.400
D3ZTR1	Mrps17	NA	-0.244	0.066	-0.191	0.257	-0.297	0.200	-0.033	0.914	-0.139	0.371
F6Q5K7	Mrps18b	NA	-0.307	0.010	-0.273	0.143	-0.340	0.057	0.068	0.657	0.001	0.971
D3ZIN7	Mrps23	NA	-0.399	0.006	-0.364	0.114	-0.435	0.057	0.094	0.771	0.023	0.857

Table C.1 Cont.

A9UMV2	Mrps24	NA	-0.371	0.002	-0.322	0.029	-0.420	0.086	0.187	0.429	0.089	0.486
Q4QR80	Mrps25	297459	-0.446	< 0.001	-0.390	0.029	-0.502	0.029	0.088	0.629	-0.024	0.914
D4A833	Mrps30	NA	-0.279	0.034	-0.306	0.171	-0.252	0.229	0.012	0.971	0.067	0.743
B0BN56	Mrps31	290850	-0.344	< 0.001	-0.338	0.029	-0.350	0.029	0.072	0.714	0.060	0.571
Q0ZF54	Mrps33	296995	-0.348	0.017	-0.354	0.171	-0.342	0.086	0.154	0.314	0.165	0.514
D4ABM5	Mrps34	NA	-0.348	0.005	-0.312	0.086	-0.383	0.057	0.118	0.457	0.047	0.743
D4A9Z6	Mrps35	NA	-0.581	0.005	-0.169	0.257	-0.993	0.029	0.678	0.029	-0.147	0.371
M0R776	Mrps36	NA	-0.083	0.643	-0.103	0.829	-0.063	0.800	-0.069	0.886	-0.029	0.886
D3ZVT2	Mrps5	NA	-0.712	< 0.001	-0.760	0.029	-0.665	0.057	0.056	0.800	0.152	0.400
Q5I0K8	Mrps7	113958	-0.483	0.002	-0.578	0.029	-0.388	0.171	-0.007	1.000	0.183	0.314
B0BN68	Mrps9	301371	-0.413	0.001	-0.429	0.029	-0.397	0.057	0.072	0.686	0.104	0.371
Q8HIC8	Mt-atp8	NA	-2.625	< 0.001	-2.640	0.029	-2.610	0.029	-0.004	1.000	0.026	0.886
Q8HIC9	Mt-co1	NA	-0.103	0.667	0.018	0.971	-0.223	0.314	-0.119	0.714	-0.360	0.514
Q8SEZ5	Mt-co2	NA	-2.363	< 0.001	-2.341	0.029	-2.385	0.029	-0.059	0.914	-0.102	0.914
Q8HIC6	Mt-nd4	NA	-0.321	0.034	-0.262	0.371	-0.381	0.029	0.004	1.000	-0.115	0.857
Q7H113	Mt-nd4l	NA	-0.418	0.058	-0.557	0.143	-0.279	0.371	-0.237	0.600	0.042	0.886
Q8SEZ0	Mt-nd5	NA	-0.209	0.019	-0.204	0.086	-0.214	0.229	0.077	0.571	0.067	0.457
B0BN52	Mtch2	295922	-0.105	0.238	-0.251	0.143	0.042	0.600	-0.089	0.143	0.204	0.200
Q5XIG9	Mtftp1	NA	-0.170	0.150	-0.206	0.257	-0.134	0.657	-0.030	0.857	0.041	0.686
B0BN02	Mtx1	NA	-0.313	0.011	-0.359	0.057	-0.266	0.171	-0.066	0.771	0.027	0.829
Q5U1Z9	Mtx2	288150	-0.109	0.341	-0.003	1.000	-0.215	0.257	0.083	0.457	-0.129	0.571
D4A1H7	Mul1	NA	0.079	0.868	0.340	0.743	-0.182	0.486	0.025	0.943	-0.496	0.571
F1LPV0	Nars	NA	-0.700	0.001	-1.047	0.029	-0.353	0.143	-0.486	0.314	0.208	0.314
G3V9S6	Ndufa1	NA	-0.343	0.397	-0.581	0.343	-0.105	0.857	0.081	0.886	0.558	0.371
Q80W89	Ndufa11	301123	-0.136	0.287	-0.105	0.629	-0.167	0.486	0.090	0.714	0.027	0.943
D3Z5S8	Ndufa2	NA	-0.002	0.990	-0.062	0.743	0.059	0.857	-0.162	0.514	-0.040	0.857
F1M8L6	Ndufa3	NA	-0.135	0.299	-0.052	0.771	-0.217	0.314	0.096	0.714	-0.069	0.743
B2RZD6	Ndufa4	NA	0.265	0.049	0.251	0.343	0.279	0.229	-0.102	0.600	-0.075	0.629
Q63362	Ndufa5	25488	-0.033	0.836	-0.175	0.429	0.108	0.629	-0.073	0.657	0.210	0.429
D4A3V2	Ndufa6	NA	-0.088	0.463	-0.318	0.114	0.142	0.343	-0.160	0.343	0.300	0.114
Q7TP78	Ndufa8	296658	0.032	0.875	-0.184	0.314	0.248	0.514	-0.305	0.457	0.126	0.400
Q5BK63	Ndufa9	NA	-0.135	0.197	-0.157	0.400	-0.114	0.457	0.008	0.971	0.051	0.800
F1LWG4	Ndufa11	NA	-0.133	0.221	-0.206	0.171	-0.060	0.829	-0.013	0.943	0.133	0.229
Q08776	Ndufa3	NA	-0.276	0.003	-0.372	0.029	-0.180	0.171	-0.054	0.743	0.138	0.114
Q9NQR8	Ndufa4	NA	-0.115	0.119	-0.100	0.171	-0.130	0.343	0.054	0.714	0.024	0.743
B2GV71	Ndufa5	NA	-0.203	0.216	-0.264	0.514	-0.143	0.514	-0.064	0.829	0.057	0.600
D3ZN43	Ndufa6	NA	0.030	0.827	0.105	0.686	-0.044	0.857	0.168	0.486	0.019	0.943
Q5XI79	Ndufa7	NA	-0.644	0.003	-0.752	0.114	-0.536	0.029	-0.163	0.829	0.053	0.800
D4A0T0	Ndufb10	NA	-0.209	0.060	-0.127	0.543	-0.290	0.057	0.060	0.571	-0.102	0.686
D4A7L4	Ndufb11	NA	-0.106	0.403	-0.025	0.886	-0.188	0.429	0.086	0.771	-0.078	0.571
B2RYU0	Ndufb2	362344	-0.565	0.001	-0.606	0.086	-0.524	0.029	-0.111	0.686	-0.030	0.857
D4A565	Ndufb5	NA	0.028	0.794	0.000	0.971	0.057	0.857	-0.041	1.000	0.016	0.857
D3ZZ21	Ndufb6	NA	-0.229	0.003	-0.266	0.057	-0.193	0.057	0.082	0.343	0.155	0.143
D3ZLT1	Ndufb7	NA	-0.361	0.043	-0.381	0.171	-0.341	0.229	-0.006	1.000	0.035	0.800
B2RYS8	Ndufb8	293991	-0.206	0.013	-0.174	0.114	-0.238	0.143	0.045	0.857	-0.020	0.829
B2RYW3	Ndufb9	299954	-0.139	0.084	-0.183	0.200	-0.095	0.400	-0.002	1.000	0.085	0.486
D3Z575	Ndufc1	NA	0.299	0.296	0.283	0.486	0.316	0.486	-0.526	0.286	-0.493	0.229
Q5PQZ9	Ndufc2	293130	-0.309	0.003	-0.388	0.057	-0.231	0.114	0.051	0.571	0.028	0.200
Q66HF1	Ndufc3	301458	-0.116	0.096	-0.111	0.257	-0.120	0.171	0.034	0.657	0.025	0.657
Q641Y2	Ndufc4	NA	-0.195	0.002	-0.222	0.029	-0.168	0.086	-0.008	0.914	0.045	0.629
D3ZG43	Ndufc5	NA	-0.080	0.305	0.011	0.914	-0.172	0.143	0.081	0.686	-0.102	0.314
Q5XIF3	Ndufc6	NA	-0.077	0.682	-0.220	0.486	0.066	0.857	-0.166	0.514	0.120	0.657
B5DEL8	Ndufc7	362588	-0.220	0.314	-0.359	0.343	-0.080	0.743	-0.029	0.914	0.251	0.486
Q5RJN0	Ndufc8	362837	-0.106	0.030	-0.056	0.400	-0.157	0.029	0.012	0.800	-0.089	0.314
B0BNE6	Ndufc9	293652	-0.075	0.340	-0.043	0.714	-0.106	0.429	0.048	0.743	-0.015	0.914
Q5XIH3	Ndufv1	293655	-0.085	0.438	-0.194	0.371	0.023	0.886	-0.092	0.457	0.124	0.571
P19234	Ndufv2	81728	-0.111	0.030	-0.134	0.086	-0.088	0.257	0.045	0.571	0.091	0.114
G3V644	Ndufv3	NA	-0.394	< 0.001	-0.450	0.029	-0.338	0.057	-0.030	0.857	0.082	0.571
Q6PCU8	Ndufv4	NA	-0.172	0.125	-0.182	0.343	-0.163	0.429	-0.094	0.771	-0.075	0.371
D3ZA85	Nfu1	NA	-0.190	0.085	-0.069	0.657	-0.311	0.057	0.128	0.543	-0.114	0.257
P42676	Nln	117041	-0.317	0.022	-0.343	0.171	-0.290	0.143	0.033	0.800	0.087	0.571
Q5FVQ8	Nlrx1	NA	-0.284	0.001	-0.310	0.029	-0.257	0.057	0.035	0.629	0.088	0.257
P19804	Nme2	83782	-0.163	0.028	-0.205	0.114	-0.121	0.229	0.048	0.514	0.133	0.200
B2GUX5	Nt5c3a	NA	-0.289	0.006	-0.298	0.057	-0.280	0.086	0.118	0.486	0.136	0.114
Q6AYD9	Nudt19	308518	-0.278	0.038	-0.295	0.057	-0.262	0.257	0.019	0.971	0.052	0.514
D3ZEH6	Nudt8	NA	-0.106	0.344	-0.174	0.343	-0.039	0.857	-0.010	0.971	0.125	0.400
P04182	Oat	64313	-0.252	0.035	-0.168	0.371	-0.336	0.086	0.146	0.371	-0.022	0.857
Q5XIG4	Ociad1	289590	-0.167	0.072	-0.154	0.257	-0.179	0.314	-0.002	1.000	-0.027	0.829
Q5X178	Ogdh	NA	-0.011	0.790	0.020	0.771	-0.042	0.429	0.004	0.943	-0.058	0.286
D3Z574	Oma1	NA	-0.293	0.015	-0.337	0.171	-0.249	0.114	0.072	0.571	0.160	0.371
D3ZRH1	Oxa1l	NA	-0.300	0.004	-0.363	0.029	-0.237	0.143	0.047	0.829	0.173	0.171
B2GV06	Oxct1	NA	0.102	0.157	0.060	0.571	0.143	0.229	0.024	0.600	0.106	0.457
D4A0Y4	Oxna1	NA	-0.080	0.418	-0.041	0.571	-0.120	0.629	0.184	0.143	0.106	0.543
G3V6R7	Oxsm	NA	-0.266	0.026	-0.201	0.200	-0.330	0.057	0.193	0.229	0.064	0.686
D3ZZV1	Pam16	NA	-0.057	0.506	-0.006	1.000	-0.108	0.514	0.023	0.857	-0.078	0.543
O88767	Park7	364583	-0.255	0.036	-0.364	0.057	-0.146	0.400	-0.039	0.829	0.178	0.286
P52873	Pc	NA	-0.123	0.247	-0.171	0.429	-0.075	0.514	0.032	0.857	0.128	0.229
P14882	Pcca	687008	-0.115	0.523	-0.216	0.514	-0.015	0.943	0.085	0.600	0.286	0.457
Q68FZ8	Pccb	24624	-0.155	0.269	-0.094	0.743	-0.216	0.257	0.130	0.457	0.008	1.000
P49432	Pdhb	289950	0.058	0.511	0.157	0.200	-0.041	0.886	0.143	0.371	-0.055	0.686
Q64536	Pdk2	81530	-0.036	0.721	0.003	0.943	-0.076	0.629	0.188	0.314	0.109	0.371
A11L14	Pdp1	NA	-0.095	0.306	-0.057	0.657	-0.132	0.457	0.039	0.771	-0.036	0.771
D3ZX46	Pdpr	NA	0.010	0.910	0.059	0.686	-0.039	0.829	0.106	0.486	0.008	0.971

Table C.1 Cont.

Q75Q41	Tomm22	300075	-0.212	0.092	-0.183	0.314	-0.240	0.314	0.021	1.000	-0.035	0.943
Q3KRD5	Tomm34	311621	-0.507	0.001	-0.628	0.029	-0.387	0.057	0.026	0.886	0.267	0.257
D3ZJ53	Tomm6	NA	-0.251	0.063	-0.311	0.229	-0.190	0.200	0.046	0.771	0.168	0.371
Q75Q39	Tomm70a	680142	-0.334	0.001	-0.364	0.057	-0.303	0.057	-0.050	0.829	0.011	0.886
Q5XH20	Trap1	287069	-0.494	< 0.001	-0.427	0.029	-0.561	0.029	0.150	0.286	0.016	0.971
P24329	Tst	25274	-0.059	0.644	0.061	0.714	-0.178	0.457	0.060	0.829	-0.179	0.143
D4A6D7	Ttc19	NA	-0.276	0.009	-0.368	0.057	-0.184	0.257	-0.085	0.543	0.099	0.457
P85834	Tufm	293481	0.075	0.202	0.081	0.343	0.068	0.457	0.086	0.371	0.074	0.400
P97615	Txn2	79462	-0.288	0.113	-0.374	0.171	-0.201	0.486	0.055	0.829	0.228	0.314
Q89049	Txnrd1	NA	-0.396	0.003	-0.492	0.029	-0.301	0.114	-0.018	0.943	0.173	0.286
Q920J5	Txnrd2	50551	-0.089	0.295	-0.116	0.286	-0.062	0.686	0.054	0.743	0.108	0.286
P56499	Ucp3	25708	0.266	0.035	0.156	0.286	0.376	0.114	-0.092	0.771	0.128	0.457
Q68FY0	Uqcrc1	301011	0.010	0.872	0.001	1.000	0.019	0.829	-0.006	0.914	0.012	0.971
P32551	Uqcrc2	NA	0.031	0.730	0.076	0.486	-0.014	0.914	-0.098	0.286	-0.188	0.257
P20788	Uqcrcf1	291103	0.034	0.649	0.133	0.200	-0.066	0.714	0.104	0.086	-0.095	0.543
Q77Q16	Uqcrq	NA	0.048	0.803	-0.087	0.800	0.183	0.457	-0.108	0.714	0.162	0.600
P81155	Vdac2	83531	-0.028	0.704	-0.051	0.600	-0.005	0.971	0.016	0.914	0.062	0.629
Q9R1Z0	Vdac3	83532	-0.226	0.329	-0.070	0.971	-0.381	0.143	-0.074	0.743	-0.385	0.371
F1M8H2	Wars2	NA	-0.348	0.044	-0.302	0.286	-0.395	0.086	0.183	0.371	0.090	0.686
D3ZTR5	Zbed5	NA	-0.039	0.717	0.039	0.829	-0.116	0.514	-0.052	0.714	-0.206	0.171

## Table C.2

Table C.2 Phospho-site fold change.

Uniprot ID	Gene Symbol	Entrez	Site	HCR/LCR		HCR Rest / LCR Rest		HCR Run / LCR Run		LCR Run / LCR Rest		HCR Run / HCR Rest	
				log2 fold change	Permutation P-value	log2 fold change	Permutation P-value	log2 fold change	Permutation P-value	log2 fold change	Permutation P-value	log2 fold change	Permutation P-value
Q5RKI8	Abcb8	362302	S697	0.388	0.005	0.552	0.029	0.224	0.200	0.169	0.371	-0.159	0.400
Q5RKI8	Abcb8	362302	T621	-0.208	0.097	-0.114	0.629	-0.302	0.171	0.053	0.714	-0.135	0.657
Q5RKI8	Abcb8	362302	S700	0.273	0.046	0.158	0.286	0.387	0.143	-0.222	0.543	0.007	0.914
P15650	Acadl	25287	S193	0.198	0.255	0.209	0.486	0.187	0.429	-0.102	0.629	-0.124	0.657
Q9ER34	Aco2	79250	S559	-0.522	0.004	-0.393	0.057	-0.651	0.057	0.146	0.629	-0.112	0.600
P18163	Acs1	25288	S424	0.178	0.113	0.203	0.143	0.153	0.429	0.134	0.486	0.084	0.514
P18163	Acs1	25288	S230	-0.257	0.385	-0.355	0.657	-0.159	0.314	-0.162	0.829	0.035	0.600
D4A1G1	Acyp2	NA	S69	0.039	0.902	-0.108	0.857	0.186	0.657	0.108	0.714	0.402	0.457
Q9JM53	Aifm1	83533	S374	0.147	0.062	0.262	0.086	0.033	0.686	0.122	0.457	-0.107	0.114
Q9JM53	Aifm1	83533	S267	-0.036	0.944	-0.364	0.571	0.292	0.686	0.321	0.714	0.977	0.314
Q9JM53	Aifm1	83533	S370	0.215	0.008	0.187	0.143	0.242	0.086	-0.061	0.686	-0.006	0.886
Q5U1W6	Apool	317191	T34	0.451	0.027	0.641	0.143	0.261	0.057	0.063	0.771	-0.316	0.400
Q5U1W6	Apool	317191	Y49	0.228	0.418	-0.029	0.971	0.484	0.057	-0.619	0.229	-0.106	0.629
B1WBW4	Armc10	NA	S43	0.023	0.921	0.075	0.829	-0.030	0.800	-0.275	0.143	-0.380	0.371
P19511	Atp5f1	NA	S228	0.117	0.332	-0.013	1.000	0.247	0.229	-0.025	0.914	0.234	0.229
P19511	Atp5f1	NA	Y165	0.149	0.357	0.106	0.629	0.193	0.343	0.119	0.571	0.206	0.429
P29419	Atp5i	140608	S68	-0.140	0.459	-0.340	0.029	0.151	0.714	-0.321	0.314	0.260	0.257
P29419	Atp5i	140608	Y32	0.365	0.423	0.434	0.457	0.297	0.771	0.224	0.629	0.087	0.943
D3ZAF6	Atp5j2	NA	S32	0.278	0.167	0.179	0.457	0.377	0.314	-0.344	0.143	-0.146	0.686
D3ZY50	Atpaf1	NA	S76	-0.696	0.044	-0.736	0.171	-0.657	0.200	-0.547	0.257	-0.468	0.371
B1WBN3	Bckdha	25244	S348	0.027	0.876	0.209	0.457	-0.155	0.314	-0.140	0.400	-0.504	0.114
B1WBN3	Bckdha	25244	S338	-0.292	0.506	0.157	0.800	-0.741	0.086	-0.048	0.971	-0.946	0.114
Q00972	Bckdk	29603	S31	0.135	0.302	0.257	0.343	0.013	0.914	-0.018	0.943	-0.262	0.171
D3ZUX5	Chchd3	NA	Y49	-0.003	0.987	-0.221	0.429	0.215	0.543	-0.014	1.000	0.422	0.143
D3ZUX5	Chchd3	NA	Y179	-0.220	0.312	-0.494	0.200	0.053	0.829	-0.231	0.571	0.316	0.143
D3ZUX5	Chchd3	NA	S51	-0.416	0.370	-0.570	0.629	-0.263	0.657	0.168	0.600	0.475	0.486
D3ZUX5	Chchd3	NA	T188	0.131	0.560	0.023	0.943	0.240	0.571	-0.128	0.743	0.088	0.771
D3ZUX5	Chchd3	NA	S29	-0.016	0.908	-0.047	0.800	0.015	0.914	-0.028	0.857	0.035	0.857
D3ZUX5	Chchd3	NA	S112	0.143	0.351	0.151	0.343	0.135	0.657	-0.005	1.000	-0.020	0.971
Q68FT1	Coq9	NA	S80	-0.122	0.236	-0.199	0.229	-0.046	0.800	-0.080	0.714	0.074	0.343
P10888	Cox4i1	29445	Y44	-0.585	0.090	-0.270	0.457	-0.901	0.143	-0.131	0.771	-0.762	0.171
P10888	Cox4i1	29445	S26	0.367	0.314	0.334	0.571	0.400	0.429	-0.171	0.714	-0.105	0.771
P10888	Cox4i1	29445	S58	0.100	0.360	0.208	0.143	-0.007	0.971	0.208	0.257	-0.007	0.914
D3ZD09	Cox6b1	NA	S52	0.283	0.203	0.637	0.029	-0.071	0.914	0.183	0.686	-0.525	0.114
P80432	Cox7c	NA	S17	-0.024	0.892	0.238	0.286	-0.286	0.400	0.279	0.371	-0.245	0.257
Q3B7D0	Cpox	304024	S101	0.179	0.094	0.381	0.029	-0.023	0.886	0.112	0.229	-0.292	0.143
B2GV15	Dbt	29611	S220	-0.016	0.894	-0.210	0.429	0.179	0.200	-0.145	0.486	0.244	0.114
G3V6P2	Dlst	NA	T162	-0.061	0.889	0.239	0.771	-0.361	0.543	0.202	0.743	-0.398	0.600
P13803	Etfp	300726	S172	-0.427	0.274	-0.694	0.371	-0.160	0.629	-0.555	0.171	-0.021	0.971
Q5M964	Fh	NA	S362	-0.279	0.329	-0.259	0.571	-0.299	0.571	-0.144	0.771	-0.184	0.514
P10860	Glud1	24399	Y451	0.176	0.170	0.216	0.400	0.137	0.314	0.119	0.400	0.040	0.914
P00507	Got2	314123	S306	-0.051	0.705	-0.044	0.771	-0.058	0.800	-0.047	0.857	-0.061	0.800
P00507	Got2	314123	S133	-0.269	0.113	-0.301	0.457	-0.237	0.229	-0.076	0.829	-0.012	0.914
Q35077	Gpd1	60666	S308	0.601	0.003	0.652	0.143	0.551	0.029	0.104	0.714	0.003	0.971
Q9WVK7	Hadh	113965	S13	-0.357	0.398	-0.171	0.771	-0.544	0.514	-0.067	0.971	-0.440	0.286
Q64428	Hadha	170670	S641	0.061	0.630	0.122	0.714	0.000	1.000	0.195	0.343	0.073	0.714
Q64428	Hadha	170670	S643	0.015	0.908	0.070	0.857	-0.041	0.829	0.129	0.486	0.017	0.971
Q64428	Hadha	170670	T395	0.156	0.458	0.198	0.371	0.113	0.771	0.084	0.857	-0.001	1.000
Q6MG85	Hsd17b8	361802	S58	0.055	0.556	0.075	0.743	0.036	0.800	0.053	0.743	0.013	0.914
P56574	Idh2	361596	S423	0.167	0.403	0.142	0.629	0.192	0.514	-0.020	1.000	0.031	0.971
Q5XU3	Idh3g	25179	T120	0.130	0.683	0.423	0.343	-0.162	0.771	0.515	0.171	-0.070	0.886
Q3KR86	Immt	312444	Y578	0.050	0.623	0.123	0.514	-0.023	0.886	0.008	1.000	-0.138	0.200
Q3KR86	Immt	312444	T185	-0.202	0.147	-0.211	0.429	-0.194	0.314	-0.135	0.629	-0.119	0.371
Q3KR86	Immt	312444	S69	0.073	0.666	0.185	0.486	-0.039	0.914	0.091	0.771	-0.133	0.629
Q3KR86	Immt	312444	S302	0.186	0.110	0.264	0.057	0.108	0.657	0.136	0.543	-0.020	0.829
Q3KR86	Immt	312444	S507	-0.188	0.160	-0.265	0.143	-0.111	0.657	-0.125	0.600	0.029	0.829
Q3KR86	Immt	312444	S399	-0.071	0.759	-0.036	0.943	-0.178	0.600	0.270	0.429	0.056	0.943
Q3KR86	Immt	312444	T192	-0.202	0.265	-0.190	0.857	-0.213	0.200	0.012	0.943	-0.011	1.000
P04642	Ldha	366355	Y239	0.056	0.642	0.164	0.229	-0.052	0.857	-0.118	0.400	-0.334	0.114
P04642	Ldha	366355	T307	0.266	0.020	0.338	0.029	0.194	0.114	-0.066	0.657	-0.211	0.114
P04642	Ldha	366355	T86	0.425	0.008	0.554	0.029	0.297	0.229	0.008	1.000	-0.250	0.143
P04642	Ldha	366355	S84	0.029	0.907	-0.125	0.857	0.183	0.571	0.053	0.914	0.362	0.429
P04642	Ldha	366355	T322	0.355	0.002	0.355	0.086	0.356	0.029	-0.063	0.714	-0.062	0.514
Q5XIT9	Mccc2	361884	S499	0.334	0.031	0.273	0.343	0.396	0.086	-0.046	0.886	0.076	0.857
O88989	Mdh1	24551	S241	-0.062	0.665	0.150	0.514	-0.273	0.229	0.334	0.029	-0.089	0.543
P04636	Mdh2	81829	T235	0.252	0.080	0.291	0.200	0.213	0.286	0.011	0.971	-0.067	0.743
P04636	Mdh2	81829	S246	-0.034	0.814	-0.083	0.771	0.014	0.943	-0.026	0.943	0.070	0.743
B0BN52	Mtch2	295922	S116	0.457	0.071	0.761	0.029	0.153	0.771	0.160	0.771	-0.448	0.171
B0BN52	Mtch2	295922	S283	-0.036	0.845	0.311	0.171	-0.382	0.200	0.276	0.086	-0.416	0.286
F1M8L6	Ndufa3	NA	S68	0.045	0.727	0.004	1.000	0.086	0.800	-0.201	0.314	-0.118	0.543
B2RZD6	Ndufa4	NA	S67	-0.095	0.801	-0.511	0.429	0.321	0.457	-0.622	0.200	0.210	0.743
D4A0T0	Ndufb10	NA	S4	0.241	0.264	-0.004	1.000	0.485	0.171	0.006	0.943	0.495	0.229
D4A0T0	Ndufb10	NA	T31	-0.316	0.186	-0.573	0.143	-0.059	0.800	-0.317	0.514	0.197	0.400
D4A0T0	Ndufb10	NA	S25	0.149	0.281	0.078	0.714	0.221	0.171	0.033	0.829	0.176	0.486
D4A0T0	Ndufb10	NA	S21	-0.210	0.668	-0.275	0.829	-0.144	0.829	0.151	0.771	0.281	0.743
D4A0T0	Ndufb10	NA	T17	-0.410	0.367	-0.160	0.857	-0.659	0.343	0.287	0.743	-0.211	0.771

Table C.2 Cont.

D4A0T0	Ndufb10	NA	T133	0.307	0.047	0.324	0.229	0.290	0.114	0.080	0.686	0.046	0.829
D4A0T0	Ndufb10	NA	Y32	-0.310	0.252	-0.082	0.829	-0.538	0.200	0.436	0.371	-0.019	1.000
D4A7L4	Ndufb11	NA	S39	-0.114	0.251	-0.125	0.514	-0.102	0.143	-0.090	0.629	-0.067	0.543
D4A565	Ndufb5	NA	Y181	-0.094	0.722	-0.006	0.971	-0.182	0.771	0.024	0.971	-0.151	0.714
D4A565	Ndufb5	NA	S182	0.120	0.648	0.219	0.600	0.022	1.000	0.142	0.857	-0.055	0.914
D3ZLT1	Ndufb7	NA	Y62	0.342	0.014	0.416	0.086	0.268	0.171	0.098	0.571	-0.050	0.743
B2RYS8	Ndufb8	293991	Y184	0.056	0.710	0.089	0.800	0.022	0.886	-0.086	0.743	-0.154	0.486
B2RYS8	Ndufb8	293991	S175	0.064	0.342	0.132	0.314	-0.004	0.943	0.066	0.486	-0.070	0.571
Q5XIF3	Ndufs4	NA	S144	0.428	0.077	0.544	0.171	0.313	0.457	0.205	0.486	-0.026	0.971
Q5RJN0	Ndufs7	362837	S58	-0.021	0.839	-0.067	0.486	0.026	0.943	0.054	0.629	0.147	0.486
Q5RJN0	Ndufs7	362837	S39	-0.086	0.589	0.023	0.943	-0.196	0.429	0.090	0.771	-0.128	0.629
G3V644	Ndufv3	NA	S154	-0.312	0.216	-0.428	0.257	-0.195	0.600	0.167	0.657	0.400	0.343
Q6PCU8	Ndufv3	NA	S54	-0.157	0.255	-0.155	0.457	-0.158	0.457	0.008	0.971	0.005	0.971
P19804	Nme2	83782	T94	-0.012	0.942	-0.147	0.629	0.123	0.057	-0.189	0.543	0.081	0.286
Q5XIG4	Ociad1	289590	S143	-0.265	0.289	-0.183	0.743	-0.348	0.343	0.395	0.314	0.230	0.486
Q5XIG4	Ociad1	289590	S198	0.057	0.775	0.082	0.743	0.032	0.914	-0.008	1.000	-0.057	0.971
Q5XIH7	Phb2	114766	S14	-0.051	0.767	0.041	0.857	-0.143	0.571	0.255	0.429	0.071	0.657
Q5XIH7	Phb2	114766	T155	0.271	0.235	0.501	0.086	0.042	0.914	0.406	0.371	-0.053	0.857
Q5XIH7	Phb2	114766	S151	0.032	0.899	0.193	0.543	-0.129	0.800	0.344	0.457	0.022	1.000
MORBK9	Pnknd	NA	S121	0.342	0.049	0.551	0.114	0.132	0.571	0.352	0.257	-0.068	0.686
D4A7X5	Ppm1k	NA	S248	0.431	0.050	0.525	0.286	0.338	0.171	0.138	0.486	-0.049	0.943
Q66H15	Rmdn3	NA	S46	0.092	0.560	0.283	0.343	-0.099	0.371	0.288	0.029	-0.094	0.829
Q920L2	Sdha	157074	S331	-0.121	0.367	-0.095	0.714	-0.147	0.457	-0.084	0.600	-0.137	0.543
Q920L2	Sdha	157074	S522	0.059	0.495	0.112	0.286	0.006	1.000	0.055	0.743	-0.050	0.743
Q920L2	Sdha	157074	S497	0.015	0.893	0.056	0.743	-0.026	0.971	0.042	0.743	-0.040	0.800
P21913	Sdhb	298596	T121	-0.023	0.885	0.088	0.657	-0.133	0.600	-0.013	0.943	-0.234	0.257
P21913	Sdhb	298596	S224	-0.178	0.318	-0.018	0.914	-0.338	0.200	0.162	0.629	-0.158	0.400
P53987	Slc16a1	25027	S213	-0.355	0.201	-0.385	0.486	-0.325	0.200	0.006	0.971	0.065	0.971
P53987	Slc16a1	25027	S492	-0.183	0.258	-0.201	0.543	-0.165	0.171	-0.048	0.886	-0.011	0.971
P53987	Slc16a1	25027	S210;S213	-0.101	0.302	-0.055	0.771	-0.147	0.086	0.099	0.629	0.007	0.971
D4A4W6	Slirp	NA	T104	-0.032	0.847	-0.015	0.886	-0.049	0.800	-0.073	0.743	-0.107	0.629
D4A4W6	Slirp	NA	T104;S105	0.234	0.124	-0.022	0.829	0.489	0.029	-0.492	0.029	0.019	0.857
D4A4W6	Slirp	NA	S105	0.277	0.437	0.212	0.714	0.342	0.543	-0.101	0.857	0.029	0.971
F1LM47	Sucla2	NA	S281	0.026	0.899	-0.074	0.800	0.126	0.714	-0.028	0.886	0.171	0.343
B0BN86	Tmem11	303196	S15;S16	-0.670	0.064	-0.999	0.114	-0.340	0.543	-0.091	0.857	0.568	0.257
B0BN86	Tmem11	303196	S15	-0.244	0.280	-0.115	0.743	-0.372	0.257	0.171	0.686	-0.086	0.743
Q3KRD5	Tomm34	311621	S186	0.119	0.320	0.136	0.543	0.102	0.286	0.130	0.571	0.096	0.714
Q75Q39	Tomm70a	680142	S94	-0.126	0.209	-0.101	0.457	-0.151	0.343	-0.124	0.429	-0.174	0.229
Q75Q39	Tomm70a	680142	S84	-0.421	0.253	-0.315	0.657	-0.527	0.343	0.434	0.457	0.222	0.686
Q75Q39	Tomm70a	680142	S78	-0.444	0.209	-0.509	0.429	-0.380	0.457	-0.098	0.800	0.031	0.971
P85834	Tufm	293481	S312	-0.183	0.534	-0.365	0.543	-0.001	1.000	0.060	0.857	0.423	0.286
Q68FY0	Uqcrc1	301011	S221	-0.002	0.988	-0.098	0.686	0.094	0.629	-0.255	0.400	-0.063	0.743
P32551	Uqcrc2	NA	S367	0.268	0.057	0.312	0.057	0.224	0.371	0.220	0.286	0.132	0.543
P20788	Uqcrcf1	291103	S99	-0.041	0.877	-0.359	0.457	0.278	0.400	-0.364	0.457	0.274	0.371
P20788	Uqcrcf1	291103	S157	0.131	0.092	0.040	0.286	0.221	0.143	-0.112	0.343	0.069	0.543
Q7TQ16	Uqcrcq	NA	Y30	0.087	0.769	-0.004	1.000	-0.179	0.714	0.140	0.771	0.324	0.429
P81155	Vdac2	83531	S116	0.036	0.720	0.223	0.086	-0.151	0.486	0.125	0.600	-0.249	0.057
P81155	Vdac2	83531	S253	0.302	0.003	0.428	0.029	0.176	0.200	0.223	0.057	-0.029	0.800
P81155	Vdac2	83531	S252	0.141	0.495	0.028	0.943	0.254	0.114	-0.205	0.771	0.020	1.000

Table C.3

Table C.3 Acetyl-site fold change.

Uniprot ID	Gene Symbol	Entrez ID	Site	HCR/LCR		HCR Rest / LCR Rest		HCR Run / LCR Run		LCR Run / LCR Rest		HCR Run / HCR Rest	
				log2 fold change	Permutation	log2 fold change	P-value	log2 fold change	P-value	log2 fold change	P-value	log2 fold change	P-value
P15650	Acadl	25287	K419	-0.718	0.042	-0.787	0.286	-0.649	0.143	-0.355	0.343	-0.217	0.771
P15650	Acadl	25287	K92	-0.118	0.131	-0.208	0.086	-0.029	0.800	-0.114	0.200	0.065	0.629
Q6IMX3	Acads	64304	K308	-0.378	0.099	-0.632	0.143	-0.124	0.657	-0.330	0.314	0.179	0.600
P70584	Acadsb	25618	K284	-0.791	0.010	-0.882	0.086	-0.700	0.200	-0.318	0.457	-0.136	0.686
P17764	Acat1	25014	K254	-0.134	0.726	0.107	0.800	-0.376	0.343	-0.356	0.400	-0.839	0.200
P17764	Acat1	25014	K80	-0.057	0.874	0.199	0.629	-0.313	0.571	-0.189	0.800	-0.702	0.200
P17764	Acat1	25014	K187	0.236	0.460	0.658	0.229	-0.185	0.743	0.282	0.571	-0.562	0.257
P17764	Acat1	25014	K171	-0.125	0.652	-0.006	1.000	-0.244	0.629	-0.087	0.829	-0.325	0.400
P17764	Acat1	25014	K242	0.136	0.439	0.203	0.429	0.069	0.829	-0.114	0.686	-0.249	0.429
P17764	Acat1	25014	K220	-0.282	0.087	-0.264	0.257	-0.300	0.286	-0.143	0.514	-0.179	0.429
P17764	Acat1	25014	K210	-0.200	0.084	-0.106	0.514	-0.293	0.143	0.053	0.771	-0.134	0.343
P17764	Acat1	25014	K335	-0.080	0.759	0.035	1.000	-0.195	0.571	0.171	0.657	-0.059	0.886
P17764	Acat1	25014	K248	-0.209	0.453	-0.164	0.743	-0.255	0.543	0.132	0.857	0.041	0.886
Q9ER34	Aco2	79250	K523	-0.663	0.000	-0.525	0.057	-0.801	0.029	-0.068	0.829	-0.343	0.086
Q9ER34	Aco2	79250	K723	-0.195	0.272	-0.173	0.429	-0.217	0.629	-0.071	0.886	-0.115	0.486
Q9ER34	Aco2	79250	K517	-0.621	0.000	-0.598	0.029	-0.644	0.029	0.094	0.629	0.048	0.800
Q9ER34	Aco2	79250	K50	-0.328	0.077	-0.353	0.171	-0.304	0.343	0.249	0.314	0.299	0.086
Q9ER34	Aco2	79250	K689	-0.648	0.000	-0.728	0.057	-0.569	0.029	0.145	0.543	0.304	0.371
D3ZA93	Acot13	NA	K43	-0.431	0.044	-0.380	0.400	-0.481	0.057	-0.239	0.600	-0.341	0.171
D3ZA93	Acot13	NA	K127	-0.375	0.132	-0.112	0.714	-0.639	0.057	0.206	0.600	-0.321	0.371
Q6IMX8	Acot2	192272	K83	-0.356	0.010	-0.415	0.057	-0.298	0.200	-0.019	0.943	0.098	0.657
Q9JM53	Aifm1	83533	K592	0.262	0.385	0.650	0.114	-0.126	0.829	0.230	0.571	-0.547	0.229
G3V7J0	Aldh6a1	NA	K55	-0.281	0.242	-0.624	0.057	0.063	0.829	0.037	0.943	0.725	0.086
P19511	Atp5f1	NA	K233	-0.101	0.470	-0.041	0.886	-0.161	0.657	-0.118	0.600	-0.238	0.086
P19511	Atp5f1	NA	K162	-0.015	0.889	0.005	0.971	-0.034	0.857	-0.049	0.886	-0.088	0.286
P19511	Atp5f1	NA	K188	0.113	0.622	0.194	0.629	0.031	1.000	0.100	0.829	-0.063	0.914
P19511	Atp5f1	NA	K238	-0.079	0.714	0.012	0.971	-0.170	0.629	0.122	0.714	-0.059	0.800
P19511	Atp5f1	NA	K194	-0.227	0.489	-0.200	0.714	-0.254	0.629	0.015	0.971	-0.039	0.943
P19511	Atp5f1	NA	K244	0.020	0.857	0.040	0.857	0.000	1.000	0.148	0.314	0.108	0.600
P31399	Atp5h	641434	K85	0.229	0.681	0.432	0.600	0.026	0.971	-0.035	0.971	-0.442	0.600
P31399	Atp5h	641434	K95	0.023	0.958	0.331	0.543	-0.285	0.771	0.208	0.743	-0.409	0.600
P31399	Atp5h	641434	K63:K71	-0.243	0.441	-0.106	0.886	-0.381	0.343	-0.103	0.800	-0.377	0.086
P31399	Atp5h	641434	K71	0.003	0.991	0.295	0.314	-0.290	0.429	0.208	0.486	-0.376	0.286
P31399	Atp5h	641434	K73	0.468	0.234	0.446	0.543	0.489	0.343	-0.284	0.629	-0.242	0.686
P31399	Atp5h	641434	K63	-0.227	0.117	-0.095	0.686	-0.360	0.057	0.067	0.829	-0.197	0.200
P31399	Atp5h	641434	K117	0.050	0.606	0.191	0.171	-0.092	0.514	0.090	0.600	-0.193	0.029
P31399	Atp5h	641434	K48	-0.302	0.056	-0.219	0.400	-0.384	0.114	0.051	0.829	-0.113	0.657
P31399	Atp5h	641434	K78	-0.238	0.178	-0.084	0.800	-0.392	0.143	0.196	0.514	-0.112	0.514
P31399	Atp5h	641434	K121	0.152	0.593	0.031	0.886	0.274	0.771	-0.276	0.857	-0.033	0.914
P29419	Atp5i	140608	K48	-0.058	0.926	0.028	0.971	-0.145	0.857	-0.871	0.571	-1.045	0.286
P29419	Atp5i	140608	K34	-0.063	0.849	0.013	1.000	-0.139	0.600	-0.142	0.886	-0.294	0.343
P21571	Atp5j	500560	K79	-0.417	0.127	-0.473	0.314	-0.362	0.400	-0.174	0.629	-0.063	0.829
P21571	Atp5j	500560	K41	0.002	0.996	0.064	0.886	-0.059	0.914	0.203	0.657	0.080	0.886
P21571	Atp5j	500560	K46	0.267	0.366	-0.174	0.629	0.708	0.143	-0.545	0.143	0.336	0.429
D3ZAF6	Atp5j2	NA	K16	-0.093	0.498	-0.013	0.914	-0.173	0.600	0.181	0.571	0.021	0.771
Q06647	Atp5o	192241	K70	-0.114	0.646	-0.102	0.600	-0.125	0.857	0.234	0.629	0.210	0.457
Q06647	Atp5o	192241	K93	-0.396	0.129	-0.486	0.143	-0.306	0.486	0.039	0.914	0.219	0.629
Q06647	Atp5o	192241	K60	-0.025	0.918	-0.037	0.886	-0.012	1.000	0.231	0.486	0.257	0.629
Q06647	Atp5o	192241	K192	0.019	0.932	0.056	0.829	-0.018	0.971	0.387	0.343	0.313	0.286
Q06647	Atp5o	192241	K204	-0.089	0.738	-0.229	0.457	0.052	0.914	0.317	0.400	0.598	0.114
Q00972	Bckdk	29603	K245	-0.079	0.743	-0.312	0.486	0.153	0.543	-0.449	0.371	0.016	0.914
D3ZUX5	Chchd3	NA	K130	-0.245	0.562	-0.407	0.657	-0.084	0.771	-0.413	0.771	-0.091	0.771
B0K020	Cisd1	NA	K55	0.233	0.435	0.108	0.771	0.359	0.371	-0.581	0.257	-0.329	0.371
B0K020	Cisd1	NA	K68	-0.156	0.497	-0.292	0.486	-0.021	0.914	-0.083	0.857	0.188	0.400
P10888	Cox4i1	29445	K168	-0.235	0.675	-0.040	1.000	-0.429	0.400	-0.347	0.886	-0.735	0.400
P10888	Cox4i1	29445	K67	-0.316	0.008	-0.291	0.143	-0.341	0.057	-0.016	0.943	-0.067	0.657
P10888	Cox4i1	29445	K78	-0.204	0.162	-0.183	0.371	-0.226	0.371	0.030	0.886	-0.014	0.971
P11240	Cox5a	252934	K83	-0.831	0.040	-0.807	0.314	-0.856	0.114	-0.104	0.771	-0.153	0.657
P11240	Cox5a	252934	K109	-0.464	0.085	-0.421	0.457	-0.507	0.143	-0.021	0.971	-0.107	0.771
P12075	Cox5b	94194	K74	-0.404	0.415	-0.424	0.629	-0.383	0.343	-0.651	0.543	-0.610	0.314
P12075	Cox5b	94194	K121	-0.318	0.241	-0.321	0.629	-0.315	0.286	0.204	0.571	0.210	0.714
D3ZD09	Cox6b1	NA	K85	-0.435	0.286	-0.238	0.771	-0.633	0.143	-0.239	0.686	-0.634	0.429
P35171	Cox7a2	NA	K33	-0.373	0.018	-0.325	0.114	-0.421	0.086	-0.043	0.914	-0.140	0.600
P80431	Cox7b	303393	K36	-0.522	0.531	-0.189	0.971	-1.233	0.086	0.114	0.857	-1.308	0.257
P80431	Cox7b	303393	K75	-0.604	0.185	-0.337	0.514	-0.872	0.200	0.703	0.371	0.168	0.686
P80432	Cox7c	NA	K25	-0.473	0.047	-0.151	0.457	-0.795	0.086	0.185	0.543	-0.459	0.114
P80432	Cox7c	NA	K62	-0.338	0.109	-0.253	0.657	-0.422	0.086	0.064	0.886	-0.105	0.657
Q704S8	Crat	311849	K486	-0.164	0.517	0.057	0.971	-0.385	0.057	0.064	0.743	-0.378	0.514
Q704S8	Crat	311849	K268	-0.297	0.000	-0.282	0.029	-0.313	0.057	0.070	0.686	0.040	0.657
Q704S8	Crat	311849	K609	-0.533	0.138	-0.750	0.200	-0.317	0.514	-0.014	0.971	0.419	0.371
P04166	Cyb5b	NA	K101	-0.224	0.323	-0.203	0.657	-0.244	0.314	0.180	0.371	0.139	0.771
D3ZDE4	Dguok	NA	K212	-0.093	0.347	-0.161	0.371	-0.024	0.886	-0.014	0.943	0.123	0.086
Q6P6R2	Dld	298942	K410	0.012	0.964	0.280	0.229	-0.256	0.600	0.035	0.943	-0.501	0.057
Q6P6R2	Dld	298942	K122	-0.412	0.080	-0.319	0.257	-0.504	0.286	-0.033	0.943	-0.218	0.600
Q6P6R2	Dld	298942	K66	-0.131	0.485	0.011	0.971	-0.273	0.457	0.131	0.743	-0.153	0.429
Q6P6R2	Dld	298942	K267	-0.112	0.517	0.116	0.629	-0.340	0.171	0.420	0.200	-0.036	0.857
Q6P6R2	Dld	298942	K273	0.052	0.741	0.219	0.286	-0.114	0.686	0.309	0.229	-0.024	0.886
Q6P6R2	Dld	298942	K143	-0.331	0.075	-0.315	0.343	-0.346	0.200	0.067	0.800	0.037	0.857

Table C.3 Cont.

Q6P6R2	Dld	298942	K104	-0.326	0.103	-0.305	0.429	-0.346	0.229	0.091	0.743	0.050	0.886
Q6P6R2	Dld	298942	K155	-0.355	0.030	-0.428	0.029	-0.281	0.400	-0.046	0.971	0.100	0.514
Q6P6R2	Dld	298942	K420	-0.293	0.032	-0.293	0.114	-0.294	0.229	0.163	0.514	0.161	0.314
Q6P6R2	Dld	298942	K271	0.037	0.787	0.018	0.943	0.056	0.657	0.131	0.429	0.168	0.543
G3V6P2	Dlst	NA	K274	0.589	0.295	0.142	0.914	1.037	0.229	-0.984	0.229	-0.089	0.914
G3V6P2	Dlst	NA	K268	-0.089	0.731	-0.101	0.800	-0.077	0.800	0.217	0.629	0.241	0.629
G3V6P2	Dlst	NA	K155	-0.268	0.425	-0.622	0.286	0.087	0.914	-0.210	0.714	0.499	0.314
G3V6P2	Dlst	NA	K273	-0.438	0.336	-0.736	0.229	-0.139	0.829	0.126	0.857	0.723	0.343
P14604	Echs1	140547	K101	0.023	0.802	0.099	0.371	-0.054	0.743	0.031	0.829	-0.122	0.343
Q68G41	Eci1	NA	K255	-0.024	0.915	-0.028	0.943	-0.019	0.971	-0.081	0.829	-0.071	0.857
Q68G41	Eci1	NA	K76	0.216	0.370	0.320	0.400	0.113	0.743	0.171	0.629	-0.036	0.914
Q68G41	Eci1	NA	K229	-0.241	0.281	-0.315	0.400	-0.167	0.629	-0.046	0.857	0.102	0.829
Q5XIC0	Eci2	NA	K79	-0.542	0.017	-0.484	0.057	-0.600	0.200	-0.125	0.429	-0.241	0.600
Q5XIC0	Eci2	NA	K158	-0.022	0.826	-0.019	0.971	-0.026	0.943	0.164	0.057	0.157	0.457
P56571	ES1	NA	K98	-0.174	0.562	-0.069	0.800	-0.279	0.686	-0.196	0.657	-0.406	0.429
P56571	ES1	NA	K231	-0.090	0.552	-0.031	0.943	-0.148	0.600	-0.026	0.943	-0.142	0.486
P56571	ES1	NA	K162	-0.156	0.243	-0.113	0.571	-0.199	0.314	0.059	0.743	-0.026	0.886
P56571	ES1	NA	K155	-0.115	0.404	-0.147	0.371	-0.082	0.771	0.021	0.943	0.086	0.571
P13803	Etfa	300726	K69	-0.183	0.607	-0.195	0.029	-0.170	0.514	-0.068	0.714	-0.043	0.686
P13803	Etfa	300726	K162	-0.173	0.297	-0.171	0.657	-0.174	0.257	0.190	0.286	0.187	0.629
Q68FU3	Etfb	292845	K110	-0.421	0.090	-0.396	0.286	-0.446	0.343	0.026	0.971	-0.024	0.971
Q66HF3	Etfdh	295143	K95	-0.241	0.213	-0.218	0.571	-0.384	0.143	0.014	0.971	-0.152	0.771
Q66HF3	Etfdh	295143	K283	-0.217	0.120	-0.087	0.543	-0.348	0.229	0.112	0.771	-0.149	0.257
Q66HF3	Etfdh	295143	K131	-0.375	0.096	-0.475	0.229	-0.275	0.371	-0.269	0.629	-0.068	0.686
B0BNJ4	Ethe1	292710	K172	-0.117	0.341	-0.206	0.286	-0.029	0.971	0.187	0.257	0.364	0.029
Q5M964	Fh	NA	K63	-0.445	0.330	-0.173	0.829	-0.716	0.343	-0.003	1.000	-0.545	0.229
Q5M964	Fh	NA	K289	-0.157	0.660	-0.052	0.971	-0.262	0.771	0.242	0.829	0.032	0.886
Q5M964	Fh	NA	K77	-0.494	0.152	-0.733	0.143	-0.255	0.600	-0.035	0.971	0.443	0.229
Q5RK08	Gbas	498174	K94	-0.141	0.598	0.004	1.000	-0.286	0.457	0.156	0.714	-0.134	0.829
P10860	Glud1	24399	K415	-0.228	0.501	-0.344	0.629	-0.112	0.686	-0.541	0.343	-0.309	0.314
P10860	Glud1	24399	K84	0.120	0.364	0.166	0.343	0.073	0.857	-0.198	0.286	-0.292	0.171
P10860	Glud1	24399	K503	-0.018	0.851	-0.042	0.857	0.005	0.943	-0.125	0.429	-0.078	0.571
P10860	Glud1	24399	K527	-0.023	0.848	0.010	0.971	-0.056	0.629	0.044	0.800	-0.023	0.857
P00507	Got2	314123	K296	-0.132	0.334	-0.023	0.943	-0.242	0.343	0.154	0.571	-0.064	0.657
P00507	Got2	314123	K73	-0.101	0.326	-0.048	0.571	-0.155	0.457	0.067	0.686	-0.041	0.714
P00507	Got2	314123	K396	-0.432	0.016	-0.547	0.086	-0.317	0.171	-0.259	0.286	-0.029	0.914
P00507	Got2	314123	K90	0.004	0.986	0.017	0.943	0.009	1.000	0.053	0.914	0.027	1.000
P00507	Got2	314123	K363	-0.127	0.329	-0.193	0.400	-0.061	0.714	-0.012	0.943	0.119	0.571
P00507	Got2	314123	K302	-0.141	0.173	-0.177	0.057	-0.104	0.571	0.067	0.629	0.141	0.314
P00507	Got2	314123	K404	-0.329	0.030	-0.347	0.086	-0.310	0.314	0.122	0.686	0.158	0.371
P00507	Got2	314123	K122	-0.447	0.202	-0.872	0.029	-0.022	1.000	-0.644	0.200	0.206	0.714
P00507	Got2	314123	K159	-0.048	0.827	-0.062	0.914	-0.034	0.886	0.224	0.457	0.252	0.400
Q9WVK7	Hadh	113965	K241	-0.037	0.861	0.178	0.543	-0.252	0.571	0.003	0.971	-0.426	0.057
Q9WVK7	Hadh	113965	K185	-0.145	0.598	-0.102	0.857	-0.188	0.543	-0.060	0.914	-0.146	0.800
Q64428	Hadha	170670	K411	-0.300	0.035	-0.207	0.314	-0.394	0.057	0.063	0.829	-0.123	0.571
Q64428	Hadha	170670	K540	-0.738	0.021	-0.850	0.171	-0.626	0.171	-0.287	0.486	-0.063	0.886
Q64428	Hadha	170670	K129	-0.349	0.229	-0.390	0.686	-0.309	0.200	-0.126	0.971	-0.046	0.800
Q64428	Hadha	170670	K406	-0.342	0.147	-0.348	0.371	-0.336	0.400	-0.019	1.000	-0.007	1.000
Q64428	Hadha	170670	K289	-0.227	0.268	-0.149	0.543	-0.304	0.400	0.204	0.629	0.049	0.857
Q64428	Hadha	170670	K163	-0.155	0.166	-0.093	0.514	-0.217	0.257	0.180	0.286	0.055	0.800
Q64428	Hadha	170670	K353	-0.170	0.248	-0.118	0.543	-0.221	0.371	0.253	0.229	0.150	0.543
Q64428	Hadha	170670	K60	-0.166	0.420	-0.091	0.743	-0.241	0.371	0.372	0.171	0.222	0.429
Q64428	Hadha	170670	K728	-0.532	0.002	-0.526	0.029	-0.538	0.057	0.290	0.314	0.278	0.029
Q60587	Hadhb	171155	K244	-0.396	0.051	-0.325	0.371	-0.468	0.086	0.040	0.800	-0.103	0.686
P29266	Hibadh	NA	K78	0.359	0.361	0.542	0.229	0.177	0.800	-0.088	0.800	-0.452	0.343
P29266	Hibadh	NA	K144	-0.086	0.571	-0.069	0.743	-0.103	0.743	-0.074	0.629	-0.108	0.686
P29266	Hibadh	NA	K237	-0.050	0.647	0.003	1.000	-0.102	0.429	0.131	0.371	0.026	0.886
P97519	Hmgcl	79238	K48	-0.617	0.001	-0.610	0.029	-0.624	0.029	-0.320	0.029	-0.334	0.057
F1M953	Hspa9	NA	K600	-0.129	0.727	0.065	0.857	-0.323	0.714	-0.339	0.514	-0.726	0.200
F1M953	Hspa9	NA	K612	-0.146	0.594	0.050	0.914	-0.343	0.571	0.046	0.971	-0.348	0.343
F1M953	Hspa9	NA	K135	-0.248	0.090	-0.102	0.600	-0.394	0.029	-0.044	0.829	-0.336	0.143
F1M953	Hspa9	NA	K300	-0.276	0.475	-0.570	0.457	0.017	0.943	-0.744	0.229	-0.157	0.514
F1M953	Hspa9	NA	K288	-0.330	0.015	-0.349	0.143	-0.311	0.143	0.087	0.686	0.124	0.486
P63039	Hspd1	289614	K455	0.057	0.715	0.151	0.429	-0.037	0.914	0.038	0.914	-0.151	0.400
P63039	Hspd1	289614	K130	-0.196	0.108	-0.085	0.514	-0.308	0.229	0.078	0.686	-0.144	0.400
P63039	Hspd1	289614	K125	-0.273	0.009	-0.251	0.029	-0.294	0.200	0.034	0.857	-0.009	0.914
P63039	Hspd1	289614	K202	-0.365	0.002	-0.474	0.029	-0.256	0.143	-0.186	0.200	0.032	0.800
P56574	ldh2	361596	K199	-0.210	0.455	-0.385	0.486	-0.035	1.000	-0.389	0.457	-0.039	0.943
P56574	ldh2	361596	K275	-0.114	0.662	-0.110	0.857	-0.118	0.857	0.034	1.000	0.026	1.000
P56574	ldh2	361596	K384	-0.128	0.490	-0.194	0.571	-0.063	0.771	-0.039	0.800	0.092	0.771
P56574	ldh2	361596	K166	-0.122	0.468	-0.214	0.457	-0.030	0.943	-0.085	0.543	0.099	0.714
P56574	ldh2	361596	K180	-0.199	0.163	-0.247	0.371	-0.150	0.429	0.030	0.857	0.127	0.657
P56574	ldh2	361596	K280	0.036	0.875	0.034	0.943	0.038	0.943	0.180	0.571	0.183	0.571
P56574	ldh2	361596	K133	-0.143	0.479	-0.149	0.800	-0.138	0.514	0.212	0.343	0.222	0.629
P56574	ldh2	361596	K155	0.030	0.857	-0.034	0.886	0.093	0.686	0.127	0.629	0.255	0.314
P56574	ldh2	361596	K48	-0.414	0.133	-0.786	0.057	-0.041	0.886	-0.453	0.371	0.291	0.343
P56574	ldh2	361596	K282	-0.139	0.485	-0.241	0.486	-0.037	0.829	0.101	0.800	0.305	0.343
Q5XUJ3	ldh3g	25179	K159	-0.298	0.059	-0.445	0.171	-0.151	0.086	-0.066	0.743	0.228	0.371
Q5XUJ3	ldh3g	25179	K115	-0.538	0.057	-0.848	0.057	-0.228	0.600	-0.218	0.657	0.402	0.286
Q3KR86	lmmt	312444	K251	-0.120	0.816	-0.153	0.886	-0.393	0.571	-0.316	0.714	-0.862	0.343
P12007	lvd	24513	K56	-0.265	0.078	-0.393	0.029	-0.136	0.629	-0.071	0.514	0.186	0.543
P12007	lvd	24513	K76	-1.173	0.001	-1.576	0.029	-0.770	0.114	-0.574	0.343	0.232	0.600
P04642	Ldha	366355	K224	-0.147	0.775	0.105	0.943	-0.400	0.257	-0.608	0.571	-1.113	0.171
P04642	Ldha	366355	K228	-0.150	0.724	0.119	0.943	-0.418	0.114	-0.376	0.714	-0.913	0.200

Table C.3. Cont.

P04642	Ldha	366355	K232	-0.084	0.891	0.089	0.943	-0.257	0.429	-0.470	0.800	-0.816	0.343
P04642	Ldha	366355	K126	-0.055	0.578	0.073	0.714	-0.182	0.229	0.014	0.943	-0.241	0.086
P04642	Ldha	366355	K243	-0.362	0.322	-0.407	0.600	-0.318	0.429	-0.201	0.800	-0.112	0.800
F1LXA0	LOC100910710	NA	K43	-0.243	0.385	-0.050	0.914	-0.436	0.314	-0.269	0.514	-0.655	0.029
F1LXA0	LOC100910710	NA	K101	-0.559	0.037	-0.364	0.371	-0.753	0.029	0.094	0.914	-0.295	0.429
D3ZC29	LOC100912591	NA	K112	-0.350	0.182	-0.375	0.143	-0.325	0.543	-0.099	0.857	-0.049	0.886
D3ZC29	LOC100912591	NA	K41	-0.394	0.007	-0.483	0.086	-0.304	0.086	-0.017	0.971	0.162	0.400
D3ZF13	LOC683884	NA	K92	-0.286	0.606	0.064	0.943	-0.636	0.257	-0.298	0.829	-0.998	0.086
M0RD15	Mcu	NA	K331	-0.102	0.665	-0.250	0.543	0.046	0.914	-0.352	0.257	-0.057	0.771
P04636	Mdh2	81829	K239	-0.409	0.299	0.014	1.000	-0.832	0.029	-0.058	0.914	-0.905	0.057
P04636	Mdh2	81829	K91	-0.420	0.411	-0.411	0.657	-0.428	0.314	-0.643	0.457	-0.661	0.514
P04636	Mdh2	81829	K185	-0.199	0.312	-0.164	0.686	-0.234	0.371	-0.179	0.629	-0.249	0.229
P04636	Mdh2	81829	K335	-0.515	0.004	-0.412	0.086	-0.619	0.086	0.020	0.943	-0.187	0.314
P04636	Mdh2	81829	K301	-0.058	0.616	0.087	0.486	-0.203	0.343	0.213	0.286	-0.078	0.600
P04636	Mdh2	81829	K165	-0.437	0.224	-0.521	0.514	-0.354	0.371	0.299	0.457	0.466	0.486
P04636	Mdh2	81829	K329	-0.389	0.350	-0.632	0.286	-0.146	0.829	0.177	0.657	0.662	0.371
Q3B8R7	Mrp147	NA	K146	0.000	1.000	-0.206	1.000	0.206	0.600	-0.687	0.457	-0.275	0.286
D3Z558	Ndufa2	NA	K62	-0.406	0.051	-0.471	0.057	-0.340	0.486	0.043	0.943	0.174	0.286
B2R2D6	Ndufa4	NA	K56	-0.263	0.175	-0.276	0.314	-0.250	0.429	0.180	0.629	0.206	0.486
Q63362	Ndufa5	25488	K55	-0.278	0.642	-0.096	0.914	-0.461	0.457	-0.855	0.429	-1.220	0.057
Q63362	Ndufa5	25488	K46	-0.330	0.135	-0.026	0.943	-0.634	0.086	0.125	0.743	-0.483	0.057
Q63362	Ndufa5	25488	K60	-0.383	0.186	-0.219	0.714	-0.547	0.114	0.045	0.857	-0.283	0.286
Q63362	Ndufa5	25488	K36	-0.404	0.075	-0.219	0.486	-0.589	0.114	0.180	0.686	-0.191	0.543
Q63362	Ndufa5	25488	K40	-0.481	0.065	-0.335	0.457	-0.627	0.171	0.161	0.743	-0.130	0.686
Q5BK63	Ndufa9	NA	K189	-0.392	0.026	-0.243	0.400	-0.541	0.029	0.083	0.714	-0.215	0.400
D3ZZ21	Ndufb6	NA	K24	-0.147	0.154	-0.060	0.543	-0.234	0.171	-0.021	0.914	-0.195	0.314
B2RYW3	Ndufb9	299954	K52	-0.127	0.793	-0.115	0.857	-0.138	0.743	-0.778	0.371	-0.801	0.086
B2RYW3	Ndufb9	299954	K121	-0.200	0.343	-0.135	0.829	-0.265	0.200	-0.161	0.657	-0.291	0.171
B2RYW3	Ndufb9	299954	K59	-0.251	0.084	-0.221	0.343	-0.280	0.171	-0.027	0.886	-0.085	0.686
D3Z575	Ndufc1	NA	K38	-0.744	0.042	-0.716	0.286	-0.772	0.114	0.386	0.514	0.329	0.371
Q66HF1	Ndufs1	301458	K84	-0.287	0.013	-0.295	0.086	-0.278	0.257	0.013	0.971	-0.029	0.686
Q66HF1	Ndufs1	301458	K709	-0.287	0.074	-0.373	0.143	-0.201	0.429	-0.102	0.714	0.070	0.686
Q66HF1	Ndufs1	301458	K289	-0.367	0.025	-0.531	0.029	-0.203	0.400	-0.193	0.543	0.135	0.543
D3ZG43	Ndufs3	NA	K264	-0.374	0.227	-0.374	0.514	-0.532	0.171	-0.320	0.486	-0.636	0.086
D3ZG43	Ndufs3	NA	K260	-0.343	0.141	-0.287	0.457	-0.399	0.200	-0.309	0.400	-0.421	0.114
B5DEL8	Ndufs5	362588	K101	-0.150	0.735	-0.276	0.657	-0.023	1.000	-0.231	0.771	0.021	1.000
Q5XIH3	Ndufv1	293655	K36	-0.329	0.293	0.106	0.857	-0.764	0.086	0.026	0.914	-0.843	0.086
Q5XIH3	Ndufv1	293655	K126	-0.514	0.217	-0.424	0.543	-0.603	0.229	-0.272	0.571	-0.451	0.571
Q5XIH3	Ndufv1	293655	K64	-0.322	0.042	-0.098	0.514	-0.545	0.086	0.297	0.343	-0.150	0.371
Q5XIH3	Ndufv1	293655	K104	-0.479	0.066	-0.360	0.429	-0.598	0.200	0.274	0.543	0.036	0.943
Q5XIH3	Ndufv1	293655	K81	-0.245	0.428	-0.310	0.600	-0.180	0.629	0.133	0.771	0.263	0.571
P19234	Ndufv2	81728	K124	-0.219	0.182	-0.319	0.371	-0.119	0.343	-0.364	0.029	-0.164	0.629
Q5XI78	Ogdh	NA	K947	0.035	0.943	0.483	0.514	-0.414	0.686	0.016	1.000	-0.882	0.171
Q5XI78	Ogdh	NA	K401	-0.025	0.878	0.277	0.229	-0.326	0.114	0.224	0.371	-0.378	0.200
B2GV06	Oxct1	NA	K480	-0.204	0.452	-0.036	0.857	-0.372	0.086	-0.259	0.600	-0.595	0.171
B2GV06	Oxct1	NA	K274	-0.245	0.091	-0.118	0.714	-0.373	0.029	0.017	0.914	-0.238	0.171
B2GV06	Oxct1	NA	K296	-0.421	0.183	-0.522	0.429	-0.321	0.257	-0.051	0.943	0.150	0.857
Q68FZ8	Pccb	24624	K103	-0.312	0.442	0.144	0.800	-0.768	0.114	0.788	0.229	-0.123	0.971
Q920L2	Sdha	157074	K530	-0.931	0.157	-0.407	0.686	-1.455	0.086	-0.540	0.743	-1.588	0.114
Q920L2	Sdha	157074	K490	-0.284	0.491	-0.016	0.971	-0.553	0.171	-0.213	0.914	-0.750	0.057
Q920L2	Sdha	157074	K472	-0.204	0.280	-0.133	0.571	-0.276	0.457	-0.123	0.714	-0.267	0.314
Q920L2	Sdha	157074	K171	-0.564	0.002	-0.465	0.200	-0.662	0.029	0.016	0.943	-0.182	0.400
Q920L2	Sdha	157074	K600	-0.127	0.325	-0.111	0.629	-0.143	0.514	-0.114	0.571	-0.147	0.371
Q920L2	Sdha	157074	K327	-0.400	0.000	-0.397	0.029	-0.404	0.057	-0.050	0.743	-0.057	0.543
Q920L2	Sdha	157074	K628	-0.194	0.305	-0.113	0.743	-0.275	0.400	0.190	0.600	0.028	0.943
P21913	Sdhb	298596	K270	-0.097	0.879	0.168	0.886	-0.362	0.629	-0.781	0.486	-1.312	0.114
P21913	Sdhb	298596	K57	-0.353	0.154	-0.293	0.514	-0.414	0.171	-0.050	0.943	-0.171	0.600
P21913	Sdhb	298596	K53	-0.341	0.076	-0.355	0.286	-0.328	0.314	-0.016	0.943	0.010	0.971
P21913	Sdhb	298596	K64	-0.397	0.027	-0.437	0.114	-0.358	0.114	0.106	0.800	0.185	0.371
G3V741	Sic25a3	NA	K200	-0.169	0.475	0.046	0.886	-0.384	0.429	0.094	0.914	-0.336	0.257
G3V741	Sic25a3	NA	K289	-0.273	0.416	-0.417	0.543	-0.129	0.714	-0.482	0.457	-0.194	0.371
G3V741	Sic25a3	NA	K203	-0.259	0.130	-0.141	0.686	-0.378	0.200	0.165	0.657	-0.073	0.514
G3V741	Sic25a3	NA	K93	-0.368	0.193	-0.445	0.486	-0.291	0.314	-0.193	0.857	-0.039	0.914
G3V741	Sic25a3	NA	K228	-0.811	0.041	-1.197	0.114	-0.425	0.229	-0.244	0.886	0.528	0.057
P07895	Sod2	24787	K122	-0.204	0.317	-0.030	0.971	-0.379	0.086	0.048	0.914	-0.300	0.400
P07895	Sod2	24787	K114	-0.190	0.205	0.011	0.971	-0.391	0.114	0.176	0.343	-0.226	0.429
P07895	Sod2	24787	K130	-0.131	0.421	0.044	0.714	-0.305	0.371	0.219	0.400	-0.131	0.686
P07895	Sod2	24787	K68	-0.229	0.057	-0.124	0.543	-0.333	0.086	0.083	0.486	-0.126	0.543
F1LM47	Sucla2	NA	K440	-0.434	0.040	-0.470	0.200	-0.397	0.200	-0.252	0.400	-0.179	0.486
P13086	Suclg1	114597	K105	-0.407	0.025	-0.221	0.486	-0.592	0.057	0.110	0.829	-0.260	0.229
P13086	Suclg1	114597	K54	-0.159	0.306	-0.053	0.829	-0.265	0.229	0.180	0.400	-0.033	0.886
Q68FY0	Uqcrc1	301011	K138	-0.046	0.649	0.031	0.857	-0.123	0.371	0.029	0.800	-0.125	0.486
P32551	Uqcrc2	NA	K97	-0.261	0.125	-0.321	0.257	-0.201	0.571	0.029	0.914	0.149	0.571
P32551	Uqcrc2	NA	K158	-0.157	0.322	-0.184	0.343	-0.130	0.657	0.151	0.600	0.205	0.229
P32551	Uqcrc2	NA	K91	0.103	0.609	-0.133	0.600	0.340	0.286	0.056	0.857	0.529	0.114
Q77Q16	Uqcrcq	NA	K77	-0.393	0.534	-0.102	0.971	-0.684	0.229	-0.322	0.829	-0.904	0.257
Q77Q16	Uqcrcq	NA	K33	-0.291	0.225	-0.367	0.229	-0.214	0.629	0.135	0.800	0.288	0.286
P81155	Vdac2	83531	K73	0.231	0.282	0.382	0.229	0.079	0.800	0.129	0.686	-0.175	0.657
P81155	Vdac2	83531	K75	0.133	0.433	0.155	0.514	0.110	0.743	-0.043	0.857	-0.088	0.600



## References

- Alsted, T.J., Ploug, T., Prats, C., Serup, A.K., Hoeg, L., Schjerling, P., Holm, C., Zimmermann, R., Fledelius, C., Galbo, H., et al. (2013). Contraction-induced lipolysis is not impaired by inhibition of hormone-sensitive lipase in skeletal muscle. *The Journal of physiology* 591, 5141-5155.
- Anderson, R.M., and Weindruch, R. (2010). Metabolic reprogramming, caloric restriction and aging. *Trends in endocrinology and metabolism: TEM* 21, 134-141.
- Badawy, A.A.B., Morgan, C.J., and Turner, J.A. (2007). Application of the Phenomenex EZ:faast™ amino acid analysis kit for rapid gas-chromatographic determination of concentrations of plasma tryptophan and its brain uptake competitors. *Amino Acids* 34, 587-596.
- Batch, B.C., Shah, S.H., Newgard, C.B., Turer, C.B., Haynes, C., Bain, J.R., Muehlbauer, M., Patel, M.J., Stevens, R.D., Appel, L.J., et al. (2013). Branched chain amino acids are novel biomarkers for discrimination of metabolic wellness. *Metabolism: clinical and experimental*.
- Blair, S.N., Kampert, J.B., Kohl, H.W., 3rd, Barlow, C.E., Macera, C.A., Paffenbarger, R.S., Jr., and Gibbons, L.W. (1996). Influences of cardiorespiratory fitness and other precursors on cardiovascular disease and all-cause mortality in men and women. *JAMA : the journal of the American Medical Association* 276, 205-210.
- Bligh, E.G., and Dyer, W.J. (1959). A rapid method of total lipid extraction and purification. *Canadian journal of biochemistry and physiology* 37, 911-917.
- Blomstrand, E., Hassmn, P., Ekblom, B., and Newsholme, E.A. (1991). Administration of branched-chain amino acids during sustained exercise--effects on performance and on plasma concentration of some amino acids. *European journal of applied physiology and occupational physiology* 63, 83-88.
- Bonen, A., Campbell, S.E., Benton, C.R., Chabowski, A., Coort, S.L., Han, X.X., Koonen, D.P., Glatz, J.F., and Luiken, J.J. (2004). Regulation of fatty acid transport by fatty acid translocase/CD36. *The Proceedings of the Nutrition Society* 63, 245-249.
- Bouzakri, K., Austin, R., Rune, A., Lassman, M.E., Garcia-Roves, P.M., Berger, J.P., Krook, A., Chibalin, A.V., Zhang, B.B., and Zierath, J.R. (2008). Malonyl CoenzymeA decarboxylase regulates lipid and glucose metabolism in human skeletal muscle. *Diabetes* 57, 1508-1516.

- Bruss, M.D., Khambatta, C.F., Ruby, M.A., Aggarwal, I., and Hellerstein, M.K. (2010). Calorie restriction increases fatty acid synthesis and whole body fat oxidation rates. *American journal of physiology. Endocrinology and metabolism* *298*, E108-116.
- Buchholz, A.C., and Schoeller, D.A. (2004). Is a calorie a calorie? *The American journal of clinical nutrition* *79*, 899S-906S.
- Burniston, J.G., Kenyani, J., Wastling, J.M., Burant, C.F., Qi, N.R., Koch, L.G., and Britton, S.L. (2011). Proteomic analysis reveals perturbed energy metabolism and elevated oxidative stress in hearts of rats with inborn low aerobic capacity. *Proteomics* *11*, 3369-3379.
- Butler, J.A., Mishur, R.J., Bhaskaran, S., and Rea, S.L. (2013). A metabolic signature for long life in the *Caenorhabditis elegans* Mit mutants. *Aging cell* *12*, 130-138.
- Camargo, A., Azuaje, F., Wang, H., and Zheng, H. (2008). Permutation - based statistical tests for multiple hypotheses. *Source code for biology and medicine* *3*, 15.
- Campbell, P.J., Carlson, M.G., Hill, J.O., and Nurjhan, N. (1992). Regulation of free fatty acid metabolism by insulin in humans: role of lipolysis and reesterification. *The American journal of physiology* *263*, E1063-1069.
- Chebotareva, N.A., Kurganov, B.I., Harding, S.E., and Winzor, D.J. (2005). Effect of osmolytes on the interaction of flavin adenine dinucleotide with muscle glycogen phosphorylase b. *Biophysical chemistry* *113*, 61-66.
- Chen, E.Y., Tan, C.M., Kou, Y., Duan, Q., Wang, Z., Meirelles, G.V., Clark, N.R., and Ma'ayan, A. (2013). Enrichr: interactive and collaborative HTML5 gene list enrichment analysis tool. *BMC bioinformatics* *14*, 128.
- Choudhary, C., Weinert, B.T., Nishida, Y., Verdin, E., and Mann, M. (2014). The growing landscape of lysine acetylation links metabolism and cell signalling. *Nature reviews. Molecular cell biology* *15*, 536-550.
- Church, T.S., Cheng, Y.J., Earnest, C.P., Barlow, C.E., Gibbons, L.W., Priest, E.L., and Blair, S.N. (2004). Exercise capacity and body composition as predictors of mortality among men with diabetes. *Diabetes care* *27*, 83-88.
- Clifford, G.M., Londos, C., Kraemer, F.B., Vernon, R.G., and Yeaman, S.J. (2000). Translocation of hormone-sensitive lipase and perilipin upon lipolytic stimulation of rat adipocytes. *The Journal of biological chemistry* *275*, 5011-5015.
- Coggan, A.R., Raguso, C.A., Gastaldelli, A., Sidossis, L.S., and Yeckel, C.W. (2000). Fat metabolism during high-intensity exercise in endurance-trained and untrained men. *Metabolism: clinical and experimental* *49*, 122-128.

- Connor, S.C., Hansen, M.K., Corner, A., Smith, R.F., and Ryan, T.E. (2010). Integration of metabolomics and transcriptomics data to aid biomarker discovery in type 2 diabetes. *Molecular bioSystems* 6, 909-921.
- Constantin-Teodosiu, D., Carlin, J.I., Cederblad, G., Harris, R.C., and Hultman, E. (1991). Acetyl group accumulation and pyruvate dehydrogenase activity in human muscle during incremental exercise. *Acta physiologica Scandinavica* 143, 367-372.
- Coyle, E.F., Jeukendrup, A.E., Wagenmakers, A.J., and Saris, W.H. (1997). Fatty acid oxidation is directly regulated by carbohydrate metabolism during exercise. *The American journal of physiology* 273, E268-275.
- de Magalhaes, J.P., Curado, J., and Church, G.M. (2009). Meta-analysis of age-related gene expression profiles identifies common signatures of aging. *Bioinformatics (Oxford, England)* 25, 875-881.
- DeMarco, V.G., Johnson, M.S., Ma, L., Pulakat, L., Mugerfeld, I., Hayden, M.R., Garro, M., Knight, W., Britton, S.L., Koch, L.G., et al. (2012). Overweight female rats selectively breed for low aerobic capacity exhibit increased myocardial fibrosis and diastolic dysfunction. *American journal of physiology. Heart and circulatory physiology* 302, H1667-1682.
- Doisaki, M., Katano, Y., Nakano, I., Hirooka, Y., Itoh, A., Ishigami, M., Hayashi, K., Goto, H., Fujita, Y., Kadota, Y., et al. (2010). Regulation of hepatic branched-chain alpha-keto acid dehydrogenase kinase in a rat model for type 2 diabetes mellitus at different stages of the disease. *Biochemical and biophysical research communications* 393, 303-307.
- Du Bois, E. (1933). Graham Lusk 1866–1932. *Ergebnisse der Physiologie und exper. Pharmakologie* 35, 10-12.
- Egan, B., and Zierath, J.R. (2013). Exercise metabolism and the molecular regulation of skeletal muscle adaptation. *Cell metabolism* 17, 162-184.
- Enea, C., Seguin, F., Petitpas-Mulliez, J., Boildieu, N., Boisseau, N., Delpech, N., Diaz, V., Eugene, M., and Dugue, B. (2010). (1)H NMR-based metabolomics approach for exploring urinary metabolome modifications after acute and chronic physical exercise. *Analytical and bioanalytical chemistry* 396, 1167-1176.
- Eto, I. (2013). Expression of p27Kip1, a cell cycle repressor protein, is inversely associated with potential carcinogenic risk in the genetic rodent models of obesity and long-lived Ames dwarf mice. *Metabolism: clinical and experimental* 62, 873-887.
- Evans, C.R., Karnovsky, A., Kovach, M.A., Standiford, T.J., Burant, C.F., and Stringer, K.A. (2013). Untargeted LC–MS Metabolomics of Bronchoalveolar Lavage

Fluid Differentiates Acute Respiratory Distress Syndrome from Health. *Journal of proteome research* 13, 640-649.

Fay, M.P.S., P. A. (2010). Exact and Asymptotic Weighted Logrank Tests for Interval Censored Data: The interval R Package. *Journal of Statistical Software* 36, 1-34.

Fernandez, C., Hansson, O., Nevsten, P., Holm, C., and Klint, C. (2008). Hormone-sensitive lipase is necessary for normal mobilization of lipids during submaximal exercise. *American journal of physiology. Endocrinology and metabolism* 295, E179-186.

Fiehn, O., Garvey, W.T., Newman, J.W., Lok, K.H., Hoppel, C.L., and Adams, S.H. (2010). Plasma metabolomic profiles reflective of glucose homeostasis in non-diabetic and type 2 diabetic obese African-American women. *PLoS one* 5, e15234.

Finley, L.W., Haas, W., Desquirit-Dumas, V., Wallace, D.C., Procaccio, V., Gygi, S.P., and Haigis, M.C. (2011). Succinate dehydrogenase is a direct target of sirtuin 3 deacetylase activity. *PLoS one* 6, e23295.

Fischer, E.H., and Krebs, E.G. (1955). Conversion of phosphorylase b to phosphorylase a in muscle extracts. *The Journal of biological chemistry* 216, 121-132.

Fuchs, S., Bundy, J.G., Davies, S.K., Viney, J.M., Swire, J.S., and Leroi, A.M. (2010). A metabolic signature of long life in *Caenorhabditis elegans*. *BMC biology* 8, 14.

Fueger, P.T., Heikkinen, S., Bracy, D.P., Malabanan, C.M., Pencek, R.R., Laakso, M., and Wasserman, D.H. (2003). Hexokinase II partial knockout impairs exercise-stimulated glucose uptake in oxidative muscles of mice. *American journal of physiology. Endocrinology and metabolism* 285, E958-963.

Fujii, H., Tokuyama, K., Suzuki, M., Popov, K.M., Zhao, Y., Harris, R.A., Nakai, N., Murakami, T., and Shimomura, Y. (1995). Regulation by physical training of enzyme activity and gene expression of branched-chain 2-oxo acid dehydrogenase complex in rat skeletal muscle. *Biochimica et biophysica acta* 1243, 277-281.

Galgani, J.E., Heilbronn, L.K., Azuma, K., Kelley, D.E., Albu, J.B., Pi-Sunyer, X., Smith, S.R., and Ravussin, E. (2008). Metabolic flexibility in response to glucose is not impaired in people with type 2 diabetes after controlling for glucose disposal rate. *Diabetes* 57, 841-845.

Garcia-Martinez, C., Marotta, M., Moore-Carrasco, R., Guitart, M., Camps, M., Busquets, S., Montell, E., and Gomez-Foix, A.M. (2005). Impact on fatty acid metabolism and differential localization of FATP1 and FAT/CD36 proteins delivered

in cultured human muscle cells. *American journal of physiology. Cell physiology* *288*, C1264-1272.

Geer, L.Y., Markey, S.P., Kowalak, J.A., Wagner, L., Xu, M., Maynard, D.M., Yang, X., Shi, W., and Bryant, S.H. (2004). Open mass spectrometry search algorithm. *Journal of proteome research* *3*, 958-964.

Ghoshal, A., Guo, T., Soukhova, N., and Soldin, S. (2005). Rapid measurement of plasma acylcarnitines by liquid chromatography–tandem mass spectrometry without derivatization. *Clinica Chimica Acta* *358*, 104-112.

Giblin, W., Skinner, M.E., and Lombard, D.B. (2014). Sirtuins: guardians of mammalian healthspan. *Trends in genetics : TIG* *30*, 271-286.

Gollnick, P.D., Piehl, K., and Saltin, B. (1974). Selective glycogen depletion pattern in human muscle fibres after exercise of varying intensity and at varying pedalling rates. *The Journal of physiology* *241*, 45-57.

Goodpaster, B.H., and Brown, N.F. (2005). Skeletal muscle lipid and its association with insulin resistance: what is the role for exercise? *Exercise and sport sciences reviews* *33*, 150-154.

Gregory R. Warnes, B.B., Lodewijk Bonebakker, Robert Gentleman, Wolfgang Huber, Andy Liaw, Thomas Lumley, Martin Maechler, Arni Magnusson, Steffen Moeller, Marc Schwartz, Bill Venables (2013). *gplots: Various R programming tools for plotting data.*

Guitart, M., Osorio-Conles, O., Pentinat, T., Cebria, J., Garcia-Villoria, J., Sala, D., Sebastian, D., Zorzano, A., Ribes, A., Jimenez-Chillaron, J.C., et al. (2014). Fatty acid transport protein 1 (FATP1) localizes in mitochondria in mouse skeletal muscle and regulates lipid and ketone body disposal. *PLoS one* *9*, e98109.

Haemmerle, G., Lass, A., Zimmermann, R., Gorkiewicz, G., Meyer, C., Rozman, J., Heldmaier, G., Maier, R., Theussl, C., Eder, S., et al. (2006). Defective lipolysis and altered energy metabolism in mice lacking adipose triglyceride lipase. *Science (New York, N.Y.)* *312*, 734-737.

Hakimi, P., Yang, J., Casadesus, G., Massillon, D., Tolentino-Silva, F., Nye, C.K., Cabrera, M.E., Hagen, D.R., Utter, C.B., Baghdy, Y., et al. (2007). Overexpression of the cytosolic form of phosphoenolpyruvate carboxykinase (GTP) in skeletal muscle repatterns energy metabolism in the mouse. *The Journal of biological chemistry* *282*, 32844-32855.

Hall, L.M.L., Moran, C., Milne, G., Wilson, J., MacFarlane, N., Forouhi, N., Hariharan, N., Salt, I., Sattar, N., and Gill, J.M.R. (2010). Fat oxidation, fitness and skeletal

muscle expression of oxidative/lipid metabolism genes in South Asians: implications for insulin resistance? *PloS one* 5, e14197-e14197.

Haller, R.G., and Vissing, J. (2004). No spontaneous second wind in muscle phosphofructokinase deficiency. *Neurology* 62, 82-86.

Hallows, W.C., Yu, W., Smith, B.C., Devries, M.K., Ellinger, J.J., Someya, S., Shortreed, M.R., Prolla, T., Markley, J.L., Smith, L.M., et al. (2011). Sirt3 promotes the urea cycle and fatty acid oxidation during dietary restriction. *Molecular cell* 41, 139-149.

Hansen, C., and Spuhler, K. (1984). Development of the National Institutes of Health genetically heterogeneous rat stock. *Alcoholism, clinical and experimental research* 8, 477-479.

Hardie, D.G., Salt, I.P., Hawley, S.A., and Davies, S.P. (1999). AMP-activated protein kinase: an ultrasensitive system for monitoring cellular energy charge. *The Biochemical journal* 338 ( Pt 3), 717-722.

Hebert, A.S., Dittenhafer-Reed, K.E., Yu, W., Bailey, D.J., Selen, E.S., Boersma, M.D., Carson, J.J., Tonelli, M., Balloon, A.J., Higbee, A.J., et al. (2013). Calorie restriction and SIRT3 trigger global reprogramming of the mitochondrial protein acetylome. *Molecular cell* 49, 186-199.

Helge, J.W., Rehrer, N.J., Pilegaard, H., Manning, P., Lucas, S.J., Gerrard, D.F., and Cotter, J.D. (2007). Increased fat oxidation and regulation of metabolic genes with ultraendurance exercise. *Acta physiologica (Oxford, England)* 191, 77-86.

Hiatt, W.R., Regensteiner, J.G., Wolfel, E.E., Ruff, L., and Brass, E.P. (1989). Carnitine and acylcarnitine metabolism during exercise in humans. Dependence on skeletal muscle metabolic state. *The Journal of clinical investigation* 84, 1167-1173.

Hill, A.V., and Lupton, H. (1923). Muscular Exercise, Lactic Acid, and the Supply and Utilization of Oxygen. *QJM os-16*, 135-171.

Hirschey, M.D., Shimazu, T., Goetzman, E., Jing, E., Schwer, B., Lombard, D.B., Grueter, C.A., Harris, C., Biddinger, S., Ilkayeva, O.R., et al. (2010). SIRT3 regulates mitochondrial fatty-acid oxidation by reversible enzyme deacetylation. *Nature* 464, 121-125.

Hirschey, M.D., Shimazu, T., Jing, E., Grueter, C.A., Collins, A.M., Aouizerat, B., Stancakova, A., Goetzman, E., Lam, M.M., Schwer, B., et al. (2011). SIRT3 deficiency and mitochondrial protein hyperacetylation accelerate the development of the metabolic syndrome. *Molecular cell* 44, 177-190.

- Hollenberg, M., Ngo, L.H., Turner, D., and Tager, I.B. (1998). Treadmill exercise testing in an epidemiologic study of elderly subjects. *The journals of gerontology. Series A, Biological sciences and medical sciences* 53, B259-267.
- Hollenberg, M., Yang, J., Haight, T.J., and Tager, I.B. (2006). Longitudinal changes in aerobic capacity: implications for concepts of aging. *The journals of gerontology. Series A, Biological sciences and medical sciences* 61, 851-858.
- Holloszy, J.O., and Coyle, E.F. (1984). Adaptations of skeletal muscle to endurance exercise and their metabolic consequences. *Journal of applied physiology: respiratory, environmental and exercise physiology* 56, 831-838.
- Holloszy, J.O., Kohrt, W.M., and Hansen, P.A. (1998). The regulation of carbohydrate and fat metabolism during and after exercise. *Frontiers in bioscience : a journal and virtual library* 3, D1011-1027.
- Holloway, G.P., Lally, J., Nickerson, J.G., Alkhateeb, H., Snook, L.A., Heigenhauser, G.J., Calles-Escandon, J., Glatz, J.F., Luiken, J.J., Spriet, L.L., et al. (2007). Fatty acid binding protein facilitates sarcolemmal fatty acid transport but not mitochondrial oxidation in rat and human skeletal muscle. *The Journal of physiology* 582, 393-405.
- Hong, F., Breitling, R., McEntee, C.W., Wittner, B.S., Nemhauser, J.L., and Chory, J. (2006). RankProd: a bioconductor package for detecting differentially expressed genes in meta-analysis. *Bioinformatics (Oxford, England)* 22, 2825-2827.
- Horowitz, J.F. (2003). Fatty acid mobilization from adipose tissue during exercise. *Trends in endocrinology and metabolism: TEM* 14, 386-392.
- Horowitz, J.F., Mora-Rodriguez, R., Byerley, L.O., and Coyle, E.F. (1997). Lipolytic suppression following carbohydrate ingestion limits fat oxidation during exercise. *The American journal of physiology* 273, E768-775.
- Houten, S.M., Herrema, H., Te Brinke, H., Denis, S., Ruiten, J.P., van Dijk, T.H., Argmann, C.A., Ottenhoff, R., Muller, M., Groen, A.K., et al. (2013). Impaired amino acid metabolism contributes to fasting-induced hypoglycemia in fatty acid oxidation defects. *Human molecular genetics* 22, 5249-5261.
- Houtkooper, R.H., Argmann, C., Houten, S.M., Canto, C., Jenning, E.H., Andreux, P.A., Thomas, C., Doenlen, R., Schoonjans, K., and Auwerx, J. (2011). The metabolic footprint of aging in mice. *Scientific reports* 1, 134.
- Howlett, R.A., Parolin, M.L., Dyck, D.J., Hultman, E., Jones, N.L., Heigenhauser, G.J., and Spriet, L.L. (1998). Regulation of skeletal muscle glycogen phosphorylase and PDH at varying exercise power outputs. *The American journal of physiology* 275, R418-425.

Hue, L., and Taegtmeyer, H. (2009). The Randle cycle revisited: a new head for an old hat. *American journal of physiology. Endocrinology and metabolism* 297, E578-591.

Huffman, K.M., Redman, L.M., Landerman, L.R., Pieper, C.F., Stevens, R.D., Muehlbauer, M.J., Wenner, B.R., Bain, J.R., Kraus, V.B., Newgard, C.B., et al. (2012). Caloric restriction alters the metabolic response to a mixed-meal: results from a randomized, controlled trial. *PloS one* 7, e28190.

Huffman, K.M., Shah, S.H., Stevens, R.D., Bain, J.R., Muehlbauer, M., Slentz, C.A., Tanner, C.J., Kuchibhatla, M., Houmard, J.A., Newgard, C.B., et al. (2009). Relationships between circulating metabolic intermediates and insulin action in overweight to obese, inactive men and women. *Diabetes care* 32, 1678-1683.

Huijsman, E., van de Par, C., Economou, C., van der Poel, C., Lynch, G., Schoiswohl, G., Haemmerle, G., Zechner, R., and Watt, M. (2009). Adipose triacylglycerol lipase deletion alters whole body energy metabolism and impairs exercise performance in mice. *American journal of physiology: endocrinology and metabolism* 297, E505-E513.

Ibrahimi, A., Bonen, A., Blinn, W.D., Hajri, T., Li, X., Zhong, K., Cameron, R., and Abumrad, N.A. (1999). Muscle-specific overexpression of FAT/CD36 enhances fatty acid oxidation by contracting muscle, reduces plasma triglycerides and fatty acids, and increases plasma glucose and insulin. *The Journal of biological chemistry* 274, 26761-26766.

Jensen, J., Rustad, P.I., Kolnes, A.J., and Lai, Y.C. (2011). The role of skeletal muscle glycogen breakdown for regulation of insulin sensitivity by exercise. *Frontiers in physiology* 2, 112.

Jeppesen, J., Jordy, A.B., Sjoberg, K.A., Fullekrug, J., Stahl, A., Nybo, L., and Kiens, B. (2012). Enhanced fatty acid oxidation and FATP4 protein expression after endurance exercise training in human skeletal muscle. *PloS one* 7, e29391.

Jeppesen, J., and Kiens, B. (2012). Regulation and limitations to fatty acid oxidation during exercise. *The Journal of physiology* 590, 1059-1068.

Jeukendrup, A.E. (2002). Regulation of fat metabolism in skeletal muscle. *Annals of the New York Academy of Sciences* 967, 217-235.

Jeukendrup, A.E., and Wallis, G.A. (2005). Measurement of substrate oxidation during exercise by means of gas exchange measurements. *International journal of sports medicine* 26 Suppl 1, S28-37.

John, S., Weiss, J.N., and Ribalet, B. (2011). Subcellular localization of hexokinases I and II directs the metabolic fate of glucose. *PloS one* 6, e17674.



- Karamanou, M., and Androustos, G. (2013). Antoine-Laurent de Lavoisier (1743-1794) and the birth of respiratory physiology. *Thorax* 68, 978-979.
- Katewa, S.D., Demontis, F., Kolipinski, M., Hubbard, A., Gill, M.S., Perrimon, N., Melov, S., and Kapahi, P. (2012). Intramyocellular fatty-acid metabolism plays a critical role in mediating responses to dietary restriction in *Drosophila melanogaster*. *Cell metabolism* 16, 97-103.
- Kelley, D.E., and Mandarino, L.J. (2000). Fuel selection in human skeletal muscle in insulin resistance: a reexamination. *Diabetes* 49, 677-683.
- Kerner, J., Minkler, P.E., Lesnfsky, E.J., and Hoppel, C.L. (2014). Fatty acid chain elongation in palmitate-perfused working rat heart: mitochondrial acetyl-CoA is the source of two-carbon units for chain elongation. *Journal of Biological Chemistry* 289, 10223-10234.
- Keung, W., Ussher, J.R., Jaswal, J.S., Raubenheimer, M., Lam, V.H., Wagg, C.S., and Lopaschuk, G.D. (2013). Inhibition of carnitine palmitoyltransferase-1 activity alleviates insulin resistance in diet-induced obese mice. *Diabetes* 62, 711-720.
- Kiens, B. (2006). Skeletal muscle lipid metabolism in exercise and insulin resistance. *Physiological reviews* 86, 205-243.
- Kiens, B., Essen-Gustavsson, B., Christensen, N.J., and Saltin, B. (1993). Skeletal muscle substrate utilization during submaximal exercise in man: effect of endurance training. *The Journal of physiology* 469, 459-478.
- Kivela, R., Silvennoinen, M., Lehti, M., Rinnankoski-Tuikka, R., Purhonen, T., Ketola, T., Pullinen, K., Vuento, M., Mutanen, N., Sartor, M.A., et al. (2010). Gene expression centroids that link with low intrinsic aerobic exercise capacity and complex disease risk. *FASEB journal : official publication of the Federation of American Societies for Experimental Biology* 24, 4565-4574.
- Klein, S., Coyle, E.F., and Wolfe, R.R. (1994). Fat metabolism during low-intensity exercise in endurance-trained and untrained men. *The American journal of physiology* 267, E934-940.
- Koch, L.G., and Britton, S.L. (2001). Artificial selection for intrinsic aerobic endurance running capacity in rats. *Physiological genomics* 5, 45-52.
- Koch, L.G., and Britton, S.L. (2005). Divergent selection for aerobic capacity in rats as a model for complex disease. *Integrative and comparative biology* 45, 405-415.
- Koch, L.G., and Britton, S.L. (2008). Aerobic metabolism underlies complexity and capacity. *The Journal of physiology* 586, 83-95.

Koch, L.G., Kemi, O.J., Qi, N., Leng, S.X., Bijma, P., Gilligan, L.J., Wilkinson, J.E., Wisloff, H., Hoydal, M.A., Rolim, N., et al. (2011). Intrinsic aerobic capacity sets a divide for aging and longevity. *Circulation research* 109, 1162-1172.

Koch, L.G., Meredith, T.A., Fraker, T.D., Metting, P.J., and Britton, S.L. (1998). Heritability of treadmill running endurance in rats. *The American journal of physiology* 275, R1455-1460.

Kodama, S., Saito, K., Tanaka, S., Maki, M., Yachi, Y., Asumi, M., Sugawara, A., Totsuka, K., Shimano, H., Ohashi, Y., et al. (2009). Cardiorespiratory fitness as a quantitative predictor of all-cause mortality and cardiovascular events in healthy men and women: a meta-analysis. *JAMA (Chicago, Ill.)* 301, 2024-2035.

Koves, T.R., Ussher, J.R., Noland, R.C., Slentz, D., Mosedale, M., Ilkayeva, O., Bain, J., Stevens, R., Dyck, J.R., Newgard, C.B., et al. (2008). Mitochondrial overload and incomplete fatty acid oxidation contribute to skeletal muscle insulin resistance. *Cell metabolism* 7, 45-56.

Larsen, F.J., Anderson, M., Ekblom, B., and Nystrom, T. (2012). Cardiorespiratory fitness predicts insulin action and secretion in healthy individuals. *Metabolism: clinical and experimental* 61, 12-16.

Lass, A., Zimmermann, R., Oberer, M., and Zechner, R. (2011). Lipolysis - a highly regulated multi-enzyme complex mediates the catabolism of cellular fat stores. *Progress in lipid research* 50, 14-27.

Lauritzen, H.P., Galbo, H., Brandauer, J., Goodyear, L.J., and Ploug, T. (2008). Large GLUT4 vesicles are stationary while locally and reversibly depleted during transient insulin stimulation of skeletal muscle of living mice: imaging analysis of GLUT4-enhanced green fluorescent protein vesicle dynamics. *Diabetes* 57, 315-324.

Lauritzen, H.P., Galbo, H., Toyoda, T., and Goodyear, L.J. (2010). Kinetics of contraction-induced GLUT4 translocation in skeletal muscle fibers from living mice. *Diabetes* 59, 2134-2144.

Lee, D.-c., Artero, E., Sui, X., and Blair, S. (2010). Mortality trends in the general population: the importance of cardiorespiratory fitness. *Journal of psychopharmacology* 24, 27-35.

Lee, S.H., and Davis, E.J. (1986). Amino acid catabolism by perfused rat hindquarter. The metabolic fates of valine. *The Biochemical journal* 233, 621-630.

Lehmann, R., Zhao, X., Weigert, C., Simon, P., Fehrenbach, E., Fritsche, J., Machann, J., Schick, F., Wang, J., Hoene, M., et al. (2010). Medium chain acylcarnitines dominate the metabolite pattern in humans under moderate intensity exercise and support lipid oxidation. *PloS one* 5, e11519.

Leite, S.A., Monk, A.M., Upham, P.A., and Bergenstal, R.M. (2009). Low cardiorespiratory fitness in people at risk for type 2 diabetes: early marker for insulin resistance. *Diabetol Metab Syndr* 1, 8.

Leskinen, T., Rinnankoski-Tuikka, R., Rintala, M., Seppnen-Laakso, T., Pllnen, E., Alen, M., Sipil, S., Kaprio, J., Kovanen, V., Rahkila, P., et al. (2010). Differences in muscle and adipose tissue gene expression and cardio-metabolic risk factors in the members of physical activity discordant twin pairs. *PLoS one* 5.

Lessard, S.J., Rivas, D.A., Chen, Z.P., van Denderen, B.J., Watt, M.J., Koch, L.G., Britton, S.L., Kemp, B.E., and Hawley, J.A. (2009). Impaired skeletal muscle beta-adrenergic activation and lipolysis are associated with whole-body insulin resistance in rats bred for low intrinsic exercise capacity. *Endocrinology* 150, 4883-4891.

Lessard, S.J., Rivas, D.A., Stephenson, E.J., Yaspelkis, B.B., 3rd, Koch, L.G., Britton, S.L., and Hawley, J.A. (2011). Exercise training reverses impaired skeletal muscle metabolism induced by artificial selection for low aerobic capacity. *American journal of physiology. Regulatory, integrative and comparative physiology* 300, R175-182.

Lewis, G., Farrell, L., Wood, M., Martinovic, M., Arany, Z., Rowe, G., Souza, A., Cheng, S., McCabe, E., Yang, E., et al. (2010). Metabolic signatures of exercise in human plasma. *Science translational medicine* 2, 33ra37-33ra37.

Lombard, D.B., Alt, F.W., Cheng, H.L., Bunkenborg, J., Streeper, R.S., Mostoslavsky, R., Kim, J., Yancopoulos, G., Valenzuela, D., Murphy, A., et al. (2007). Mammalian Sir2 homolog SIRT3 regulates global mitochondrial lysine acetylation. *Molecular and cellular biology* 27, 8807-8814.

Lopez-Otin, C., Blasco, M.A., Partridge, L., Serrano, M., and Kroemer, G. (2013). The hallmarks of aging. *Cell* 153, 1194-1217.

Lorenz, M.A., Burant, C.F., and Kennedy, R.T. (2011). Reducing Time and Increasing Sensitivity in Sample Preparation for Adherent Mammalian Cell Metabolomics. *Analytical Chemistry* 83, 3406-3414.

Luiken, J.J., Dyck, D.J., Han, X.X., Tandon, N.N., Arumugam, Y., Glatz, J.F., and Bonen, A. (2002). Insulin induces the translocation of the fatty acid transporter FAT/CD36 to the plasma membrane. *American journal of physiology. Endocrinology and metabolism* 282, E491-495.

Lundby, A., Lage, K., Weinert, B.T., Bekker-Jensen, D.B., Secher, A., Skovgaard, T., Kelstrup, C.D., Dmytriiev, A., Choudhary, C., Lundby, C., et al. (2012). Proteomic analysis of lysine acetylation sites in rat tissues reveals organ specificity and subcellular patterns. *Cell reports* 2, 419-431.

Lustgarten, M.S., Price, L.L., Logvinenko, T., Hatzis, C., Padukone, N., Reo, N.V., Phillips, E.M., Kirn, D., Mills, J., and Fielding, R.A. (2013). Identification of serum analytes and metabolites associated with aerobic capacity. *European journal of applied physiology* *113*, 1311-1320.

Lynch, C.J., Hutson, S.M., Patson, B.J., Vaval, A., and Vary, T.C. (2002). Tissue-specific effects of chronic dietary leucine and norleucine supplementation on protein synthesis in rats. *American journal of physiology. Endocrinology and metabolism* *283*, E824-835.

MacLean, D.A., and Graham, T.E. (1993). Branched-chain amino acid supplementation augments plasma ammonia responses during exercise in humans. *Journal of applied physiology* *74*, 2711-2717.

Magkos, F., Bradley, D., Schweitzer, G.G., Finck, B.N., Eagon, J.C., Ilkayeva, O., Newgard, C.B., and Klein, S. (2013). Effect of Roux-en-Y gastric bypass and laparoscopic adjustable gastric banding on branched-chain amino acid metabolism. *Diabetes* *62*, 2757-2761.

Mailloux, R.J., Dumouchel, T., Aguer, C., deKemp, R., Beanlands, R., and Harper, M.E. (2011). Hexokinase II acts through UCP3 to suppress mitochondrial reactive oxygen species production and maintain aerobic respiration. *The Biochemical journal* *437*, 301-311.

Marquis, N.R., and Fritz, I.B. (1965). THE DISTRIBUTION OF CARNITINE, ACETYLCARNITINE, AND CARNITINE ACETYLTRANSFERASE IN RAT TISSUES. *The Journal of biological chemistry* *240*, 2193-2196.

Martin, F.P., Spanier, B., Collino, S., Montoliu, I., Kolmeder, C., Giesbertz, P., Affolter, M., Kussmann, M., Daniel, H., Kochhar, S., et al. (2011). Metabotyping of *Caenorhabditis elegans* and their culture media revealed unique metabolic phenotypes associated to amino acid deficiency and insulin-like signaling. *Journal of proteome research* *10*, 990-1003.

Masri, S., Patel, V.R., Eckel-Mahan, K.L., Peleg, S., Forne, I., Ladurner, A.G., Baldi, P., Imhof, A., and Sassone-Corsi, P. (2013). Circadian acetylome reveals regulation of mitochondrial metabolic pathways. *Proceedings of the National Academy of Sciences of the United States of America* *110*, 3339-3344.

Menni, C., Fauman, E., Erte, I., Perry, J.R., Kastenmuller, G., Shin, S.Y., Petersen, A.K., Hyde, C., Psatha, M., Ward, K.J., et al. (2013). Biomarkers for type 2 diabetes and impaired fasting glucose using a nontargeted metabolomics approach. *Diabetes* *62*, 4270-4276.

Mitchell, H.H. (1937). Carl von Voit. *The Journal of nutrition* *13*, 2-13.

Mittendorfer, B., and Klein, S. (2001). Effect of aging on glucose and lipid metabolism during endurance exercise. *International journal of sport nutrition and exercise metabolism* 11 Suppl, S86-91.

Morris, C., Grada, C.O., Ryan, M., Roche, H.M., De Vito, G., Gibney, M.J., Gibney, E.R., and Brennan, L. (2013). The relationship between aerobic fitness level and metabolic profiles in healthy adults. *Molecular nutrition & food research* 57, 1246-1254.

Mullen, E., and Ohlendieck, K. (2010). Proteomic profiling of non-obese type 2 diabetic skeletal muscle. *International journal of molecular medicine* 25, 445-458.

Munkacsy, E., and Rea, S.L. (2014). The paradox of mitochondrial dysfunction and extended longevity. *Experimental gerontology* 56, 221-233.

Muoio, D., and Koves, T. (2007). Skeletal muscle adaptation to fatty acid depends on coordinated actions of the PPARs and PGC1 alpha: implications for metabolic disease. *Applied physiology, nutrition, and metabolism* 32, 874-883.

Naples, S.P., Borengasser, S.J., Rector, R.S., Uptergrove, G.M., Morris, E.M., Mikus, C.R., Koch, L.G., Britton, S.L., Ibdah, J.A., and Thyfault, J.P. (2010). Skeletal muscle mitochondrial and metabolic responses to a high-fat diet in female rats bred for high and low aerobic capacity. *Applied physiology, nutrition, and metabolism = Physiologie appliquee, nutrition et metabolisme* 35, 151-162.

Narkar, V.A., Fan, W., Downes, M., Yu, R.T., Jonker, J.W., Alaynick, W.A., Banayo, E., Karunasiri, M.S., Lorca, S., and Evans, R.M. (2011). Exercise and PGC-1alpha-independent synchronization of type I muscle metabolism and vasculature by ERRgamma. *Cell metabolism* 13, 283-293.

Neary, C.L., and Pastorino, J.G. (2013). Akt inhibition promotes hexokinase 2 redistribution and glucose uptake in cancer cells. *Journal of cellular physiology* 228, 1943-1948.

Nesvizhskii, A.I., and Aebersold, R. (2005). Interpretation of shotgun proteomic data: the protein inference problem. *Molecular & cellular proteomics : MCP* 4, 1419-1440.

Newgard, C.B., An, J., Bain, J.R., Muehlbauer, M.J., Stevens, R.D., Lien, L.F., Haqq, A.M., Shah, S.H., Arlotto, M., Slentz, C.A., et al. (2009). A branched-chain amino acid-related metabolic signature that differentiates obese and lean humans and contributes to insulin resistance. *Cell metabolism* 9, 311-326.

Nickerson, J.G., Alkhateeb, H., Benton, C.R., Lally, J., Nickerson, J., Han, X.X., Wilson, M.H., Jain, S.S., Snook, L.A., Glatz, J.F., et al. (2009). Greater transport efficiencies of the membrane fatty acid transporters FAT/CD36 and FATP4 compared with FABPpm and FATP1 and differential effects on fatty acid

esterification and oxidation in rat skeletal muscle. *The Journal of biological chemistry* 284, 16522-16530.

Noland, R.C., Koves, T.R., Seiler, S.E., Lum, H., Lust, R.M., Ilkayeva, O., Stevens, R.D., Hegardt, F.G., and Muoio, D.M. (2009). Carnitine insufficiency caused by aging and overnutrition compromises mitochondrial performance and metabolic control. *The Journal of biological chemistry* 284, 22840-22852.

Noland, R.C., Thyfault, J.P., Henes, S.T., Whitfield, B.R., Woodlief, T.L., Evans, J.R., Lust, J.A., Britton, S.L., Koch, L.G., Dudek, R.W., et al. (2007). Artificial selection for high-capacity endurance running is protective against high-fat diet-induced insulin resistance. *American journal of physiology. Endocrinology and metabolism* 293, E31-41.

Nordby, P., Saltin, B., and Helge, J.W. (2006). Whole-body fat oxidation determined by graded exercise and indirect calorimetry: a role for muscle oxidative capacity? *Scandinavian journal of medicine & science in sports* 16, 209-214.

Novak, C.M., Escande, C., Burghardt, P.R., Zhang, M., Barbosa, M.T., Chini, E.N., Britton, S.L., Koch, L.G., Akil, H., and Levine, J.A. (2010). Spontaneous activity, economy of activity, and resistance to diet-induced obesity in rats bred for high intrinsic aerobic capacity. *Horm Behav* 58, 355-367.

Odland, L.M., Heigenhauser, G.J., Wong, D., Hollidge-Horvat, M.G., and Spriet, L.L. (1998a). Effects of increased fat availability on fat-carbohydrate interaction during prolonged exercise in men. *The American journal of physiology* 274, R894-902.

Odland, L.M., Howlett, R.A., Heigenhauser, G.J., Hultman, E., and Spriet, L.L. (1998b). Skeletal muscle malonyl-CoA content at the onset of exercise at varying power outputs in humans. *The American journal of physiology* 274, E1080-1085.

Orngreen, M.C., Jeppesen, T.D., Andersen, S.T., Taivassalo, T., Hauerslev, S., Preisler, N., Haller, R.G., van Hall, G., and Vissing, J. (2009). Fat metabolism during exercise in patients with McArdle disease. *Neurology* 72, 718-724.

Pagliarini, D.J., Calvo, S.E., Chang, B., Sheth, S.A., Vafai, S.B., Ong, S.E., Walford, G.A., Sugiana, C., Boneh, A., Chen, W.K., et al. (2008). A mitochondrial protein compendium elucidates complex I disease biology. *Cell* 134, 112-123.

Palacios, O.M., Carmona, J.J., Michan, S., Chen, K.Y., Manabe, Y., Ward, J.L., 3rd, Goodyear, L.J., and Tong, Q. (2009). Diet and exercise signals regulate SIRT3 and activate AMPK and PGC-1alpha in skeletal muscle. *Aging* 1, 771-783.

Park, S.K., and Prolla, T.A. (2005). Gene expression profiling studies of aging in cardiac and skeletal muscles. *Cardiovascular research* 66, 205-212.

Peel, J.B., Sui, X., Adams, S.A., Hebert, J.R., Hardin, J.W., and Blair, S.N. (2009). A prospective study of cardiorespiratory fitness and breast cancer mortality. *Medicine and science in sports and exercise* 41, 742-748.

Perez-Schindler, J., Summermatter, S., Salatino, S., Zorzato, F., Beer, M., Balwierz, P.J., van Nimwegen, E., Feige, J.N., Auwerx, J., and Handschin, C. (2012). The corepressor NCoR1 antagonizes PGC-1alpha and estrogen-related receptor alpha in the regulation of skeletal muscle function and oxidative metabolism. *Molecular and cellular biology* 32, 4913-4924.

Peronnet, F., and Massicotte, D. (1991). Table of nonprotein respiratory quotient: an update. *Canadian journal of sport sciences = Journal canadien des sciences du sport* 16, 23-29.

Phanstiel, D.H., Brumbaugh, J., Wenger, C.D., Tian, S., Probasco, M.D., Bailey, D.J., Swaney, D.L., Tervo, M.A., Bolin, J.M., Ruotti, V., et al. (2011). Proteomic and phosphoproteomic comparison of human ES and iPS cells. *Nature methods* 8, 821-827.

Pietilainen, K.H., Naukkarinen, J., Rissanen, A., Saharinen, J., Ellonen, P., Keranen, H., Suomalainen, A., Gotz, A., Suortti, T., Yki-Jarvinen, H., et al. (2008). Global transcript profiles of fat in monozygotic twins discordant for BMI: pathways behind acquired obesity. *PLoS medicine* 5, e51.

Pohjanen, E., Thysell, E., Jonsson, P., Eklund, C., Silfver, A., Carlsson, I.B., Lundgren, K., Moritz, T., Svensson, M.B., and Antti, H. (2007). A multivariate screening strategy for investigating metabolic effects of strenuous physical exercise in human serum. *Journal of proteome research* 6, 2113-2120.

Power, R.A., Hulver, M.W., Zhang, J.Y., Dubois, J., Marchand, R.M., Ilkayeva, O., Muoio, D.M., and Mynatt, R.L. (2007). Carnitine revisited: potential use as adjunctive treatment in diabetes. *Diabetologia* 50, 824-832.

Quinn, L.S., Anderson, B.G., Conner, J.D., and Wolden-Hanson, T. (2013). IL-15 overexpression promotes endurance, oxidative energy metabolism, and muscle PPARdelta, SIRT1, PGC-1alpha, and PGC-1beta expression in male mice. *Endocrinology* 154, 232-245.

R Core Team (2013). R: A language and environment for statistical computing. (Vienna, Austria: R Foundation for Statistical Computing).

Ramnanan, C.J., Edgerton, D.S., Kraft, G., and Cherrington, A.D. (2011). Physiologic action of glucagon on liver glucose metabolism. *Diabetes, obesity & metabolism* 13 Suppl 1, 118-125.

Ramsay, R.R., and Zammit, V.A. (2004). Carnitine acyltransferases and their influence on CoA pools in health and disease. *Molecular Aspects of Medicine* 25, 475-493.

Randle, P.J. (1998). Regulatory interactions between lipids and carbohydrates: the glucose fatty acid cycle after 35 years. *Diabetes/metabolism reviews* 14, 263-283.

Randle, P.J., Garland, P.B., Hales, C.N., and Newsholme, E.A. (1963). The glucose fatty-acid cycle. Its role in insulin sensitivity and the metabolic disturbances of diabetes mellitus. *Lancet* 1, 785-789.

Rapp, J.P. (1982). Dahl salt-susceptible and salt-resistant rats. A review. *Hypertension* 4, 753-763.

Rardin, M.J., Newman, J.C., Held, J.M., Cusack, M.P., Sorensen, D.J., Li, B., Schilling, B., Mooney, S.D., Kahn, C.R., Verdin, E., et al. (2013). Label-free quantitative proteomics of the lysine acetylome in mitochondria identifies substrates of SIRT3 in metabolic pathways. *Proceedings of the National Academy of Sciences of the United States of America* 110, 6601-6606.

Ren, Y.Y., Overmyer, K.A., Qi, N.R., Treutelaar, M.K., Heckenkamp, L., Kalahar, M., Koch, L.G., Britton, S.L., Burant, C.F., and Li, J.Z. (2013). Genetic analysis of a rat model of aerobic capacity and metabolic fitness. *PloS one* 8, e77588.

Richards, S.E., Wang, Y., Claus, S.P., Lawler, D., Kochhar, S., Holmes, E., and Nicholson, J.K. (2013). Metabolic phenotype modulation by caloric restriction in a lifelong dog study. *Journal of proteome research* 12, 3117-3127.

Richter, E.A., and Hargreaves, M. (2013). Exercise, GLUT4, and skeletal muscle glucose uptake. *Physiological reviews* 93, 993-1017.

Rivas, D.A., Lessard, S.J., Saito, M., Friedhuber, A.M., Koch, L.G., Britton, S.L., Yaspelkis, B.B., 3rd, and Hawley, J.A. (2011). Low intrinsic running capacity is associated with reduced skeletal muscle substrate oxidation and lower mitochondrial content in white skeletal muscle. *American journal of physiology. Regulatory, integrative and comparative physiology* 300, R835-843.

Roepstorff, C., Halberg, N., Hillig, T., Saha, A.K., Ruderman, N.B., Wojtaszewski, J.F., Richter, E.A., and Kiens, B. (2005). Malonyl-CoA and carnitine in regulation of fat oxidation in human skeletal muscle during exercise. *American journal of physiology. Endocrinology and metabolism* 288, E133-142.

Rogowski, M.P., Flowers, M.T., Stamatikos, A.D., Ntambi, J.M., and Paton, C.M. (2013). SCD1 activity in muscle increases triglyceride PUFA content, exercise capacity, and PPARdelta expression in mice. *Journal of lipid research* 54, 2636-2646.



Romijn, J.A., Coyle, E.F., Sidossis, L.S., Gastaldelli, A., Horowitz, J.F., Endert, E., and Wolfe, R.R. (1993). Regulation of endogenous fat and carbohydrate metabolism in relation to exercise intensity and duration. *The American journal of physiology* *265*, E380-391.

Romijn, J.A., Coyle, E.F., Sidossis, L.S., Zhang, X.J., and Wolfe, R.R. (1995). Relationship between fatty acid delivery and fatty acid oxidation during strenuous exercise. *Journal of applied physiology* (Bethesda, Md. : 1985) *79*, 1939-1945.

Rush, J.W., MacLean, D.A., Hultman, E., and Graham, T.E. (1995). Exercise causes branched-chain oxoacid dehydrogenase dephosphorylation but not AMP deaminase binding. *Journal of applied physiology* *78*, 2193-2200.

Sahlin, K. (1990). Muscle carnitine metabolism during incremental dynamic exercise in humans. *Acta physiologica Scandinavica* *138*, 259-262.

Sahlin, K., Sallstedt, E.K., Bishop, D., and Tonkonogi, M. (2008). Turning down lipid oxidation during heavy exercise--what is the mechanism? *Journal of physiology and pharmacology : an official journal of the Polish Physiological Society* *59 Suppl 7*, 19-30.

Schneider, C.A., Rasband, W.S., and Eliceiri, K.W. (2012). NIH Image to ImageJ: 25 years of image analysis. *Nature methods* *9*, 671-675.

Schoiswohl, G., Schweiger, M., Schreiber, R., Gorkiewicz, G., Preiss-Landl, K., Taschler, U., Zierler, K.A., Radner, F.P., Eichmann, T.O., Kienesberger, P.C., et al. (2010). Adipose triglyceride lipase plays a key role in the supply of the working muscle with fatty acids. *Journal of lipid research* *51*, 490-499.

Schrauwen, P., Timmers, S., and Hesselink, M.K. (2013). Blocking the entrance to open the gate. *Diabetes* *62*, 703-705.

Schrauwen, P., van Aggel-Leijssen, D.P., Hul, G., Wagenmakers, A.J., Vidal, H., Saris, W.H., and van Baak, M.A. (2002). The effect of a 3-month low-intensity endurance training program on fat oxidation and acetyl-CoA carboxylase-2 expression. *Diabetes* *51*, 2220-2226.

Schwarzer, M., Britton, S., Koch, L., Wisloff, U., and Doenst, T. (2010). Low intrinsic aerobic exercise capacity and systemic insulin resistance are not associated with changes in myocardial substrate oxidation or insulin sensitivity. *Basic Research in Cardiology* *105*, 357-364.

Schweiger, M., Schreiber, R., Haemmerle, G., Lass, A., Fledelius, C., Jacobsen, P., Tornqvist, H., Zechner, R., and Zimmermann, R. (2006). Adipose triglyceride lipase and hormone-sensitive lipase are the major enzymes in adipose tissue triacylglycerol catabolism. *The Journal of biological chemistry* *281*, 40236-40241.

Sears, D.D., Hsiao, G., Hsiao, A., Yu, J.G., Courtney, C.H., Ofrecio, J.M., Chapman, J., and Subramaniam, S. (2009). Mechanisms of human insulin resistance and thiazolidinedione-mediated insulin sensitization. *Proceedings of the National Academy of Sciences* *106*, 18745-18750.

Seifert, E.L., Bastianelli, M., Aguer, C., Moffat, C., Estey, C., Koch, L.G., Britton, S.L., and Harper, M.E. (2012). Intrinsic aerobic capacity correlates with greater inherent mitochondrial oxidative and H<sub>2</sub>O<sub>2</sub> emission capacities without major shifts in myosin heavy chain isoform. *Journal of applied physiology* *113*, 1624-1634.

Shah, S.H., Crosslin, D.R., Haynes, C.S., Nelson, S., Turer, C.B., Stevens, R.D., Muehlbauer, M.J., Wenner, B.R., Bain, J.R., Laferrere, B., et al. (2012). Branched-chain amino acid levels are associated with improvement in insulin resistance with weight loss. *Diabetologia* *55*, 321-330.

She, P., Zhou, Y., Zhang, Z., Griffin, K., Gowda, K., and Lynch, C. (2010). Disruption of BCAA metabolism in mice impairs exercise metabolism and endurance. *Journal of applied physiology* *108*, 941-949.

Shimomura, Y., Fujii, H., Suzuki, M., Murakami, T., Fujitsuka, N., and Nakai, N. (1995). Branched-chain alpha-keto acid dehydrogenase complex in rat skeletal muscle: regulation of the activity and gene expression by nutrition and physical exercise. *The Journal of nutrition* *125*, 1762S-1765S.

Sidossis, L.S., Gastaldelli, A., Klein, S., and Wolfe, R.R. (1997). Regulation of plasma fatty acid oxidation during low- and high-intensity exercise. *The American journal of physiology* *272*, E1065-1070.

Smith, B.K., Jain, S.S., Rimbaud, S., Dam, A., Quadriatero, J., Ventura-Clapier, R., Bonen, A., and Holloway, G.P. (2011). FAT/CD36 is located on the outer mitochondrial membrane, upstream of long-chain acyl-CoA synthetase, and regulates palmitate oxidation. *The Biochemical journal* *437*, 125-134.

Spydevold, O. (1979). The effect of octanoate and palmitate on the metabolism of valine in perfused hindquarter of rat. *European journal of biochemistry / FEBS* *97*, 389-394.

Starritt, E.C., Howlett, R.A., Heigenhauser, G.J., and Spriet, L.L. (2000). Sensitivity of CPT I to malonyl-CoA in trained and untrained human skeletal muscle. *American journal of physiology. Endocrinology and metabolism* *278*, E462-468.

Still, A.J., Floyd, B.J., Hebert, A.S., Bingman, C.A., Carson, J.J., Gunderson, D.R., Dolan, B.K., Grimsrud, P.A., Dittenhafer-Reed, K.E., Stapleton, D.S., et al. (2013). Quantification of mitochondrial acetylation dynamics highlights prominent sites of metabolic regulation. *The Journal of biological chemistry* *288*, 26209-26219.

Stump, D.D., Zhou, S.L., and Berk, P.D. (1993). Comparison of plasma membrane FABP and mitochondrial isoform of aspartate aminotransferase from rat liver. *The American journal of physiology* 265, G894-902.

Tarnopolsky, M.A., Parise, G., Gibala, M.J., Graham, T.E., and Rush, J.W. (2001). Myoadenylate deaminase deficiency does not affect muscle anaplerosis during exhaustive exercise in humans. *The Journal of physiology* 533, 881-889.

Thyfault, J.P., Rector, R.S., and Noland, R.C. (2006). Metabolic inflexibility in skeletal muscle: a prelude to the cardiometabolic syndrome? *Journal of the cardiometabolic syndrome* 1, 184-189.

Thyfault, J.P., Rector, R.S., Uptergrove, G.M., Borengasser, S.J., Morris, E.M., Wei, Y., Laye, M.J., Burant, C.F., Qi, N.R., Ridenhour, S.E., et al. (2009). Rats selectively bred for low aerobic capacity have reduced hepatic mitochondrial oxidative capacity and susceptibility to hepatic steatosis and injury. *The Journal of physiology* 587, 1805-1816.

Timmers, S., Nabben, M., Bosma, M., van Bree, B., Lenaers, E., van Beurden, D., Schaart, G., Westerterp-Plantenga, M.S., Langhans, W., Hesselink, M.K., et al. (2012). Augmenting muscle diacylglycerol and triacylglycerol content by blocking fatty acid oxidation does not impede insulin sensitivity. *Proceedings of the National Academy of Sciences of the United States of America* 109, 11711-11716.

Tomas-Loba, A., Bernardes de Jesus, B., Mato, J.M., and Blasco, M.A. (2013). A metabolic signature predicts biological age in mice. *Aging cell* 12, 93-101.

Tunstall, R.J., Mehan, K.A., Wadley, G.D., Collier, G.R., Bonen, A., Hargreaves, M., and Cameron-Smith, D. (2002). Exercise training increases lipid metabolism gene expression in human skeletal muscle. *American journal of physiology. Endocrinology and metabolism* 283, E66-72.

Turner, N., Cooney, G.J., Kraegen, E.W., and Bruce, C.R. (2014). Fatty acid metabolism, energy expenditure and insulin resistance in muscle. *The Journal of endocrinology* 220, T61-79.

van Hall, G., MacLean, D.A., Saltin, B., and Wagenmakers, A.J. (1996). Mechanisms of activation of muscle branched-chain alpha-keto acid dehydrogenase during exercise in man. *The Journal of physiology* 494 ( Pt 3), 899-905.

van Loon, L.J., Greenhaff, P.L., Constantin-Teodosiu, D., Saris, W.H., and Wagenmakers, A.J. (2001). The effects of increasing exercise intensity on muscle fuel utilisation in humans. *The Journal of physiology* 536, 295-304.

- Venables, M.C., Achten, J., and Jeukendrup, A.E. (2005). Determinants of fat oxidation during exercise in healthy men and women: a cross-sectional study. *Journal of applied physiology* (Bethesda, Md. : 1985) *98*, 160-167.
- Wagenmakers, A.J., Beckers, E.J., Brouns, F., Kuipers, H., Soeters, P.B., van der Vusse, G.J., and Saris, W.H. (1991). Carbohydrate supplementation, glycogen depletion, and amino acid metabolism during exercise. *The American journal of physiology* *260*, E883-890.
- Wagenmakers, A.J., Brookes, J.H., Coakley, J.H., Reilly, T., and Edwards, R.H. (1989). Exercise-induced activation of the branched-chain 2-oxo acid dehydrogenase in human muscle. *European journal of applied physiology and occupational physiology* *59*, 159-167.
- Wagenmakers, A.J., Salden, H.J., and Veerkamp, J.H. (1985). The metabolic fate of branched-chain amino acids and 2-oxo acids in rat muscle homogenates and diaphragms. *The International journal of biochemistry* *17*, 957-965.
- Wagner, G.R., and Payne, R.M. (2013). Widespread and enzyme-independent Nepsilon-acetylation and Nepsilon-succinylation of proteins in the chemical conditions of the mitochondrial matrix. *The Journal of biological chemistry* *288*, 29036-29045.
- Wall, B.T., Stephens, F.B., Constantin-Teodosiu, D., Marimuthu, K., Macdonald, I.A., and Greenhaff, P.L. (2011). Chronic oral ingestion of L-carnitine and carbohydrate increases muscle carnitine content and alters muscle fuel metabolism during exercise in humans. *The Journal of physiology* *589*, 963-973.
- Wang, Q., Zhang, Y., Yang, C., Xiong, H., Lin, Y., Yao, J., Li, H., Xie, L., Zhao, W., Yao, Y., et al. (2010). Acetylation of metabolic enzymes coordinates carbon source utilization and metabolic flux. *Science (New York, N.Y.)* *327*, 1004-1007.
- Wang, T.J., Larson, M.G., Vasan, R.S., Cheng, S., Rhee, E.P., McCabe, E., Lewis, G.D., Fox, C.S., Jacques, P.F., Fernandez, C., et al. (2011). Metabolite profiles and the risk of developing diabetes. *Nature medicine* *17*, 448-453.
- Wasserman, D.H., and Ayala, J.E. (2005). Interaction of physiological mechanisms in control of muscle glucose uptake. *Clinical and experimental pharmacology & physiology* *32*, 319-323.
- Wei, M., Gibbons, L.W., Mitchell, T.L., Kampert, J.B., Lee, C.D., and Blair, S.N. (1999). The association between cardiorespiratory fitness and impaired fasting glucose and type 2 diabetes mellitus in men. *Annals of internal medicine* *130*, 89-96.

Wenger, C.D., Lee, M.V., Hebert, A.S., McAlister, G.C., Phanstiel, D.H., Westphall, M.S., and Coon, J.J. (2011a). Gas-phase purification enables accurate, multiplexed proteome quantification with isobaric tagging. *Nature methods* *8*, 933-935.

Wenger, C.D., Phanstiel, D.H., Lee, M.V., Bailey, D.J., and Coon, J.J. (2011b). COMPASS: a suite of pre- and post-search proteomics software tools for OMSSA. *Proteomics* *11*, 1064-1074.

West, J.B. (2013). The collaboration of Antoine and Marie-Anne Lavoisier and the first measurements of human oxygen consumption. *American journal of physiology. Lung cellular and molecular physiology* *305*, L775-785.

Westbrook, R., Bonkowski, M.S., Strader, A.D., and Bartke, A. (2009). Alterations in oxygen consumption, respiratory quotient, and heat production in long-lived GHRKO and Ames dwarf mice, and short-lived bGH transgenic mice. *The journals of gerontology. Series A, Biological sciences and medical sciences* *64*, 443-451.

Whaley, M.H., Kampert, J.B., Kohl, H.W., 3rd, and Blair, S.N. (1999). Physical fitness and clustering of risk factors associated with the metabolic syndrome. *Medicine and science in sports and exercise* *31*, 287-293.

White, A.T., and Schenk, S. (2012). NAD(+)/NADH and skeletal muscle mitochondrial adaptations to exercise. *American journal of physiology. Endocrinology and metabolism* *303*, E308-321.

White, T.P., and Brooks, G.A. (1981). [U-14C]glucose, -alanine, and -leucine oxidation in rats at rest and two intensities of running. *American journal of physiology* *240*, E155-E165.

Widdowson, E.M. (1955). Assessment of the energy value of human foods. *The Proceedings of the Nutrition Society* *14*, 142-154.

Wijeyesekera, A., Selman, C., Barton, R.H., Holmes, E., Nicholson, J.K., and Withers, D.J. (2012). Metabotyping of long-lived mice using <sup>1</sup>H NMR spectroscopy. *Journal of proteome research* *11*, 2224-2235.

Wilder, R.M. (1959). Calorimetry: the-basis of the science of nutrition. *A.M.A. archives of internal medicine* *103*, 146-154.

Wilmore, J.H., and Costill, D.L. (2004). *Physiology of sport and exercise*. (Champaign, IL: Human Kinetics).

Wisloff, U., Najjar, S.M., Ellingsen, O., Haram, P.M., Swoap, S., Al-Share, Q., Fernstrom, M., Rezaei, K., Lee, S.J., Koch, L.G., et al. (2005). Cardiovascular risk factors emerge after artificial selection for low aerobic capacity. *Science (New York, N.Y.)* *307*, 418-420.

- Wone, B., Donovan, E.R., and Hayes, J.P. (2011). Metabolomics of aerobic metabolism in mice selected for increased maximal metabolic rate. *Comparative biochemistry and physiology. Part D, Genomics & proteomics* 6, 399-405.
- Wurtz, P., Soininen, P., Kangas, A.J., Ronnema, T., Lehtimäki, T., Kahonen, M., Viikari, J.S., Raitakari, O.T., and Ala-Korpela, M. (2013). Branched-chain and aromatic amino acids are predictors of insulin resistance in young adults. *Diabetes care* 36, 648-655.
- Xiong, Y., and Guan, K.L. (2012). Mechanistic insights into the regulation of metabolic enzymes by acetylation. *The Journal of cell biology* 198, 155-164.
- Xu, F., Tavintharan, S., Sum, C.F., Woon, K., Lim, S.C., and Ong, C.N. (2013). Metabolic signature shift in type 2 diabetes mellitus revealed by mass spectrometry-based metabolomics. *The Journal of clinical endocrinology and metabolism* 98, E1060-1065.
- Yamamoto, H., Williams, E.G., Mouchiroud, L., Canto, C., Fan, W., Downes, M., Heligon, C., Barish, G.D., Desvergne, B., Evans, R.M., et al. (2011). NCoR1 is a conserved physiological modulator of muscle mass and oxidative function. *Cell* 147, 827-839.
- Yoshida, Y., Jain, S.S., McFarlan, J.T., Snook, L.A., Chabowski, A., and Bonen, A. (2013). Exercise- and training-induced upregulation of skeletal muscle fatty acid oxidation are not solely dependent on mitochondrial machinery and biogenesis. *The Journal of physiology* 591, 4415-4426.
- Zahn, J.M., and Kim, S.K. (2007). Systems biology of aging in four species. *Current Opinion in Biotechnology* 18, 355-359.
- Zhang, T., Wang, S., Lin, Y., Xu, W., Ye, D., Xiong, Y., Zhao, S., and Guan, K.L. (2012). Acetylation negatively regulates glycogen phosphorylase by recruiting protein phosphatase 1. *Cell metabolism* 15, 75-87.
- Zhao, S., Xu, W., Jiang, W., Yu, W., Lin, Y., Zhang, T., Yao, J., Zhou, L., Zeng, Y., Li, H., et al. (2010). Regulation of cellular metabolism by protein lysine acetylation. *Science (New York, N.Y.)* 327, 1000-1004.
- Zisman, A., Peroni, O.D., Abel, E.D., Michael, M.D., Mauvais-Jarvis, F., Lowell, B.B., Wojtaszewski, J.F., Hirshman, M.F., Virkamäki, A., Goodyear, L.J., et al. (2000). Targeted disruption of the glucose transporter 4 selectively in muscle causes insulin resistance and glucose intolerance. *Nature medicine* 6, 924-928.